Thermophilic Methanotrophy in the Taupō Volcanic Zone

A thesis
submitted in fulfilment
of the requirements for the degree
of
Doctor of Philosophy
in the School of Science
at
The University of Waikato
by
KAREN HOUGHTON

THE UNIVERSITY OF
WAIKATO
Te Whare Wānanga o Waikato

2018

Abstract

Methanotrophs are widely distributed in the environment and play an important role in the global methane cycle by oxidising the majority of methane produced each year. Geological sources of methane contribute substantial volumes of this greenhouse gas to the atmosphere, but research on methanotrophs to date has focused on low temperature environments. This study aimed to investigate thermophilic methanotrophy in geothermal environments within the Taupō Volcanic Zone.

A comprehensive survey of methane oxidation in geothermal soils and sediments was carried out, in conjunction with DNA sequencing of 16S rRNA genes from each sample. Methane oxidation is prevalent within the geothermal samples. This is the first survey of methane oxidation of multiple geothermal samples, and emphasises the importance of these ecosystems to the biogeochemical methane cycle. Geothermal samples encompassed highly diverse microbial communities with few ubiquitous genera, and communities were significantly different between methane oxidizing and non-oxidising microcosms. Some methane-oxidising communities did not include 16S rRNA gene sequences from known methanotrophs, suggesting the presence in geothermal ecosystems of taxa currently not recognised as capable of methane oxidation.

Enrichment microcosms were created using the methane-oxidising geothermal samples, and evaluated in terms of methane oxidation and transcriptional activity. Methanotrophy was observed at temperatures between 37 and 75 °C, which complemented the detection of mRNA transcripts for the complete oxidation of methane. Stress response genes were also highly expressed in the microcosms, identifying a variety of mechanisms within the communities to adapt to environmental change. This is the first example of using metatranscriptomics to investigate methanotrophs from geothermal environments and gives insight into the metabolic pathways involved in thermophilic methanotrophy.

Methane-oxidising bacteria were obtained in axenic culture from five enrichment microcosms, confirming the hypothesis that thermophilic methanotrophs could be enriched and isolated from geothermal environments. Many methanotrophs are poorly described in terms of their physiology and ecology, and to address these knowledge gaps, the strains isolated in this study were subjected to thorough phylogenetic and phenotypic characterisation. This research will also facilitate future cultivation, cryostorage and revival of methane oxidisers.

Several described methanotrophs are capable of oxidising hydrogen in addition to methane, but the association between hydrogen oxidation and cell growth is poorly understood. This research aimed to investigate if mixotrophic hydrogen oxidation was used to optimise growth, and if this could be linked to survival at elevated temperatures. [NiFe]- hydrogenases were identified in four of the methanotrophs isolated in this study but hydrogen oxidation was observed in only three of the isolates, which highlights the importance of culture-based investigations to confirm phenotypes predicted by metagenomics. One isolate showed increasing hydrogen oxidation with increasing temperature, but this did not appear to be linked to survival at elevated temperatures.

This study used a combination of culture-independent and cultivation studies to demonstrate that methanotrophs are both abundant and highly active within geothermal environments. Methanotrophs from these ecosystems have also been successfully isolated and characterised, adding to our knowledge both of their physiology and ecological role in methane cycling.

Acknowledgements

This work was supported by the GNS Science research programme New Zealand's Geothermal Future - Biodiversity & Ecology; and a Postgraduate Scholarship from Freemasons New Zealand.

Firstly, I would like to thank my supervisors, Professor Ian McDonald at Waikato, Dr Matthew Stott at Canterbury and Dr Carlo Carere at GNS Science, for all their suggestions, support and draft-editing over the last few years. I would also like to thank Dr Kirill Lagutin at Callaghan Innovation, for determination of the phospholipid fatty acid composition of the novel methanotrophs described in this study.

Thank you to Jean Power, for keeping me on the right track and giving me constant reassurance. I wish you all the best with your own never-ending project and hope I can give you back even a little of what you have given me through this journey.

Thanks are also due to past and present colleagues at GNS Science, in particular Hanna, Dora, Sarah, Kat, Laura and Dave, for all the support and for allowing me to monopolise lab equipment for long periods of time, and supplying Thursday chocolate.

But, mostly, thanks to Paul for your support and your belief in me. I couldn't have done it without you.

"Quoth the Raven "Nevermore.""

Contents

List of Figures

List of Tables

Abbreviations

ABC	ATP-binding cassette
ANME	Anaerobic methane oxidising archaea
ANMS	Ammonia nitrate mineral salts media
AOB	Ammonia oxidising bacteria
BLAST	Basic Local Alignment Search Tool
BSA	Bovine serum albumin
CBB	Calvin-Benson-Bassham cycle
CD-ART	Conserved Domain-Architecture Retrieval Tool
CH_3OH	Methanol
CoA	Co-enzyme A
COM	Craters of the Moon
DMSO	Dimethyl sulfoxide
dNTP	Deoxyribose nucleoside triphosphate
DTT	Dithiothreitol
EC x.x.x.x	Enzyme Commission number for enzyme nomenclature
ECL	Equivalent chain length
EDTA	Ethylenediaminetetraacetic acid
ETC	Electron transport chain
FAME	Fatty acid methyl ester
FID	Flame ionisation detector
FISH	Fluorescent in situ hybridization
G+C	Guanine-cytosine content
GC	Gas chromatography
GC-MS	Gas chromatography-mass spectrometry
GDS	Golden Springs
H_2O_2	Hydrogen peroxide
HAMO	High affinity methane oxidation
HCl	Hydrochloric acid
ICM	Intracytoplasmic membranes
IRMS	Isotope ratio mass spectrometry
JTT	Jones-Taylor-Thornton
Kxxxxx	KEGG Orthology number for enzyme nomenclature

KEGG	Kyoto Encyclopedia of Genes and Genomes
K_m	Half-saturation constant
kPa	Kilopascal
LPR	Loop Road
LPS	Lipopolysaccharide
MAG	Metagenome-assembled genome
MAR	Microautoradiography
MG- RAST	Metagenomic Rapid Annotations using Subsystems Technology
MMO	Methane monooxygenase
MOB	Methane oxidising bacteria
MPN	Most Probable Number (of viable cells in a culture)
NAD^+	Nicotinamide adenine dinucleotide (oxidised)
NADH	Nicotinamide adenine dinucleotide (reduced)
NAG	N-acetylglucosamine
NAM	N-acetylmuramic acid
NaOH	Sodium hydroxide
NCBI	National Center for Biotechnology Information
ND	Not determined
NGM	Ngatamariki
NMS	Nitrate mineral salts media
OD	Optical density
OH	Hydroxyl
OKO	Orakei Korako
OTU	Operational taxonomic unit
PCoA	Principal Coordinates Analysis
PLFA	Phospholipid-derived fatty acids
pMMO	Particulate (membrane-bound) methane monooxygenase
PQQ	Pyrroloquinoline quinone
PVC	*Planctomycetes-Verrucomicrobia-Chlamydiae* superphylum
pXMO	Alternative particulate methane monooxygenase
R^2	Coefficient of determination for linear regression
RCP	Reducing compound photometer
REE	Rare earth elements; lanthanum, cerium, praseodymium and neodymium

ROS	Reactive oxygen species
RO	Reverse osmosis
r.p.m.	Revolutions per minute
RTK	Rotokawa
RT-PCR	Reverse transcription-polymerase chain reaction
RuBisCO	Ribulose-1,5-bisphosphate carboxylase/oxygenase
RuMP	Ribulose monophosphate pathway
SIMS	Secondary ion mass spectrometry
SIP	Stable isotope probing
sMMO	Soluble methane monooxygenase
SOD	Superoxide dismutase
TCD	Thermal conductivity detector
Tg	Teragram=megatonne=10^{12} grams
TKA	Te Kopia
TKT	Tikitere
T_{max}	Maximum temperature for growth
TMCS	Trimethylchlorosilane
TOK	Tokaanu
T_{opt}	Optimum temperature for growth
TPM	Transcripts per million
TPS	Trehalose-6-phosphate synthase
Tris	Tris(hydroxymethyl)aminomethane
TSA	Transcriptome shotgun assembly
TSB	Tryptic soy broth
TVZ	Taupō volcanic zone
USC	Upland soil cluster
V_{max}	Maximum rate for reaction
WAM	Waimangu
WAP	Waipahihi
WFPS	Water filled pore spaces
WHV	Whakarewarewa Village
WKT	Waikite Valley
WTV	Wairakei Thermal Valley

Gene abbreviations used in KEGG metabolism pathway maps

ACDS	Acetyl-CoA decarbonylase/synthase complex
AmoCAB	Methane/ammonia monooxygenase subunits
AnfG	Nitrogenase delta subunit
COX11, COX15	Cytochrome *c* oxidase assembly protein subunits
CoxA-D	Cytochrome *c* oxidase subunits
CydABX	Cytochrome bd ubiquinol oxidase subunits
CyoA-E	Heme o synthase subunits
Cyt b and Cyt 1	Cytochrome *c* reductase b/c1 subunits
Hao	Hydroxylamine dehydrogenase
Hdh	Hydrazine dehydrogenase
HoxEFU	Bidirectional [NiFe] hydrogenase diaphorase subunits
Hzs	Hydrazine synthase
ISP	Cytochrome *c* reductase iron-sulfur subunit
MtaA	[methyl-Co (III) methanol-specific corrinoid protein]:coenzyme M methyltransferase
MtaB	Methanol---5-hydroxybenzimidazolylcobamide Co-methyltransferase
MtaC	Methanol corrinoid protein
MtbA	[methyl-Co(III) methylamine-specific corrinoid protein]:coenzyme M methyltransferase
MtbB	Dimethylamine---corrinoid protein Co-methyltransferase
MtbC	Dimethylamine corrinoid protein
MtmB	Methylamine---corrinoid protein Co-methyltransferase
MtmC	Monomethylamine corrinoid protein
MttB	Trimethylamine---corrinoid protein Co-methyltransferase
MttC	Trimethylamine corrinoid protein
NapAB	Periplasmic nitrate reductase
NarB	Ferredoxin-nitrate reductase
NarGHI	Nitrate reductase / nitrite oxidoreductase subunits
NasAB	Assimilatory nitrate reductase subunits
NdHA-N	NAD(P)H-quinone oxidoreductase subunits
NifDKH	Nitrogenase molybdenum-iron protein

NirA	Ferredoxin-nitrite reductase
NirBD	Nitrite reductase (NADH) subunits
NirK	Nitrite reductase (NO-forming)
NirS	Nitrite reductase (NO-forming) / hydroxylamine reductase
NIT-6	Nitrite reductase (NAD(P)H)
NorBC	Nitric oxide reductase subunit
NosZ	Nitrous-oxide reductase
NR	Nitrate reductase (NAD(P)H)
NrfAH	Nitrite reductase (cytochrome c_{552}) subunits
NuoA-N	NADH-quinone oxidoreductase subunits
NxrAB	Nitrate reductase / nitrite oxidoreductase subunits
QoxA-D	Cytochrome aa_3-600 menaquinol oxidase subunits
SdhA-D and FrdA-D	Succinate dehydrogenase / fumarate reductase, flavoprotein subunits

1. Literature Review

1.1 Introduction

Methane (CH_4) is a potent greenhouse gas, of both anthropogenic and natural origin, which plays an important role in global warming. Methane is 25 times more effective at absorbing infra-red radiation than carbon dioxide [1], and is predicted to be responsible for up to 47 % of the global temperature response to greenhouse gases over a ten-year period [2]. The global methane budget is ~ 500-600 Tg per year; with the majority of methane produced via anaerobic methanogenic archaea [3] and often associated with carbon sources under human management such as ruminant animals, rice fields, sewage treatment facilities and landfills. Wetland environments are the major source of non-human-associated methane emissions, accounting for the release of up to 284 Tg per year [4]. Geothermal emissions of geologic methane, produced from magma and lithosphere degassing (Figure 1.1), also contribute to the global methane budget. Microseepages, mud volcanoes and other geological sources emit 33 to 75 Tg per year [4, 5]. Other high temperature environments with sizable methane emissions include natural gas fields (up to 95 % methane of total gas emitted [6]); oil reservoirs (up to 95 % methane [7]); deep subsurface fracture water within mines (up to 5.15 % methane [8]; and permanently burning coal fires (up to 0.6 % methane [9]) (all v/v).

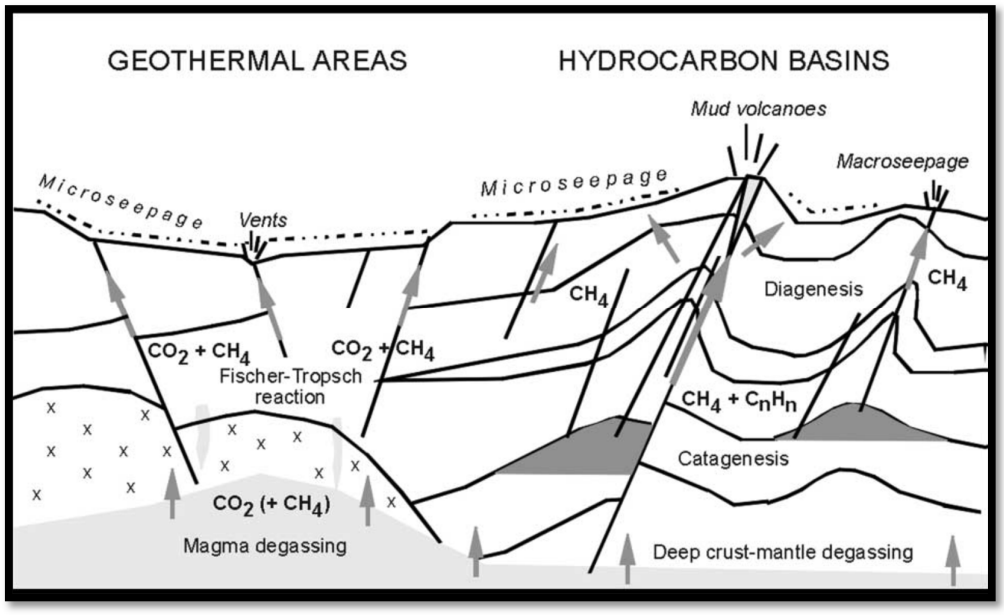

Figure 1.1 Sketch of geologic methane production and release. Taken from [10].

Geothermal systems often release high volumes of methane, principally via the Fischer-Tropsch reaction (conversion of carbon monoxide and hydrogen to methane and other hydrocarbons) and magmatic degassing (Figure 1.1) [10]. In some cases, the methane content in geothermal gases can be significant, for example emissions from Awakeri in the Bay of Plenty, New Zealand contained up to 27 % (v/v) methane [11]. However, methane emissions are highly variable; the methane emissions from a range of geothermal soils in Italy varied from 0.008 to 43 kg per day [12].

1.2 Abiotic and biotic methane consumption

Methane emissions can be consumed during biotic and abiotic pathways. The largest sink for methane degradation is via photochemically-induced oxidation with hydroxyl radicals ($^{\bullet}OH$) present in the troposphere [3]. This process removes ~ 80 % of the methane that reaches the atmosphere; while the remaining 20 % either diffuses into the stratosphere or is consumed by microorganisms that oxidise methane (methanotrophs), in approximately equal proportions [13]. There are two primary methanotrophic phenotypes that are distinguishable on the basis of the terminal electron acceptor utilised; aerobic methanotrophs that employ oxygen as the terminal electron acceptor in their metabolic pathways, and anaerobic methane oxidisers that employ alternate electron acceptors such as sulfate or nitrate [3].

Both aerobic and anaerobic methane oxidisers often inhabit marine and terrestrial settings where they effectively act as biofilters and reduce the total methane flux to the atmosphere [14]. Aerobic methanotrophic bacteria (methanotrophs) are the principle oxidisers of methane diffusing to the atmosphere [13]. A total of 72 aerobic methanotrophs have been characterised from 31 genera (a full list of methanotrophic isolates is available in Extended Data Set 1), distributed between the phyla *Proteobacteria* and *Verrucomicrobia*.

Anaerobic methane oxidising archaea (ANME) use alternative terminal electron acceptors, such as iron or manganese [15], sulfate [16], or nitrate [17]. Currently, ANME have not yet been fully isolated [18]. There has also been speculation that members of the *Bathyarchaeota* may be involved in a dissimilatory methane-

oxidising process [19], although metagenomic sequencing of consortia containing either *Bathyarchaeota* [20] or the closely related phylum *Verstraetearchaeota* [21] suggests that strains from these phyla may instead be responsible for methylotrophic methanogenesis (production of methane from methanol and methylated compounds). Of the anaerobic methane oxidising bacteria, *Methylomirabilis oxyfera* and *M. sinica* are proposed to employ a metabolic process whereby the reduction of nitrate (and the intracellular conversion of nitric oxide to dinitrogen and oxygen) is coupled to an aerobic methane oxidation pathway [22]. This review will focus on aerobic methanotrophs, as ANME are mainly found in marine environments [23], although some have been identified in mesophilic freshwater and paddy soil samples [24].

1.3 Methanotrophs

All characterised aerobic methane oxidising bacteria to date belong to the phyla *Proteobacteria* and *Verrucomicrobia*, and represent only a limited number of species (a full list of phenotypic characteristics of methanotrophic isolates is available in Extended Data Set 1). Most isolates are obligate methanotrophs, exclusively dependent on methane or methanol as their sole carbon and energy source. However, in contrast to the proteobacterial methanotrophs that assimilate carbon as via one of two pathways (RuMP or Serine – discussed in detail below), verrucomicrobial isolates use methane only for energy generation and assimilate carbon dioxide (CO_2) into biomass using the Calvin-Benson-Bassham (CBB) pathway [25, 26].

The scope of known carbon and energy substrates in methanotrophs is currently expanding. Some members of the *Beijerinckiaceae* family (*Alphaproteobacteria*) including *Methylocapsa aurea* [27] and *Methylocystis bryophila* [28] strains are "limited facultative" [29] and can oxidise acetate. *Methylocella* strains are defined as facultative, as they can also oxidise pyruvate, succinate, malate and ethanol [30], and even propane [31]. In moderately acidic environments (> pH 3.5), where these strains have been found, organic acids such as acetate (pKa 4.76) and succinate (pKa 4.16) are deprotonated. Below pH 3.5, many organic acids become protonated and diffuse across the plasma membrane, depleting the proton gradient [32]. Relatively low concentrations (< 50 μM) of organic acids in soil or in

laboratory media could therefore lead to acidification of the cytosol [33], which may explain why the obligately acidophilic methanotrophic *Verrucomicrobia* strains cannot oxidise organic acids. However, *Methylacidiphilum fumariolicum* SolV [34] and *M. infernorum* RTK17.1 [35] grow hydrogenotrophically and/or mixotrophically, using both methane and hydrogen as energy sources.

Methanotrophs are part of a wider guild of microorganisms, known as methylotrophs, which use reduced carbon substrates with no carbon-carbon bonds [36]. These substrates include methanol, methylated amines, halogenated methane, and methylated sulfur species such as dimethylsulfoniopropionate (DMSP). Aerobic methylotrophs are more phylogenetically diverse than methanotrophs, with representatives from the phyla *Firmicutes* [36], *Actinobacteria* [37], *Bacteroidetes* [38], *Chloroflexi* [39], and *Deinococcus-Thermus* [40], as well as other *Proteobacteria* genera [37].

Aerobic methanotrophs have specialised metabolic pathways in order to catabolise C1 compounds. Methanotrophs express either a soluble or a membrane-bound variant of the methane monooxygenase enzyme (sMMO or pMMO; more information can be found in the section *Methane monooxygenase*) in order to catalyse the oxidation of methane to methanol, which in turn is oxidised to either formaldehyde [41] or, in the verrucomicrobial species, *M. fumariolicum*, to formate [42] via methanol dehydrogenase. Some formaldehyde is assimilated into biomass through the ribulose monophosphate (RuMP) or serine pathways [36], while the remainder is terminally oxidised into carbon dioxide for respiratory energy production (Figure 1.2).

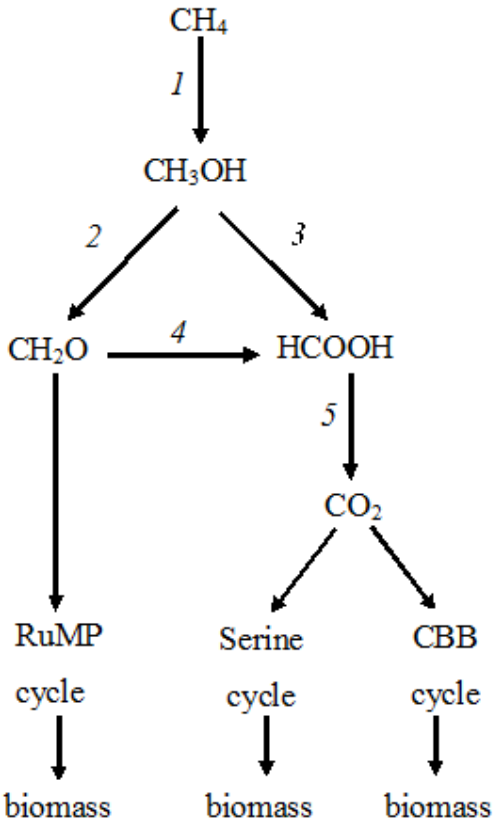

Figure 1.2 Schematic of C1 compound metabolic pathways in aerobic methanotrophs. *1*, particulate or soluble methane monooxygenase; *2*, methanol dehydrogenase enzymes; *3*, methanol dehydrogenase in *M. fumariolicum*; *4,* formaldehyde oxidation systems; *5*, formate dehydrogenase enzymes. RuMP, Ribulose monophosphate; CBB, Calvin-Benson-Bassham. Only some verrucomicrobial methanotrophs fix carbon via the CBB cycle pathway.

Before the discovery of the verrucomicrobial methanotrophs in 2007 [14, 43], methane oxidising bacteria were divided into two groups; Type I (*Gammaproteobacteria*) and Type II (*Alphaproteobacteria*) [44, 45]. This classification was based on phenotypic characteristics; Type I methanotrophs were defined as containing bundles of intracytoplasmic discs throughout the cell and using the ribulose monophosphate (RuMP) pathway for carbon assimilation; whereas Type II methanotrophs displayed intracytoplasmic membranes (ICM) on the cell periphery, used the serine pathway for carbon assimilation and could fix nitrogen [46]. In addition, their average genomic %mol G+C content was higher than Type I methanotrophs (60-67 mol%, compared to 43-65 mol%) [47].

Although still useful as general observations for groups within *Proteobacteria*, in recent years expanded isolation and characterisation efforts of novel methane oxidising bacteria has revealed that these criteria are no longer entirely accurate. For example, some members of the *Gammaproteobacteria* Type I group (*Methylosphaera*, *Methylosoma*, *Methylogaea* and *Methylococcus*) were found to fix nitrogen despite Type I methanotrophs being originally believed to be incapable of diazotrophy [46]. Similarly, the location of intracytoplasmic membranes is variable within the Type II genera *Methylocella* and *Methylocapsa* [48] where they were previously considered only peripheral. In addition, the gammaproteobacterium *Crenothrix polyspora*, which is closely related to *Methylosoma difficile* [49], may be capable of facultative methanotrophy, a trait previously attributed only to Type II methanotrophs. Enrichment cultures containing 99 % *C. polyspora* were shown to not only oxidise methane, but also assimilate acetate and glucose [50].

Type II methanotrophs are more tolerant to environmental stress such as nitrogen limitation, hypoxia, or periods of substrate (CH_4) starvation [46, 51, 52]. With respect to methane limitation, the serine pathway of carbon assimilation uses one molecule of carbon from both formaldehyde (derived from CH_4) and CO_2 to synthesise acetyl CoA; whereas in the RuMP pathway all the carbon is derived from methane. It is speculated that this gives Type II methanotrophs a competitive advantage over Type I strains in environments where methane availability may be periodically limiting [53].

In contrast, the verrucomicrobial methanotrophs exhibit electron dense structures that may be membrane vesicles or carboxysome-like protein structures [47] that differ in appearance from either Type I or Type II intracytoplasmic vesicles, except in *Methylacidimicrobium fagopyrum*, which has stacks of ICM. The RuMP and serine pathways are largely absent [54], and only two species, *Methylacidiphilum kamchatkense* Kam1 [55] and *Methylacidiphilum infernorum* V4 [14] fix dinitrogen (N_2). *Methylacidiphilum* strains have much lower G+C values than the *Methylacidimicrobium* isolates: (40.8 – 45.5 mol%, compared to 60.9- 63.8 mol%).

1.3.1 Thermophilic methanotrophs

The majority of described methanotrophs are mesophilic, growing optimally between 10 and 35 °C [45], and at circum-neutral pH (Extended Data Set 1). For the purposes of this review, methanotrophs will be classified as either mesophilic, thermotolerant or thermophilic (Table 1.1) on the basis of their reported growth temperature optima and maxima, as defined by Schlegel [56].

Table 1.1 Methanotroph growth temperature classification.

	Mesophilic	Thermotolerant	Thermophilic
Temperature optima and maxima	T_{opt} 20-42 °C	not given	T_{opt} > 40 °C
	T_{max} < 42 °C	T_{max} < 50 °C	T_{max}< 70 °C

There are currently 15 isolated methanotrophs that are thermophilic (T_{opt} > 40 °C and T_{max} < 70 °C). These have been isolated from hot springs in Japan [57], Hungary [58, 59] and Russia [55], and warm soil or mud in New Zealand [14], Italy [43] and Russia [60] (Table 1.2). Currently, the highest recorded growth temperature for a methanotroph, *Methylothermus thermalis*, is 67 °C [57]. Previously another *Methylothermus* species, "*Methylothermus* strain HB" was enriched and isolated from a Hungarian hot spring with a reported maximum growth temperature of 72 °C [59]. This strain, however, was difficult to maintain and is no longer extant.

Table 1.2 Characteristics of thermophilic and thermotolerant aerobic methanotrophic isolates. Thermotolerant strains are highlighted with *

Taxonomy	Isolation sites	Temperature range (optimum) (°C)	pH range (optimum)	Morphology	Internal membrane structures	sMMO	C_1 assimilation pathway	N_2 fixation	Major PLFA (>15% of total)	DNA G+C mol%	References
Alphaproteobacteria											
Methylocystis											
sp. "Se48"*	Hot spring, Russia	15-53 (37)	5.0-7.5	Vibrioid	Type II ICM	-	serine	+	18:1ω7c, 18:1ω9c	62.0	[61]
Gammaproteobacteria											
Methylothermus											
M. subterraneus	Hot spring, Japan	37-65 (55-60)	5.2-7.5 (5.8-6.3)	Coccoid	Type I ICM	-	RuMP	-	16:0, 18:1ω7c	54.4	[62]
M. thermalis	Hot spring, Japan	37-67 (57-59)	6.5-7.5 (6.8)	Coccoid	Type I ICM	-	RuMP	-	16:0, 18:1ω7c	62.5	[57]
sp. "HB"	Hot spring, Hungary	40-72 (55-62)	ND	Coccoid	ND	-	ND	ND	ND	ND	[59]

Taxonomy	Isolation sites	Temperature range (optimum) (°C)	pH range (optimum)	Morphology	Internal membrane structures	sMMO	C_1 assimilation pathway	N_2 fixation	Major PLFA (>15% of total)	DNA G+C mol%	References
Methylomarinovum											
M. caldicuralii	Hydrothermal sediment, Japan	30-55 (45-50)	5.3-6.9	Coccoid or rod	Type I ICM	-	RuMP	-	16:0, 18:1ω7c	66.0	[63]
Methylococcus											
*M. capsulatus**	Sewage sludge, USA	28-55 (37)	5.5-8.5	Coccoid	Parallel ICM	+	RuMP	+	16:0, 16:1 ω7c	62.5	[45, 64]
M. thermophilus	Mud, Russia	37-62 (50-56)	ND	Coccoid	Parallel ICM	ND	RuMP	-	16:0, 16:1 ω7c, *cy*17:0	63.3	[45, 60]
Methylocaldum											
M. gracile	Soil, Russia	20-47 (42)	(6.8)	Coccoid or rod	ND	ND	RuMP, serine	-	16:1ω5t	59.0	[58, 60, 65]
*M. marinum**	Hydrothermal sediment, japan	20-47 (36)	6.0-8.0 (7.0)	Coccoid or rod	ND	+	RuMP, serine	-	16:0, 16:1ω7c	59.7	[66]

Taxonomy	Isolation sites	Temperature range (optimum) (°C)	pH range (optimum)	Morphology	Internal membrane structures	sMMO	C_1 assimilation pathway	N_2 fixation	Major PLFA (>15% of total)	DNA G+C mol%	References
M. szegediense	Hot spring, Hungary/ compost, Germany	37-62 (55)	(6.8)	Coccoid or rod	ND	-	RuMP	-	ND	56.5	[58, 67]
M. tepidum	Soil, UK	30-47 (42)	(6.8)	Coccoid or rod	ND	-	RuMP	-	ND	57.2	[58]
sp. "H-11"	Manure, Russia	30-59 (55)	6.0-8.5 (7.1)	Rod	Type I ICM	-	RuMP, serine	ND	16:0	58.5	[68]
sp. "O-12"	Silage, Russia	30-61 (55)	6.0-8.5 (7.2)	Rod	Type I ICM	-	RuMP, serine	ND	16:0	58.5	[69]
sp. "BFH1"	Soil, Bangladesh	30-60 (51-55)	4.2-7.5 (5.5-6.0)	Coccoid	Type I ICM	-	ND	+	16:0	62.7	[70]
sp. "BFH2"	Soil, Bangladesh	30-60 (51-55)	4.5-7.5 (5.5-6.0)	Coccoid	Type I ICM	-	ND	+	ND	62.7	[70]

Taxonomy	Isolation sites	Temperature range (optimum) (°C)	pH range (optimum)	Morphology	Internal membrane structures	sMMO	C_1 assimilation pathway	N_2 fixation	Major PLFA (>15% of total)	DNA G+C mol %	References
Verrucomicrobia											
Methylacidiphilum											
M. fumariolicum	Geothermal soil, Italy	40-65 (55)	0.8-5.8	Rod	Electron dense inclusions	-	CBB	-	18:0, *a*15:0	40.8	[43, 47]
M. infernorum	Geothermal soil, New Zealand	40-60 (60)	1.0-6.0 (2.0-2.5)	Rod	Electron dense inclusions	-	CBB	+	18:0	45.5	[14, 47]
M. kamchatkense	Hot spring, Russia	37-60	2.0-5.0	Rod	Electron dense inclusions	-	CBB	+	*a*15:0, *i*14:0	ND	[47, 55]

*, thermotolerant; ND, not determined; +, positive; -, negative; ICM, intracytoplasmic membranes; RuMP, ribulose monophosphate pathway; CBB, Calvin-Benson-Bassham pathway; PLFA, phospholipid-derived fatty acids. All species were positive for pMMO.

1.3.2 Methane monooxygenase

All known aerobic methanotrophs encode at least a single methane monooxygenase enzyme; which catalyses the energy-dependent oxidation of methane to methanol. Methane monooxygenase enzymes may be membrane-bound (particulate form, pMMO) or cytoplasmic (soluble form, sMMO), with the two enzyme forms not sharing sequence or structural homology, requiring different reductants (Figure 1.3) and are unlikely to have arisen through lateral gene transfer and subsequent evolution [71]. The reductant required for pMMO catalysis may be cytochrome c [46] or a type 2 NADH:quinone oxoreductase (NDH-2) [72], whereas sMMO catalysis uses NADH as the reductant [73].

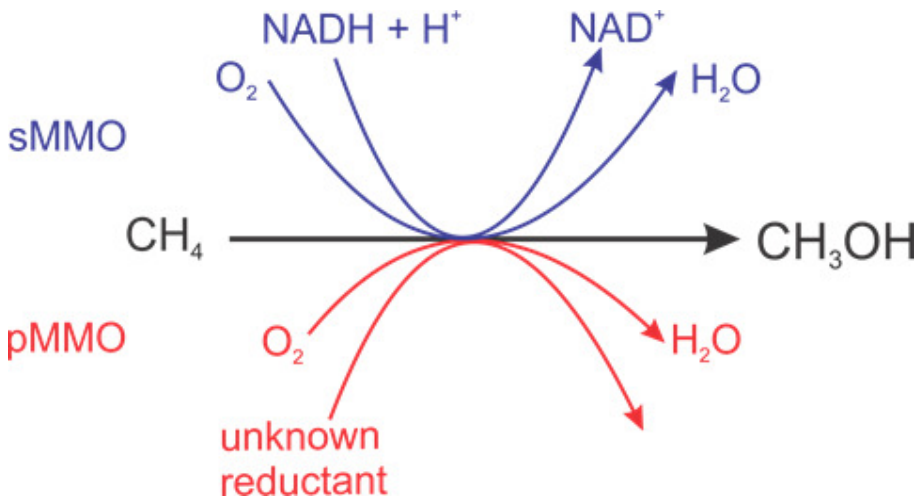

Figure 1.3 Schematic of the two known methane oxidation pathways in aerobic bacteria. Blue, soluble MMO pathway; red, particulate MMO pathway.

The pMMO, which contains copper, and possibly iron [74], is found in the cytoplasmic membrane of almost all methanotrophic isolates, with the exception of *Methylocella* and *Methyloferula* strains, which express only sMMO [48]. Membrane-bound MMO (pMMO) has a greater affinity for methane, but slower reaction kinetics [75], than sMMO, an iron-containing enzyme. Soluble MMO is only expressed in the cytoplasm by a small number of described methanotroph isolates and typically only under conditions of copper deficiency [76].

Methanotrophs that express both forms of MMO typically utilise a "copper-switch", consisting of methanobactin, which has a high affinity for binding to copper ions, and the polypeptide MmoD [77]. MmoD is encoded as part of the sMMO operon and controls differential expression of the pMMO and sMMO operons during conditions of either high or low copper availability. In the absence of copper, methanobactin will bind a variety of transition and near-transition elements [78], protecting the host from metal toxicity.

The activities of both pMMO and sMMO are non-specific [79-81] with ammonia, carbon monoxide, and a range of alkanes, alkenes and aromatics serving as possible substrates for oxidisation; although with no net energy gain to the bacterium [77]. Several studies have investigated the use of methanotrophs for bioremediation with their ability to degrade pollutants such as chlorinated solvents [75, 82-84]. Following the methane oxidation step are sequential energy-generating dehydrogenase reactions that oxidise methanol through formaldehyde and/or formate and finally to carbon dioxide.

1.3.3 Thermal Adaptations

Thermophilic *Bacteria* and *Archaea* require specific adaptations of cell components to survive at high temperatures. These may include protein composition and structure [85, 86], lipid membrane composition [87], synthesis and accumulation of small organic compounds [88-90], and responses to reactive oxygen species [85, 91]. Thermally stable proteins may have a higher optimum temperature for activity than their counterparts from mesophilic organisms. For example, formate dehydrogenase, hexulose phosphate synthase, and hydroxypyruvate reductase from *M. szegediense* O-12, which are all involved in carbon assimilation using either the serine or RuMP pathways, have higher temperature optima than those from *M. capsulatus* or *M. echinoides* 2 [85].

With respect to methane oxidation, the sMMO in a strain closely related to *M. capsulatus* is stable for one hour following heat shock at 60 °C [92]. Although there are no reports on the potential thermal stability of pMMO, the enzyme shares high homology to ammonia monooxygenase [93], and the ammonia-

oxidising archaeon, *Candidatus* “Nitrosocaldus yellowstonii”, grows at up to 74 °C. This finding suggests that the structurally similar pMMO may also be stable at high temperatures. Subsequent enzymatic reactions catalysing the conversion of methanol to formaldehyde or formate via methanol dehydrogenase have been widely studied in other bacteria and do not appear to be restricted by temperature.

There are many facultative methanol-oxidising, aerobic bacteria able to grow at elevated temperatures [38-40], which suggests that methanol dehydrogenases and other enzymes within carbon assimilation pathways are stable at high temperatures. NAD-dependent methanol dehydrogenases, such as those found in *Bacillus methanolicus*, actually become more active at higher temperatures [94]. Many different metabolic pathways exist for the oxidation of formaldehyde, from single-enzyme systems (e.g. glutathione-dependent formaldehyde dehydrogenase) to much more complex systems involving several enzymes (e.g. tetrahydromethanopterin- and tetrahydrofolate-linked pathways) [95, 96], but there is little information available on the heat stability of these enzymes.

Some thermostable proteins have significant amino acid substitutions from their mesophilic counterparts, including increases in charged amino acid residues (e.g. arginine) and residues with side chains (e.g. alanine, isoleucine and glutamine) [86]. RuBisCO enzymes found in thermophilic bacteria and hyperthermophilic archaea, are more thermally stable than the homologous enzymes from mesophiles; through amino acid substitutions of alanine, isoleucine and glutamine; or by forming a decameric structure by interactions between glutamic acid, arginine and asparagine residues [97, 98]. It is likely that the homologs of RuBisCO found in the thermophilic strains of *Methylocaldum* [99], *Methylococcus* [99], and *Methylacidiphilum* [34] will also contain similar substitutions, although these have not yet been investigated.

Another common adaptation to high temperatures by thermophilic microorganisms is a change in lipid composition, e.g. chain length. Long chain fatty acids are frequently found in the lipid membranes of thermophiles, as

longer length chains have higher melting points [87]. However, thermophilic methanotrophs do not appear to adhere to this rule, as the *Methylacidiphilum* strains produce predominantly 18:0 fatty acids, but also high proportions of *a*15:0 and *i*14:0, while some *Methylocaldum* strains produce 16:1ω7c. *Methylococcus* strains synthesise various hopanoids [100] and sterols [101], which may stabilise cell membranes at increased temperatures, by maintaining core membrane rigidity while allowing lipid bilayer head groups to remain fluid [102].

Microorganisms may respond to the thermal stress induced by rising temperatures in a number of other ways. As growth temperatures rise, the number of reactive oxygen species (ROS) such as superoxide anions (O_2^-, a by-product of oxygen metabolism) and hydrogen peroxide (H_2O_2, produced through the action of the RuBisCO oxygenase) also increase. *M. szegediense* O-12 and *M. capsulatus* respond to this oxidative stress by increasing levels of cytochrome c peroxidases, which reduce H_2O_2 to water. However, the activities of superoxide dismutase (SOD), which catalyses the disproportionation reaction of superoxide anions to water and hydrogen peroxide, were independent of growth temperature in both strains [85]. In addition, *Methylomonas* species synthesise carotenoids [91] that both scavenge ROS [103] and reinforce lipid bilayer stability [104].

Thermophilic bacteria accumulate compatible solutes or thermolytes, such as polyamines, sucrose, α -glutamate, di-myo-inositol phosphate or hydoxyectoine, in response to both osmotic and heat stress [88-90]. *M. szegediense* O-12 accumulates sucrose as the growth temperature increases, reaching a maximum of 1.2 % at 57 °C [85]. The enzyme lactate dehydrogenase from this isolate was shown to be stabilised at high temperatures when preheated in the presence of sucrose. Other thermophilic methanotrophs may have similar adaptations to those outlined above, or may have evolved entirely new methods of adapting to high-temperature environments. Transcriptional responses to heat stress have not yet been investigated in methanotrophs, although the transcriptomes of *Methylocystis* SC2 cultures under salt stress [105] and *Methylacidiphilum fumariolicum* under

nitrosative and oxidative stresses [106] have been studied.

1.4 Genes for detecting methanotrophs

Microorganisms that can be cultivated in a laboratory are thought to be only a small subset of total microbial diversity [107], due to the difficulty in replicating environmental conditions [108]. Culture-independent techniques, such as sequencing DNA from environmental samples, are necessary to identify unculturable microbes, to understand their phylogeny, and to investigate their potential effects on biogeochemical cycles [109, 110].

1.4.1 Particulate methane mono-oxygenase

The *pmoCAB* operon, which encodes for pMMO, is found in multiple copies in most methanotrophs [111] and there is evidence that the different homologs possess different affinities for methane and may be differentially expressed. In *Methylocystis* SC2, the conventional pMMO is only expressed and oxidising methane when cells are exposed to more than 600 ppmv methane, while a second pMMO isozyme, encoded by *pmoCAB2*, is expressed constitutively and oxidises methane at near atmospheric concentrations (1.75 ppmv) [112]. The expression of *pmoCAB2*, but not *pmoCAB1*, was significantly downregulated in the presence of ammonia [113] In *M. kamchatkense*, the *pmoCAB2* operon is transcribed at levels up to 1000-fold greater than the two other *pmo* operons during growth on methane, but conversely, expression is downregulated ten-fold when cells are grown on methanol [114].

The α-subunit of pMMO, encoded by *pmoA*, is structurally similar to that of ammonia monooxygenase (AMO) and shares a similar range of catalysable substrates; although with differing affinities. The genes *pmoA* and *amoA* share high levels of nucleotide homology [93], with the PmoA of methanotrophs from *Alpha-* and *Gammaproteobacteria* clustering phylogenetically with the AmoA of ammonia oxidising bacteria (AOB) from *Gammaproteobacteria*, and some verrucomicrobial PmoA clustering with AmoA from *Thaumarchaeota* [115] (Figure 1.4). Interestingly, the *pmoA* sequence of the anaerobic methane oxidising bacterium, *M. oxyfera*, was divergent from other known sequences, but signature residues were conserved, including those surrounding the ligand

to the zinc centre of pMMO [22, 116]. In phylogenetic analyses, the *M. oxyfera* *pmoA* gene clustered more closely with *pmoA* sequences from uncultured soil methanotrophs and verrucomicrobial methanotrophs than proteobacterial *pmoA*s [22]. Finally, some methanotrophs within the genera *Crenothrix*, *Methylobacter*, *Methylomicrobium* and *Methylomonas* also encode a second particulate methane monooxygenase (pXMO) encoded by a *pxmABC* operon [115, 117]. This enzyme is thought to be involved in methane oxidation under hypoxic conditions and coupled to respiratory nitrate reduction. Transcripts of *pxmABC* increase significantly in the presence of NO_3^-. The PxmA amino acid sequences cluster with PmoA from ethane-oxidising bacteria from a marine hydrocarbon seep [118], and to AmoA from ammonia oxidisers within *Betaproteobacteria*.

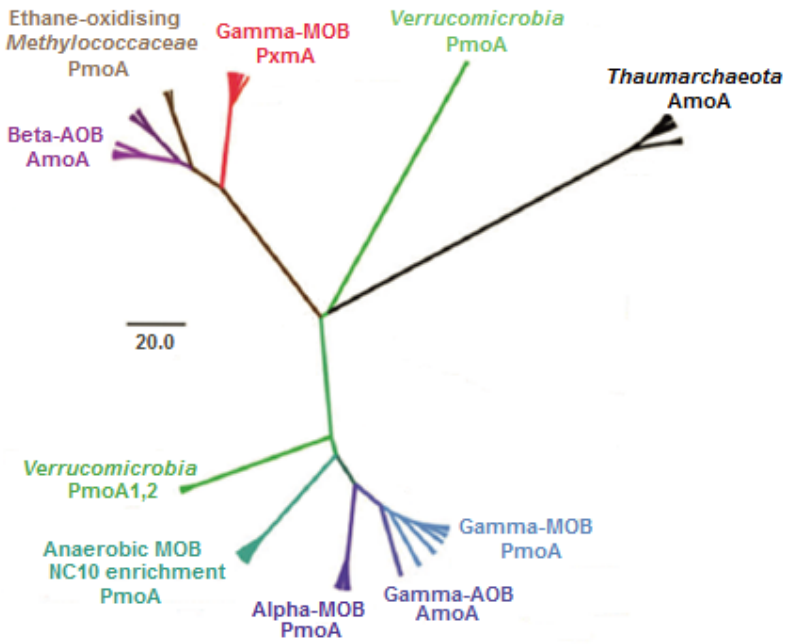

Figure 1.4 Unrooted phylogenetic consensus trees of PmoA, PxmA and AmoA protein sequences (adapted from [115]). The mean branch lengths are characterized by a scale bar indicating the evolutionary distance (changes per amino acid position).

The *pmoA* gene is often used to calculate phylogenetic relationships between methanotrophic bacteria (Figure 1.5), and this is generally in good agreement with phylogenies determined using the 16S rRNA gene (Figure 1.6) [119]. A range of PCR primers have been designed to probe for the presence of the *pmoA* gene in environmental samples for proteobacterial [58, 120, 121], verrucomicrobial [26, 122] and anaerobic methanotrophs [123]. However, the relatively high degree of sequence variation in the conserved regions (primer target sites) of the known *pmoA* genes has made the designing of universal primers for detection in environmental samples difficult, and likely means novel *pmoA* genes still remain undetected.

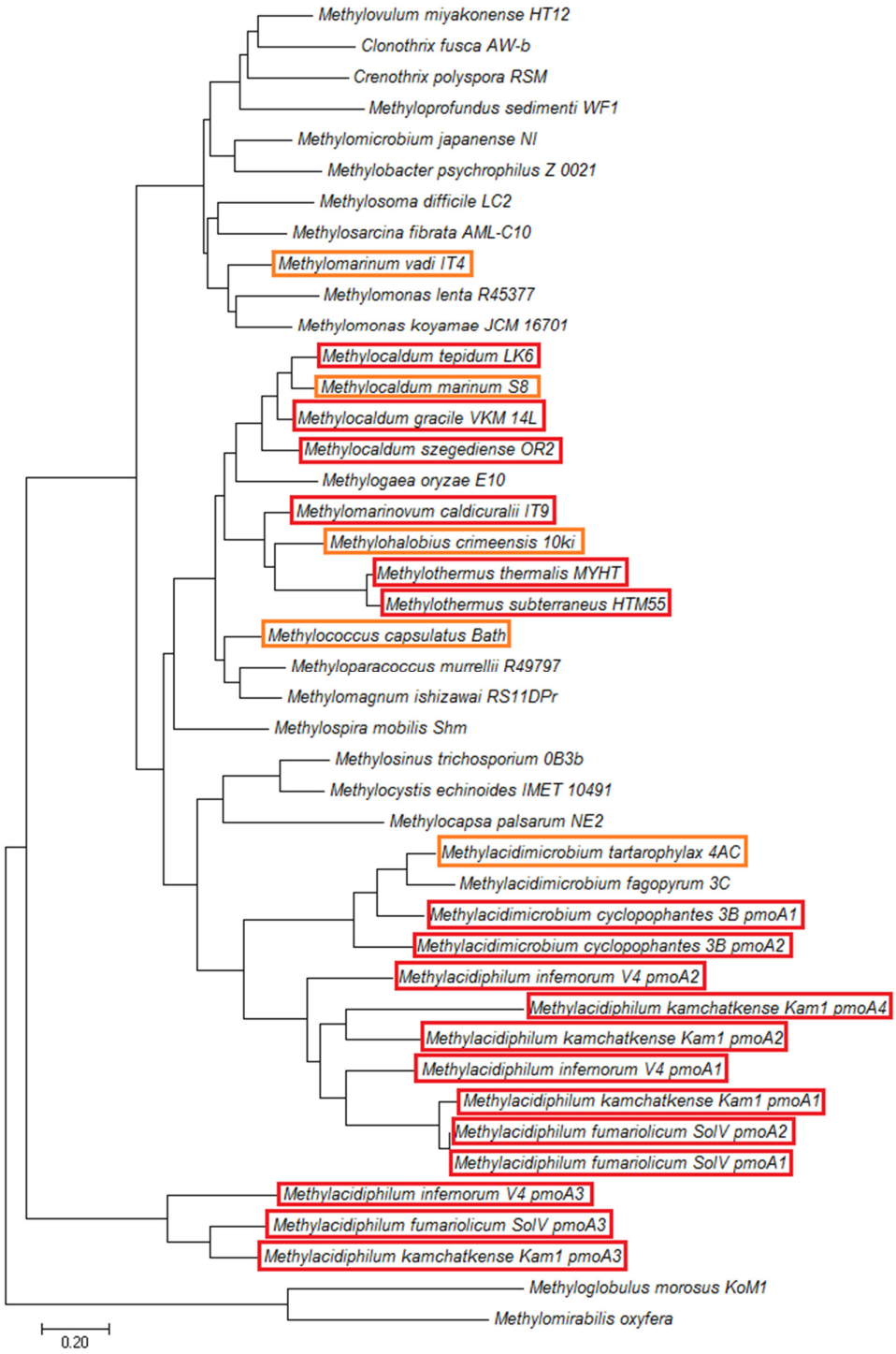

Figure 1.5 Phylogenetic relationships between known methanotrophs based on derived amino acid sequences encoded by *pmoA* genes. Thermophilic isolates are highlighted in red, thermotolerant strains in orange. The evolutionary history was inferred using Neighbour-Joining [124] and the evolutionary distances were computed using the Poisson correction method [125]. Scale bar represents 0.2 nucleotide substitutions per site. Evolutionary analyses were conducted in MEGA7 [126].

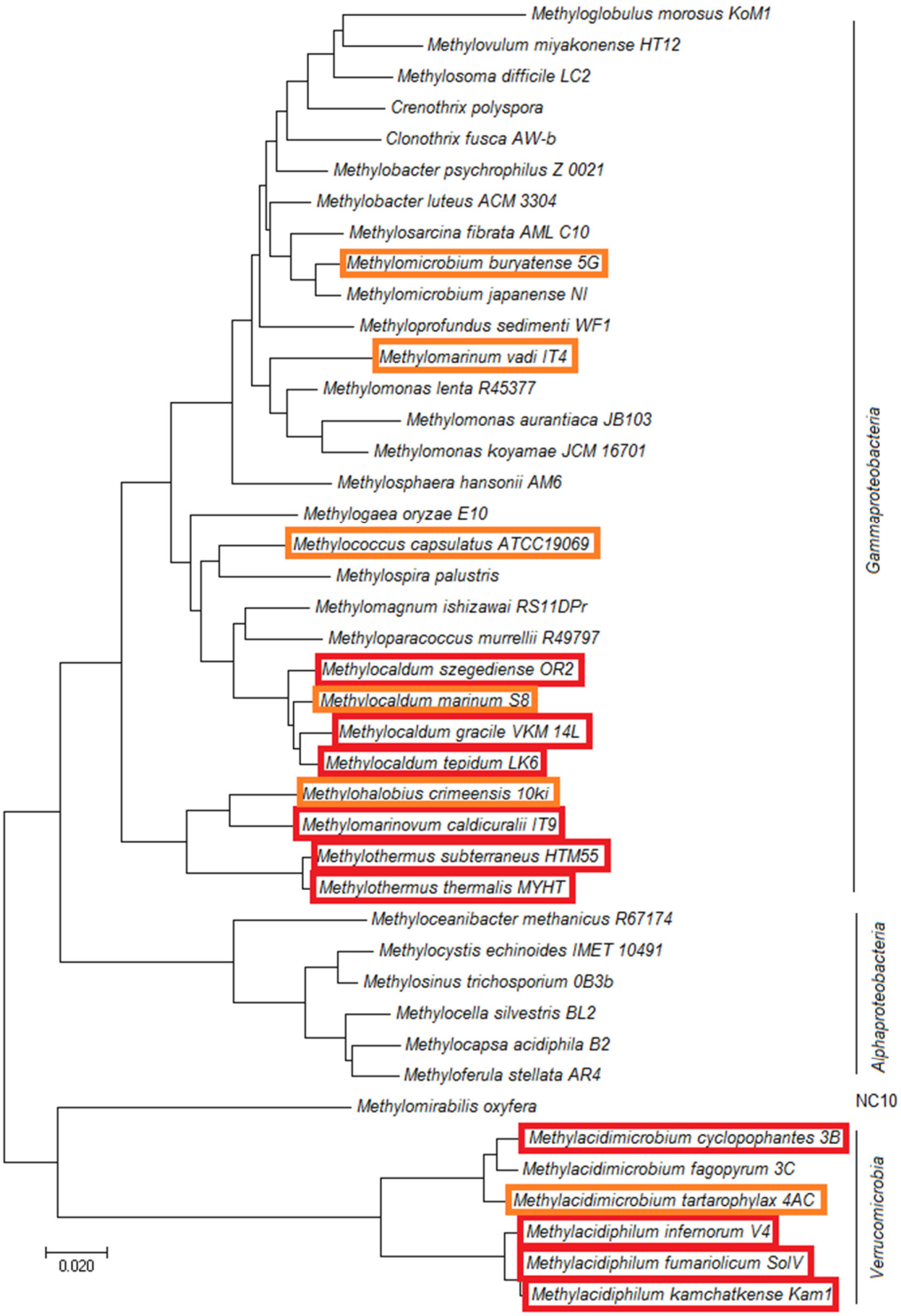

Figure 1.6 Phylogenetic tree of 16S rRNA gene sequences from aerobic methanotrophs. Thermophilic isolates are highlighted in red, thermotolerant strains in orange. The evolutionary history was inferred using Neighbour-Joining [124] and the evolutionary distances were computed using the Maximum Composite Likelihood method [127]. Scale bar represents 0.2 nucleotide substitutions per site. Made with MEGA7 [126].

The significant sequence divergence in *pmoA* genes suggests that they may have evolved from a distant common ancestor rather than as the result of recent horizontal gene transfer [78]. However, this appears to not be true for all MMO genes. The sMMO in facultative *Methylocella* strains may have been acquired via horizontal gene transfer, suggesting that the predecessor of *Methylocella* may have originally been a methylotroph, and only developed the ability to oxidise methane after the acquisition of sMMO [128]. Gene transfer may also occur in individual species; a recently discovered strain of the methylotrophic genus *Methyloceanibacter*, *M. methanicus*, has acquired sMMO and is capable of oxidising methane. In addition, the *Methylocapsa* strains *M. acidophila* and *M. aurea* both express pMMO, but only *M. aurea* shows facultative growth, suggesting that this strain may have become able to oxidise acetate through the acquisition of new genes from an acetotroph.

1.4.2 Soluble methane mono-oxygenase

The sMMO is encoded by an operon consisting of genes encoding a hydrolase element (*mmoXYZ*), reductases or regulatory elements (*mmoB* and *mmoC*), and the MMO "copper-switch" (*mmoD*) [129]. Primers have been used to detect the presence of *mmoX* [58, 130, 131], as well as *mmoC* [132] in environmental samples, and even *mmoX* genes specific to *Methylocella* species [133]. However, as most methanotrophs possess only pMMO, *mmoX* or *mmoC* primers must be used in conjunction with other genetic markers, such as *pmoA*, to determine community structure.

1.4.3 Methanol dehydrogenase

Another useful functional marker is *mxaF*, which encodes for the large subunit of a methanol dehydrogenase found in Gram-negative methylotrophs [132] and which appears to be ubiquitous in methanotrophs [134]. Many methanotrophs also possess a *xoxF* gene, an orthologue of *mxaF* [41], which encodes for a polypeptide that shares approximately 50 % amino acid identity to MxaF [135], has methanol dehydrogenase activity, and requires lanthanides as a co-factor [136]. There are at least seven clades of XoxF (XoxF1 – XoxF5, in addition to XoxF products from *Methylosinus trichosporium* and *Acidiphilium cryptum*) [41, 42] and PCR primers have been designed to target the five major

phylogenetic groups [137]. However, at least one methanotroph, *M. oxyfera*, is encodes *xoxF* genes from two different clades [42], which indicates that *xoxF* may not be a suitable proxy for phylogenetic relatedness.

1.4.4 High-throughput sequencing of methanotrophs and methanogens

Using next-generation sequencing, *pmoA s*equences from proteobacterial methanotrophs have been detected in several high temperature ecosystems; at 71.5 °C in a geothermal stream within a gold mine in Japan [138], at up to 83 °C in an Italian geothermal soil [139], from 50-100 °C in a deep sea hydrothermal chimney [140], and at up to 99 °C in hot springs in Russia [141]. Many of the retrieved *pmoA* sequences from these studies were found to be most closely related to *Methylothermus* "HB". It is worth mentioning that the Russian hot springs were situated within intertidal areas and therefore regularly experienced temperature fluctuation, possibly allowing for the growth of bacteria with lower maximum growth temperatures. Verrucomicrobial methanotroph *pmoA* sequences have been detected from geothermal soil samples in New Zealand at up to 81.6 °C [122]. However, the identification of *pmoA*, or other functional genes, does not necessarily indicate the presence of an active community of methanotrophs transcribing and translating these genes into proteins.

In some instances, the detection of *pmoA* sequences within environmental samples has been coupled to observations of methane oxidation at high temperature. For instance, geothermal soils from New Zealand incubated at 65 °C [26], hot springs in Russia at 74 °C [141], and volcanic soil from Italy at up to 80 °C [139] biologically oxidise methane. Incorporation of ^{13}C labelled methane into bacterial biomass was detected at temperatures of at least 60 °C in the Russian study [141]. Anaerobic methane oxidation has been demonstrated at up to 60 °C in cultures from hydrothermal sediments [142].

Methanogenic *Archaea* have been detected in high temperature environments; in a Japanese natural gas field at 53.1 °C [6], coal fires in Wyoming of up to 82.2 °C, and oil reservoirs at 60 °C in Western Siberia [143], 65 °C in China [144] and 75 °C off the coast of California [145]. The presence of such thermophilic methane producers suggests the intriguing possibility that these environments may also harbour populations of extremophilic methanotrophs taking advantage of an abundant energy source.

1.4.5 Transcriptomics

Although identification of specific gene sequences can identify genetic potential, (meta)transcriptomics (the analysis of mRNA transcripts), can be used to determine active methanotrophy in both pure cultures under controlled laboratory conditions, or in environmental samples. Early studies used the Reverse Transcription-Polymerase Chain Reaction (RT-PCR) on extracted mRNA to determine the expression of specific genes involved in methane oxidation, including *pmoA* in forest soils [146], landfills [147], peatland [148] and in *Methylocystis* cultures [112]; and *mmoX* in landfill [147], peatland [131] and pure cultures of *Methylococcus capsulatus* [149] and *Methylocella silvestris* BL2 [150]. More recent studies have analysed total mRNA profiles to identify differential gene expression under defined experimental conditions, such as oxygen exposure in the anaerobic *M. oxyfera* [151] and in response to ammonia availability in cultures of *Methylocystis* SC2[113].

Metatranscriptomics can be used to analyse whole community mRNA profiles. Individual reads can either be compared to a database of known sequences, such as the NCBI Transcriptome Shotgun Assembly (TSA) Database, or assembled into (near)-complete transcriptomes for individual organisms. The database approach is more rapid, but many sequences fail to match any currently available in databases, as microbial diversity is not proportionally-represented in public archives. The read mapping approach has been used to identify active methanotrophs in a hydrothermal plume [152] and those responsible for high affinity methane oxidation (HAMO) in paddy soil [52], but no metatranscriptome studies of geothermal environments specifically targeting methanotrophy have been published.

1.4.6 Other methods of identifying methanotrophic activity

Stable Isotope Probing (SIP)

Stable isotope probing is a method used to identify active microorganisms within an environmental sample, by incubating with a metabolizable substrate that has been labelled with a stable isotope that is heavier than the more commonly occurring isotope e.g. ^{13}C. The labelled substrate is taken up and incorporated into cellular biomass, which can then be separated from the "light" or unlabelled fractions by density gradient centrifugation. Identification of microorganisms can be achieved by studying labelled biomarkers such as phospholipid-derived fatty acids (PLFA) [153], DNA [154, 155], RNA [156] or proteins [157].

Early studies showed that the morphology and growth of some organisms can be adversely affected by exposure to multiple isotopes; cultures of *E. coli* B and K12 showed morphological changes and an increase in lag phase when transferred from media containing $^{2}H_2O$ to media containing H_2O, as well as vice versa [158].

As an applied ecological technique, DNA-stable isotope probing can be used to determine the genetic potential of an ecosystem when it is used in conjunction with DNA/RNA sequencing technologies (e.g. 16S RNA or functional genes). However, long incubation times are necessary to label sufficient DNA for separation and this may result in cross-feeding; with non-target microorganisms eventually assimilating the labelled by-products of initial substrate metabolism [154]. This is also true for labelling proteins, and using DNA- or protein-SIP may bias against slow-growing organisms, as labelling is directly related to the rate of synthesis or replication. Nevertheless, DNA-SIP has been used to identify active methanotrophs in environments as diverse as coal mines [159], arctic soils [160], an alkaline saline lake [37], oil sands tailings ponds [161] and peat bogs [162]. RNA sequencing, in conjunction with mRNA-SIP, has been successfully used to obtain a meta-transcriptome to detect functional methanotrophs within lake sediment [163]. In active cells, RNA synthesis occurs at a high rate, enabling more rapid labelling, and therefore reducing the need for long incubation times or increased substrate [164]. Proteins labelled

with ^{13}C, ^{15}N and ^{36}S can be identified using mass spectrometry of peptides and used to give high resolution of both species and function within environmental samples. Protein-SIP is also highly sensitive, as it requires only ~ 0.1 % of ^{13}C to be incorporated [157].

Autotrophic methanotrophs can be difficult to detect using SIP, as they do not directly assimilate $^{13}CH_4$, but experiments with $^{13}CO_2$ and DNA-SIP have detected verrucomicrobial methanotrophs in geothermal systems [26]. Studies on the intra-aerobic methanotroph *M. oxyfera* have also shown that lipids were significantly more enriched in ^{13}C after incubation with ^{13}C bicarbonate than $^{13}CH_4$ [165], suggesting this species was assimilating CO_2 into biomass via the CBB pathway.

Another radioisotope commonly used in microbial ecology studies is ^{14}C. The conversion of $^{14}CH_4$ into $^{14}CO_2$ or its assimilation into ^{14}C-labelled biomass has been used to demonstrate aerobic methane oxidation in forest soils [166, 167], lake sediments [168] and hot springs [141, 169], and the carbon conversion efficiency can be calculated by the relative proportions of the pathways [170]. The incorporation of radiolabel into biomass can be visualised using a combination of fluorescent *in situ* hybridization (FISH) and microautoradiography (MAR) [50, 171], or by exposing phosphor imaging plates [172, 173].

Fluorescent In-Situ Hybridization (FISH) has been used to identify RNA or DNA from microbial populations by using probes that hybridize specifically to target sequences [174]. The Secondary Ion Mass Spectrometry (SIMS) process, which analyses secondary C_2^- ions ejected from the target surface using a caesium ion beam, allows isotopic analysis of individual cells from within mixed consortia [175]. The two-step process was successfully used in the first evidence that anaerobic archaea (ANME-2) were capable of methane oxidation [176].

Isotope Ratio Mass Spectrometry (IRMS) can be used to analyse the ratio of stable isotopes of various compounds, allowing the detection of isotope fractionation due to microbial respiration and assimilation [177]. The technique has been used successfully to identify anaerobic methane oxidation in marine sediments [174], toluene metabolism in aquifers [178], and phenanthrene degradation in soils [179].

1.4.7 Ecological factors influencing methanotroph biogeography

The distribution and abundance of microbes will be affected by their interactions with their environment as well as with other organisms. In many environments, temperature and pH are important drivers of microbial diversity [180-182]. The abundance and fitness of aerobic methanotrophs will additionally be strongly affected by factors such as methane and oxygen availability, which, in turn, is influenced by physical characteristics of the environment such as soil mineralogy and porosity. In this section, factors that may influence the growth and survival of methanotrophs in high temperature environments are reviewed. These include influence of the soil type and structure, the availability of organic carbon, nitrogen and essential trace metals, and the solubility and availability of gases such as methane, oxygen and hydrogen.

The texture of soils and the size of their grains can be an important determinant of methane oxidation capability. Methane oxidation correlates with both very fine (< 0.06 mm) and with coarse (> 2 mm) grains [183]; coarse particles allow methane and oxygen to diffuse easily through the soil, while the time taken for induction of methane oxidation increases as the size of soil particles decreased [184]. The incorporation of fine particles within a soil matrix provides a large surface area to volume ratio for microorganisms, and allows greater access to nutrients such as potassium, calcium and phosphorus that may be essential for biological activity. However, finer soils can also be compacted more through aggregation [185] and thus will lose porosity. Bender and Conrad [184] found no correlation between soil particle size and overall methanotroph abundance. Soils that contain large amounts of clay minerals retain methane and slow diffusion of gas through the matrix [186], possibly explaining why soils with a

high clay content show greater rates of methane oxidation than soils with a high sand content [183, 187].

Soil methane consumption also appears to be influenced by seasonality [172, 188, 189]. The majority of these effects appear to be related to soil moisture content rather than soil temperature. The optimum soil water content for methanotrophs must balance the physiological requirement for water with the rapid transport of methane in the aqueous phase [190]. Soils with a larger proportion of water filled pore spaces (WFPS) will have lower methane availability, as the diffusion rate of methane is 10,000 times slower in water than in air [191]. However, very low soil humidity will also subject cells to desiccation and reduce methane oxidation [192].

The optimum water content of ambient temperature soils for methanotrophy appears to be between 9 and 22 % [184, 187, 190, 193] with a slightly higher optimum required for initial induction of methane oxidation activity [184]. This difference may reflect a resting population of methanotrophs surviving as cysts or exospores, becoming active. The response of methane oxidation activity to drying below the optimum was reported to be more sensitive than to wetting above the optimum [194]. Higher water content may also stimulate the soil methane oxidation rate by increasing the availability of other water-soluble substrates [195]. The availability of water changes soils from a net source of methane when waterlogged, to a net sink during drought conditions; in a swamp [196], a wetland [197], and peatlands [198]. This may be due to methanotrophic populations undertaking high affinity methane oxidation (HAMO), which can be induced in rice paddy soils flushed with high volumes of methane over a period of weeks. Transcripts from the soil indicated the presence of active *Methylosarcina, Methylosinus* and *Methylocystis* species [52].

The composition and size of the methanotroph community may also be affected by the mineralogy of soils. Soils with a high organic carbon content in general support fewer methanotrophs than soils with lower levels of organic matter [187, 199]. This may be due to decreased oxygen availability, as soils with a

high level of organic matter may rapidly become anoxic. In addition, Jensen *et al* [199] demonstrated that the diversity of methanotrophs was slightly higher in soils that had lower sand and more organic carbon content.

The fertilisation of soils with nitrogen, as nitrate, ammonium or urea, affects methanotroph community size and composition. At low concentrations, nitrate stimulates methane oxidation in some soils [200, 201]. Similarly, the addition of urea stimulates the growth of Type I methanotrophs in rice paddy soils [202], and ammonium added to landfill cover soils showed the same effect [203]. However, the addition of elevated concentrations of ammonium often cause a decrease in methane uptake rates [184, 190], an observation that is corroborated by experiments showing that elevated ammonium concentrations inhibits methane oxidation by the Type II methanotroph *Methylocystis* sp. strain SC2 in axenic cultures [113]. The cause of this inhibition is likely a result of two factors; firstly, because of its similar molecular structure to methane, ammonium will compete for the MMO binding site with methane [204] that in effect will reduce the flux of methane oxidised, and secondly, the intermediate products from ammonia oxidation, (particularly hydroxylamine, but also nitrite) are also toxic to methanotrophic soil microorganisms [205]. Methanotrophs may also be sensitive to ionic effects, such as an increase in osmotic potential, caused by the presence of ammonium or other salts such as K^+, Na^+ and Cl^-. KCl inhibits methanotrophic activity, although not to the same extent as the addition of NH_4Cl [194]. Methanotrophs are sensitive to ions including NO_2^-, NO_3^-, Cl^-, and Na^+, but less sensitive to K^+, HCO_3^- and SO_4^{2-}[192].

The effect of *in situ* temperature is likely to influence the abundance and activity of methanotrophs in heated ecosystems. Methane solubility in water has a parabolic-like relationship with temperature, with the minimum solubility peaking at ~ 90 °C (Figure 1.7). The solubility of methane drops about 33 % as the temperature increases from 30 to 60 °C [206]. This therefore suggests that while methane is available to microorganisms in the thermophilic temperature range (Table 1.1), accessing this methane as a substrate will be more challenging than it would be for mesophilic methanotrophs. The solubility of oxygen in pure water is inversely correlated with temperature (Figure 1.8) and

this may also restrict the growth of aerobic microorganisms, including methanotrophs, at high temperatures.

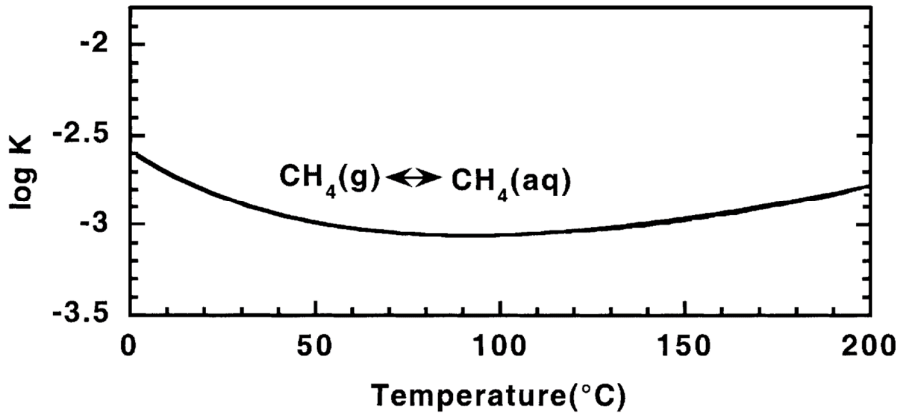

Figure 1.7 Log of the equilibrium constant (K) for the solubility of gaseous methane, plotted against temperature at the saturation pressure for water. Adapted from [207].

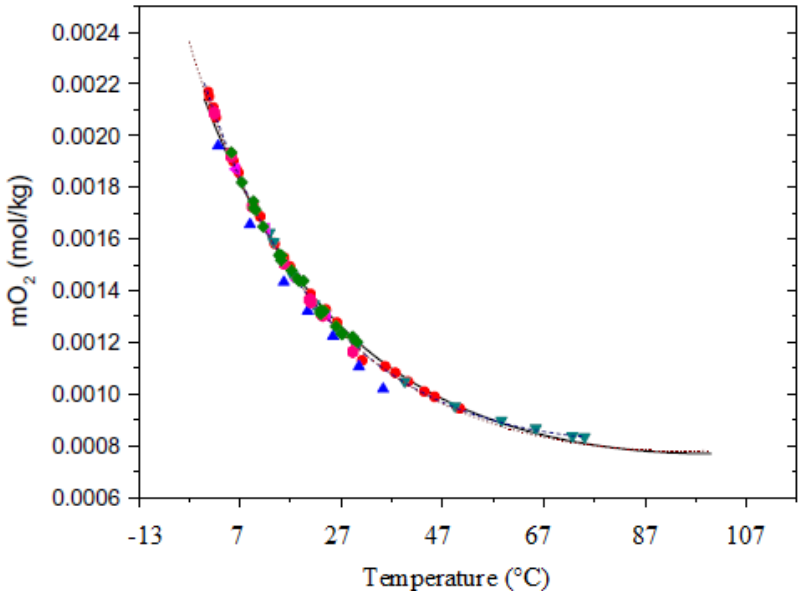

Figure 1.8 Oxygen solubility in pure water at atmospheric pressure. The different colours represent data from multiple studies. Adapted from [208].

Soil temperature does not appear to have a significant effect on methane oxidation rates. At low temperatures, up to 10 °C, an increase in temperature may lead to an increase in oxidation [191, 209], but above 10 °C, temperature increases do not appear to be consistently related to oxidation rates [210]. Instead, soil moisture appears to be responsible for the majority of seasonal effects seen in methane-oxidising soils [187], although thermophilic soils have not been investigated.

1.4.8 Effects of soil gases on methanotrophs

Soil gas composition and concentrations can vary markedly in geothermal ecosystems. In this section, methane, oxygen and hydrogen gases will be considered with respect to their possible influence on the activities, abundances and diversity of thermophilic methanotrophic soil communities. The concentration of methane within the gas phase of soils appears to play a strong part in the selection and growth and maintenance of methanotrophic soil communities. In soil ecosystems, the application of high methane concentrations increases the rate of *in situ* methane consumption [170, 205] and it is generally accepted that the observed methane oxidation rates are limited by methane availability [211, 212], possibly because of gas diffusion limitation.

However, some proteobacterial methanotrophs oxidise methane to below tropospheric concentrations of ~1.84 ppmv [52]. High affinity methane oxidation (HAMO) may be limited to the Upland Soil Clusters (USC-α and -γ), but HAMO also occurs in paddy soils, mainly in *Methylocystis* and *Methylosinus* strains. The HAMO activity was induced by flushing the soils first with high concentrations of methane (10,000 ppmv), and although this activity ceased after two weeks, it could be regained after further soil exposure to methane [52]. Low methane conditions may lead to the induction of high affinity enzymes or isozymes [112], to cells switching to oxidation of alternative carbon sources such as methanol [213], or cells reverting to resting forms such as exospores and cysts [214]. Under methane starvation conditions, a decrease in the half-saturation constant (K_m) and maximum rate for reaction (V_{max}) for methane oxidation in *Methylocystis* LR2 was observed, but the specific affinity of pMMO, and the rate of uptake of methane, remained the

same [215]. This may be due to the availability of oxygen and reductant (e.g. NADH for sMMO) becoming a rate-limiting factor.

Oxygen is an essential substrate for both the catalysis of methane oxidation via methane monooxygenase and as a terminal electron acceptor for aerobic respiration. The growth of methanotrophs in many soil ecosystems is therefore obligately dependent on the continual diffusion of oxygen into these habitats, and many methanotrophs are found at oxic/anoxic interfaces within soils [216]. Curiously, in the absence of methane, the presence of oxygen can be detrimental to the survival of methanotrophic bacteria. Methane starvation of WP12, a Type I methanotroph, resulted in a 10-fold greater loss of biomass in an oxic environment (over 240 hours) than under anoxic conditions, with biomass loss largely attributed to the exogenous breakdown of proteins and lipids [51]. Recovery of methane oxidation occurred up to 35 % more quickly in WP12, *M. trichosporium* OB3b or *Methylomicrobium album* following periods of methane starvation under anaerobic compared to aerobic conditions. Methane oxidation decreases in methanotrophic soils or pure cultures following a period of exposure to air without methane [217], and the effect may be caused by changes in sMMO enzyme affinity following starvation.

The oxygen level within a lake sediment environment also altered community composition [218]. Sediment microcosms incubated under an atmosphere with 25 % (v/v) methane and 5 % (v/v) oxygen were dominated by *Methylobacter* species and methylotrophs from *Methylotenera*, while microcosms incubated with 25 % (v/v) methane and 75 % (v/v) oxygen consisted mainly of *Methylosarcina* and methylotrophs within *Methylophilus.* As the oxygen levels used were above reported K_m values for methanotrophs, the differences may result from different strategies used during periods of hypoxia. Comparative genomic analysis indicated that the *Methylobacter* species possessed a *pxmA* gene that was upregulated during hypoxia, as well as the more common *pmoA*, nitrate and nitrite reductases, and multiple hydrogenases [218].

Nitrate reduction has also been linked to methane oxidation during hypoxia in a variety of methanotrophs. For example, in *Methylomonas denitrificans* FJG1,

the dissimilatory nitrate reduction pathway, which comprises the nitrate reductase *narGHJI*, the nitrite reductase *nirK* and the nitric oxide reductase *norBC*, is only upregulated under oxygen limitation when nitrate is plentiful [219]. The substitution of oxygen with nitrate as a terminal electron acceptor would reduce the oxygen requirement of the cell by half, thereby allowing the small quantities of oxygen available in a hypoxic environment to be used solely for methane oxidation (via MMO). Interestingly, *pxmA* was also transcriptionally upregulated in *M. denitrificans* FJG1 under hypoxic conditions, although nitrate was not necessary to induce expression [219]. In addition, *Methylocystis* SC2 was shown to produce N_2O when grown with methanol as a carbon source in the presence of nitrate [220] In *Methylocystis* MTS cells grown on methanol under high oxygen conditions (25-35 %, v/v), formaldehyde rapidly built up, which inhibited further reactions of both methanol to formaldehyde, and formaldehyde to formate and CO_2 [221]. Conversely, in low oxygen conditions (1-3 %, v/v), formaldehyde was converted rapidly to formate, which can accumulate in the cell or be excreted. The accumulation of intermediates under low oxygen conditions suggests that pMMO has a higher affinity for oxygen than the electron transport chain [221].

Hydrogen is ubiquitous in the atmosphere and in geothermally-vented gases, and is used by many *Bacteria*, *Archaea* and eukaryotes as an energy source [222]. Dominant soil phyla including *Acidobacteria*, *Actinobacteria* and *Proteobacteria* use hydrogen either for growth or for survival during periods of starvation [223-225], and genes for hydrogen-uptake and/or hydrogen-evolving hydrogenases have been found in a wide variety of genomes, including all currently sequenced methanotrophs [35, 226]. *M. trichosporium* OB3b possesses two hydrogenases, one expressed constitutively and one expressed in response to hydrogen in the absence of methane [227]. The oxidation of hydrogen provides reductant to both pMMO and sMMO to oxidise substrates such as methane, propane, chloroform and trichloroethylene [228]. *M. capsulatus* Bath also has two hydrogenases, one soluble and one membrane bound, which are both expressed constitutively. The soluble hydrogenase reduces NAD^+ and can drive both sMMO and pMMO activity [229]. Hydrogen oxidation by a membrane-bound hydrogenase has also been found to enhance

growth of *Methylacidiphilum* spp. RTK17.1 and *M. fumariolicum* SolV, particularly under hypoxic conditions. Utilisation of hydrogen continued in both cultures under methane and/or oxygen partial pressures, suggesting that this may also be a mechanism for subsistence [34, 35].

1.4.9 Trace metals

The availability of trace metals, particularly copper, iron, nickel and rare earth elements (lanthanides) are critical to the growth of many methanotrophs. For example, methanotrophs that express pMMO have an obligate requirement for Cu^{2+} for methane oxidation activity. The complete structure and biochemistry of pMMO has not yet been fully elucidated, but the metalloenzyme complex contains between 4 and 30 mol of copper [230]. However, very high concentrations of copper, above 4.3 mM Cu^{2+}, inhibit methane oxidation activity [184]. In methanotrophs that also express sMMO, a chalkophore, known as methanobactin, and a polypeptide (MmoD) are responsible for the switch in transcription from pMMO to sMMO under low copper conditions [77]. Copper can be found in relatively high concentrations in geothermal surface waters compared to freshwater, particularly in low pH systems [231] that may stimulate growth of methanotrophs that use pMMO. Conversely, higher pH systems with lower levels of copper leached from sulfide minerals may harbour methanotrophs only able to express sMMO. Growth of *M. fumariolicum* SolV, a methanotroph isolated from volcanic mud, is dependent on the presence of the rare earth elements (REE) lanthanum, cerium, praseodymium or neodymium [136]. The lanthanides are essential as a cofactor in the methanol dehydrogenase XoxF. These elements have been observed in high concentrations in sand, and in magmatic and metamorphic rocks that are often found in geothermal areas [232]. It is generally considered that the *in situ* access to the metals by methanotrophs in geothermal ecosystems should not be restrictive due to the mobility of the metals and lack of leaching of young soils [214]. However, ensuring that the trace metal requirements of thermophilic methanotrophs during laboratory-based cultivations can be potentially problematic. In the case of *M. fumariolicum* SolV, sterile geothermal mud was added to all cultivations to ensure this need was being met [43].

1.5 Conclusions and Hypotheses

The recent increased focus on factors contributing to global climate change emphasises the importance of understanding the sources and sinks of climate modifying gases such as methane. While the extent and distribution of low and moderate temperature methanotrophy is relatively well understood, little is known about thermophilic methanotrophs, even though approximately 5-15 % of the flux of methane originates from geothermal resources. Despite the impact of geothermal environments, there are less than 20 characterised thermophilic methanotrophs and only 3 thermotolerant methanotrophs.

A satisfactory explanation for the paucity of extant thermophilic methanotrophs is elusive. The constraints around the solubility of both methane and oxygen at high temperatures may define an upper temperature limit above which aerobic methane oxidisers cannot be isolated. Similarly, competitive exclusion of methane oxidation by geothermally plentiful ammonia (as ammonium ion) to the active site of MMO similarly may also restrict growth to a point that it becomes energetically unfavourable. Conversely, there are several sound physical reasons why geothermal systems may harbour potential populations of active and currently undescribed thermophilic methanotrophs. Many geothermal fields at high temperatures release high volumes of methane and hydrogen, and geothermal soils are frequently clay-based, contain low levels of organic carbon, and contain relatively high concentrations of trace metals required by methanotrophs, including copper and lanthanides.

Nonetheless, the diversity of cultured methanotrophs has expanded greatly over the last ten years, and several thermophilic methane-oxidising bacteria have now been isolated and characterised. Some well-studied methanotrophs have known thermal adaptations; others may utilise unusual mechanisms for heat tolerance. The modularity of enzymes involved in the known methane oxidation pathways may contribute to the ability of methanotrophic microorganisms to respond to high temperature conditions.
Recent work using culture-independent and stable-isotope techniques, has clearly demonstrated methanotrophy in thermophilic ecosystems. Proteobacterial methanotroph *pmoA* sequences have been detected in several

high temperature geothermal systems; at 71.5 °C in Japan [138], at up to 83 °C in Italian soil [139] and at up to 99 °C in Russia [141]. Similarly, verrucomicrobial *pmoA* sequences have also been detected in geothermal soils in New Zealand at up to 81.6 °C [122]. Methane oxidation has also been demonstrated in geothermal samples from New Zealand incubated at 65 °C [26], from Russia at 74 °C [141], and from Italy at up to 80 °C [139].

Incorporation of ^{13}C labelled methane into bacterial biomass was detected at temperatures of at least 60 °C in the Russian study [141]. Furthermore, next-generation sequencing technology, particularly metagenomics and metatranscriptomics, is likely to reveal pathways in which methanotrophy can operate in geothermal ecosystems, by potentially avoiding the biases associated with primer annealing and cultivation techniques.

Considering the above literature review, this research proposes that thermophilic methanotrophic microorganisms will be present and detectable within the Taupō Volcanic Zone (TVZ) of New Zealand's central North Island. To address this proposal the research in this thesis will investigate:

1) The microbial ecology of methanotrophs in TVZ geothermal systems

Both molecular and functional studies have shown the potential for geothermal systems to harbour populations of active methanotrophs, and I hypothesise that thermophilic methane-oxidising strains can be detected, enriched and isolated from these areas. For the first section of this thesis, my aims are to: i) quantify rates of methane oxidation in geothermal microcosms across a wide range of pH and temperature; ii) evaluate the effects of temperature, pH, soil type and environmental methane concentrations on microcosm methane oxidation rates; and iii) determine the microbial community composition within these geothermal microcosms through 16S rRNA gene sequencing.

2) The enrichment of thermophilic methanotrophs

If geothermal areas are ecosystems for active, thermophilic methanotrophs, these may be enriched using standard minimal media used for methanotroph isolation. My aims are to: i) determine methane oxidation rates of enrichment cultures in standard media; and ii) to perform comparative functional transcriptomics on methanotrophic consortia.

3) Isolation of methanotrophs from geothermal areas

If methanotrophs can be enriched from geothermal microcosms and identified through measurement of methane oxidation and analysis of mRNA transcripts, my aims for this section of the thesis are to: i) isolate thermophilic methanotrophs; and ii) to characterise isolates in terms of their growth temperature and pH ranges, preferred carbon and nitrogen sources, rates of methane oxidation and the presence or absence of specific functional genes.

4) Hydrogen oxidation and survival at elevated temperatures

Several methanotrophs oxidise hydrogen in addition to methane, or during periods of methane starvation. I hypothesise that hydrogen and methane co-utilisation will allow thermophilic methanotrophs to extend their temperature range by using alternative energy sources. My aims for this section of the thesis are i) to determine if any isolates encode hydrogenases; ii) to determine if any isolates oxidise hydrogen; and iii) to establish if hydrogen oxidation can contribute to methanotroph survival at temperatures above growth $T_{max.}$

2. Microbial Ecology of Thermophilic Methanotrophs within the Taupō Volcanic Zone

2.1 Introduction

The greenhouse gas methane (CH_4), being 25 times more effective than carbon dioxide (CO_2) at absorbing infra-red radiation, is responsible for 20-30 % of global climate change [1]. The global methane budget is around 600 Tg/year from both natural and anthropogenic sources [3], yet much of this methane is consumed by methanotrophic bacteria before it reaches the atmosphere. It is therefore important to understand the distribution and diversity of methanotrophic bacteria to enable a more complete understanding of ecological processes that modulate methane emissions and oxidation.

Aerobic methanotrophic bacteria have now been detected and/or isolated from nearly all known sources of methane, including wetlands [233], freshwater lakes [163], rice paddy fields [234], landfills [235], coal mines [159] and geothermal areas [57]. While our knowledge of methanotroph ecology in many of these ecosystems is extensive [46, 78, 81], our understanding of the distribution and diversity of methane oxidising bacteria in geothermal fields remains limited to a few studies [139, 141, 236, 237]. Geothermal emissions of geologic methane from magma degassing are thought to be the second largest natural source of methane [4], emitting up to 75 Tg/year, but geothermal and volcanic areas are inhospitable for most known species of methanotrophs, due to acidic pH, high temperatures and low oxygen concentrations [184]. Evidence of methanotrophic activity in geothermal areas was first shown in 2005 [238], and even though a number of thermophilic aerobic methanotrophs have recently been isolated from geothermal soil, including the discovery of a new class of methane-oxidising bacteria within *Verrucomicrobia* [14, 43], very little is known about the phylogenetic and metabolic diversity of thermophilic methanotrophs from these areas. It is unclear if this disparity is due to a difficulty in culturing methane-oxidisers, from a failure to replicate environmental conditions *in vitro* [108], or because there are biological restrictions on methane oxidation at high temperatures, such as methane solubility [207] or enzyme instability [92].

This study will use culture-independent methods (e.g. 16S rRNA gene amplicon sequencing) on geothermal soil and sediment samples from throughout the Taupō Volcanic Zone (TVZ), New Zealand, to detect the activity of thermophilic methanotrophs and, if present, to assess whether specific environmental conditions may promote or conversely limit biological methane oxidation in particular areas. To achieve these aims I will: i) quantify rates of aerobic methane oxidation in geothermal samples across a wide range of pH and temperature; ii) evaluate the effects of temperature, pH, soil type and environmental methane concentrations on observed methane oxidation rates; and iii) determine the microbial community composition within these geothermal samples. The overall workflow for this study is shown in Figure 2.1.

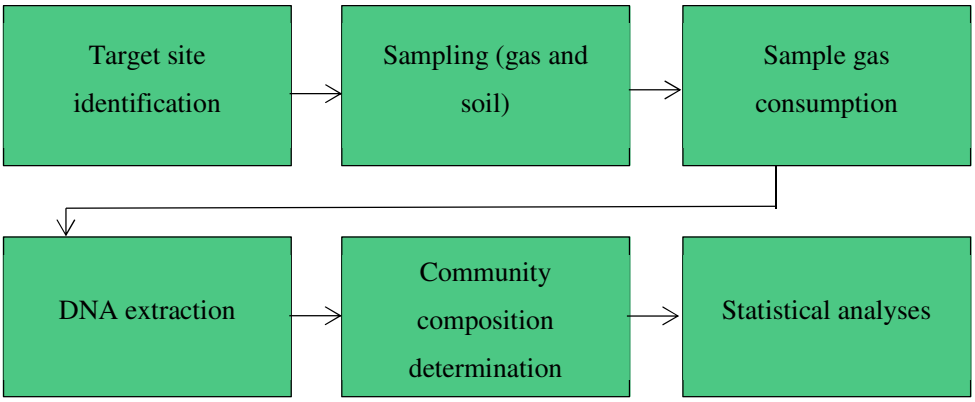

Figure 2.1 Workflow diagram of the sampling and community analysis procedure for detecting methanotrophic activity in the TVZ.

2.1.1 Experimental Rationale

The TVZ covers 6000 km^2 of the central North Island in New Zealand and extends from the active volcanoes of White Island to Mount Ruapehu (Figure 2.2). The area contains >20 geothermal fields that are characterised by an abundance of hot springs, geysers, and mud pools [11]. Analysis of gas emitted from geothermal fields within the TVZ found that most systems contain 0.1 to 5.0 % methane (v/v), but there are certain sites that have much higher proportions, such as a Golden Springs site where the emitted gas consists of up to 19.3 % methane (v/v) [11]. My hypothesis is that thermophilic methanotrophs will be detected in geothermal areas within this highly active volcanic region.

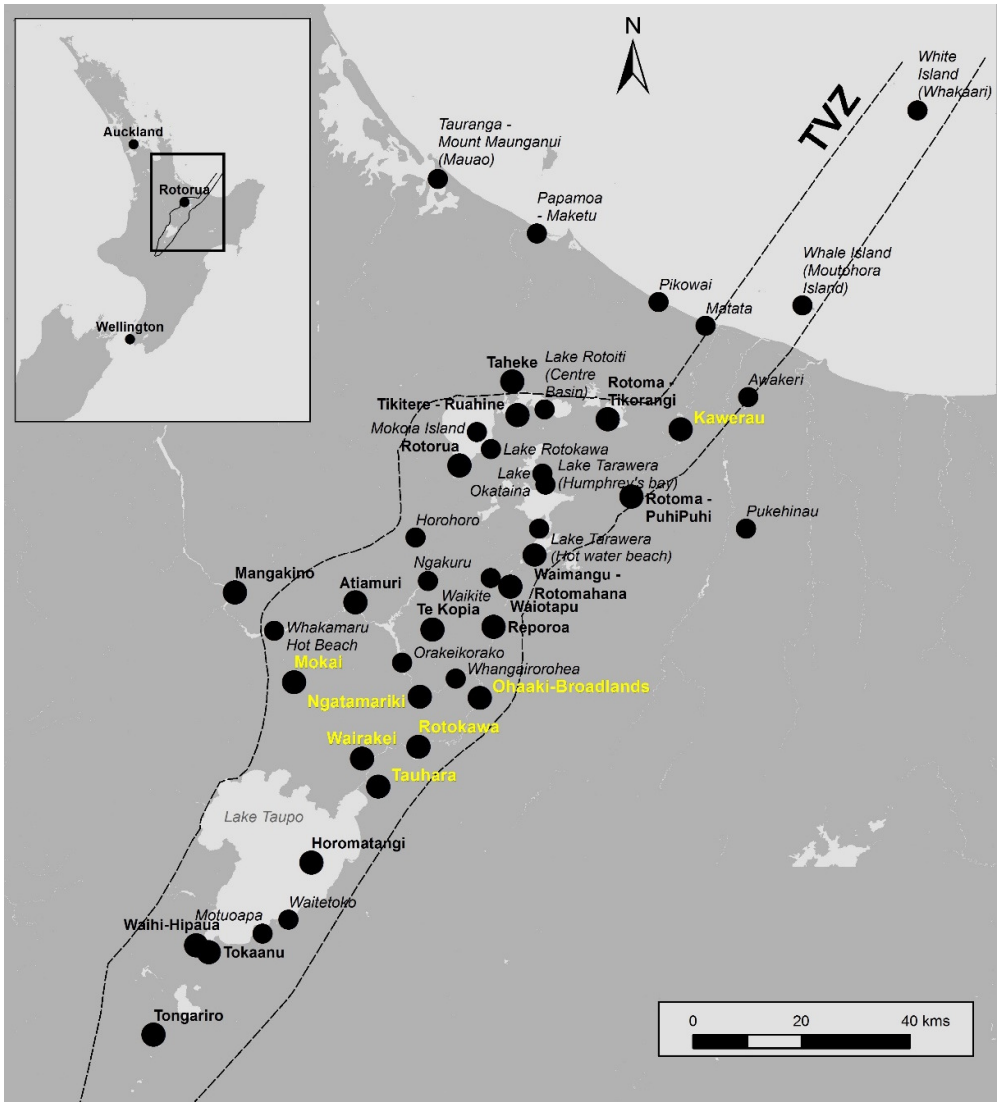

Figure 2.2 Map of geothermal systems within the Taupō Volcanic Zone. Black circles represent geothermal upflows resulting in surface geothermal features. Locations of geothermal power stations are highlighted with yellow text. Copyright GNS Science.

Methanotrophs have been identified in geothermal areas around the world at temperatures ≤ 99 °C using molecular surveys. These surveys use either the 16S rRNA gene or *pmoA,* which encodes for the alpha subunit of particulate methane monooxygenase [139, 141, 236, 237] and is therefore diagnostic of methanotrophy. Despite its utility, there are several caveats when using *pmoA* as a diagnostic tool: there is a great deal of sequence diversity between known methanotrophs so more unusual *pmoA* genes may not be detected [115, 239];

several isolated methanotrophs contain multiple different copies of the gene [43, 240, 241]; and at least three genera within *Alphaproteobacteria* do not contain the gene at all [45, 242]. In this study, I will use primers that universally target the V4 region of the 16S rRNA gene (515F-806R [243]) as part of an NGS amplicon-based survey of microbial communities in geothermal soils in the TVZ.

This study focuses on the diversity and distribution of methanotrophs within geothermal soils. The rationale for targeting soils and sediments over aqueous environments is two-fold. Firstly, soils and sediments have a much greater abundance and diversity of microbes than freshwater aquatic systems [244]. With pH and temperature being strong drivers of microbial diversity [180, 181] within geothermal habitats [180, 181], I anticipate that the greater diversity and richness within soils provides this study with a stronger opportunity to select and enrich for strains of thermophilic methanotrophs. Secondly, the solubility of methane in water is low, and decreases by approximately 33 % as the temperature increases from 30 to 60 °C [206]. Oxygen solubility additionally drops about 37 % over the same temperature range [245]. The limited availability of these essential gases in hot springs is likely to restrict growth of methanotrophs within water columns as compared to soils of similar temperatures. For these reasons it was felt that the likelihood of detecting thermophilic methanotrophs was greatest in geothermally-heated or steam-fed soils, so mainly soil samples were collected for the purposes of this study. However, it should be noted that in several instances hot spring sediments and/or water column samples were collected from sites with known elevated fluxes of methane.

In this study, a variety of soil types were collected from geothermally-heated soils to assess the influence of soil structure on the presence and activity of thermophilic methanotrophs. Gas availability in soils is affected primarily by soil moisture content, measured as the percentage of water-filled pore spaces (WFPS) within the soil, which is a function of soil porosity [246]. High moisture contents can reduce or completely inhibit methane consumption [190, 194], by affecting either gas transport within soils and between soils and the

atmosphere or inducing water stress responses in cells. As methane diffuses through water at a rate ~ 10,000x slower than through air [209], it follows that a high proportion of WFPS in a soil will reduce the availability of methane for methanotrophs. The physiological effects of water stress on methanotrophs are also not well known – some studies have shown that *Methylosinus* and *Methylomonas* species have little tolerance to moderate water stress [190]. However, the rapid recovery of methane oxidation as soils dry [246] suggests that these elevated WFPS effects are not permanent. Other soil characteristics, such as grain size [183, 184] and clay content [186, 187] affect methane oxidation capability, and for this reason samples were chosen to also cover a range of soil attributes.

2.2 Materials and Methods

2.2.1 Sampling Overview

The majority of sample locations were chosen from steaming soils at geothermal sites with an observed surface temperature of > 55 °C. Other sites were identified from the 1000 Springs dataset [247] as having either high *in situ* levels of methane, or with a high proportion of 16S rRNA gene sequences from the location assigned as putative methanotrophs. Sampling locations were chosen to cover a wide range of temperatures, pH values and different soil characteristics (see *2.2.2 Sample characterisation* for how these were determined). Samples were collected from 14 geothermal fields within the TVZ, between Rotorua in the North and Tokaanu in the South (Figure 2.3, Figure 2.4, and Figure 2.5).

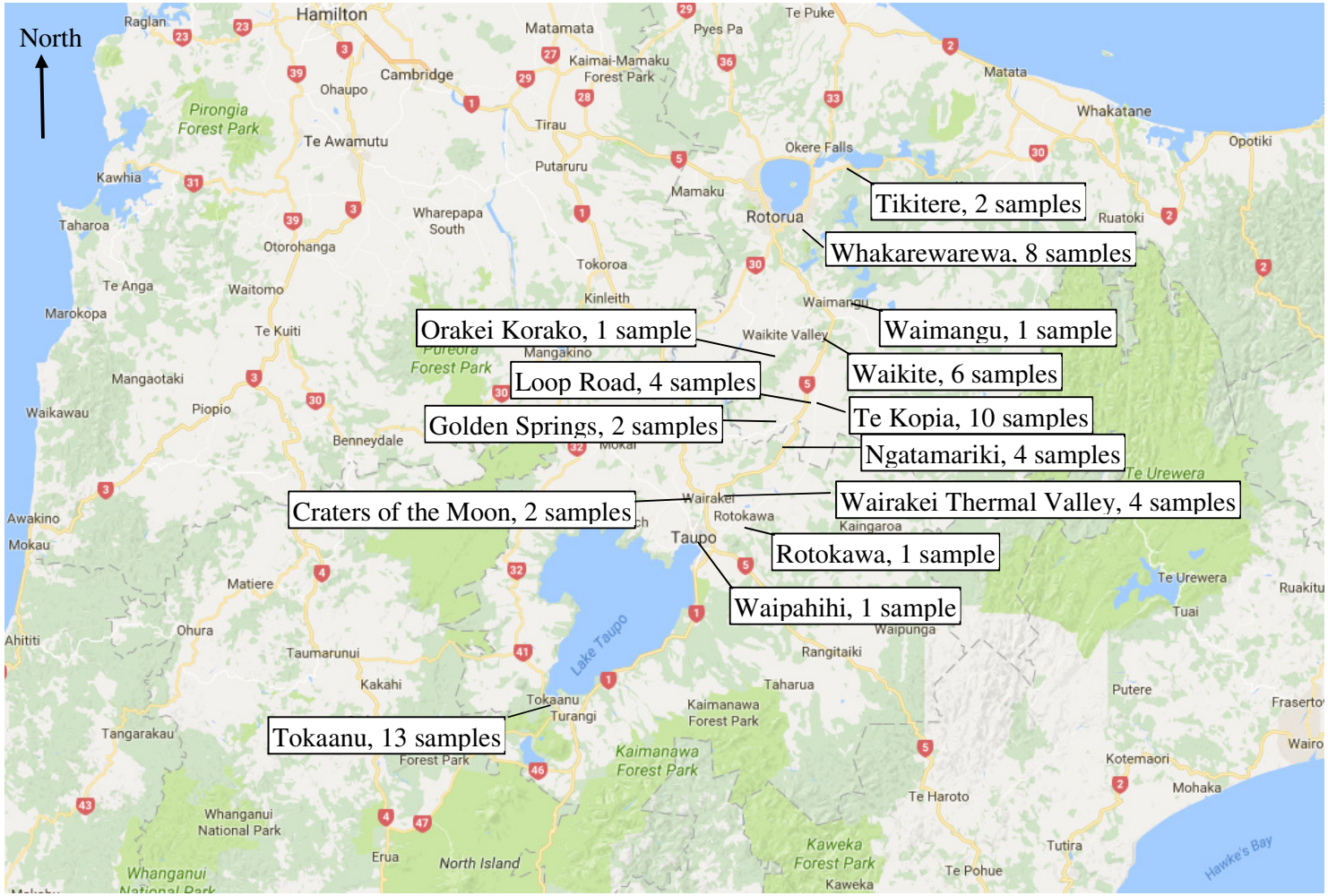

Figure 2.3 Map of the sampling locations within the Taupō Volcanic Zone, New Zealand. Map data copyright 2017 Google.

Figure 2.4 Satellite imagery (Google Earth) showing the locations of selected sample sites for this study. All map data © Google[NZ]

a) Whakarewarewa Village (WHV) sample sites.

b) Wairakei Thermal Valley (WTV) sampling sites.

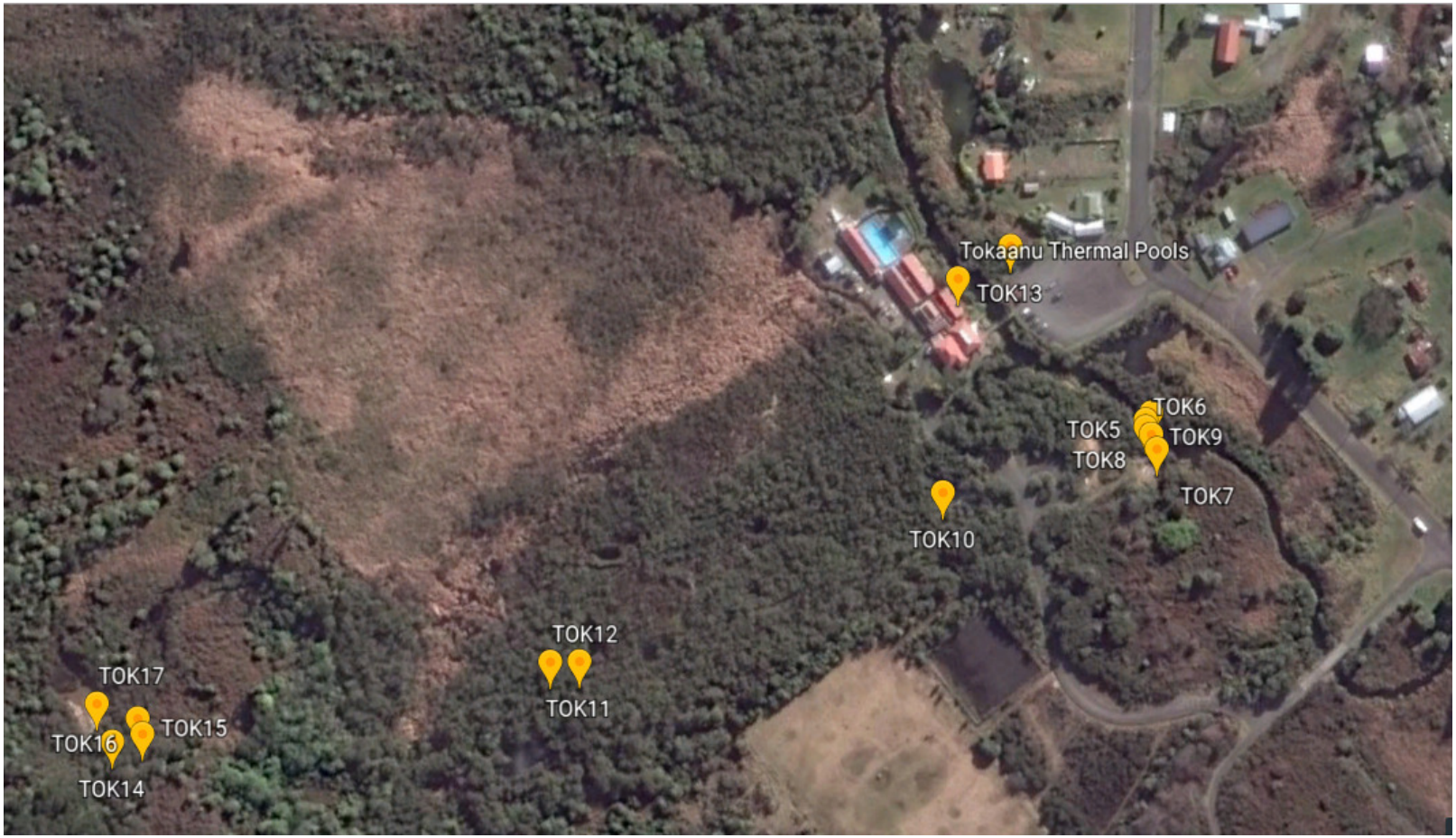

c) Tokaanu (TOK) sampling sites.

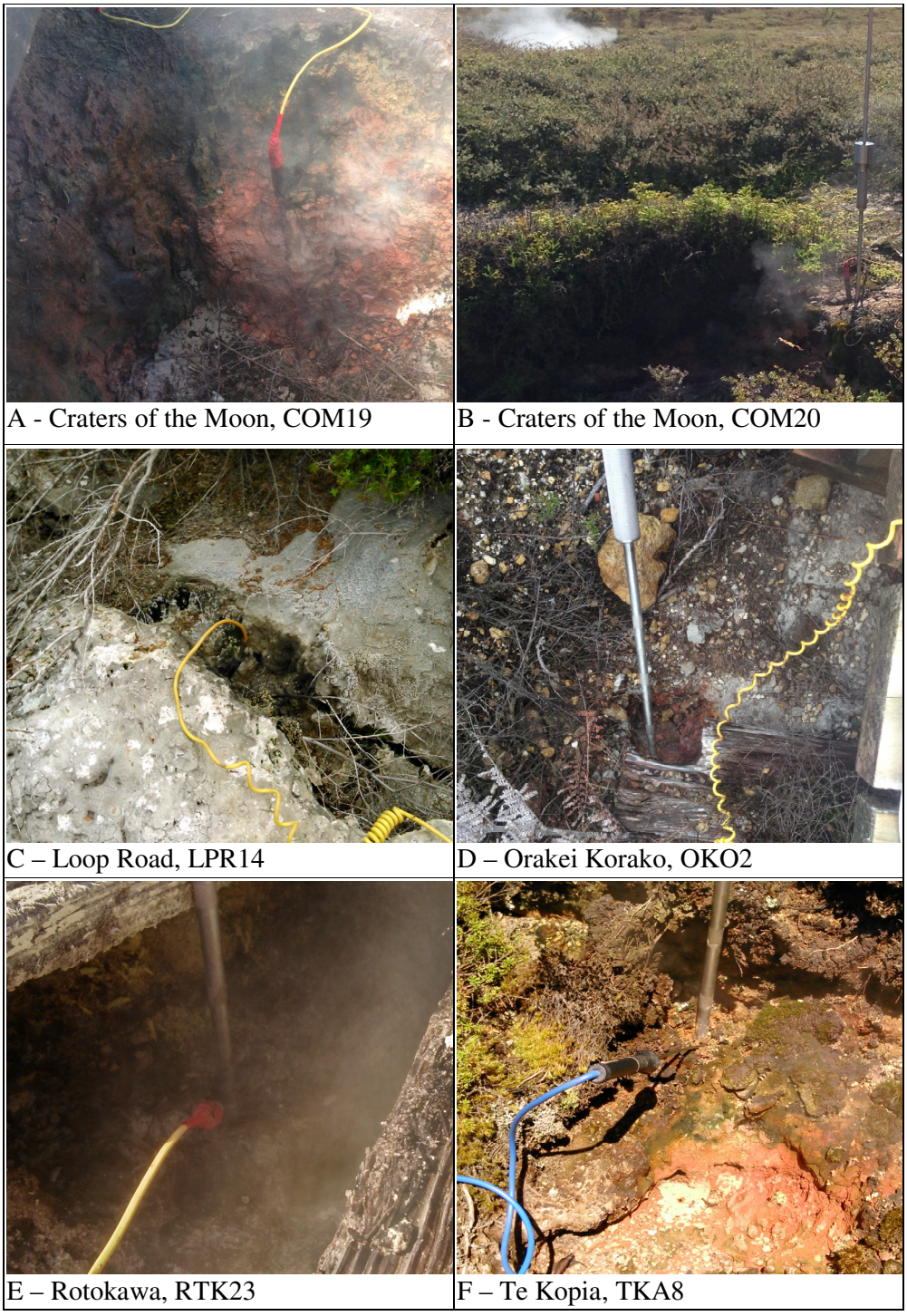

Figure 2.5 Photographs of selected sample sites chosen for this study.

G - Te Kopia, TKA15

H - Tikitere, TKT67 and TKT68

I – Whakarewarewa Village, WHV12

J - Whakarewarewa Village, WHV14

K – Waikite Valley, WKT44

L – Waikite Valley, WKT46

Figure 2.5 Photographs of selected sample sites chosen for this study.

2.2.2 Sample characterisation

Ground temperatures were measured using a thermal probe inserted into the soil at 2, 10 or 20 cm depth and a 51 II digital thermometer (Fluke, WA). Soil gas microcosms were collected, where possible, using a custom-built sampling pole inserted into the soil to 10 or 20 cm depth (Figure 2.6). 700 ml of gas was drawn through the sampling pole and discarded, to avoid atmospheric contamination. 25 ml of gas was then slowly extracted from the soil and injected through a three-way valve into a pre-evacuated Air and Gas Sampling Bag (Calibrated Instruments, MD). Gas samples were processed within 24 hours on a Peak Performer 1 Gas Analyzer (Peak Laboratories, CA) equipped with a flame ionization detector (FID) and a Unibeads 60/80 column.

Figure 2.6 Sampling pole being used to sample gas from soil at Whakarewarewa Village WHV20. The pole is driven into the ground using the central weight. Soil gases are withdrawn from the subsurface soil environment via perforations in the tip of the pole through the central bore to a 50 ml syringe connected to the top of the pole.

Soil characteristics were determined using a version of the British Soil Classification System [248]. “Clay” soils were soft and primarily composed of

fine, sticky particles that were often wet or moist. The identity of specific clay minerals was not determined. “Sand” soils were loose rather than soft and had small rounded particles less than 2 mm in size. Soils were classified as “loam” when they consisted of sand, silt, and clay, as well as organic material. These soils were loose, easily compacted and appeared most like ordinary garden soil. Samples that contained a mixture of these three soil classes were defined as either “clay/loam”, “clay/loam/sand”, “clay/sand”, or “loam/sand”. “Sediments” were defined as sand, silt or clay particles that were under water at the time of sampling, while “biomass” was used for material attached to the side of a hot spring that appeared biological in origin. One final sample was classified as “water”; this was taken from a hot spring without disturbing the sediment below, and was selected because the 1000 Springs dataset [247] indicated the presence of high numbers of methanotrophs.

Soil samples of approximately 2 g were harvested using a trowel and spatula previously sterilised with ethanol, and were immediately transferred to autoclaved 114 ml glass vials (122 °C, 15 PSI, 20 minutes, P52014 Pressure Vessel (Mercer Stainless Limited, Henderson, New Zealand), which were then capped with sterile butyl rubber stoppers and sealed with aluminium crimps. A separate accompanying soil sample was stored in a sterile 50 ml Falcon tube; soil pH was measured at room temperature on returning to the laboratory, by suspending approximately 1 g of soil in 10 ml RO H_2O. A model 320 HI11310 pH probe (Hanna Instruments, RI) was used to determine pH.

2.2.3 Methane consumption assessment by thermophilic soil microcosms

A gas mixture (v/v), consisting of 80 % CH_4, 15 % CO_2 and 5 % O_2 (14.3 ml), was injected into the sample vial headspace through a sterile filter resulting in final gas headspace concentrations of 10 % CH_4, 1.3 % CO_2 and 21.6 % O_2 (approximately 10-12 kPa). Vials were placed in incubators at temperatures that reflected the *in situ* sample temperature (40, 46, 50, 60, 68, 70, 75 or 80 °C). At 3-4 day intervals, vials were moved to a water bath at 20 °C and equilibrated to room temperature (20 °C) for 5 hours before headspace pressure was measured with a XP2i digital pressure gauge (Crystal Engineering Corporation, CA) to enable determination of moles of gas. Headspaces were quantified by GC-FID by

removing 500 µl with a gastight syringe (SGE Analytical Science, Melbourne) and diluting to 5 ml with air.

Methane oxidation rates (µmol/g soil/day) were calculated using linear regression. If microcosms showed a greater loss of methane than controls (sampling without replacement) for five consecutive readings, and if the coefficient of determination of linear regression (R^2) was > 0.5, microcosms were designated as positive for methane oxidation. Graphs showing the calculation of rates of oxidation for all positive microcosms are shown in Appendix 7.1. After positive oxidation was determined, or after at least four weeks of headspace measurements for microcosms that did not oxidise methane, all microcosms were opened in a Hera Safe Biosafety Cabinet (Heraeus, Germany) and soils were distributed into 2 ml bead-beating tubes (Macherey-Nagel, Germany; 2 x 0.25 g) for DNA extraction. Residual soils were transferred into sterile 15 ml tubes for archival storage at -80 °C.

2.2.4 Microcosm DNA extraction and sequencing

DNA was extracted from soil and sediment microcosms using a modified protocol for the NucleoSpin Soil kit (Macherey-Nagel, Germany). A 0.25 g of sample was placed into bead beating tubes along with 200 µl of Difco™ sterile skimmed milk solution (5 % w/v), 150 µl Enhancer SX and 700 µl of either Lysis Buffer SL1 or SL2, provided with the kit. Cells had two cycles of disruption in a bead beater (Biospec, OK) at maximum speed for 30 seconds followed by cooling at 4 °C for > 5 minutes. Samples were next centrifuged at 11,000 x *g* for one minute and the supernatant removed to a 2 ml microfuge tube. Lysis Buffer SL3 (150 µl) was then added, the tubes were briefly vortexed and centrifuged again at 11,000 x *g* for one minute and the supernatant transferred into a new tube. 125 µl of a 7.5 M potassium acetate solution was added and vortexed and the resultant mix was centrifuged at 17,000 x *g* for five minutes. Finally, the supernatant was removed to a new tube containing 250 µl of Binding Buffer SB and vortexed briefly before being applied to a spin filter column and centrifuged at 11,000 x *g* for one minute. The remainder of the manufacturer's protocol was then followed, with the exception that DNA was eluted twice with 40 µl Elution Buffer SE heated to 70 °C.

DNA was amplified using universal primers for the V4 region of the 16S rRNA gene [243] with adaptor sequences for the Illumina MiSeq: 515F 5'-TCG TCG GCA GCG TCA GAT GTG TAT AAG AGA CAG GTG YCA GCM GCC GCG GTA A-3'; 806R 5'-GTC TCG TGG GCT CGG AGA TGT GTA TAA GAG ACA GGG ACT ACN VGG GTW TCT AAT-3'. PCR was carried out in 50 µl reaction volumes containing 100 µM dNTPs, 0.5 µM primers, 1U i-Taq (iNtRON Biotechnology, South Korea) and 7 µl of an enhancer solution (2.7 M betaine, 0.2 M trehalose, 6.7 mM DTT, 0.055 mg ml^{-1} BSA and 0.067 % DMSO). The final concentration of $MgCl_2$ was 1.5 mM. DNA templates from microcosms were used at final concentrations of 10 – 50 ng/reaction. PCR amplifications were performed using a CGI-96 thermal cycler (Corbett Research, Australia) with PalmCycler™ software, v2.1.10 (Corbett Research). Three PCR amplicons (~300 bp) for each sample were pooled and purified using the NucleoSpin Gel and PCR Clean-up kit (Macherey-Nagel) and Agencourt AmPure XP (Beckman Coulter, IN). Amplicon libraries using the PCR products were prepared and sequenced by Macrogen Inc. (South Korea).

Two samples were selected to test the ability to replicate sequencing results. NGM91R was a physical replicate; a duplicate sample taken from the same geothermal site and tested for methane oxidation in the same manner as NGM91, before DNA extraction from both. WKT46R was an extraction replicate; a second subsample was taken from the WKT46 microcosm after methane oxidation was shown to be negative for this sample, and DNA was extracted in duplicate. The duplicate samples WKT46R and NGM91R were sequenced using the same protocol but on different Illumina runs to WKT46 and NGM91.

2.2.5 Community 16S rRNA gene sequence processing and diversity metric assessment

The quality of raw read data was assessed using FastQC [249]. Paired-end sequence reads were merged and filtered using USEARCH v7.0, with a maximum expected error of 1 [250]. Remaining sequences either greater than 500 bp (to remove poor quality sequences at the end of long reads) or less than 200 bp (the minimum required for taxonomy classification) were removed using mothur v1.35.1 [251]. A *de novo* database of ≥ 97 % similar sequence centroids or OTUs

was created in USEARCH [250]. Raw sequences were mapped against this *de novo* database to generate counts of sequences matching OTUs (i.e. taxons) for each sample. Using QIIME v1.9.1[252], taxonomy was assigned to each OTU by using the RDP classifier v2.2 [253] with a confidence threshold of 0.5 and trained on the Silva 16S rRNA gene database (version 123) [254]. Chloroplast and mitochondrial OTUs were removed and all samples were rarefied to the lowest sample read count (n=149,400). The full sequencing pipeline is shown in Appendix 7.2.

All Operational Taxonomic Units (OTUs) identified by the RDP Classifier as belonging to the methanotrophic families *Beijerinckiaceae* or *Methylocystaceae* (*Alphaproteobacteria*); the order *Methylococcales* (*Gammaproteobacteria*); or as *Methylacidiphilum* (*Verrucomicrobia*) were manually checked against the NCBI database using a discontiguous megablast. OTUs that were > 90 % related to a described methanotrophic species were identified as putative methanotrophs. Although there are no universal definitions for higher taxa using 16S rRNA gene sequences, the 90 % similarity level is commonly used to denote the boundary of an order within a phylum (e.g. [255, 256]). The full list of these OTUs is shown in Appendix 7.3.

The core diversity workflow within QIIME [252] was used to analyse sequencing data, by creating multiple rarefactions of the data, calculating and comparing alpha and beta diversity of the samples, and summarising taxa across all samples and as a function of methane oxidation status. Standard parameters were used for this script, with the exception that Chao1 (a non-parametric estimate of species richness [257]) and the Shannon [258] and Simpson [259] indices (quantitative measures of diversity and abundance) were selected as the alpha diversity metrics.

$$chao1 = S_{obs} + \frac{F_1(F_1 - 1)}{2(F_2 + 1)}$$

where S is the number of OTUs in the sample, and F_1 and F_2 are the count of singletons and doubletons, respectively.

$$\text{Shannon Diversity Index (H)} = -\sum_{i=1}^{s}(p_i \log_2 p_i)$$

where *s* is the number of OTUs and p_i is the proportion of the community represented by OTU *i*.

Simpson's Diversity Index is calculated by

$$1 - \sum p_i^2$$

where p_i is the proportion of the community represented by OTU *i*.

Beta diversity metrics were weighted UniFrac and unweighted UniFrac [260], which compare community compositions while taking into account the phylogenetic distances between taxa.

2.2.6 Statistical analyses of community composition data

The statistical analyses of the microcosm microbial communities used custom scripts to generate the described outputs. All scripts are listed in Appendix 7.2. The QIIME script distance_matrix_from_mapping.py was used to create distance matrices of *in situ* methane concentration, sample type, sample temperatures and pH, the latitude and longitude of individual samples, and μmol of methane oxidised per gram of soil per day. Mantel tests [261] were then performed using the script compare_distance_matrices.py to determine any correlation between methane oxidation rates and sample characteristics, using 999 permutations of a two-tailed test. Correlations between methane oxidation rates and the categorical sample characteristics of geothermal field and sample type were identified using a Kruskal-Wallis [262] test, which is a non-parametric, one-way analysis of variance used where sample means are not equal and the distribution is not normal.

Correlations between geothermal field and the UniFrac distance matrices were calculated in QIIME using the script compare_categories.py, using 999 permutations with PERMANOVA [263] that describes the strength and significance of any correlation. PERMANOVA is a non-parametric test that uses

values within distance matrices and is less sensitive to differences in variance between sample groups than ANOSIM analyses [264]. The null hypothesis for PERMANOVA is that the "centroids" of the groups are equivalent for all groups. Mantel tests were also performed between the sample characteristic distance matrices previously mentioned, and the unweighted and weighted UniFrac distance matrices of the OTUs. These tests were undertaken using the compare_distance_matrices.py script, using a two-tailed test and 999 permutations.

All OTUs were grouped according to assigned phyla, and a Kruskal-Wallis test [262] was performed to determine significant taxonomic differences using a Microsoft Excel spreadsheet downloaded from [262]. To assess significant differences between genera, OTUs from all microcosms were filtered to remove unclassified sequences, and Kruskal-Wallis tests performed on genus clusters. Statistically significant differences in OTU frequencies between sample groups clustered by geothermal field were also determined using Kruskal-Wallis tests.

2.3 Results

2.3.1 Geothermal soil and sediment sampling for thermophilic methanotrophic communities

A total of 59 samples from 14 geothermal fields were collected, with temperatures ranging between 35.0 and 85.3 °C, and with a pH range between pH 1.5 and 9.2. Twenty-five samples were characterised primarily as clay, six as primarily loam, and twelve as sediments (permanently covered with hot spring water). Another 12 samples were classified as mixed soils; either clay/loam, clay/loam/sand, clay/sand or loam/sand. Of the remaining samples, there were two biomass samples (from biofilms attached to the side of a hot spring), one sandy soil, and one water sample (Table 2.1).

It was not possible to measure methane concentrations *in situ* for every sample, due to the nature of some samples (e.g. waterlogged sediments), and the difficulty in inserting the sampling pole at some sites to the depth required for gas sampling. For samples taken at the same location as the 1000 Springs project, the *in situ* concentration of methane measured in the spring water is given.

Table 2.1 Physical characteristics and methane oxidation of microcosms from geothermal sites. Methane oxidation is shown as µmol of methane per gram of soil per day. The methane oxidation value for the Waipahihi sample WAP11 is from an enrichment culture, and is in µmol/day.

Geothermal field	Sample ID	Latitude	Longitude	Temperature (°C)	pH	ppm CH4 *in situ*	Sample description	Soil classification	Incubation temperature (°C)	Soil oxidation	Soil methane oxidation rate µmol/g/day µmol/g/day
Craters of the Moon	COM19	-38.6478	176.0683	70.2	7.6		Orange-red clay soil	C	70	N	0.00
	COM20	-38.6454	176.0693	76.0	6.4		Steaming pink clay	C	70	N	0.00
Golden Springs	GDS1	-38.4651	176.3104	38.9	7.2		Water	W	37	Y	1.35
	GDS2	-38.4651	176.3104	38.0	7.0		Sediment	D	37	Y	1.89
Loop Road	LPR14	-38.4136	176.3611	85.0	2.8		Thick black clay	C	75	Y	2.96
	LPR16	-38.4135	176.3609	67.4	1.5	1593.1	Crumbly brown loam with sinter	L	70	Y	0.57
	LPR17	-38.4135	176.3609	59.4	1.6	3896.2	Loam and clay with lots of leaf litter	C/L	60	Y	1.00
	LPR19	-38.4113	176.3610	50.0	5.4	9.2	Crumbly loam	L	50	N	0.00
Ngatamariki	NGM89	-38.5335	176.1718	70.0	3.0		Beige to orange soil	L	60	Y	1.90

Geothermal field	Sample ID	Latitude	Longitude	Temperature (°C)	pH	ppm CH4 *in situ*	Sample description	Soil classification	Incubation temperature (°C)	Soil oxidation	Soil methane oxidation rate µmol/g/day µmol/g/day
	NGM90	-38.5335	176.1718	51.0	7.0		White surface biomass	D	60	N	0.00
	NGM91	-38.5334	176.1718	60.0	7.0		Sediment	D	60	Y	1.63
	NGM91R	-38.5334	176.1718	60.0	7.0		Sediment	D	60	Y	1.86
Orakei Korako	OKO2	-38.4738	176.1464	71.6	4.3	5.9	Steaming orange clay/sand mixture	C/S	70	Y	17.36
Rotokawa	RTK23	-38.6253	176.1952	77.3	2.1		Black loam + brown sand	L/S	75	N	0.00
Te Kopia	TKA8	-38.4154	176.2151	75.3	4.7	3.4	Black sinter + crumbly orange clay	C	75	Y	0.58
	TKA9	-38.4154	176.2151	66.3	4.2	25.2	Red clay and sandy pale brown loam	C/L/S	70	Y	2.50
	TKA10	-38.4154	176.2151	68.1	4.2	98.6	Purple clay	C	70	N	0.00
	TKA11	-38.4153	176.2152	51.1	4.5		Green layer and orange clay	C	50	N	0.00
	TKA12	-38.4153	176.2152	85.3	4.4		Orange clay and hard white lumps	C	75	N	0.00

Geothermal field	Sample ID	Latitude	Longitude	Temperature (°C)	pH	ppm CH4 *in situ*	Sample description	Soil classification	Incubation temperature (°C)	Soil oxidation	Soil methane oxidation rate µmol/g/day µmol/g/day
	TKA13	-38.4153	176.2152	65.6	4.1		Pink clay	C	70	Y	0.77
	TKA14	-38.4153	176.2152	77.4	4.6	4.6	Orange crumbly clay	C	75	N	0.00
	TKA15	-38.4153	176.2152	70.3	5.1	40.5	Pale orange to white clay soil	C	70	Y	0.67
	TKA16	-38.4153	176.2151	71.6	5.0	14.9	Brown loam	L	70	Y	1.40
	TKA17	-38.4153	176.2150	60.7	5.3	32.7	Dark brown soil	L	60	N	0.00
Tikitere	TKT67	-38.0597	176.3534	75.8	2.6	13.8	Liquid mud from centre	C	70	Y	9.35
	TKT68	-38.0597	176.3534	35.0	3.0		Crusted mud from outside edge	C	50	Y	7.05
Tokaanu	TOK5	-38.9677	175.7653	82.5	7.9	10.1	Clay/loam	C/L	80	N	0.00
	TOK6	-38.9678	175.7654	74.6	7.6		Clay/loam	C/L	70	N	0.00
	TOK7	-38.9679	175.7654	63.7	6.8		Clay	C	60	Y	4.40
	TOK8	-38.9677	175.7654	69.0	7.0		Very wet, thick sticky brown clay	C	70	N	0.00

Geothermal field	Sample ID	Latitude	Longitude	Temperature (°C)	pH	ppm CH4 *in situ*	Sample description	Soil classification	Incubation temperature (°C)	Soil oxidation	Soil methane oxidation rate µmol/g/day µmol/g/day
	TOK9	-38.9678	175.7653	64.0	6.7		Dry sandy soil	S	60	N	0.00
	TOK10	-38.9680	175.7643	58.3	6.9		Sediment	D	60	Y	2.72
	TOK11	-38.9687	175.7626	63.0	9.2		Very fine silky clay	C	60	N	0.00
	TOK12	-38.9687	175.7624	62.5	8.1		Sediment	D	60	Y	1.51
	TOK13	-38.9671	175.7647	82.3	7.9	4.8	Clay/loam	C/L	80	N	0.00
	TOK14	-38.9689	175.7604	71.7	5.4		Red/brown clay	C	70	N	0.00
	TOK15	-38.9689	175.7605	69.6	6.2		Steam affected reddish brown clay	C	70	Y	0.58
	TOK16	-38.9689	175.7605	76.4	6.1	21.3	Pink, brown and yellow clay	C	80	N	0.00
	TOK17	-38.9688	175.7603	63.5	7.7		Pink and gritty sediment	D	60	Y	5.48
Waimangu	WAM36	-38.2829	176.3988	73.0	4.6		Pink clay	C	75	Y	1.67
Waipahihi	WAP11	-38.7020	176.0852	45.0	6.7		Orange sediment	D	46	N/A	**4.55**

Geothermal field	Sample ID	Latitude	Longitude	Temperature (°C)	pH	ppm CH4 *in situ*	Sample description	Soil classification	Incubation temperature (°C)	Soil oxidation	Soil methane oxidation rate µmol/g/day µmol/g/day
Whakarewarewa Village	WHV8	-38.1618	176.2594	80.6	7.0	112*	Grey sediment	D	68	N	0.00
	WHV12	-38.1620	176.2565	58.5	3.0	2.4	Steaming mixture of sand and loam	L/S	60	Y	1.86
	WHV13	-38.1626	176.2583	84.8	8.7	12.3*	Grey sediment from shelf	D	75	Y	0.48
	WHV14	-38.1627	176.2582	75.1	8.3	7.2*	Soft light grey sediment	D	75	N	0.00
	WHV15	-38.1624	176.2566	82.1	6.3	20.2*	Brownish grey biomass	B	75	Y	0.68
	WHV16	-38.1612	176.2579	62.5	5.6		Sediment underneath biomass	D	60	Y	1.53
	WHV18	-38.1612	176.2579	55.7	2.5		White and brown soil	L	60	Y	1.84
	WHV20	-38.1617	176.2596	64.5	5.3		Sediment	D	70	N	0.00
Waikite Valley	WKT43	-38.3274	176.3046	72.4	7.8	47.2	Reddish brown clay mixture	C	70	N	0.00
	WKT44	-38.3274	176.3038	60.0	8.3	2.8	Red moist clay	C	60	N	0.00
	WKT45	-38.3274	176.3038	71.1	8.3	2.3	Red clay	C	70	Y	0.94

Geothermal field	Sample ID	Latitude	Longitude	Temperature (°C)	pH	ppm CH4 *in situ*	Sample description	Soil classification	Incubation temperature (°C)	Soil oxidation	Soil methane oxidation rate µmol/g/day µmol/g/day
	WKT46	-38.3272	176.3044	39.7	5.8	56.8	Brown sandy soil	L/S	40	N	0.00
	WKT46R	-38.3272	176.3044	39.7	5.8	56.8	Brown sandy soil	L/S	40	N	0.00
	WKT47	-38.3272	176.3044	68.4	6.5	732.5	Brown sandy soil + reddish clay	C/S	70	N	0.00
Wairakei Thermal Valley	WTV1	-38.6149	176.0827	69.5	4.0	3.3	Pink clay	C	70	Y	5.34
	WTV2	-38.6149	176.0829	73.2	7.7	3	Black loam and pink clay	C/L	75	Y	1.40
	WTV3	-38.6148	176.0831	79.5	3.7	1.8	White crumbly soil + light pink clay	C	75	N	0.00
	WTV4	-38.6143	176.0801	65.3	4.0		Reddish clay	C	70	Y	1.73

It was not possible to collect gas samples *in situ* for every sample. Gas measurements marked * are taken from the 1000 Springs dataset [247] at the same location. Sample classifications: B, biomass; C, clay; C/L, clay/loam; C/L/S, clay/loam/sand; C/S, clay/sand; D, sediment; L, loam; L/S, loam/sand; S, sand; W, water. Microcosms that showed a greater loss of methane than controls (sampling without replacement) for five consecutive readings, and with a coefficient of determination of linear regression (R^2) > 0.5, were designated as positive for methane oxidation.

2.3.2 Methane oxidation rates in microcosms

Geothermal soil/sediment samples were sealed into glass vials with methane added to the headspace. The headspace methane concentration was measured at regular intervals and the number of µmoles of methane oxidised was calculated. One sediment sample from Waipahihi (WAP11) was placed directly into media for methanotroph enrichment and therefore the rate of methane oxidation measured for this sample is for an enrichment microcosm. This sample was taken at the same location as a 1000 Springs sample that had shown a high proportion of putative methanotrophs, but the location at the edge of a lake meant that the site was partly covered by lake water during sampling for this study and only a small volume of sediment could be collected. Of the remaining 58 microcosms, 31 (51.7 %) were positive for methane oxidation (methane concentrations dropped more than controls five times consecutively, and linear regression R^2 values were > 0.5). Graphs for these calculations are shown in Appendix 7.1. Rates of methane oxidation ranged from 0.48 µmol/g/day (Loop Road - LPR16) to 17.36 µmol/g/day (Orakei Korako - OKO2) (Table 2.1).

The greatest rates of methane oxidation by microcosms were observed for microcosms incubated at either 60 or 70 °C. Methane oxidation was also observed in six microcosms incubated at 75 °C, with LPR14 being notable with the comparably high oxidation rate of 2.96 µmol/g/day (Figure 2.7). Methane oxidation was observed over a wide pH range, from as acidic as pH 1.5 (Loop Road - LPR16, 0.47 µmol/g/day), to pH 8.7 (Whakarewarewa Village - WHV13, 0.48 µmol/g/day). However, the greatest rates of methane oxidation were observed in microcosms with a pH of 2.6 to 7.7 (Figure 2.7).

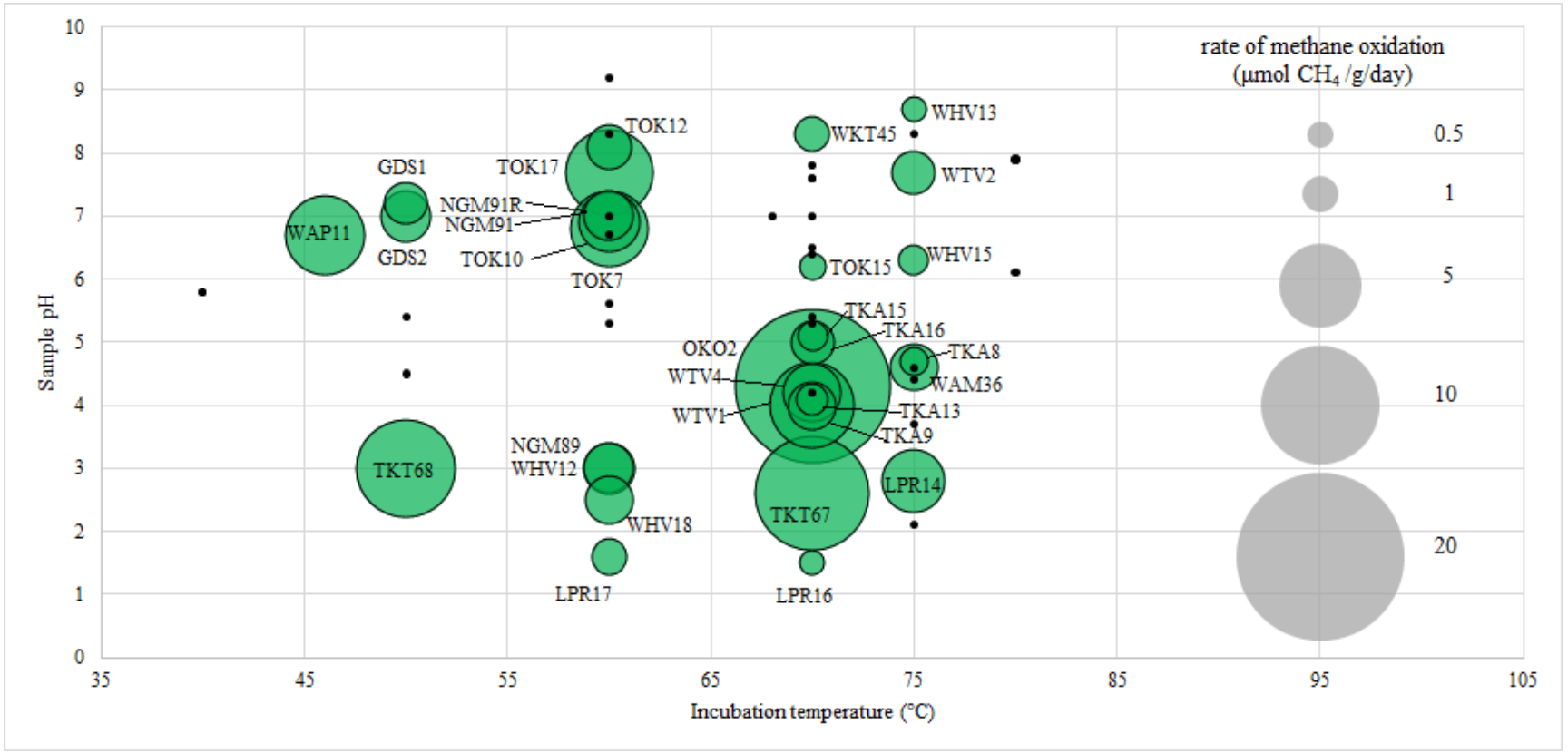

Figure 2.7 Bubble chart of methane oxidation rates of soil microcosms from all geothermal field samples. Green circles, microcosms that oxidised methane, labelled with microcosm identifier. The size of the bubble is proportional to the rate (µmol CH_4 g^{-1} d^{-1}). Black dots, microcosms that did not oxidise methane (not labelled with microcosm identifier).

2.3.3 Correlations between environmental characteristics and microcosm methane oxidation rates

Rates of methane oxidation were not obviously associated with measured soil characteristics including temperature or pH (Figure 2.7), *in situ* methane concentration (Figure 2.8) or the geographical location of the sampling sites (Figure 2.9).

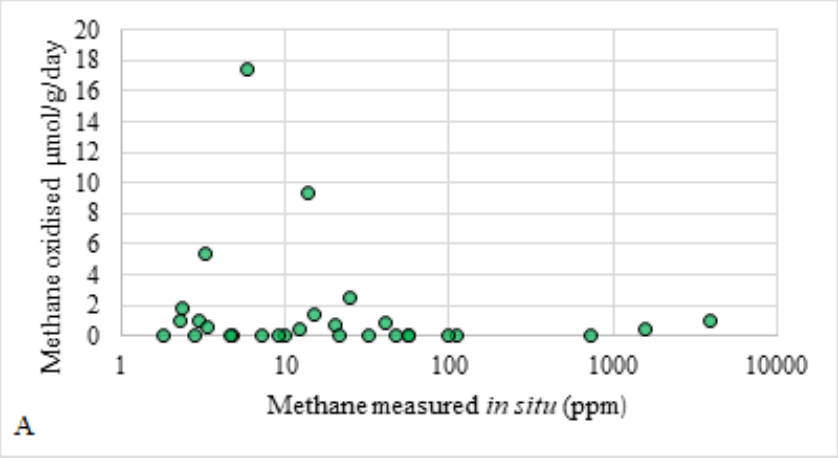

Figure 2.8 Scatter plot of methane oxidation of microcosms versus methane concentration measured *in situ.*

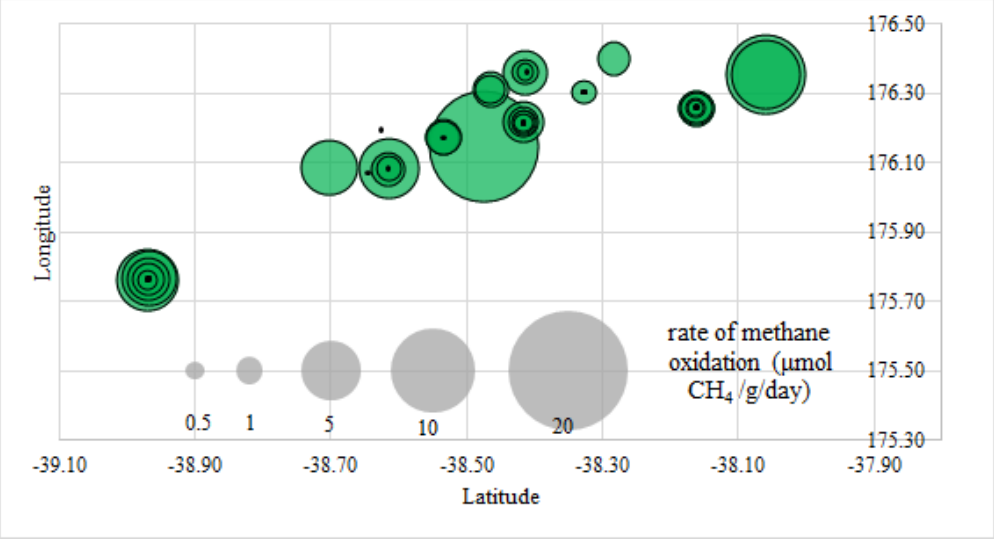

Figure 2.9 Bubble chart of methane oxidation rates of soil microcosms versus geographical location of sampling sites. Green circles, microcosms that oxidised methane. The size of the bubble is proportional to the rate (µmol CH_4 g^{-1} d^{-1}).

Statistical tests were also used to determine if observed rates of methane oxidation within microcosms correlated to any measured soil characteristics. Distance matrices for pH, temperature, *in situ* methane concentration and the latitude and longitude of the samples were tested against a distance matrix of values for μmol methane oxidised per gram of soil per day, using a Mantel test [261]. The results indicate that there were no significant correlations between the rate of methane oxidation and any of these continuous environmental factors (Table 2.2).

Table 2.2 Mantel test results between continuous environmental variables and the rate of methane oxidation of microcosms.

Variable	***p*-value**	**Test statistic (*r*)**
pH	0.501	0.04
Temperature	0.948	0.01
in situ methane concentration	0.617	-0.08
Geographical location	0.768	0.02

The discrete environmental variables of geothermal field and sample type were also plotted against methane oxidation rates, and again, no association could be identified (Figure 2.10 and Figure 2.11).

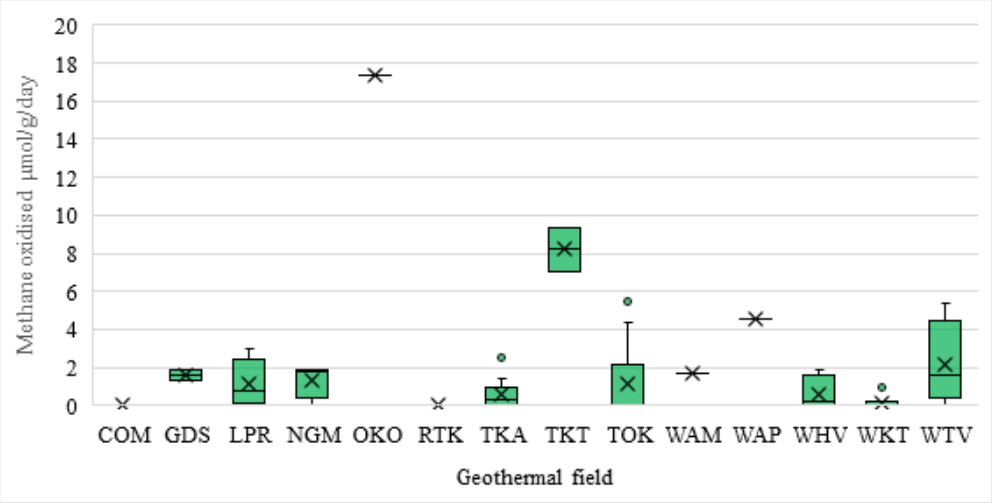

Figure 2.10 Box and whisker plot of methane oxidation rates by geothermal field. The cross indicates the mean methane oxidation rate (µmol g^{-1} d^{-1}). Dots within boxes represent individual microcosms; dots outside boxes indicate outliers. COM; Crater of the Moon (2 samples), GDS; Golden Spring (2), LPR; Loop Road (4), NGM; Ngatamariki (4), OKO; Orakei Korako (1), RTK; Rotokawa (1), TKA; Te Kopia (10), TKT; Tikitere (2), TOK; Tokaanu (13), WAM; Waimangu (1), WAP; Waipahihi (1), WHV; Whakarewarewa Village (8), WKT; Waikite (6), WTV; Wairakei Thermal Village (4).

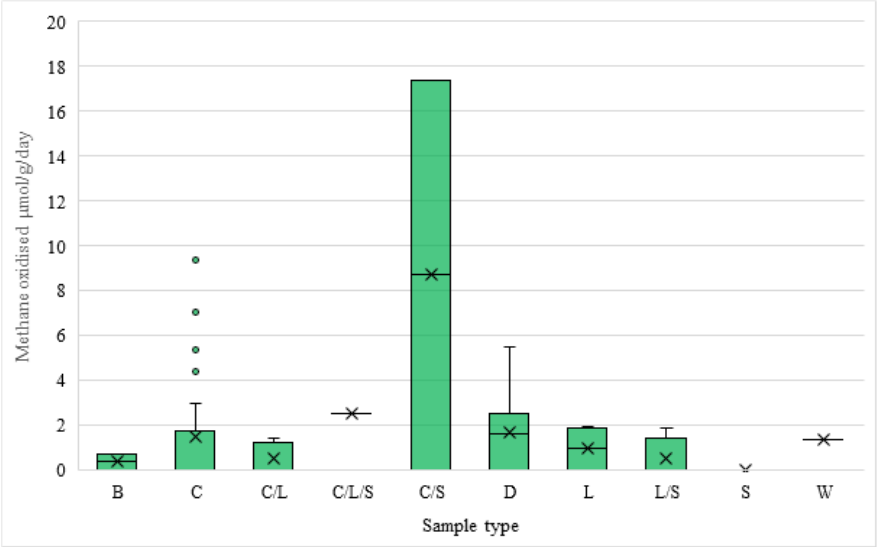

Figure 2.11 Box and whisker plot of methane oxidation rates by sample type. The cross indicates the mean methane oxidation rate (µmol g^{-1} d^{-1}). Dots within boxes represent individual microcosms; dots outside boxes indicate outliers. B, biomass (2 samples); C, clay (25); C/L, clay/loam (5); C/L/S, clay/loam/sand (1); C/S, clay/sand (2); D, sediment (12); L, loam (6); L/S, loam/sand (4); S, sand (1); W, water (1).

The discrete attributes were then analysed using a Kruskal-Wallis [262] test (Table 2.3). The Kruskal-Wallis test does not rely on the assumption that data is normally distributed, but may be less accurate when the groups used are heteroscedastic (have unequal variance) or if group sizes are small (<5) [265], so this result must be viewed with caution. Other non-parametric tests, such as the Friedman test [266] or Welch's ANOVA [262], which are less reliant on homoscedasticity, depend on an equal number of observations within each group, and so were not appropriate to use.

Table 2.3 Kruskal-Wallis test results between discrete environmental variables (sample type and geothermal field) and the rate of methane oxidation of microcosms. Significant *p*-values (< 0.05) are highlighted in bold.

Variable	*p*-value	Test statistic (H)
Sample type	0.627	7.097
Geothermal field	**0.047**	22.564

2.3.4 Microcosm 16S rRNA gene sequencing summary

After quality filtering and normalisation to 149,400 reads per microcosm, a final total of 8,605 OTUs was observed across all microcosms. The number of OTUs for each microcosm varied from 222 (Te Kopia TKA9) to 3140 (Golden Springs GDS2) (Table 2.4). The non-parametric diversity metric Chao1 [257] was used to estimate the richness of the microcosms, and rarefaction curves showed that sequencing captured most of the diversity (Figure 2.12) as the rarefaction curves tended toward an asymptote for all microcosms. A comparison between the number of OTUs found and the number of OTUs estimated by the Chao1 parameter confirmed this conclusion indicating that the sequencing effort represented between 60.08 % (Whakarewarewa WHV20) and 93.32 % (Tikitere TKT68) of the total predicted taxa (Table 2.4). The Shannon Diversity Index (H), which can take any value from zero upwards, was used to estimate the microcosm richness and evenness by analysing the diversity of OTUs and the relative abundance of each of these OTUs (Table 2.4). This confirmed that many of the microcosms were highly diverse, with the sediment microcosm Golden Springs GDS2 having the highest index of 9.06.

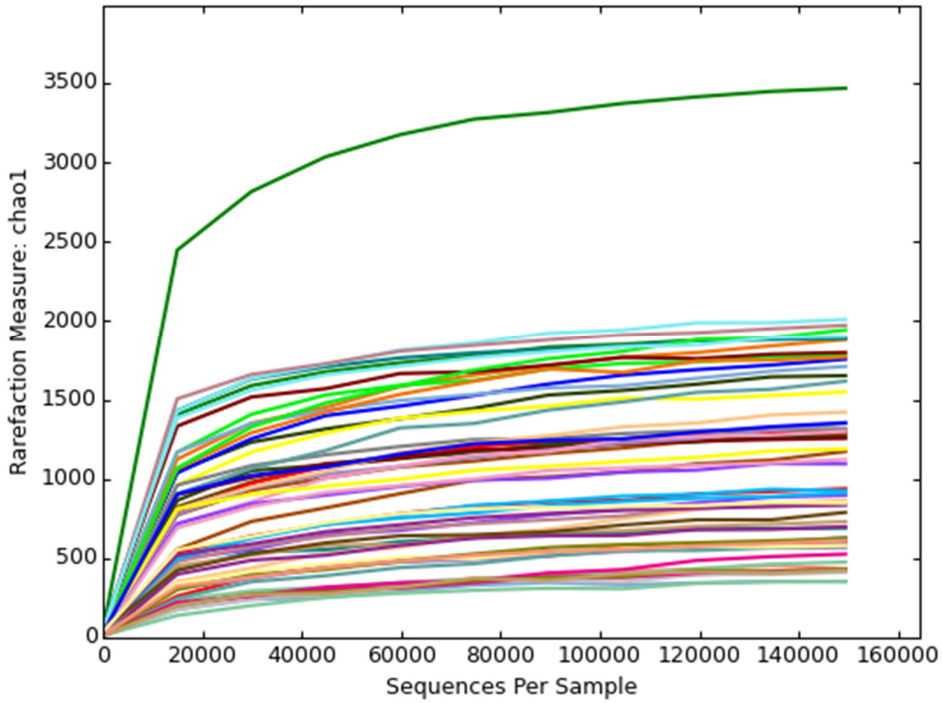

Figure 2.12 Chao1 rarefaction curves of estimated total OTUs for all geothermal microcosm, showing the estimated microcosm richness. The different colours represent sequences from each microcosm (not labelled); the highest green line represents the Golden Springs sample GDS2.

Table 2.4 Illumina 16S rRNA gene sequencing data of the microbial communities.

Microcosm ID	Number of OTUs	Chao1 estimated taxa	percentage of Chao1 estimate	Shannon index of sample	Percentage of archaeal OTUs	Percentage of bacterial OTUs	Number of unique described genera	Most abundant phylum	Percentage of *Alpha-proteobacteria* methanotrophs	Percentage of *Gamma-proteobacteria* methanotrophs	Percentage of *Verrucomicrobia* methanotrophs
COM19	731	938	77.93	5.38	91.11	8.89	87	*Bathyarchaeota*	0	0.003	0.126
COM20	1130	1354	83.46	6.08	79.76	20.24	133	*Bathyarchaeota*	0	0.003	0.173
GDS1	1527	1878	81.31	5.89	2.69	97.31	153	*Proteobacteria*	0	0.318	0.393
GDS2	3140	3467	90.57	9.06	38.28	61.72	241	*Proteobacteria*	0.002	1.465	0.034
LPR14	547	699	78.25	3.18	92.89	7.11	70	*Crenarchaeota*	0	0.146	2.657
LPR16	1010	1189	84.95	6.51	58.76	41.24	92	*Bathyarchaeota*	0	0.058	1.609
LPR17	1715	1901	90.22	7.78	41.23	58.77	176	*Thaumarchaeota*	0	0.013	10.381
LPR19	933	1122	83.16	5.77	49.66	50.34	121	*Thaumarchaeota*	0.006	0.001	0.290
NGM89	391	585	66.84	4.47	1.70	98.30	49	*Verrucomicrobia*	0	0.015	60.714
NGM90	1096	1306	83.92	7.17	15.96	84.04	133	*Thermotogae*	0.001	0.013	0.004
NGM91	451	630	71.59	5.19	0.43	99.57	66	*Armatimonadetes*	0	5.148	0.017

Microcosm ID	**Number of OTUs**	**Chao1 estimated taxa**	**percentage of Chao1 estimate**	**Shannon index of sample**	**Percentage of archaeal OTUs**	**Percentage of bacterial OTUs**	**Number of unique described genera**	**Most abundant phylum**	**Percentage of *Alpha-proteobacteria* methanotrophs**	**Percentage of *Gamma-proteobacteria* methanotrophs**	**Percentage of *Verrucomicrobia* methanotrophs**
NGM91R	1492	1943	76.79	6.76	13.36	86.64	194	*Thermotogae*	0	0.011	0.025
OKO2	288	434	66.36	4.28	92.35	7.65	40	*Bathyarchaeota*	0	0	0
RTK23	1481	1708	86.71	7.41	49.63	50.37	167	*Crenarchaeota*	0	0.058	0.677
TKA8	1099	1420	77.39	6.73	30.76	69.24	119	*Chloroflexi*	0.001	0.003	0.028
TKA9	222	354	62.71	4.07	98.26	1.74	31	*Bathyarchaeota*	0	0.001	0.037
TKA10	1057	1349	78.35	6.94	43.80	56.20	101	*Thaumarchaeota*	0.008	0.037	0.501
TKA11	455	581	78.31	5.77	37.79	62.21	35	*Thaumarchaeota*	0	0	0.003
TKA12	260	412	63.11	4.45	99.84	0.16	25	*Crenarchaeota*	0	0	0.009
TKA13	299	431	69.37	4.97	81.99	18.01	37	*Bathyarchaeota*	0	0.001	0.015
TKA14	716	913	78.42	6.12	53.29	46.71	65	*Thaumarchaeota*	0	0.005	0.077
TKA15	290	423	68.56	3.97	11.17	88.83	46	*Armatimonadetes*	0	0.002	0.021
TKA16	284	432	65.74	5.05	71.29	28.71	23	*Bathyarchaeota*	0	0	0.005

Microcosm ID	Number of OTUs	Chao1 estimated taxa	percentage of Chao1 estimate	Shannon index of sample	Percentage of archaeal OTUs	Percentage of bacterial OTUs	Number of unique described genera	Most abundant phylum	Percentage of *Alpha-proteobacteria* methanotrophs	Percentage of *Gamma-proteobacteria* methanotrophs	Percentage of *Verrucomicrobia* methanotrophs
TKA17	931	1094	85.10	5.74	67.17	32.83	99	*Thaumarchaeota*	0.007	0.027	8.598
TKT67	1816	1973	92.04	7.53	53.49	46.51	198	*Crenarchaeota*	0.011	0.111	0.641
TKT68	1759	1885	93.32	7.71	49.92	50.08	196	*Thaumarchaeota*	0.009	0.098	0.683
TOK5	1647	1796	91.70	8.08	37.36	62.64	195	*Thaumarchaeota*	0.006	0.655	0.714
TOK6	1379	1650	83.58	7.41	10.31	89.69	254	*Proteobacteria*	0	0.023	1.448
TOK7	1029	1283	80.20	6.72	40.46	59.54	144	*Bathyarchaeota*	0	11.225	17.946
TOK8	1096	1295	84.63	6.55	19.98	80.02	183	*Proteobacteria*	0.005	0.025	0.831
TOK9	1413	1754	80.56	6.73	29.75	70.25	195	*Thaumarchaeota*	0.023	0.005	0.289
TOK10	1461	1767	82.68	6.90	43.58	56.42	168	*Thaumarchaeota*	0	0.402	0.081
TOK11	1744	1892	92.18	7.06	54.61	45.39	205	*Thaumarchaeota*	0.001	0.094	0.629
TOK12	681	834	81.65	6.19	5.75	94.25	86	*Parcubacteria*	0	0.001	0.002
TOK13	1305	1548	84.30	5.87	58.32	41.68	173	*Crenarchaeota*	0	0.027	0.049

Microcosm ID	Number of OTUs	Chao1 estimated taxa	percentage of Chao1 estimate	Shannon index of sample	Percentage of archaeal OTUs	Percentage of bacterial OTUs	Number of unique described genera	Most abundant phylum	Percentage of *Alpha-proteobacteria* methanotrophs	Percentage of *Gamma-proteobacteria* methanotrophs	Percentage of *Verrucomicrobia* methanotrophs
TOK14	1805	2010	89.80	7.38	56.38	43.62	208	*Thaumarchaeota*	0.002	0.079	0.720
TOK15	1003	1299	77.21	6.46	37.33	62.67	116	*Thaumarchaeota*	0	0.003	0.033
TOK16	1209	1615	74.86	6.63	64.73	35.27	140	*Thaumarchaeota*	0	0.456	6.424
TOK17	594	789	75.29	5.85	8.47	91.53	64	*Armatimonadetes*	0	4.104	0.258
WAM36	1195	1316	90.81	6.66	73.88	26.12	134	*Crenarchaeota*	0	0.019	1.147
WAP11	1558	1775	87.77	6.00	11.62	88.38	213	*Deinococcus-Thermus*	0.001	0.012	0.524
WHV8	442	612	72.22	5.11	27.62	72.38	57	*Aquificae*	0	0	0.005
WHV12	248	352	70.45	4.05	47.26	52.74	36	*Verrucomicrobia*	0	0.001	50.602
WHV13	537	866	62.01	4.90	45.68	54.32	91	*Aquificae*	0	0.001	0.416
WHV14	323	476	67.86	5.22	22.91	77.09	36	*Thermodesulfobacteria*	0	0	0.007
WHV15	433	566	76.50	4.76	59.10	40.90	52	*Crenarchaeota*	0	0.004	0.110
WHV16	730	848	86.08	6.43	4.27	95.73	63	*Chlorobi*	0	0.001	0.002

Microcosm ID	Number of OTUs	Chao1 estimated taxa	percentage of Chao1 estimate	Shannon index of sample	Percentage of archaeal OTUs	Percentage of bacterial OTUs	Number of unique described genera	Most abundant phylum	Percentage of *Alpha-proteobacteria* methanotrophs	Percentage of *Gamma-proteobacteria* methanotrophs	Percentage of *Verrucomicrobia* methanotrophs
WHV18	276	352	78.41	3.03	99.04	0.96	48	*Euryarchaeota*	0	0.003	0.496
WHV20	316	526	60.08	4.40	57.21	42.79	45	*Aquificae*	0	0.001	0.006
WKT43	720	925	77.84	5.76	48.91	51.09	109	*Thaumarchaeota*	0.001	0.002	0.007
WKT44	570	731	77.98	6.28	17.78	82.22	63	*Deinococcus-Thermus*	0	0.003	0.003
WKT45	452	622	72.67	3.57	88.72	11.28	39	*Aigarchaeota*	0	0.001	0.015
WKT46	648	896	72.32	4.98	13.94	86.06	78	*Chloroflexi*	0.052	0	6.030
WKT46R	652	842	77.43	4.90	14.25	85.75	68	*Chloroflexi*	0.114	0	3.500
WKT47	585	690	84.78	4.69	77.19	22.81	72	*Thaumarchaeota*	0.003	0	13.936
WTV1	1138	1256	90.61	6.35	77.31	22.69	130	*Bathyarchaeota*	0.001	0.006	12.021
WTV2	1135	1265	89.72	6.16	77.87	22.13	132	*Bathyarchaeota*	0	5.483	8.689
WTV3	818	1172	69.80	4.62	92.49	7.51	131	*Bathyarchaeota*	0	0.010	0.576
WTV4	402	603	66.67	4.41	92.59	7.41	48	*Bathyarchaeota*	0	0	0.639

An assessment of the community composition of all of the microcosms indicate that many of the soil communities were highly diverse, with 618 described genera from 76 archaeal and bacterial phyla across all normalised reads (Table 2.4), and a high number of OTUs from many microcosms were affiliated to sequences from taxa known only through metagenomic sequencing and with no described or isolated representatives. Across all microcosms, the average number of OTUs were 927 from 110 described genera. However, there was a very wide range as the least diverse microcosm, Te Kopia TKA16, contained only 23 genera whilst Tokaanu TOK6 included sequences from 254 described genera. Bacterial reads comprised the majority of sequences in 56 % of the microcosms (n = 33). However, in 12 of these microcosms, an archaeal taxon was the most abundant phylum, reflecting the high diversity within these microcosms (Table 2.4). In total, *Thaumarchaeota* was the most abundant phylum in 16 of the microcosms, but in all of these the *Thaumarchaeota* were still less than 50 % of the total reads. This was reflected in other microcosms too; the 'most abundant' phylum comprised more than 30 % of the total reads in only 34 of the microcosms (57.6 %). In four microcosms, the dominant phylum was actually less than 20 % of the total reads; Tokaanu TOK5, 19 % *Thaumarchaeota*; Whakarewarewa WHV16, 18 % *Chlorobi*; Golden Springs GDS2, 17 % *Proteobacteria*; and Tokaanu TOK17, 15 % *Armatimonadetes.*

2.3.5 Differences in alpha and beta diversity between oxidising and non-oxidising communities

For further analysis, geothermal microcosms were divided into two cohorts on the basis of whether methane oxidation was observed (microcosms showed a greater loss of methane than controls and R^2 was > 0.5) or was absent. The QIIME workflow core_diversity_analyses.py (Appendix 7.2) was used to determine differences in alpha diversity, or variance between the microbial communities of the geothermal microcosms that oxidised methane and those that did not. The Shannon (Figure 2.13) and Simpson (Figure 2.14) diversity indices, which take into account both OTU richness and the relative abundances of those OTUs, both indicated that there was no significant difference in alpha diversity between the two cohorts (non-parametric two-sample t-test performed using QIIME: $p = 0.247$ for Shannon and $p = 0.195$ for Simpson). However, the methane-oxidising

microcosms showed a discernibly greater range of diversity indices and had higher numbers of OTUs (7230 compared to 5112) and slightly more unique described genera (553 vs. 506) than the non-methane-oxidising microcosms.

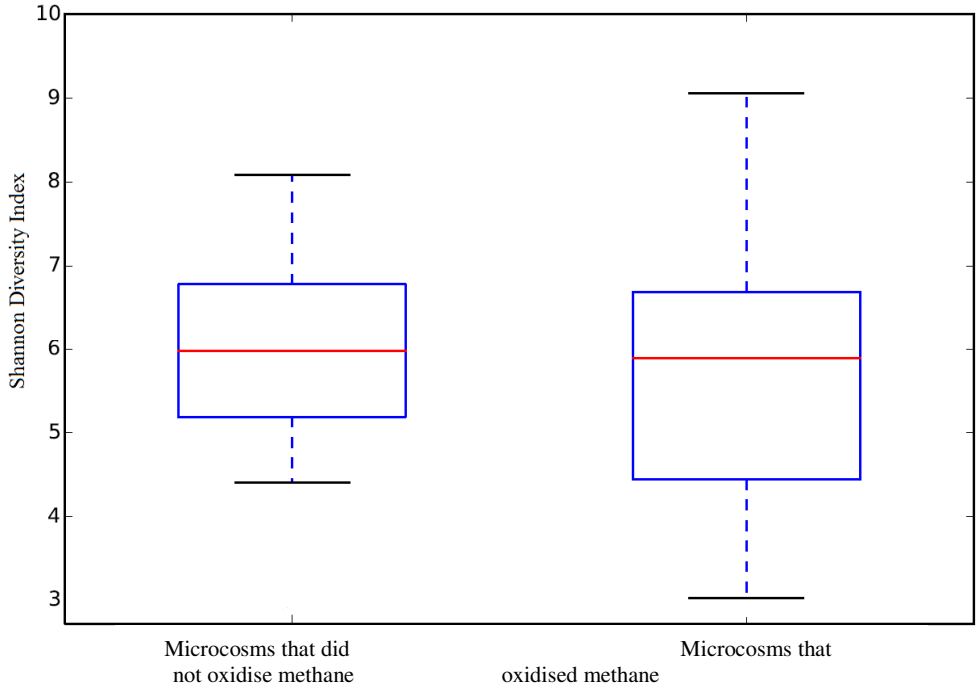

Figure 2.13 Boxplots of the Shannon index for the geothermal soil microcosms, split by methane oxidation status. Boxes, interquartile ranges; horizontal lines, medians; whiskers, highest and lowest values within 1.5x the interquartile range.

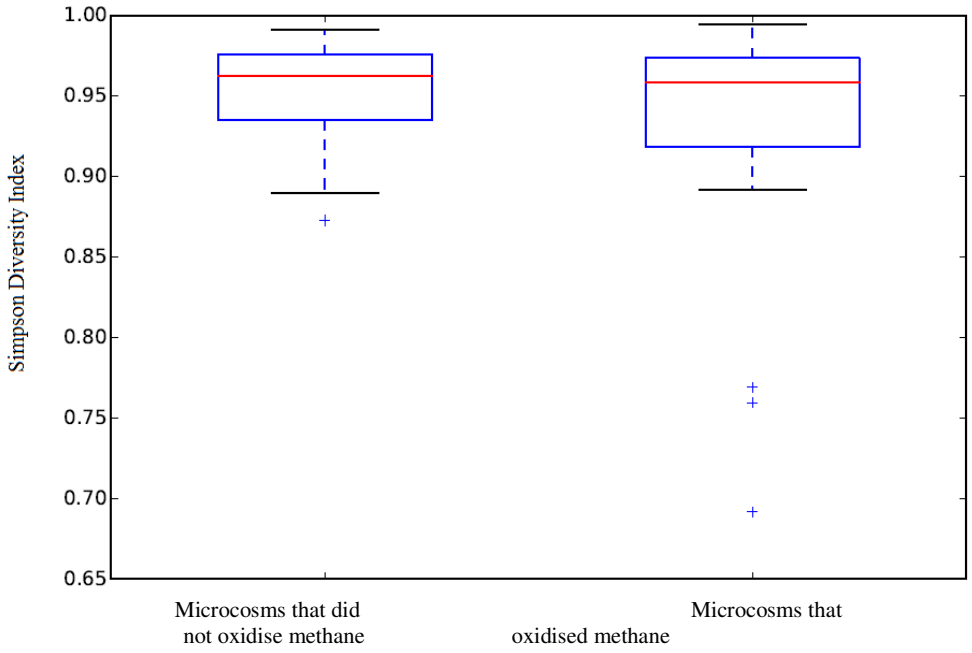

Figure 2.14 Boxplots of the Simpson index for the geothermal soil microcosms, split by methane oxidation status. Boxes, interquartile ranges; horizontal lines, medians; whiskers, highest and lowest values within 1.5x the interquartile range; +, outliers.

To compare the beta diversity (differences in microbial community composition) across the microcosm cohorts, principal coordinates analyses (PCoA) were performed on samples using both unweighted and weighted UniFrac metrics (Figure 2.15 and Figure 2.16). Unweighted UniFrac is a qualitative measure based on the presence or absence of taxa, and can be used to determine the effects of environmental factors that can constrain growth such as temperature [267]. Weighted UniFrac is a quantitative measure that analyses changes in the abundance of individual taxa, and can identify the effects of more transient environmental factors such as nutrient availability [260]. PCoA analysis using both metrics indicated that the two microcosm cohorts represented overlapping microbial communities, with factors 1 and 2 combined accounting for 28 % of the variance between communities using the unweighted metric (Figure 2.15), and for 45 % of the variance with the weighted metric (Figure 2.16), as the impact of low-abundance taxa was diminished. Regression analysis of the PCoA factors on environmental variables may have identified correlations with factors other than methane oxidation, such as temperature or pH.

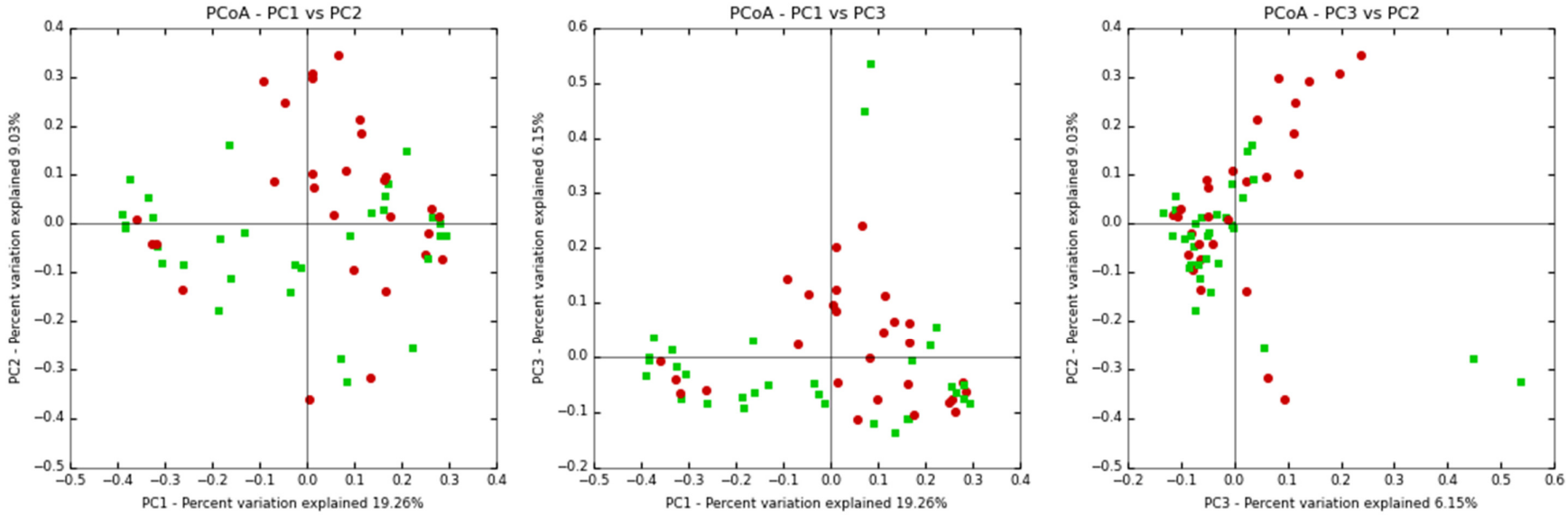

Figure 2.15 Principal Coordinates Analysis of the differences between microbial communities using an unweighted UniFrac metric across all microcosms. Microcosms that oxidised methane are represented as green squares; microcosms that did not oxidise methane as red dots.

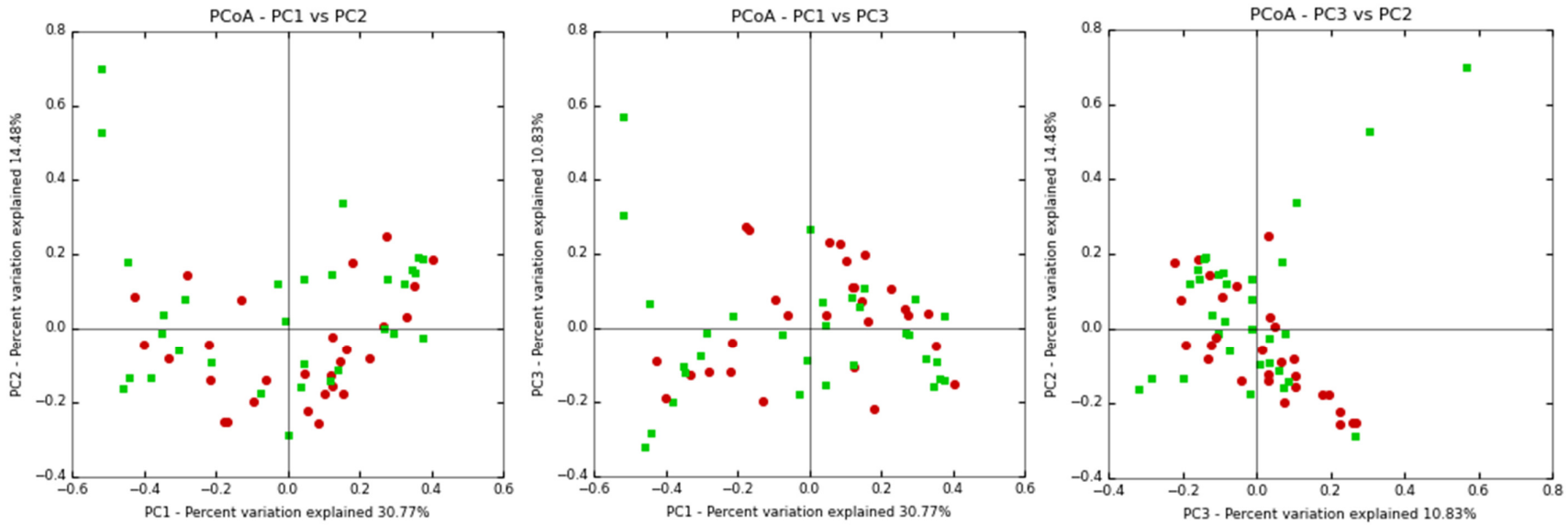

Figure 2.16 Principal Coordinates Analysis of the differences between microbial communities using a weighted UniFrac metric across all microcosms. Microcosms that oxidised methane are represented as green squares; microcosms that did not oxidise methane as red dots.

2.3.6 Differences in phyla between oxidising and non-oxidising communities

At phylum level, the microcosms within each cohort appeared to be equally diverse, containing 29-30 phyla at abundances of more than 0.2 %, with only three phyla not appearing in sequences from both cohorts (Figure 2.17 and Figure 2.18). *Korarchaeota* and *Acetothermia* were only identified at this abundance in the methane-oxidising microcosms (0.3 % and 0.7 %, respectively, of total reads across all microcosms in this group) and candidate division WD272 was only identified in the microcosms that did not oxidise methane (0.6 % of total reads in this group).

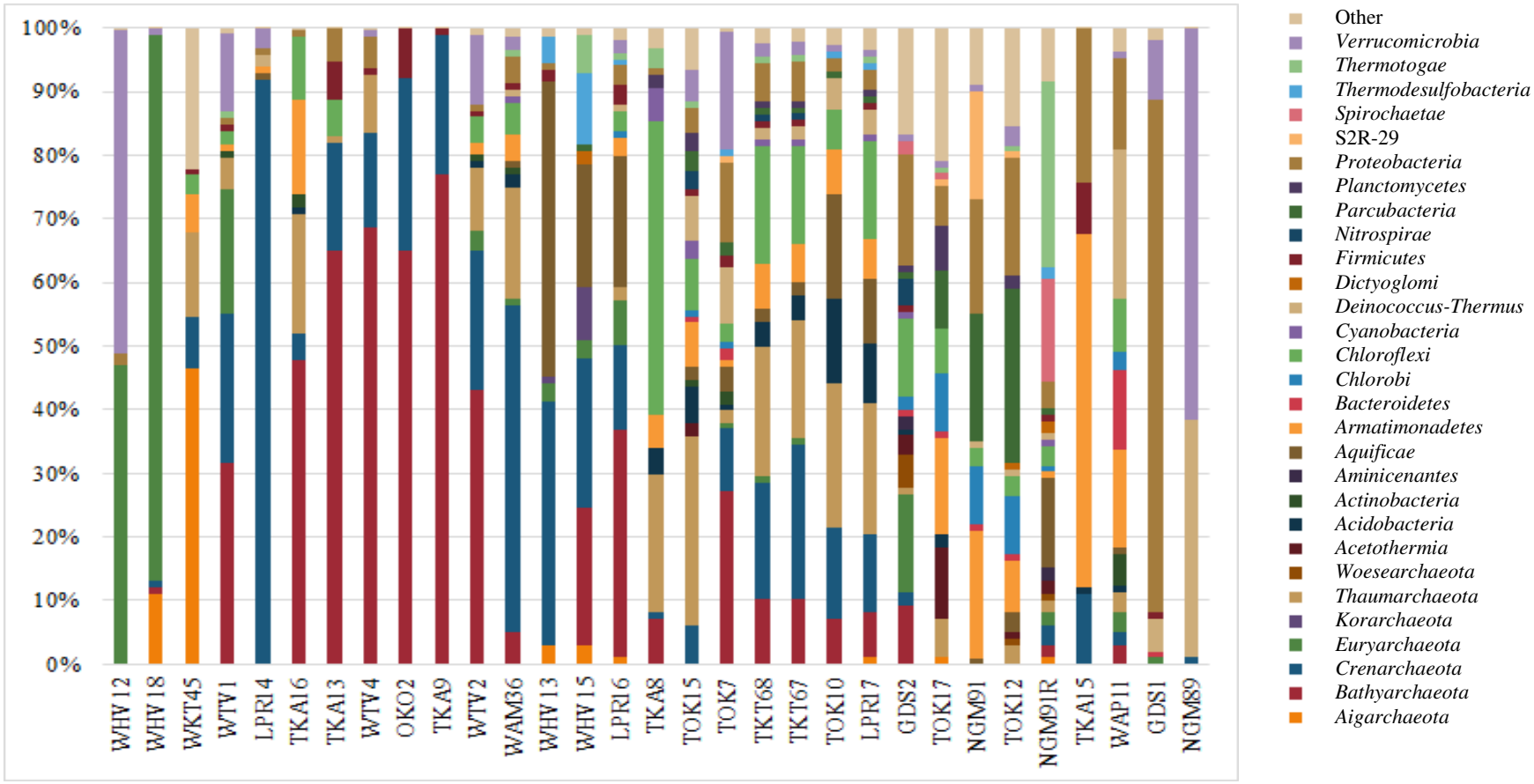

Figure 2.17 Microbial community structure at phylum-level classification of the microcosms exhibiting methane oxidisation. Taxa that formed less than 0.2 % of the reads were summed and clustered as 'Other'. Samples are clustered using a UPGMA tree based on a weighted UniFrac metric.

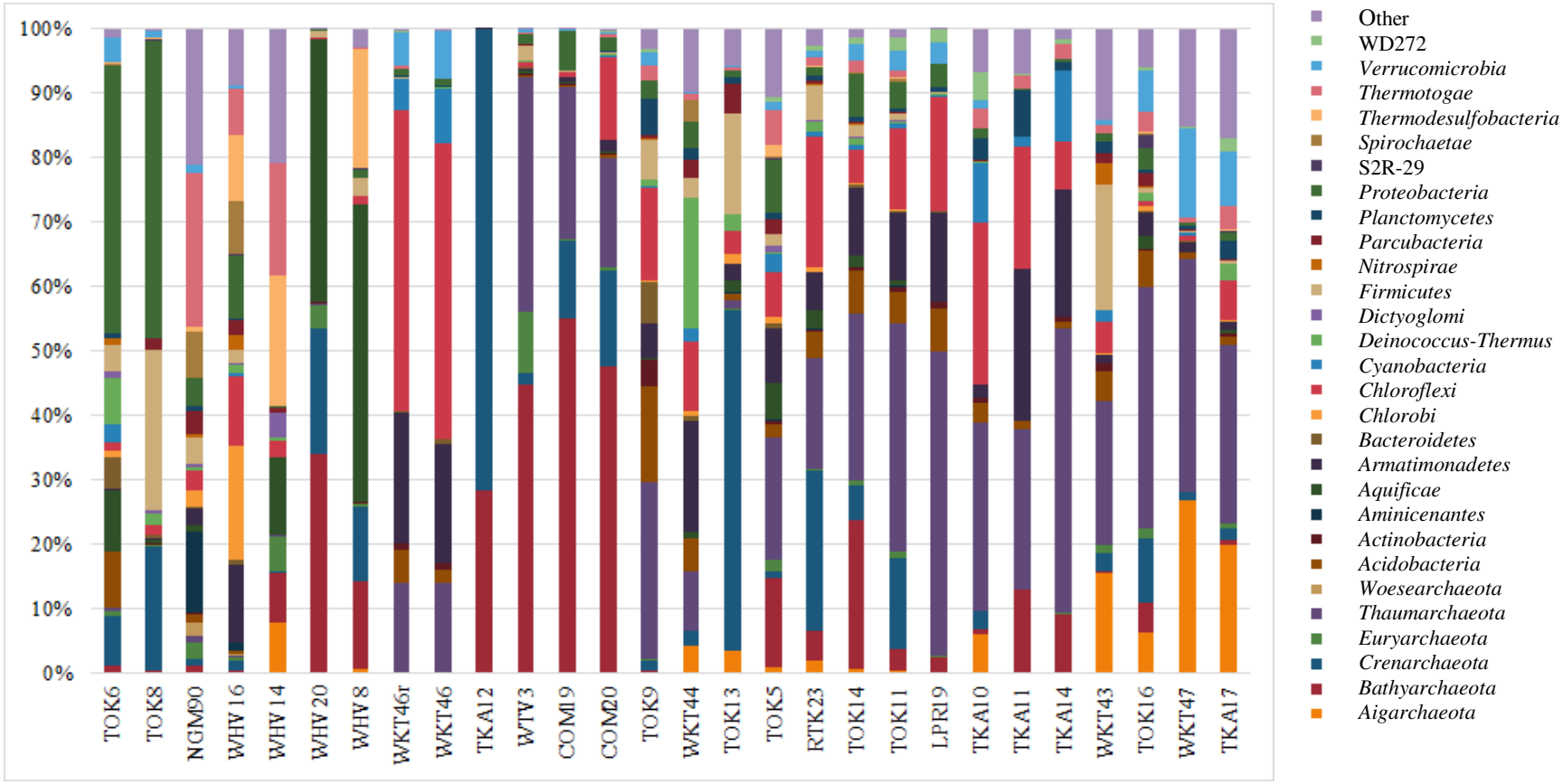

Figure 2.18 Microbial community structure at phylum-level classification of the microcosms that did not oxidise methane. Taxa that formed less than 0.2 % of the reads were summed and clustered as 'Other'. Samples are clustered using a UPGMA tree based on a weighted UniFrac metric.

The proportions of OTU sequences from phyla which comprised more than 1 % of the total reads were plotted for methane-oxidising and non-methane oxidising communities (Figure 2.19). The sum total of the normalised OTU read abundances were assessed using a Kruskal-Wallis analysis to determine significance (Table 2.5). The phylum *Proteobacteria* was separated into classes for this analysis, as there were more than 1500 OTU sequences affiliated with the phylum, and the maximum number of observations that can be used in a Kruskal-Wallis test is 1000. This indicated that of the ten phyla which were more abundant in methane-oxidising microcosms, only the differences between *Aquificae*, *Deinococcus-Thermus* and *Verrucomicrobia* populations were not significant (*p*-value < 0.05).

Table 2.5 An assessment of the significance of the differential abundance of phyla in microcosms displaying positive methane oxidation. Only taxa with an abundance of more than 1 % of total normalised reads are shown. Phyla that were significantly different (*p*-value < 0.05) using a Kruskal-Wallis analysis between the microcosm cohorts are highlighted in **bold**.

	Sum percentage of normalised reads across all microcosms			
Phylum	**Methane-oxidising**	**Non-methane-oxidising**	***p*-value**	**Test statistic (H)**
Bathyarchaeota	17.52 %	11.04 %	**<0.0001**	100.12
Crenarchaeota	14.86 %	10.04 %	**0.005**	7.34
Euryarchaeota	6.21 %	1.14 %	**<0.0001**	45.20
Aquificae	4.62 %	4.56 %	0.251	1.32
Chlorobi	0.97 %	1.23 %	**0.0003**	22.14
Deinococcus-Thermus	3.25 %	1.57 %	0.066	3.37
Deltaproteobacteria	2.14 %	1.06 %	**<0.0001**	53.76
Gammaproteobacteria	3.28 %	1.18 %	**0.012**	6.37
Parcubacteria	2.19 %	0.87 %	**<0.0001**	71.22
Verrucomicrobia	6.04 %	2.32 %	0.799	0.06

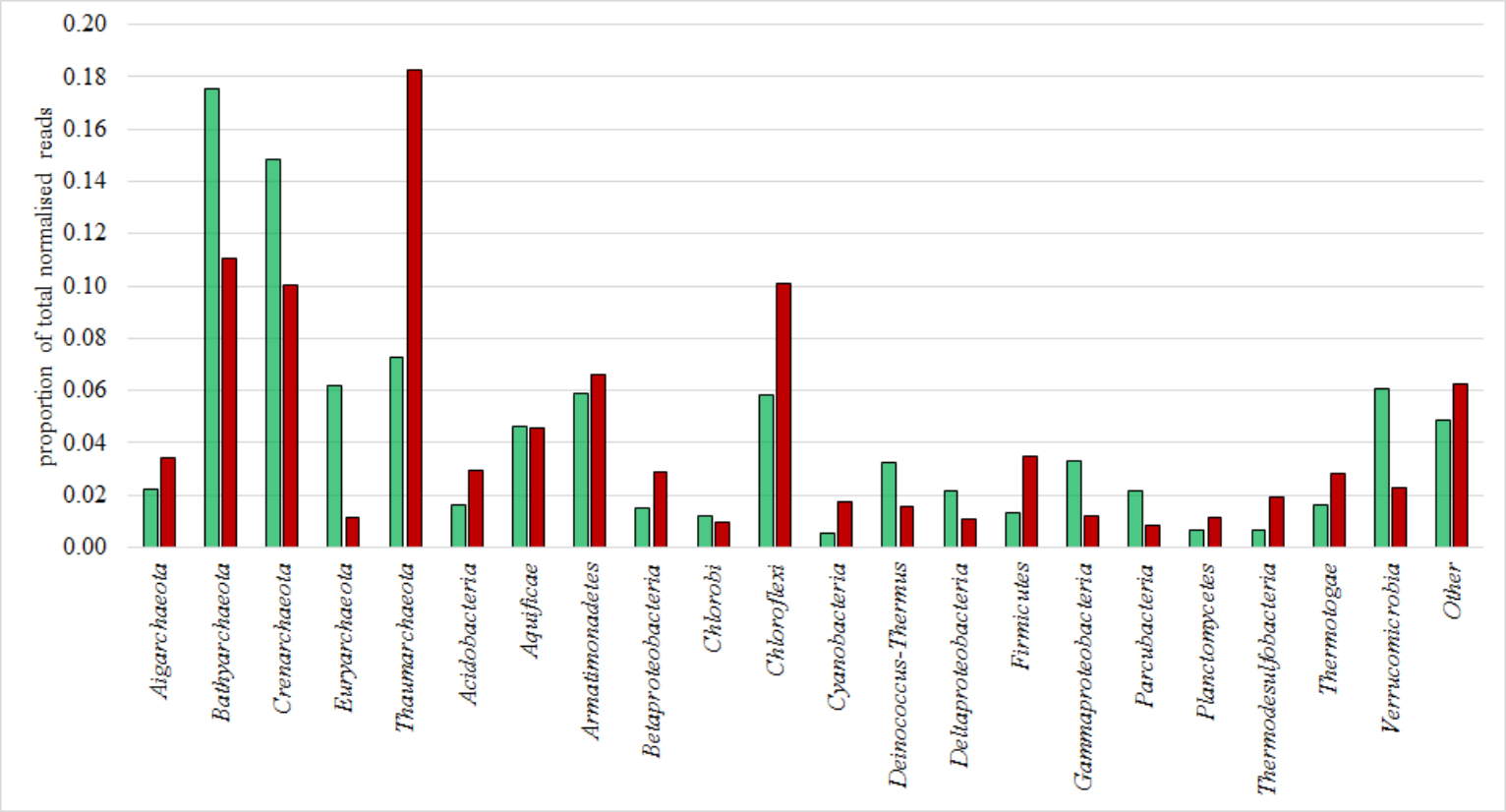

Figure 2.19 The total relative abundance of bacterial and archaeal phyla within individual microcosms, according to observed methane oxidising capability. Samples that oxidised methane are presented as green columns, and samples that did not oxidise methane as red columns. Taxa that formed less than 1 % of the total normalised reads in all samples were summed and classified as 'Other'.

2.3.7 Differences in genera between oxidising and non-oxidising communities

Across all microcosms, 6 of the described archaeal and bacterial genera (0.1 %) were found in more than 90 % of the geothermal microcosms: *Methylacidiphilum* (*Verrucomicrobia*), *Chthonomonas* (*Armatimonadetes*), *Thermus* (*Deinococcus-Thermus*), *Sulfolobus* (*Crenarchaeota*), *Thermoplasma* (*Euryarchaeota*) and *Caldimicrobium* (*Thermodesulfobacteria*). These apparently ubiquitous genera were not usually abundant however, with OTUs from each of these genera comprising an average of < 5 % of the total reads in the microcosms.

There were 66 other described genera that comprised > 1 % of the total normalised reads in any one microcosm, in addition to the six most common genera previously listed (Extended Data Set 2). Many of these are known thermophilic genera isolated from geothermal soils or hot springs, or mesophilic microorganisms that inhabit ecological niches in soils or plants. For example, OTUs related to the ubiquitous genus *Pseudomonas* [268] were identified in 32 microcosms, and made up 46.9 % of the reads from the methane-oxidising Golden Springs water column microcosm GDS1; however, the average abundance of *Pseudomonas* OTUs across all microcosms was only 0.9 % of the total microbial community. There were also some more unusual genera found during this survey. *Exilispira* (*Spirochaetae*) and *Mesoaciditoga* (*Thermotogae*) were both isolated from hydrothermal vents [269, 270], but comprised a maximum of 15.4 % and 4.6 % of the geothermal sediment microcosms from Ngatamariki NGM91R and NGM90, respectively. OTUs related to *Metallosphaera* spp. (*Crenarchaeota*), which are obligately thermoacidophilic sulfur and iron-oxidising archaea generally found in acidic springs (< pH 3.0) [271], composed 6.5 % of the reads from Wairakei Thermal Valley WTV4 (pH 4.0), and were also found to comprise more than 1 % of two pH-neutral microcosms; Wairakei Thermal Valley WTV2, pH 7.7 (1.4 %) and Tokaanu TOK7, pH 6.8 (1.1 %).

In order to further assess the taxonomic differences between the oxidising and non-oxidising communities, a Kruskal-Wallis test was performed on OTU clusters grouped at the genus level. To do this, OTUs from all microcosms were filtered to remove sequences that were unable to be classified at genus level, were termed as ‘ambiguous taxa’, and/or were taxa known only through metagenomic sequencing

with no isolates or enrichment cultures. With these OTUs removed, inferences could be made based on inferred function within a community. All OTUs were clustered according to their most similar (described) genus before a Kruskal-Wallis test was performed on each set, and this showed that 11 genera were significantly enriched in the methane-oxidising microcosms, including known methanotrophic clades such as *Methylacidiphilum* and *Methylothermus* (Table 2.6).

Table 2.6 Kruskal-Wallis assessment of the genera abundant in microcosms that were positive for methane oxidation. Only taxa with an abundance of > 0.01 % of total normalised reads and a *p*-value of < 0.05 are shown.

		Sum percentage of normalised reads across all microcosms			
Phylum	**Genus**	**Methane-oxidising microcosms**	**Non-methane oxidising microcosms**	***p*-value**	**Test statistic (H)**
Verrucomicrobia	*Methylacidiphilum*	5.74 %	1.63 %	**0.012**	6.26
Euryarchaeota	*Thermoplasma*	4.25 %	0.34 %	**<0.0001**	35.32
Proteobacteria	*Pseudomonas*	1.64 %	0.21 %	**0.011**	6.55
Proteobacteria	*Methylothermus*	1.06 %	0.05 %	**0.046**	4.00
Proteobacteria	*Sulfurimonas*	0.38 %	0.02 %	**<0.0001**	29.95
Firmicutes	*Alicyclobacillus*	0.37 %	0.24 %	**0.0005**	12.23
Proteobacteria	*Nitratifractor*	0.05 %	0.00 %	**0.0122**	6.275
Spirochaetae	*Brevinema*	0.03 %	0.02 %	**0.0339**	4.500
Proteobacteria	*Sulfurovum*	0.02 %	0.00 %	**0.0002**	13.562

As the rate of methane oxidation was weakly associated with geothermal field (Table 2.3), a PERMANOVA test was used to assess if the taxa enriched in methane-oxidising microcosms were associated with the geothermal field where the microcosm was sampled. Distance matrices of all OTUs within the methane-oxidising and non-methane-oxidising cohorts were created using both weighted and unweighted UniFrac metrics. The PERMANOVA analysis showed that geothermal field was significantly associated with differences in taxa (*p*-value < 0.05) using both the weighted and unweighted UniFrac metrics (Table 2.7), although the test statistic in both cases was low, indicating a weak association.

Table 2.7 PERMANOVA test results between UniFrac distance matrices of OTUs and geothermal field. Significant *p*-values (< 0.05) are highlighted in **bold**.

	Weighted UniFrac metric		**Unweighted UniFrac metric**	
	***p*-value**	**Test statistic (pseudo-F)**	***p*-value**	**Test statistic (pseudo-F)**
Geothermal field	**0.001**	2.355	**0.001**	2.251

A Kruskal-Wallis analysis of variance on the abundances of OTUs compared to geothermal field (Extended Data Set 4) showed that the association was primarily due to OTUs that were from either the Golden Springs GDS2 sediment sample with the most diverse community (3140 OTUs, Table 2.4), or the GDS1 water column sample taken directly above GDS2 (Extended Data Set 5). This did include three OTUs identified as *Pseudomonas* and one *Brevinema* OTU, but other OTUs identified as these genera were also found in other microcosms. The eight other genera that were significantly associated with a particular geothermal field (Table 2.8) included *Crenotalea*, a heterotroph isolated from a hot spring in Japan [272], which was represented by ten OTUs all strongly associated with the single microcosm from the Waipahihi geothermal field.

Table 2.8 Kruskal-Wallis assessment of genera significantly associated with geothermal field. Only taxa with an abundance of > 1 % of total normalised reads and a *p*-value of < 0.05 are shown. OTUs identified as "ambiguous taxa" are not shown.

OTU ID	Phylum	Genus	Geothermal field associated with	Mean number of normalised reads in this geothermal field	*p*-value	Test statistic (H)
OTU_37	*Euryarchaeota*	*Thermogymnomonas*	Whakarewarewa (WHV)	3816.0	0.048	22.5
OTU89	*Actinobacteria*	*Thermoleophilum*	Waipahihi (WAP)	7573.0	0.024	24.8
OTU_32	*Aquificae*	*Aquifex*	Whakarewarewa (WHV)	5888.8	0.046	22.6
OTU_58	*Bacteroidetes*	*Crenotalea*	Waipahihi (WAP)	8961.0	0.0007	35.6
OTU_7068	*Bacteroidetes*	*Crenotalea*	Waipahihi (WAP)	4297.0	0.0005	36.4
OTU_4613	*Bacteroidetes*	*Crenotalea*	Waipahihi (WAP)	1403.0	0.002	32.0
OTU_197	*Chloroflexi*	*Thermomicrobium*	Waipahihi (WAP)	2089.0	0.040	23.2
OTU_27	*Spirochaetae*	*Exilispira*	Ngatamariki (NGM)	5443.5	0.035	23.6
OTU_20	*Thermodesulfobacteria*	*Caldimicrobium*	Whakarewarewa (WHV)	5676.9	0.012	27.1
OTU_8772	*Thermodesulfobacteria*	*Thermodesulfobacterium*	Whakarewarewa (WHV)	2958.4	0.023	25.0

2.3.8 Sequences related to known aerobic methanotrophs

To identify potential methanotrophs, 16S rRNA gene sequences from all microcosms in both cohorts were searched and sequences of putative aerobic methanotroph OTUs were then manually checked against the NCBI database. The list of these OTUs can be found in Appendix 7.3, and the full OTU table in Extended Dataset 3. Most methanotroph OTUs from *Proteobacteria* were most closely related to *Methylothermus* (18 OTUs) and *Methylomonas* (10 OTUs) (*Gammaproteobacteria*), with smaller numbers from *Crenothrix*, *Methylocaldum*, *Methylococcus* and *Methylomicrobium* (*Gammaproteobacteria*); and *Methylocapsa*, *Methylocystis* and *Methylosinus* (*Alphaproteobacteria*) (Figure 2.20). Putative methanotrophs from *Verrucomicrobia* were almost universally closely related to *Methylacidiphilum* (74 OTUs), with the exception of one OTU that affiliated with *Methylacidimicrobium* (Figure 2.21). Putative methanotroph OTUs were found in all geothermal microcosms, covering a temperature range of 35.0 to 85.3 °C and from pH 1.5 to pH 9.2 (Figure 2.22A and B).

(Facing page)

Figure 2.20 Unrooted phylogenetic tree of the putative methanotroph OTUs from *Proteobacteria*. The evolutionary history was inferred using Neighbour-Joining [124], and evolutionary distances were computed using the Maximum Composite Likelihood method [127]. Bootstrap values are shown at the branch nodes (1000 replicates). The scale bar represents 0.02 nucleotide substitutions per site. Analyses were conducted in MEGA7 [126].

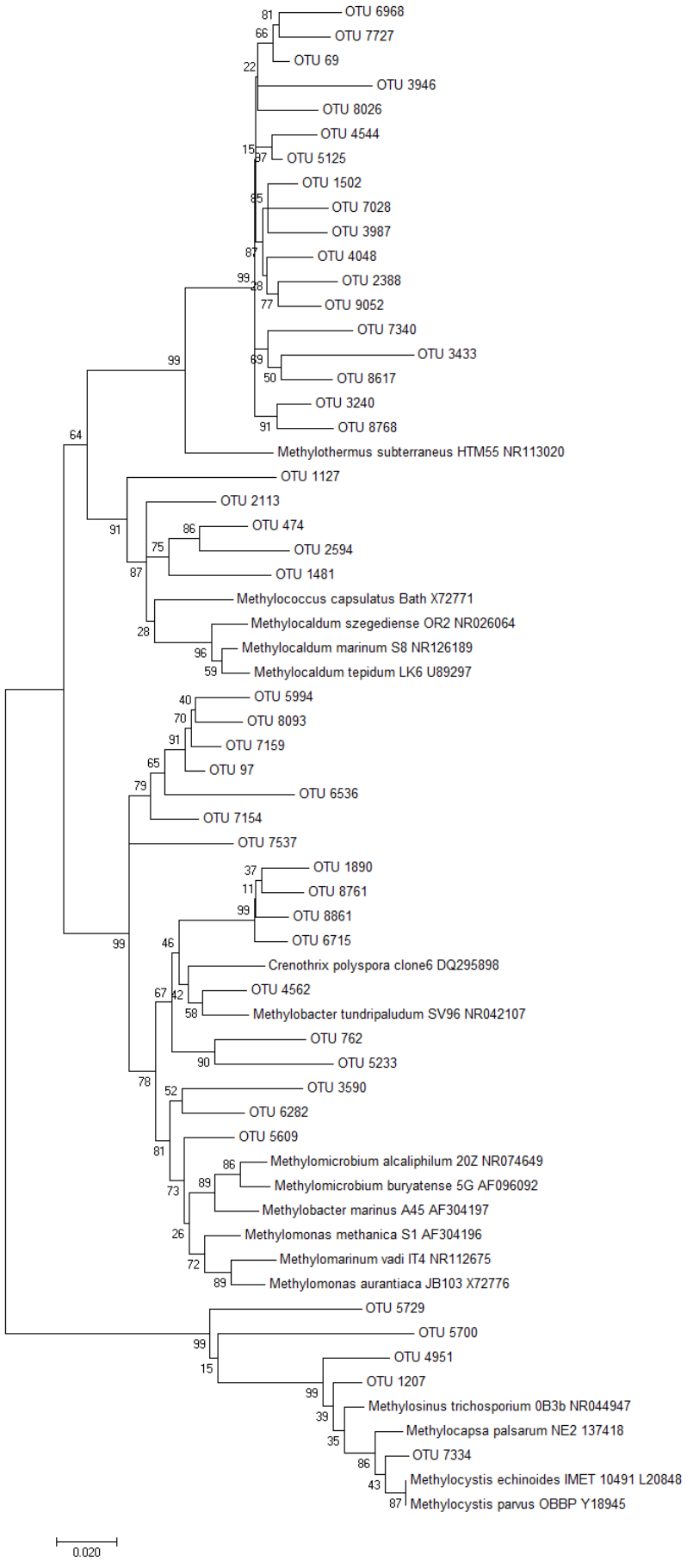
OTU 6968
OTU 7727
OTU 69
OTU 3946
OTU 8026
OTU 4544
OTU 5125
OTU 1502
OTU 7028
OTU 3987
OTU 4048
OTU 2388
OTU 9052
OTU 7340
OTU 3433
OTU 8617
OTU 3240
OTU 8768
Methylothermus subterraneus HTM55 NR113020
OTU 1127
OTU 2113
OTU 474
OTU 2594
OTU 1481
Methylococcus capsulatus Bath X72771
Methylocaldum szegediense OR2 NR026064
Methylocaldum marinum S8 NR126189
Methylocaldum tepidum LK6 U89297
OTU 5994
OTU 8093
OTU 7159
OTU 97
OTU 6536
OTU 7154
OTU 7537
OTU 1890
OTU 8761
OTU 8861
OTU 6715
Crenothrix polyspora clone6 DQ295898
OTU 4562
Methylobacter tundripaludum SV96 NR042107
OTU 762
OTU 5233
OTU 3590
OTU 6282
OTU 5609
Methylomicrobium alcaliphilum 20Z NR074649
Methylomicrobium buryatense 5G AF096092
Methylobacter marinus A45 AF304197
Methylomonas methanica S1 AF304196
Methylomarinum vadi IT4 NR112675
Methylomonas aurantiaca JB103 X72776
OTU 5729
OTU 5700
OTU 4951
OTU 1207
Methylosinus trichosporium 0B3b NR044947
Methylocapsa palsarum NE2 137418
OTU 7334
Methylocystis echinoides IMET 10491 L20848
Methylocystis parvus OBBP Y18945
0.020

(Facing page)

Figure 2.21 Unrooted Phylogenetic tree of the putative methanotroph OTUs from *Verrucomicrobia*. The evolutionary history was inferred using Neighbour-Joining [124], and the evolutionary distances were computed using the Maximum Composite Likelihood method [127]. Bootstrap values are shown at the branch nodes (1000 replicates). The scale bar represents 0.005 nucleotide substitutions per site. Analyses were conducted in MEGA7 [126].

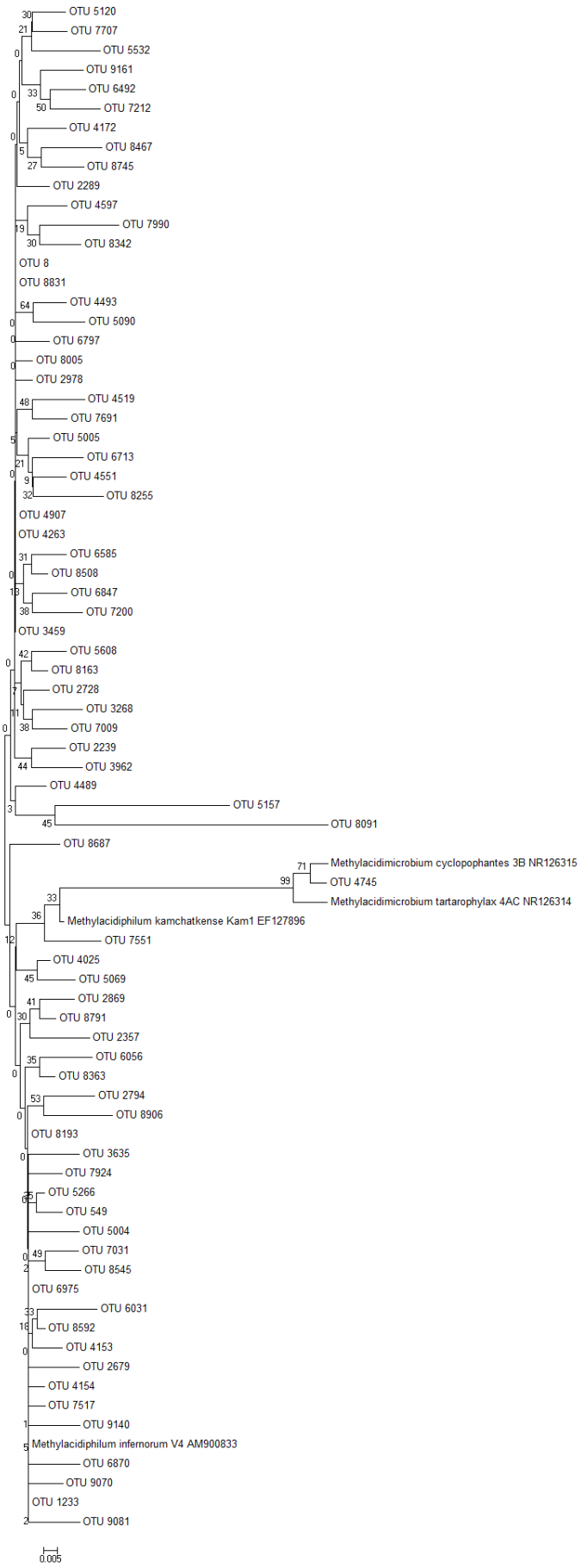
OTU 5120
OTU 7707
OTU 5532
OTU 9161
OTU 6492
OTU 7212
OTU 4172
OTU 8467
OTU 8745
OTU 2289
OTU 4597
OTU 7990
OTU 8342
OTU 8
OTU 8831
OTU 4493
OTU 5090
OTU 6797
OTU 8005
OTU 2978
OTU 4519
OTU 7691
OTU 5005
OTU 6713
OTU 4551
OTU 8255
OTU 4907
OTU 4263
OTU 6585
OTU 8508
OTU 6847
OTU 7200
OTU 3459
OTU 5608
OTU 8163
OTU 2728
OTU 3268
OTU 7009
OTU 2239
OTU 3962
OTU 4489
OTU 5157
OTU 8091
OTU 8687
Methylacidimicrobium cyclopophantes 3B NR126315
OTU 4745
Methylacidimicrobium tartarophylax 4AC NR126314
Methylacidiphilum kamchatkense Kam1 EF127896
OTU 7551
OTU 4025
OTU 5069
OTU 2869
OTU 8791
OTU 2357
OTU 6056
OTU 8363
OTU 2794
OTU 8906
OTU 8193
OTU 3635
OTU 7924
OTU 5266
OTU 549
OTU 5004
OTU 7031
OTU 8545
OTU 6975
OTU 6031
OTU 8592
OTU 4153
OTU 2679
OTU 4154
OTU 7517
OTU 9140
Methylacidiphilum infernorum V4 AM900833
OTU 6870
OTU 9070
OTU 1233
OTU 9081
0.005

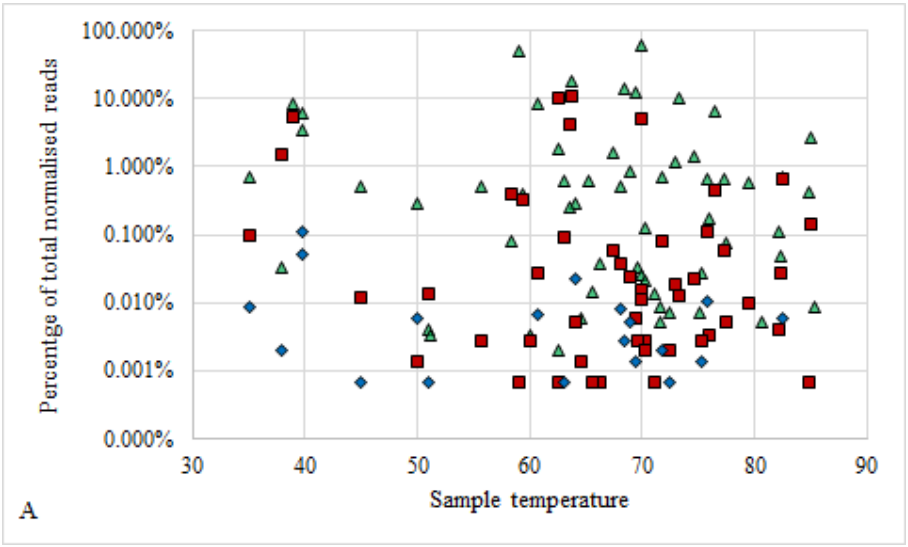

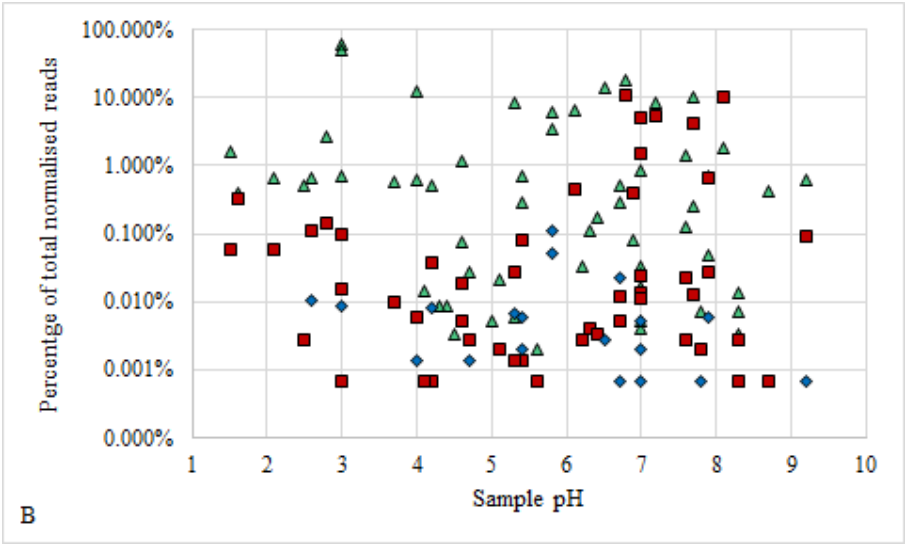

Figure 2.22 Scatter plots of temperature (A) and pH (B) versus proportion of aerobic methanotrophs from total normalised 16S rRNA gene sequences. Symbol shape indicates phylogenetic affiliation of methanotrophs; *Alphaproteobacteria,* blue diamonds; *Gammaproteobacteria*, red squares; *Verrucomicrobia,* green triangles. Temperatures plotted reflect the *in situ* microcosm temperatures.

Alphaproteobacterial methanotroph OTUs were identified in 19 of all of the microcosms but were only present in low abundance within all of these microcosms; these OTUs were present an average of 0.004 % of all reads, and the highest proportion of reads detected were 0.1 % of all normalised sequences from a Waikite soil (WKT46R). Geothermal microcosms containing

alphaproteobacterial methanotroph OTUs most closely related to the genus *Methylocystis* were detected at pHs ranging between 4.2 to 7.7, and temperatures between 38.0 and 77.3 °C.

In comparison, OTUs related to methanotrophs from *Gammaproteobacteria* were identified within 49 microcosms and were more abundant than those from *Alphaproteobacteria*, with an average abundance of 0.7 % of all reads, and a maximum of 11.2 % of all normalised reads from a Tokaanu soil, TOK7. The microcosms ranged from pH 1.5 to pH 9.2, and from 35.0 °C to 85.0 °C. The majority of methanotroph reads affiliated most closely to *Methylothermus* strains, which are thermophilic [57, 62], but the Golden Springs microcosms GDS1 (38.9 °C, pH 7.2) and GDS2 (38.0 °C, pH 7.0) also contained a small number of OTUs most similar to thermotolerant (*Methylococcus* or *Methylocaldum*) and mesophilic (*Methylomonas*, *Crenothrix* and *Methylobacter*) strains.

Methylacidiphilum strains from *Verrucomicrobia* were the most ubiquitous and the most abundant methanotrophs found in the survey. They were detected in all 59 microcosms, forming an average of 3.7 % of all reads from each microcosm, and 60.7 % of all reads from the Ngatamariki geothermal soil microcosm, NGM89. As the microcosms ranged in temperature from 35.0 to 85.0 °C, and from pH 1.5 to pH 9.2, it is unlikely that these sequences all represent active methanotrophs. Most of the OTUs were most closely related to *M. infernorum* that cannot grow below 50 °C [14], although another isolate from the same genus, *M. kamchatkense,* is able to grow at 37 °C [55]. None of the strains from either *Methylacidiphilum* or the mesophilic sister taxon *Methylacidimicrobium* can grow above pH 6 [47, 273].

2.3.9 Sequences related to putative anaerobic methanotrophs

Orakei Korako microcosm OKO2 was collected from a steam-influenced soil characterised as clay/sand (Figure 2.5D) and showed the greatest rate of methane oxidation (17.36 µmol/g/day). The soil was moderately acidic (pH 4.3) with a temperature of 71.6 °C. An analysis of the community composition revealed very few known methanotrophic OTUs within the sample. The only reads associated with a known methanotrophic phenotype were *Methylacidiphilum* OTUs, however

these were at such low levels (13 reads total) that they almost certainly are not responsible for the observed rates of methane oxidation. The microcosm was instead dominated (65.4 % of total normalised reads) by *Bathyarchaeota* sequences (Figure 2.17). As recently published genomes of this phylum suggest that some strains may be capable of anaerobic methanotrophy [20], it is tempting to suggest that these candidate taxa may be responsible for the methane oxidation observed, despite the microcosm being under aerobic conditions. Other anaerobic methanotrophs, including *Methanoperedens* and ANME-1, were only detected at low abundance in the Golden Springs microcosm GDS2, which also contained several known aerobic methanotrophs.

2.3.10 Replicability of microcosm methane oxidation and DNA extraction methodology

Two soil microcosms were selected to test the consistency of DNA extraction and sequencing procedures (Waikite WKT46R) and whether re-sampling an ecosystem yielded 16S rRNA sequences and rates of methane oxidation that were consistent with previous observations (Ngatamariki NGM91R). For the first test, DNA was extracted in duplicate from the Waikite WKT46 microcosm after methane oxidation was shown to be negative. The two DNA samples were then labelled WKT46 and WKT46R, and sequenced on separate Illumina runs. WKT46R showed a very similar community structure to its replicate pair WKT46 (Figure 2.23), demonstrating the reproducibility of the extraction and sequencing process from geothermal soils. Both samples were dominated by reads from the phylum *Chloroflexi* and had comparable numbers of OTUs (652 and 648 respectively) and numbers of unique described genera (68 and 78). There was a slight difference in the proportion of putative methanotrophs detected in the two samples; *Methylacidiphilum* sequences made up 3.5 % of the total normalised reads of WKT46R but 6.0 % of WKT46, but there were almost no methanotrophs identified from either *Alpha-* or *Gammaproteobacteria* in either sample.

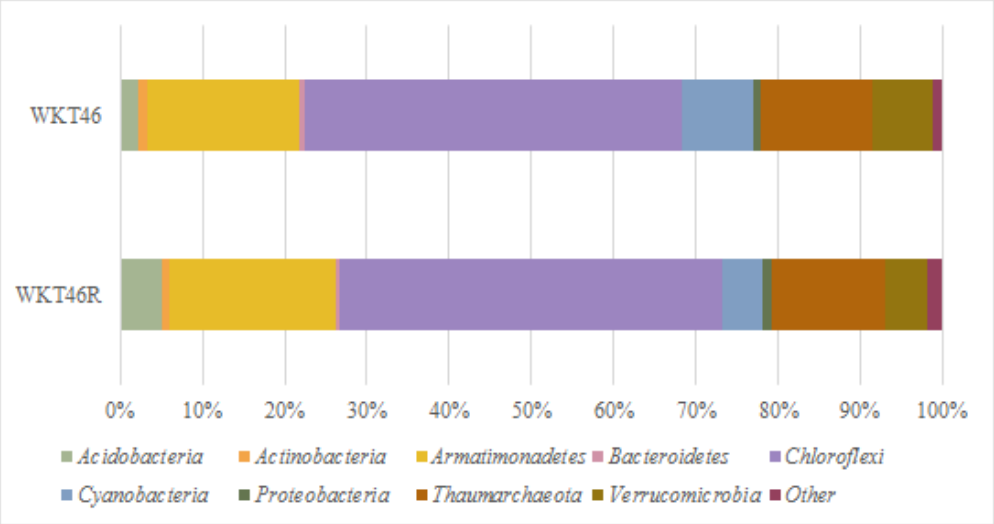

Figure 2.23 Microbial community structure of WKT46 and WKT46R. Phyla that formed < 1 % of the reads in both samples were summed and are referred to as 'Other'.

To test the replicability of re-sampling a geothermal ecosystem, a soil microcosm was collected from the same location as Ngatamariki NGM91, nine months later. The temperature and pH had remained constant (60 °C and pH 7.0). Both microcosms were positive for methane oxidation, with NGM91 oxidising 1.63 µmol CH_4 per gram of soil per day, and NGM91R oxidising 1.86 µmol/g/day. In contrast to WKT64/WKT46R, the microbial community of the duplicate NGM91R exhibited a markedly different composition from that of NGM91 (Figure 2.24). NGM1R displayed increased diversity, with 1492 OTUs compared to 451 from NGM91 and a total of 194 unique described genera in contrast to only 66 found in the first sample. NGM91 was dominated by reads affiliated to *Armatimonadetes* (20.2 % of total normalised reads) and the candidate divisions *Parcubacteria* (19.5 %) and *S2R-29* (16.8 %), but *Thermotogae* (29.2 %), *Spirochaetae* (16.4 %) and *Aquificae* (13.8 %) dominated the duplicate sample.

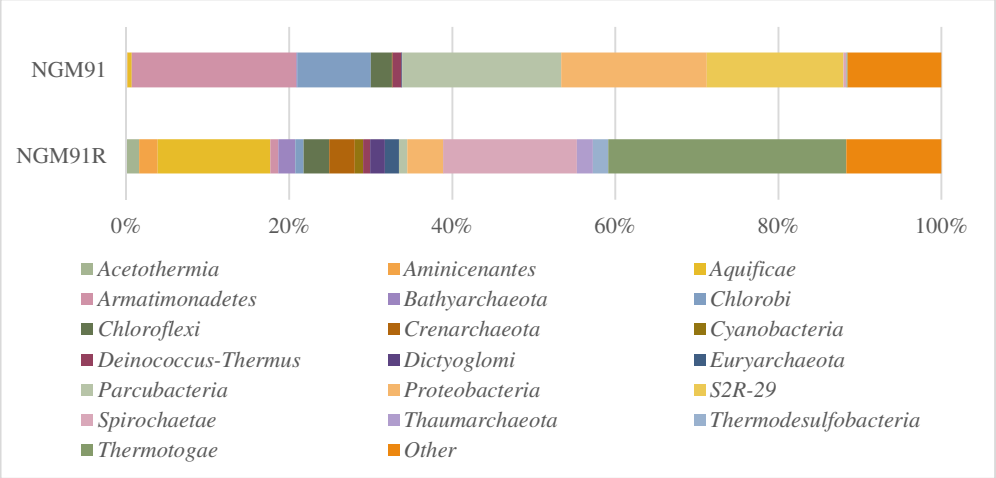

Figure 2.24 Microbial community structure of NGM91 and NGM91R. Phyla that formed < 1 % of the reads in both samples were summed and are referred to as 'Other'.

NGM91R was also assessed against its corresponding primary microcosm NGM91 for the relative proportion of putative methane oxidising OTUs detected and there were discernible differences between the duplicates. In both NGM samples, the proportion of *Alphaproteobacteria* and *Verrucomicrobia* methanotrophs were uniformly very low. However, there was an abundance of sequences related to *Methylothermus* (*Gammaproteobacteria,* 5.2 %) in NGM91 compared to only 0.01 % of reads from NGM91R, which did not correspond with the comparable levels of methane oxidation seen in the two microcosms.

2.4 Discussion

The three aims of this chapter were to quantify rates of methane oxidation in geothermal microcosms, evaluate the effects of temperature, pH, soil type and environmental methane concentrations on microcosm methane oxidation rates, and to determine the microbial community composition within these geothermal microcosms.

2.4.1 Environmental characteristics and methane oxidation

There was little correlation between methane oxidation rates and environmental variables such as temperature and sample type. Soil temperature and pH have little effect on methane oxidation rate [274, 275], and this corresponds with the

lack of correlation between these factors during this study. However, in contrast to previously published studies, there was no correlation between observed rates of methane oxidation within microcosms and soil type, although soils with a high clay content oxidise more methane than sandy soils [183, 187], and methane oxidation has also been correlated with soils containing both very fine and coarse grains [183, 187]. The difference between the outcomes of these studies and the geothermal-based research presented may be due to low numbers of individual values of each factor collected in this study (e.g. one water and two biomass samples; 14 geothermal fields) or there could be strong associations between methane oxidation and unknown environmental parameters not measured in this study (e.g. soil moisture levels or presence of essential trace elements). Increasing the number of physicochemical parameters measured (e.g. N, P, metal concentrations, potentially toxic concentrations of geothermal gases) therefore may provide increased resolution on the factors required to support microbial communities capable of thermophilic methane oxidation. Nevertheless, substantial rates (up to 17.36 μmol/g of soil/day) of methane oxidation were observed at temperatures ≤ 75 °C. These results unequivocally indicate the presence of active thermophilic methanotrophs within the geothermal microcosms. Of New Zealand methanotroph isolates, the only thermophile, *Methylacidiphilum infernorum*, is restricted in growth between pH 1.0 and pH 6.0 [14]. *Methylocaldum* species grow at up to pH 8.5 [68], but not at temperatures > 62 °C. The methane oxidising microcosms in this study included activity at pH 8.3, 70 °C and pH 8.7, 75 °C. The wide pH range of soil microcosms demonstrating positive methane consumption (between pH 1.5 and 8.7) is therefore suggestive that novel, hitherto unidentified, methanotrophs are responsible for this activity.

2.4.2 Microcosm 16S rRNA gene sequence diversity

Illumina sequencing of the 16S rRNA gene from DNA extracted from microcosms indicated that many of the communities were highly diverse, with up to 3140 OTUs observed (Golden Springs GDS2 sediment sample). Despite water samples being generally considered to be much less diverse than soils and sediments [244], the fluid sample taken just above GDS2 sediments (GDS1) also contained 1527 OTUs. Values for the Shannon index, which measures both species richness and evenness, were also extremely high for some of the

microcosms (Figure 2.13 and Figure 2.14). The index can take any value above zero, although in practice values above 10 are unlikely [276], and while soil environments ranging from dry grassland to tropical forests have values of ~3.8 [180], in this study the greatest Shannon index value for a soil was 8.08 (Tokaanu TOK5). A previous study of geothermal soil communities in New Zealand and Canada reported Shannon index values between 0.48 and 8.62 [181]. This suggests that the physicochemical conditions found in these environments may promote a high diversity of phylotypes over a wide range of pH, temperatures and sample types. Due to the high diversity observed within the sampled microbial communities, very few ubiquitous genera were present within the geothermal microcosms, and these were generally of low abundance. Consistently however, all six of these ubiquitous genera (*Methylacidiphilum*, *Chthonomonas*, *Thermus*, *Sulfolobus*, *Thermoplasma* and *Caldimicrobium*) are characterised as thermophilic and commonly found in geothermal soils and hot springs (Extended Data Set 2 and references therein).

Chthonomonas and *Methylacidiphilum* were found in all 59 samples, with an average abundance of 4.3 % and 3.7 % respectively (total normalised reads across the samples). *Chthonomonas* has notably never been detected outside the Taupō Volcanic Zone [277] and is reported to be a heterotroph that likely scavenges carbohydrates from degraded biomass. In contrast, *Methylacidiphilum* species are thermophilic methanotrophs. *Thermus*, *Thermoplasma* and *Caldimicrobium* can all grow heterotrophically with organic compounds [278-281], while sulfur and sulfur compounds commonly found in geothermal areas, including thiosulfate and sulfide, could contribute to the growth of *Sulfolobus* [271], as well as *Thermus* and *Caldimicrobium*.

Molecular hydrogen is also likely to be a primary source of energy for many of the microorganisms found in this study. H_2 may be produced both abiotically (in igneous rocks [282]) as well as through a wide range of metabolic processes [222, 226]. Hydrogen is ubiquitous in the atmosphere and due to its ability to permeate through rocks, polymers, glass and even iron [222] is a readily available source of exploitable energy to many microorganisms. Hydrogen-evolving or bidirectional hydrogenases have been identified within 51 bacterial and archaeal phyla [226]

and several of the highly prevalent genera found in this study utilise H_2 as an energy source; including *Methylacidiphilum* [34, 35], *Sulfolobus* [271] and *Caldimicrobium* [280, 281].

It should be noted that the taxa detected within the microbial communities assessed in this study do not necessarily reflect active or viable strains. For example, two of the more unexpected genera detected during this study included the obligate acidophiles *Mesoaciditoga* and *Metallosphaera* whose published growth ranges are pH 4.1-6.0 [270] and pH 1.0-4.5 [283] respectively, which were detected in several pH-neutral microcosms and sometimes at abundances that exceeded 1 % of the total population. Similarly, the presence of *Methylacidiphilum* OTUs in microcosms with soil pH up to pH 9.2, when no isolate has been described as being able to grow above pH 6.0, is not a realistic observation of metabolically active cells. It is likely that some 16S rRNA gene sequences detected in this study may be derived from dormant cysts or exospores. It is also possible that extracellular DNA has been included, as DNA from lysed cells can adsorb to minerals and persist in soil for years [284], and this "relic" DNA can overinflate observed microbial richness by as much as 55 % [285]. DNA adsorption is affected by soil mineralogy and concentration of cations and humic acids, but primarily by soil pH (with higher pH soils more likely to retain extracellular DNA) [284]. Another explanation is that multiple microniches, with varying pH values, have been consolidated during the sampling process. Extracellular DNA may also have resulted from contamination of laboratory surfaces or equipment, as *Methylacidiphilum* (and *Thermus* and *Chthonomonas*) strains are routinely cultured in rooms adjoining the laboratory in which PCR was carried out. The use of a viability PCR indicator, such as propidium monazide, which binds to and inactivates extracellular DNA [286], in future sequencing work may be able to confirm the origin of microbial DNA from geothermal samples.

2.4.3 Differences in microbial communities between oxidising and non-oxidising communities

When the microcosms were split into those that oxidised methane and those that did not, the Shannon and Simpson diversity indices demonstrated that the communities across the two categories were equally diverse, although the individual taxa differed. Methane-oxidising microcosms displayed greater species richness, and this was strongly influenced by a single hot spring sediment sample (Golden Springs GDS2) that had both the greatest Shannon index value (9.06) and the greatest number of OTUs (3140); 1324 more taxa than the next highest methane oxidising sample (Tikitere TKT67). Index ranges were also affected by microcosms of low diversity that were dominated by methanotrophs, such as the Ngatamariki NGM89 soil community that consisted of 60.7 % *Methylacidiphilum* OTUs. Whakarewarewa Village soil sample WHV12 was similarly dominated by *Methylacidiphilum* OTUs (50.6 %).

At the phyla level, *Bathyarchaeota*, *Crenarchaeota*, *Euryarchaeota*, *Chlorobi, Parcubacteria* (OD1) and *Proteobacteria* (*Deltaproteobacteria* and *Gammaproteobacteria*) were significantly more abundant in microcosms that oxidised methane (Kruskal-Wallis analysis, Table 2.5). Most *Bathyarchaeota* OTUs were at very low abundance, but one comprised 16.5 % of the total reads from methane oxidising microcosms, primarily from the OKO2 sample. Data from two near-complete *Bathyarchaeota* genomes indicates that they could be responsible for anaerobic methane oxidation [20], although other members of the phylum appear to survive by degrading detrital proteins and carbohydrates [287], or through methylotrophic methanogenesis [20, 21].

Crenarchaeota have not been described as methanotrophs, and the majority of OTUs from this phylum came from the order *Sulfolobales* that grow chemolithotrophically with sulfide, sulfur, tetrathionate and H_2 [271], which are commonly found in geothermal environments. *Euryarchaeota* sequences were also of very low abundance, except for the genus *Thermoplasma*, which can grow heterotrophically on *Bacteria*, *Archaea* and proteinaceous substances [279], and may have increased in abundance by scavenging dead microbes. Anaerobic methanotrophs have also been described within *Euryarchaeota* [17, 23, 288],

although ANME-1 and *Methanoperedens* were only found in significant numbers (805 and 251 total normalised reads) in the Golden Springs GDS2 sediment sample.

Parcubacteria (formerly known as OD1) have not yet been isolated in laboratory culture, but their small, streamlined genomes indicate that these could be symbiotic organisms [289-291]. The increased abundance of *Gammaproteobacteria* in the methane-oxidising microcosms was due in large part to the presence of known methanotrophs from *Methylothermus*, although there was also a particular increase in OTUs affiliated to *Pseudomonas*, which are facultative methylotrophs [292], able to oxidise methanol that is the first product of methane oxidation. There was also an increased abundance of *Sulfurimonas (Epsilonproteobacteria)*, sulfur-oxidising chemolithoautotrophs, in methane-oxidising microcosms, which may be due to their ability to fix carbon dioxide produced by methanotrophs, or simply that the presence of high concentrations of reduced sulfur species in the geothermal samples leads to the long-term survival of these species.

Other genera that were significantly increased in the methane-oxidising microcosms included *Methylacidiphilum* and *Alicyclobacillus*. These OTUs were most closely related to at least 11 different *Alicyclobacillus* species, making it difficult to determine the ecological function of the strains found in this study, but their metabolism of a wide range of substrates or their ability to form spores may contribute to their survival and growth in these geothermal environments.

2.4.4 Sequences related to known aerobic methanotrophs

Putative methanotroph OTUs were found in all geothermal microcosms, regardless of whether the microcosms oxidised methane or not. Potential methanotrophs from *Alphaproteobacteria* were identified in only 19 microcosms, ranging from pH 4.2 to pH 7.7, were of very low abundance in all of these samples, and were most closely related to *Methylocystis* species (Figure 2.20). The majority of methanotrophs from the *Rhizobiales* order are neutrophilic or acid-tolerant but not acidophilic, with growth optima of between pH 4.8 – 7.0 [293, 294], and no isolate has been demonstrated to grow at less than pH 3.5

(*Methyloferula stellata* [295]). The *Methylocystis* sequences were found in NZ geothermal samples with *in situ* temperatures between 38.0 and 77.3 °C, despite all validly published strains having maximum growth temperatures of approximately 37 °C [293]. The highest reported growth temperature for an isolated methanotroph within the *Alphaproteobacteria* is *Methylocystis* "Se48" [61], which has a maximum growth temperature of 53 °C but has not been formally described. It is possible geothermal sampling sites may have been contaminated with sequences from cooler areas, but it is more likely these areas experience temporal fluctuations in temperature that thus promotes the formation of cysts or exospores as resting stages of non-active Type II methanotrophs. Alternatively, these sequences may represent novel thermotolerant and thermophilic *Alphaproteobacteria*.

Other studies have detected *pmoA* sequences similar to *Methylocystis* and *Methylocapsa* in a hot spring at 51 °C [169], and in geothermal sediments at up to 76 °C [122]. While the detection of *pmoA* gene does not necessarily indicate the presence of active methanotrophy, methane oxidation in concert with *pmoA* gene detection, and in some cases low levels of ^{14}C bioassimilation, has been reported within samples from hot springs containing *Alphaproteobacteria* OTUs when incubated at 75 °C [141], which lends merit to the existence of thermophilic alphaproteobacterial methanotrophs. However, in the cited study [126], three of these four samples also contained *pmoA* sequences of *Gammaproteobacteria* origin. Gammaproteobacterial methanotrophs are known to have higher growth temperature maxima and may have been responsible for the high-temperature methane oxidation that was observed in this study. Bearing in mind the previous precautionary observations of other non-methanotrophic taxa detected in conditions beyond what can be reasonably expected knowing their currently described growth ranges, it is likely that some of the alphaproteobacterial methanotroph signatures in this study represent relic DNA rather than active thermophilic methanotrophs.

Putative methanotrophs from *Gammaproteobacteria* were detected in 49 microcosms, although there were two distinct groups of OTUs. Golden Springs GDS1 and GDS2 had OTUs that were most closely related to *Methylobacter*,

Methylocaldum, *Methylococcus*, *Methylomonas* and *Crenothrix*, and these composed up to 2.5 % of the total reads in the two samples. However, these genera were not identified in any other microcosms, with the exception of *Methylomonas* (0.04 %) in sample Tikitere TKT68. The other 47 microcosms all had OTUs that affiliated to *Methylothermus*, which was not otherwise present in the two GDS microcosms. Both extant strains of *Methylothermus* have minimum growth temperatures of 37 °C, suggesting that temperature limitations at GDS (38.0 and 38.9 °C) are unlikely, unless these OTUs, with 90 to 95 % 16S rRNA gene sequence identity to *M. subterraneus*, represent a novel methanotroph with a higher minimum growth temperature.

Potential methanotrophs from *Verrucomicrobia* were found in all microcosms and were most closely related to *Methylacidiphilum infernorum*. Again, as some of the microcosms were outside of the known temperature (40-60 °C) and pH (pH 1.0-6.0) ranges for growth for this species, it is likely that some of these OTUs represent either dormant cells, or relic DNA.

2.4.5 Replicability of microcosm methane oxidation and DNA extraction methodology

The two samples selected to test the ability to replicate results allowed very different conclusions to be drawn. DNA was extracted from two sub-samples of WKT46 soils after methane oxidation had been tested for several weeks and was shown to be negative. The sequencing results revealed the technical duplicates WKT46/WKT46R had reasonably similar communities, but there were some differences between the two samples, notably in the abundances of putative methanotrophs. Each step within the DNA extraction, amplification and sequencing process can introduce bias; including extraction method [296], annealing temperatures and PCR cycle number [297], and primer choice and sequencing platform [298]. Although these processes were replicated as closely as possible, there may have been some biases introduced, for example through differences in template concentration [299], which affected the final abundance of various OTUs.

In contrast, the NGM91/NGM91R duplicate samples showed very different results. Although both samples were taken from the sampling site and had the same temperature and pH *in situ*, the significant differences in microbial community observed with 16S rRNA gene sequencing highlighted the difficulty in reproducing sample collection. A single gram of soil can contain up to 1 x 10^{10} cells [300] and up to 5 x 10^{4} species [301], meaning that the "duplicate" samples could essentially comprise entirely different microbial communities, presumably from different microenvironments. Increasing the depth of sequencing may have shown more overlap between the communities, but as the Chao1 estimates of diversity were 71.6 % for NGM91 and 76.8 % for NGM91R, it is unlikely that the theoretical ~23-28 % of species not sequenced would have been those that were identical between the samples. In addition, differing weather patterns such as rainfall and runoff into hot springs during the sample collections nine months apart may have affected community composition.

Conclusions

Methane oxidation appears to be common in geothermal areas within the Taupō Volcanic Zone and was observed in 31 of the 59 microcosms across a wide range of pH and temperature, confirming the presence of thermophilic methanotrophs. Measurable methane oxidation rates in the sample microcosms ranged from 0.48 to 17.36 μmol/g/day, indicating that this type of metabolism is likely to be significant for microbial communities in geothermal areas.

Methane oxidation rates were not correlated with environmental factors including *in situ* methane concentration or soil type, although it was difficult to determine the influence on methane oxidation rates with small numbers of each sample category. This could have been resolved either by taking a greater number of samples, or by focusing sample collection on specific soil types, rather than using microcosms that were classified as mixed (e.g. clay/loam/sand). The ability to measure more environmental factors such as *in situ* oxygen concentrations may also have allowed for more robust determinations of the influence of physical variables on methane oxidation. Alternatively, using well-mixed hot spring water samples to reduce the complexity of sample types may have made it easier for patterns of influence to be observed. The reduced abundance of microorganisms

in water compared to soil [244] would have required much greater volumes of sample to be taken however, and the poor solubility of both methane and oxygen in water at elevated temperature [206, 245] may restrict the growth of methanotrophs in these environments.

Sample microcosms had highly diverse microbial communities, with most taxa previously identified from thermal environments including geothermal soils, hot springs, and hydrothermal fields. There were few ubiquitous genera identified but these did include *Methylacidiphilum*, a thermophilic methanotroph isolated from the TVZ, which was found in all 59 samples and at very high abundance (up to 60.7 %) in some microcosms. However, extracellular DNA, which is most likely to be found in higher pH soils with elevated levels of clay minerals, humic substances, or cations, may over-inflate these measures of diversity. There were significant differences in taxa between the microcosms that oxidised methane and the non-oxidising communities. The increased abundance of both known aerobic methanotrophs (*Methylothermus*, *Methylacidiphilum*) and putative anaerobic methanotrophs (*Bathyarchaeota*) provides some explanation for the high levels of methane oxidised in some of the geothermal microcosms. The detection of these methanotrophs at pH or temperatures outside of their known ranges for growth also indicates that there could be novel methane-oxidising bacteria within some of these samples.

The next stage of this study is to enrich methanotrophs from the geothermal microcosms, and perform functional transcriptomic analysis on nucleic acids extracted from the enrichment cultures. This will enable putative methanotrophs identified from 16S rRNA gene sequences to be linked to methanotrophic activity.

3. Enrichment of Methanotrophs and Community Transcriptomics

3.1 Introduction

The sequencing of DNA from environmental samples and enrichment microcosms has frequently been used to detect methanotrophs within environmental samples. The methods commonly used to access environmental DNA for this purpose include amplicon sequencing using the 16S rRNA gene [58] or functional genes associated with methanotrophy such as *pmoA* [26, 139] and *mmoX* [130], and metagenomic or metagenome-assembled genomes (MAGs). Both approaches have inherent limitations. Firstly, both methodologies suffer from well-documented biases during the DNA extraction, amplification and sequencing steps that can affect both diversity and abundance accuracy [297, 298, 302]. Amplicon sequencing relies on primer stringency while probing target genes within a community and therefore hybridisation efficacy is dictated by the extent of target sequence conservation [303]. Thus, while this method is excellent at detecting known genes with highly-conserved primer target sequences, it may miss genes within a community with divergent target sequences. An additional limitation when targeting the 16S rRNA gene is that some *Bacteria* and *Archaea* encode multiple copies of the 16S rRNA gene. This includes common soil microorganisms such as *Pseudomonas aeruginosa* (four copies) and *Bacillus subtilis* (ten copies) [304] and therefore abundance of these species may be over-estimated during sequencing surveys. This caveat also holds true when using specific genes to quantify functional communities, as many methanotrophs encode multiple copies of *pmoA* [47, 115, 241]. The presence of extracellular (relic) DNA within soil samples adversely affects microbial population estimates [285]. Finally, as up to 80 % of soil microorganisms are thought to exist in a state of dormancy at any time [305], sequencing of these microorganisms can obscure assessments of both microbial community identity and metabolic activity within an environment.

The use of metagenomics or MAGs as an alternative to community amplicon sequencing has often been cited as a means to assess the taxonomy of microbial communities and to hypothesise about their metabolic functions [306, 307]. However, metagenome analysis, while not prone to the gene-specific primer bias

detailed above, only reflects the metabolic potential of members of the microbial community, and does not resolve questions about microbial activity, gene expression or responses to environmental conditions [308]. Given that there is an extremely large database of sequenced 16S rRNA genes, but around 90 % of all isolates belong to just four bacterial phyla (*Actinobacteria*, *Bacteroidetes*, *Firmicutes* and *Proteobacteria*) [309], it can be very difficult to infer metabolic functions from 16S rRNA taxonomy. However, metabolic inferences can be attempted using various bioinformatics packages such as PICRUSt [310], paprica [311] and Tax4Fun [312].

Metatranscriptomics offers a direct method to identify the metabolic activity of an environmental community, rather than via inference from its genetic potential through sequencing of mRNA transcripts. This approach may be able to determine if the function of a microbial community is more important than the identification of individual taxa [313], particularly in habitats such as the human gut, where metabolic function (relative abundances of pathways) is more stable than taxonomy [314]. Metatranscriptomics offers the advantage of being culture-independent and avoids the acknowledged difficulties inherent in replicating environmental conditions *in vitro* [108]. Previous studies have investigated methanotrophs using transcriptomics within hydrothermal vents [152, 315], in peatlands [131, 162] and in landfill soil [189] ecosystems. Neither geothermal soil nor hot spring environments have yet been examined via metatranscriptomics with respect to methane-oxidising communities.

The ability to assess transcriptional activation within communities, and to predict microbial interactions within an environmental sample, can be used to determine if there is cooperative behaviour between methanotrophs and methylotrophs [316], or if methanotrophic activity is stimulated by the presence of heterotrophs [317]. However, there are some caveats with the use of metatranscriptomics; these include biases introduced during RNA extraction, reverse transcriptase polymerase chain reaction (RT-PCR) amplification and sequencing of the resultant cDNA, and that linking transcripts to metabolic functions depends on high-quality genome annotations, preferably with experimental evidence [318]. Nonetheless, in combination with other culture-independent, or culture-dependent,

methods of investigation, metatranscriptomics offers an opportunity to identify taxa, functions and gene activities within environmental samples or microcosms.

Key metabolic pathways to be investigated during this study will include methane metabolism, from methane oxidation to carbon assimilation, and oxidative phosphorylation, to identify reducing equivalents used by the microbial communities under specific culture conditions. In addition, nitrogen metabolism pathways will be examined. Nitrate can stimulate methane oxidation [200, 201], but nitrate reduction results in the production of ammonia (via nitrite) that can inhibit methane oxidation through competitive binding to the methane monooxygenase enzymes [80]. The expression of one of the two isozymes of particulate methane mono-oxygenase was significantly downregulated in the presence of ammonia in *Methylocystis* strain SC2 [113]. Ammonia oxidised by methane monooxygenase produces intermediates including hydroxylamine and nitrite, which are toxic to many methanotrophs [205].

In the previous chapter, methane oxidation from geothermal soils across the TVZ was measured and correlated with the *in situ* microbial communities. These data demonstrated that thermophilic methanotrophy was present, although in some methane-oxidising soils, such as the microcosm from Orakei Korako OKO2, known aerobic methanotrophs were not identified using 16S rRNA gene sequencing. In order to elucidate the metabolic pathways and likely methanotrophic candidates by which methane was being oxidised within these soils, I will link microbial community methane consumption with community metabolic function using metatranscriptomics. To do this, I will i) establish enrichment microcosms from geothermal microcosms showing methane oxidation from chapter two, ii) determine the rates of methane oxidation within the microcosms, and iii) extract and sequence microcosm mRNA within microcosms showing elevated methane consumption to determine methanotrophic community structure and function.

3.2 Methods

3.2.1 Enrichment cultures

All geothermal microcosms that displayed methane oxidation (microcosms showed a greater loss of methane than controls and R^2 was > 0.5, Table 2.1) were selected for enrichment of methanotrophs using a variety of media detailed in Table 3.1. All microcosms were inoculated into a modified version of Nitrate Mineral Salts media (mNMS), which was designed to be a non-specific methanotroph media based on components from several other media recipes (Appendix 7.4). In addition, each selected microcosm was tested for methane oxidation in at least one other growth medium, depending on the sample pH and the putative methanotrophs within the original microcosm as determined by 16S rRNA gene sequencing (Table 3.1, Extended Data Set 3). All media were adjusted to approximately the same pH as the original microcosm and sterilised at 121 °C at 103 kPa for 20 minutes in a P52014 Pressure Vessel (Mercer Stainless Limited, Henderson, New Zealand). All media recipes applied in this chapter are detailed in Appendix 7.4.

Microcosms with > 0.01 % 16S rRNA gene sequences identified as *Methylococcus* (Table 3.1) were inoculated into NMS media [44], which has also been used to culture *Methylobacter* and *Methylosinus* strains [44, 319], while those microcosms with more than 0.01 % of sequences assigned to *Methylomonas* were inoculated into dNMS [320, 321], which can also support the growth of *Methylocystis*, *Methylocapsa* and *Methylocella* strains [320, 322, 323]. Neutral and alkaline pH microcosms (pH > 5.5), with > 0.01 % of 16S rRNA gene sequences identified as *Methylothermus* (Table 3.1), were inoculated into mmj media [62]. This medium was used to isolate *M. subterraneus*, with which the 16S rRNA gene sequences in this study were most closely aligned. Five microcosms that had > 0.4 % of their 16S rRNA gene sequences identified as *Methylothermus* were additionally inoculated into ANMS media, which was used to isolate *M. thermalis* [57].

Table 3.1 Geothermal microcosms selected for methanotroph enrichment. Initial sample pH and putative methanotrophic genera identified via microbial community analysis are listed along with cultivation media and pH chosen for methanotrophic enrichments.

Sample location	**Sample name**	**Sample pH**	**Methanotrophic genera identified (> 0.01 % of total 16S rRNA gene sequences)**	**Media used, in addition to mNMS**	**pH of media**	**Incubation temperature (°C)**
Golden Springs	GDS1	7.2	*Methylococcus, Methylomonas, Methylacidiphilum*	NMS, dNMS	7.0	50
Golden Springs	GDS2	7.0	*Methylobacter, Methylococcus, Methylomonas, Methylacidiphilum*	NMS, dNMS	7.0	50
Loop Road	LPR14	2.8	*Methylothermus, Methylacidiphilum*	V4	3.0	75
Loop Road	LPR16	1.5	*Methylothermus, Methylacidiphilum*	V4	1.5	70
Loop Road	LPR17	1.6	*Methylothermus, Methylacidiphilum*	V4	1.5	60
Ngatamariki	NGM89	3.0	*Methylothermus, Methylacidiphilum*	V4	3.0	60
Ngatamariki	NGM91	7.0	*Methylothermus, Methylacidiphilum*	mmj, ANMS	7.0	60
Ngatamariki	NGM91R	7.0	*Methylothermus, Methylacidiphilum*	mmj	7.0	60

Orakei Korako	OKO2	4.3	None	V4	4.5	70
Te Kopia	TKA8	4.7	*Methylacidiphilum*	V4	5.0	75
Te Kopia	TKA9	4.2	*Methylacidiphilum*	V4	4.2	70
Te Kopia	TKA13	4.1	*Methylacidiphilum*	V4	4.0	70
Te Kopia	TKA15	5.1	*Methylacidiphilum*	V4	5.0	70
Te Kopia	TKA16	5.0	None	V4	5.0	70
Tikitere	TKT67	2.6	*Methylocystis, Methylothermus, Methylacidiphilum*	V4	2.5	75
Tikitere	TKT68	3.0	*Methylothermus, Methylacidiphilum*	V4	3.0	37
Tokaanu	TOK7	6.8	*Methylothermus, Methylacidiphilum*	mmj, ANMS	7.0	60
Tokaanu	TOK10	6.9	*Methylothermus, Methylacidiphilum*	mmj, ANMS	7.0	60
Tokaanu	TOK12	8.1	*Methylothermus, Methylacidiphilum*	mmj, ANMS	8.0	60
Tokaanu	TOK15*	6.2	*Methylacidiphilum*	ANMS	6.0	70
Tokaanu	TOK17	7.7	*Methylothermus, Methylacidiphilum*	mmj, ANMS	7.5	60

Waimangu	WAM36	4.6	*Methylothermus, Methylacidiphilum*	V4	4.5	70
Waipahihi	WAP11*	6.7	*Methylacidiphilum*	ANMS	7.0	46
Whakarewarewa Village	WHV12	3	*Methylacidiphilum*	V4	3.0	60
Whakarewarewa Village	WHV13*	8.7	*Methylacidiphilum*	ANMS	8.5	75
Whakarewarewa Village	WHV15*	6.3	*Methylacidiphilum*	ANMS	6.0	75
Whakarewarewa Village	WHV16*	5.6	*Methylacidiphilum*	ANMS	5.5	60
Whakarewarewa Village	WHV18	2.5	*Methylacidiphilum*	V4	2.5	50
Waikite Valley	WKT45*	8.3	*Methylacidiphilum*	ANMS	8.0	70
Wairakei Thermal Valley	WTV1	4	*Methylacidiphilum*	V4	4.0	70
Wairakei Thermal Valley	WTV2	7.7	*Methylothermus, Methylacidiphilum*	mmj	8.0	75
Wairakei Thermal Valley	WTV4	4	*Methylacidiphilum*	V4	4.0	60

*, samples of neutral or alkaline pH where more than 0.01 % of 16S gene sequences were identified as *Methylacidiphilum*, but samples were not inoculated into V4 medium.

Microcosms with a pH < 5.5, and with > 0.01 % of 16S rRNA gene sequence abundance identified as *Methylacidiphilum* (Table 3.1), were inoculated into V4 medium [14]. V4 medium has been used to successfully cultivate acidophilic *Methylacidiphilum* and *Methylacidimicrobium* species [122]. In samples Orakei Korako OKO2 and Te Kopia TKA16 the only methanotrophs identified through 16S rRNA gene sequencing were *Methylacidiphilum*; but these represented only a very small proportion of the total reads (0.009 % and 0.005 %, respectively). As these samples were < pH 5.5 (pH 4.3 and 5.0, respectively), they were also inoculated into V4 medium. Fourteen samples that had > 0.01 % of *Methylacidiphilum* sequences but a pH > 5.5, were not inoculated into V4 medium. The maximum known growth pH for strains in this genus is 6.0 [14], and as all of the sequences from geothermal samples in this study contained at least some *Methylacidiphilum* reads, this suggests that relic DNA may be present (see Discussion in chapter two). Six of these samples (Tokaanu TOK15, Waipahihi WAP11,Whakarewarewa WHV13, WHV15, WHV16 and Waikite Valley WKT45) were inoculated in ANMS medium [57] as a general methanotroph medium that contains both ammonium and nitrate as potential sources of nitrogen.

The serum bottles containing geothermal microcosms selected for further methanotrophic enrichment (Table 3.1) were opened in a Hera Safe Biosafety Cabinet (Heraeus, Hanau, Germany) and between 0.25-0.5 g of the soil or sediment sample was distributed evenly into between two and four serum bottles containing 40 ml of sterile media for enrichment. A custom gas mixture (85 % CH_4, 10 % CO_2 and 5 % O_2 v/v), was injected (14.3 ml) into the sample vial headspace through a sterile filter resulting in final gas headspace composition of ~ 10 % CH_4, 1 % CO_2 and 22 % O_2 (approximately 7-20 kPa). Serum vials were incubated at close to *in situ* temperature (37, 46, 50, 60, 70 or 75 °C), with shaking at 150 r.p.m.

At 3-4 day intervals, vials were moved to a water bath at 20 °C and equilibrated to room temperature before headspace pressure was measured with a XP2i digital pressure gauge (Crystal Engineering Corporation, CA) to enable determination of moles of gas. Headspace compositions were quantified by removing 500 µl with a gastight syringe (SGE Analytical Science, Melbourne) and diluting to 5 ml with

air before measurement on a Peak Performer 1 Gas Analyzer (Peak Laboratories, CA) equipped with a flame ionization detector (FID) and a Unibeads 60/80 column. Rates of methane oxidation (μmol/day) were subsequently calculated using linear regression. For those cultures that did not oxidise all methane in the headspace, a coefficient of determination (R^2) greater than 0.5 was designated as positive for methane oxidation. Calculations for rates of methane oxidation for all positive samples are presented in Appendix 7.6.

Where positive methane oxidation was observed in the enrichment consortium, isolation of methanotrophic strains was attempted, the details of which form chapter four. If, after at least four weeks of headspace measurements, no methane oxidation was observed, microcosms were discarded and not used again as part of this research.

3.2.2 Metatranscriptomic assessment of methanotroph enrichments

Culture conditions for RNA extraction

Three geothermal microcosms showing positive methane oxidation were selected for metatranscriptomic analysis; Golden Springs GDS1, Tokaanu TOK7, and Ngatamariki NGM89. These were chosen to cover a range of pH and temperatures, and because DNA sequencing of the original soil/sediment samples indicated an abundance of different putative methanotroph sequences (Table 3.2). The GDS1 sample was incubated at 37 °C for this experiment, the optimum temperature for *Methylococcus* species [45].

Table 3.2 Abundance of methanotroph-associated 16S rRNA gene sequences from initial inoculum of enrichment microcosms.

	Incubation temperature and pH	*Methylococcus*-related sequences	*Methylothermus*-related sequences	*Methylacidiphilum*-related sequences
GDS1	37 °C, 7.2	5.5 %	0 %	8.7 %
TOK7	46 °C, 6.8	0 %	11.2 %	17.9 %
NGM89	60 °C, 3.0	0 %	0.01 %	60.7 %

Cultivations for meta-transcriptomic assessment of methane-oxidising microbial communities were performed by inoculating enrichment microcosms Golden

Springs GDS1, Tokaanu TOK7 and Ngatamariki NGM89 in triplicate into new medium. Each of the enrichment microcosms were divided equally into three 114 ml serum vials (biological replicates) with the volumes adjusted to 30 ml of the relevant medium (NMS for GDS1, ANMS for TOK7 and V4 for NGM89). Each vial had an air headspace with supplemented with approximately 10 % (v/v) CH_4 and 1 % (v/v) CO_2.

The extent of methane oxidation of each incubation was assessed by measuring the headspace gas composition after 4, 8, 20 and 24 hours of incubation (Appendix 7.7). The headspace of the vials was sampled and quantified using GC-FID as before (Section 2.2.3). Cell density (OD_{600}) was not recorded as soil and sediment particles within the enrichment microcosm obscured the light path within the spectrophotometer and made accurate measurements impossible. After 24 hours of incubation and positive methane consumption, the vials were opened in the Biosafety Cabinet, and 20 ml of RNAlater (Invitrogen, CA) was immediately added to each vial to stabilise RNA. The entire contents of each vial were then centrifuged at 16,000 x *g* in a 1736R centrifuge (Gyrozen, Seoul, Korea), for 15 minutes at 10 °C. The cultivation media/RNAlater supernatant was then discarded and the pellet resuspended in 10 ml of RNAlater.

RNA extraction and sequencing were performed externally by Novogene (Beijing, China). Briefly, RNA was extracted from samples, and assessed for purity and integrity using agarose gel electrophoresis, and Nanodrop (Thermo-Fisher Scientific, Waltham, MA) and Bioanalyzer (Agilent, Santa Clara, CA) instruments before being quantified via Qubit (Thermo-Fisher Scientific). rRNA was then removed from the samples, mRNA was fragmented, and cDNA synthesised using random hexamers. Following first-strand synthesis, second-strand cDNA was generated by nick-translation. DNA was purified using AMPure XP beads before terminal repair, addition of 3’ terminal A overhangs and adaptors, and size selection. PCR enrichment of fragments was then completed before sequencing using Illumina HiSeq.

Bioinformatics

Raw mRNA reads were uploaded to the Galaxy web platform, and the public server (https://usegalaxy.org) was used to perform all analysis [324]. All settings for the individual pipeline wrappers were default settings unless stated otherwise. The quality of raw read data was assessed using FastQC (v0.69) [249]. Reads were trimmed using Trimmomatic (v0.36.2) [325] with a sliding window operation averaged across four bases. The average quality required was set to a Phred score of 25 for GDS samples, and 20 for TOK samples, based on their FastQC reports. Reads with a length below 120 bp after trimming were removed. Forward and reverse reads for each sample were concatenated into two files using cat (v.0.1.0) [326], and these were then assembled into contigs using Trinity (v2.2.0) [327, 328] on Bridges at the Pittsburgh Supercomputing Center.

Predicted genes within the contigs were identified using MetaGeneMark (v3.25) [329, 330] on the public server (http://www.opal.biology.gatech.edu). Identical sequences were identified and removed using the standalone Java applet, DuplicatesFinder [331]. The remaining sequences were clustered using the program h-cd-hit-est [332] on the public web server (http://weizhongli-lab.org/cdhit_suite/) with sequences clustered at 90 % nucleotide sequence identity for the GDS1 sample and at 85 % nucleotide sequence identity for the TOK7 sample. One representative sequence from each cluster identified by cd-hit-est was retained for further analysis.

The predicted genes were analysed using BLASTx [333] on a downloaded BLAST+ executable (v2.7.1) [334] and a local copy of the non-redundant (nr) protein sequences database downloaded from the National Center for Biotechnology Information (NCBI - 19/02/2018). Predicted proteins from the GDS1 and TOK7 samples were manually searched for modules within the “Methane Metabolism”, “Oxidative Phosphorylation” and “Nitrogen Metabolism” pathways in the Kyoto Encyclopaedia of Gene and Genomes (KEGG) database [335], and identified modules were then highlighted using the KEGG Mapper Search&Color Pathway tool available on the public web server (http://www.genome.jp/kegg/tool/map_pathway2.html).

Transcripts from the trimmed, non-concatenated datasets were quantified against the predicted genes from the Trinity assemblies using Salmon (0.8.2) [336], and the most highly expressed transcripts, based on transcripts per million across all three biological replicates, were identified for each sample. The full tables of all transcripts from both samples are available in Extended Data Set 6.

3.3 Results

3.3.1 Geothermal enrichment microcosms

Geothermal samples that oxidised methane (Table 2.1) were transferred to multiple media types for methanotroph enrichment experiments (Table 3.1). Of the 32 microcosms selected (including the WAP11 sediment sample with no microcosm oxidation rate and the duplicate NGM91R sample), 22 continued to show methane oxidation in one or more media (Table 3.3, Figure 3.1).

Table 3.3 Methane oxidation in enrichment microcosms. Soil classifications: B, biomass; C, clay; C/L, clay/loam; C/L/S, clay/loam/sand; C/S, clay/sand; D, sediment; L, loam; L/S, loam/sand; W, water. All microcosms were inoculated into at least two media, and the medium that resulted in the greatest rate of methane oxidation (listed, if any) is highlighted in **bold**.

Microcosm ID	Soil classification	Soil CH_4 oxidation rate (µmol/g/day)	Media	Media pH	Incubation temperature (°C)	Enrichment CH_4 oxidation rate (µmol/day)
GDS1	W	1.35	mNMS, **NMS**, dNMS	6.8	50	24.49
GDS2	D	1.89	mNMS, **NMS**, dNMS	6.8	50	22.68
LPR14	C	2.96	mNMS, V4	3.0	75	0
LPR16	L	0.57	mNMS, **V4**	1.5	70	4.56
LPR17	C/L	1.00	**mNMS**, V4	1.5	60	1.18
NGM89	L	1.90	**mNMS**, V4	3.0	60	5.54
NGM91	D	1.63	mNMS, **ANMS**, mmj	6.8	60	10.64

Microcosm ID	Soil classification	Soil CH_4 oxidation rate (µmol/g/day)	Media	Media pH	Incubation temperature (°C)	Enrichment CH_4 oxidation rate (µmol/day)
NGM91R	D	1.86	**mNMS**, mmj	6.8	60	2.33
OKO2	C/S	17.36	mNMS, V4	4.5	70	0
TKA8	C	0.58	**mNMS**, V4	5.0	75	1.32
TKA9	C/L/S	2.50	**mNMS**, V4	4.2	70	2.82
TKA13	C	0.77	**mNMS**, V4	4.0	70	5.18
TKA15	C	0.67	**mNMS**, V4	5.0	70	1.09
TKA16	L	1.40	**mNMS**, V4	5.0	70	1.82
TKT67	C	9.35	mNMS, V4	2.5	75	0
TKT68	C	7.05	mNMS, V4	3.0	37	0
TOK7	C	4.40	mNMS, mmj, **ANMS**	6.8	60	3.48
TOK10	D	2.72	mNMS, mmj, **ANMS**	6.8	60	7.67
TOK12	D	1.51	mNMS, mmj, **ANMS**	8.0	60	8.88
TOK15	C	0.58	mNMS, ANMS	6.0	70	0
TOK17	D	5.48	**mNMS**, mmj, ANMS	7.5	60	5.98
WAM36	C	1.67	mNMS, V4	4.5	70	0
WAP11	D	N/A	mNMS, **ANMS**	6.8	46	4.55
WHV12	L/S	1.86	**mNMS**, V4	3.0	60	6.54
WHV13	D	0.48	mNMS, ANMS	8.5	75	0
WHV15	B	0.68	mNMS, ANMS	6.0	75	0
WHV16	D	1.53	**mNMS**, ANMS	5.5	60	0.47
WHV18	L	1.84	**mNMS**, V4	2.5	50	2.23
WKT45	C	0.94	mNMS, ANMS	8.0	70	0
WTV1	C	5.34	**mNMS**, V4	4.0	70	2.29
WTV2	C/L	1.40	**mNMS**, mmj	8.0	75	2.40
WTV4	C	1.73	mNMS, V4	4.0	60	0

The initial rate of methane oxidation of the geothermal microcosm did not correlate with whether an enrichment would oxidise methane, or the rate of oxidation from the enrichment microcosm if this occurred (Figure 3.1).

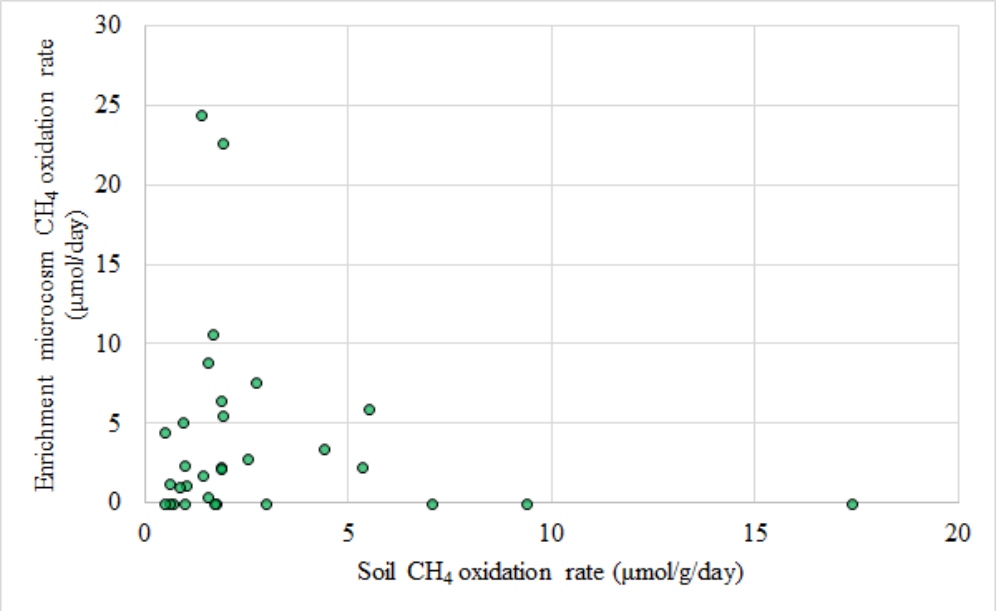

Figure 3.1 Scatter plot of methane oxidation in soil microcosms versus methane oxidation in enrichment microcosms.

Enrichment microcosms showed rates of methane oxidation of up to 24.49 µmol/day (Golden Springs GDS1) (Table 3.3). The greatest rates of CH_4 oxidation were observed at 37 °C, but consortia oxidised methane at up to 75 °C (Wairakei Thermal Valley WTV2, 2.40 µmol/day) (Figure 3.2). Enrichment consortia that oxidised methane varied between pH 1.5 (Loop Road LPR16, 4.56 µmol/day) and pH 8.1 (Tokaanu TOK12, 8.88 µmol/day), although most samples were of neutral pH (Figure 3.2).

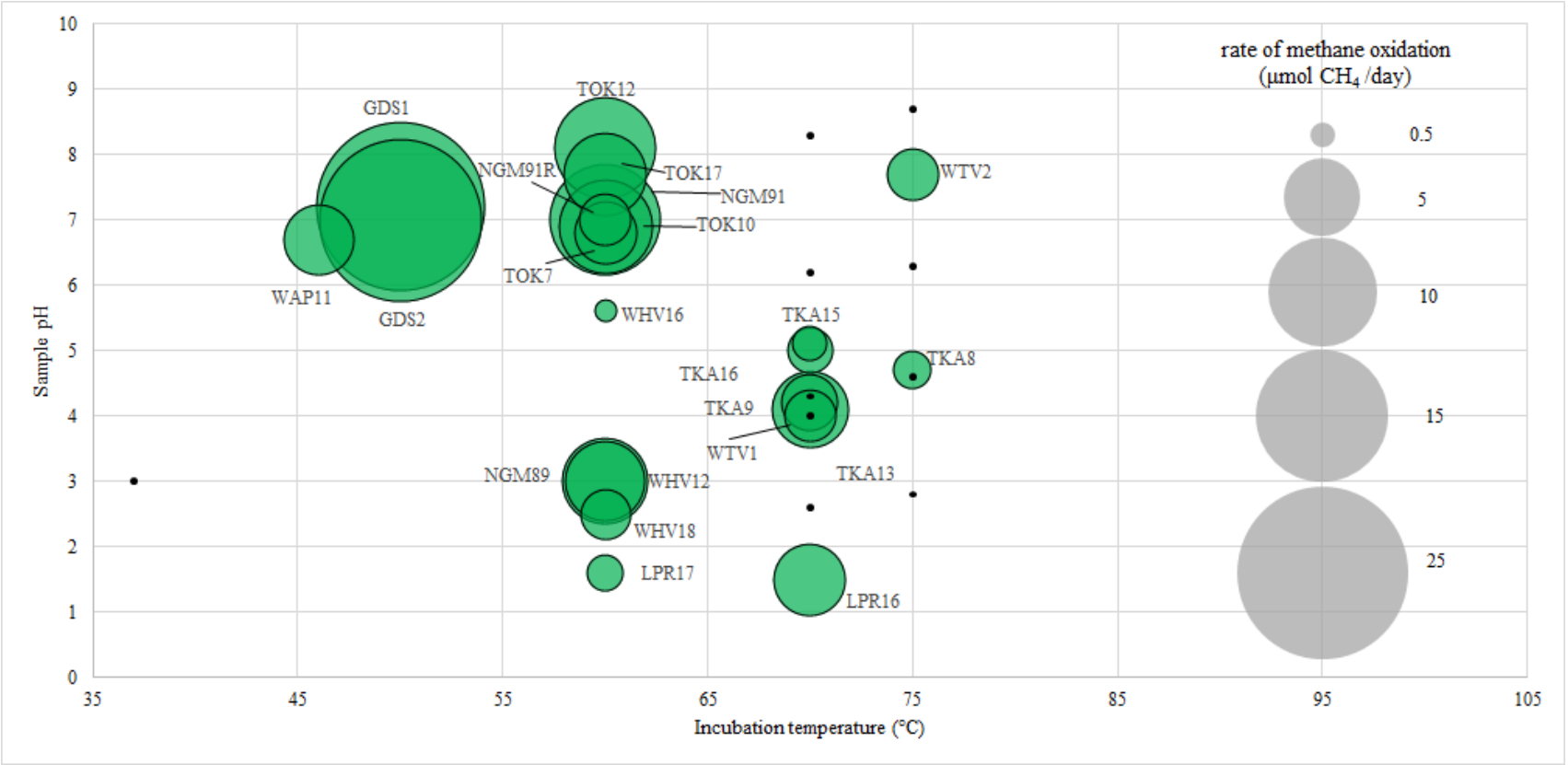

Figure 3.2 Bubble chart of showing methane oxidation rates of enrichment consortia. Green circles, samples that oxidised methane, labelled with microcosm identifier. The relative size of the bubble represents the rate of methane oxidation by the microcosm (µmol CH_4 d^{-1}). Black dots, samples that did not oxidise methane (not labelled with sample identifier).

Metatranscriptome results

To investigate the activity of microbial communities, three geothermal enrichment microcosms were selected for metatranscriptomic analysis. The microcosms were from Golden Springs (GDS1), Tokaanu (TOK7) and Ngatamariki (NGM89) and were chosen to reflect a range of pH and temperatures found across the environmental samples (Figure 3.2). The 16S rRNA gene sequences of each sample indicated that different methanotrophic genera were abundant in each sample; *Methylococcus* in GDS1, *Methylothermus* in TOK7, and *Methylacidiphilum* in NGM89 (Table 3.2). Each sample was split into three biological replicates and incubated with methane for 24 hours before stabilisation and storage of RNA using RNAlater. The samples were then shipped frozen to Novogene, Beijing where RNA was extracted, transcribed, and sequenced. RNA could not be extracted from the NGM89 sample, possibly due to the abundance of humic acids or other inhibitors present in the soil, but library preparation and sequencing were successful with GDS1 and TOK7.

3.3.2 Golden Springs sample 1 (GDS1) replicates

A total of 30.1 Gb trimmed and quality checked reads from three biological replicates (5.02 ± 0.32 Gb/sample) were co-assembled using Trinity [327, 328]. The GDS1 assembly contained 34,259 clusters, which were predicted to include 63,694 genes using heuristic models [329]. Predicted genes with a length of less than 70 bp were discarded. Sequences were clustered at 90 % nucleotide sequence identity and a single representative sequence from each cluster was retained (46,563 predicted genes). As protein:protein searches are more specific than DNA-based searches [337], the BLASTx programme from NCBI [333] was used to identify proteins with significant alignments to the translated predicted genes (based on an Expect or e-value of < 0.01). Predicted metabolic functions could be assigned to 78.6 % of these reads (36,599 proteins) (Extended Data Set 4). Modules within the KEGG "Methane Metabolism", "Oxidative Phosphorylation" and "Nitrogen Metabolism" pathways were then manually identified and mapped using the Search&Color Pathway tool.

3.3.3 GDS1 highly expressed genes

To quantify the expression of genes, trimmed sequencing reads were matched against the predicted genes from the Trinity assembly. The most highly expressed genes are shown in Table 3.4. The full set of transcripts, with their expression and BLASTx annotations, is available in Extended Data Set 6. Protein identity and taxonomy are derived from the NCBI nr protein sequence database with the most significant alignment to the query protein (lowest e-value).

The biological replicates showed a high degree of consistency, with 71.9 % of transcripts being found in all three GDS1 sets. The most highly expressed genes were related to methanotrophs, with 41 of the top 51 transcripts assigned to *Methylococcus*, *Methylomicrobium* or *Methylocystis* species (Table 3.4). The remaining transcripts were dominated by proteins assigned to *Alphaproteobacteria, Actinobacteria* and *Bacteroidetes*: 7,173 transcripts (19.6 %) were assigned to *Rhodopseudomonas*, 3,536 (9.7%) to *Aurantimonas*, and 2,756 (7.5 %) to *Novosphingobium* species; 2,342 (6.4 %) to *Streptomyces* and 1,580 (4.3 %) to *Mycobacterium*; and 1,317 (3.6 %) to *Flavobacterium.*

As expected for microcosms displaying high rates of methane oxidation (478 µmoles/hour) (Appendix 7.7), genes involved in one-carbon metabolism were highly expressed. Particulate methane monooxygenase proteins comprised between 18.5 and 22.9 % of all transcripts in the three replicates, and methanol dehydrogenase proteins 4.7 to 8.4 % of all transcripts.

Hypothetical proteins appeared to be highly expressed in the GDS1 samples (Table 3.4). The product of gene 38077 comprised between 0.7 and 2.6 % of all transcripts, and was identified as most similar to a hypothetical protein from *Methylococcus capsulatus*. The 47 most similar proteins from the NCBI database are all from *Methylococcaceae*, suggesting that this enzyme is specifically required for some aspect of methanotrophy. An alanine-zipper domain was identified using the NCBI Conserved Domain Architecture Retrieval Tool (CDART)[338], which are found in outer membrane lipoproteins such as ATP-binding Cassette (ABC) transporters. Other highly expressed transcripts identified as hypothetical proteins did not have valid domain hits using CD-ART.

Table 3.4 Most abundant transcripts from GDS1 biological replicates. Transcripts that had an average transcripts per million (TPM) > 1000 across three biological replicates are shown. Identity is based on a BLASTx search using the NCBI non-redundant (nr) database. Taxonomy is derived from the BLASTx protein sequence with the most significant similarity.

Gene	TPM (avg)	% identity	e-value	Accession	Identity	Taxonomy
38756	115475	96.6	$4.1E^{-55}$	AAB49820	particulate methane monoxygenase subunit	*Methylococcus capsulatus* str. Bath
23273	47157	96.8	$1.5E^{-109}$	AAB49820	particulate methane monoxygenase subunit	*Methylococcus capsulatus* str. Bath
23272	19414	99.2	$2.5E^{-180}$	AAB49821	particulate methane monooxygenase 27 kDa subunit	*Methylococcus capsulatus* str. Bath
38077	18242	100	$3.0E^{-29}$	WP010959950	hypothetical protein	*Methylococcus capsulatus*
23271	15301	71.3	0	BAE86886	methane monooxygenase protein B	*Methylomicrobium japanense*
15955	11251	97.0	$4.0E^{-35}$	WP016920892	hypothetical protein	*Methylocystis parvus*
4623	6858	96.0	$3.0E^{-07}$	BAW80770	hypothetical protein	*Candidatus* Nitrosoglobus terrae
32715	5049	100	$3.0E^{-41}$	WP010960118	cold-shock protein	*Methylococcus capsulatus*
12629	4505	59.5	$1.6E^{-07}$	WP014889687	methane monooxygenase/ammonia monooxygenase subunit C	*Methylocystis sp.* SC2
36297	3897	89.0	$2.0E^{-51}$	WP010962291	hypothetical protein	*Methylococcus capsulatus*
34484	3621	81.7	$5.3E^{-39}$	WP005372675	methanol dehydrogenase	*Methylomicrobium album* BG8

Gene	TPM (avg)	% identity	e-value	Accession	Identity	Taxonomy
34534	3569	96.0	$7.0E^{-45}$	WP006229561	hypothetical protein	*Methylococcus capsulatus*
39473	3564	74.0	$3.0E^{-43}$	WP007231737	prepilin-type cleavage/methylation domain-containing protein	*Methylococcus capsulatus*
37442	3071	94.0	$9.0E^{-53}$	WP010959880	HU family DNA-binding protein	*Methylococcus capsulatus*
40243	2799	100.0	$8.0E^{-33}$	WP010961245	acyl carrier protein	*Methylococcus capsulatus*
33708	2672	66.0	$9.0E^{-03}$	WP016918745	hypothetical protein	*Methylocystis parvus*
30531	2605	100	$5.0E^{-38}$	WP010959751	carbon storage regulator	*Methylococcus capsulatus*
35752	2469	98.0	$5.0E^{-64}$	WP010961831	cytochrome c-555	*Methylococcus capsulatus*
6744	2285	87.0	$4.0E^{-55}$	WP086102986	RNA-binding protein	*Chitinophagaceae* bacterium IBVUCB2
12617	2190	69.0	$3.2E^{-92}$	WP014889687	methane monooxygenase/ammonia monooxygenase subunit C	*Methylocystis sp.* SC2
39205	1874	67.0	$6.0E^{-09}$	AAU93254	hypothetical protein MCA0556	*Methylococcus capsulatus* str. Bath
40259	1849	100	$2.0E^{-45}$	WP010961228	RNA-binding protein Hfq	*Methylococcus capsulatus*
39462	1728	96.0	$5.0E^{-40}$	WP010960796	cold-shock protein	*Methylococcus capsulatus*
38111	1703	88.0	$4.0E^{-55}$	WP017366094	cytochrome C	*Methylococcus capsulatus*
22366	1649	75.7	$3.5E^{-33}$	WP027033424	cold-shock protein	*Mesorhizobium loti* R7A

Gene	TPM (avg)	% identity	e-value	Accession	Identity	Taxonomy
40306	1619	88.0	$1.0E^{-114}$	WP010960736	hypothetical protein	*Methylococcus capsulatus*
33729	1589	96.0	$5.0E^{-28}$	WP010960095	competence protein ComE	*Methylococcus capsulatus*
36906	1565	86.0	$1.0E^{-101}$	WP017365582	hypothetical protein	*Methylococcus capsulatus*
4485	1563	77.0	$5.0E^{-38}$	PPD46695	hypothetical protein CTY15_00670	*Methylocystis sp.*
36904	1397	96.0	$3.0E^{-59}$	WP010959847	pterin-4-alpha-carbinolamine dehydratase	*Methylococcus capsulatus*
34481	1378	82.6	0	WP005372670	PQQ-dependent dehydrogenase, methanol/ethanol family	*Methylomicrobium album* BG*8*
12628	1308	98.0	$1.0E^{-168}$	WP026016563	ammonia monooxygenase	*Methylocystis parvus*
18723	1306	98.0	$5.. E^{-51}$	WP010960311	RNA-binding protein	*Methylococcus capsulatus*
32714	1306	89.0	$1.0E^{-91}$	WP010960984	Hsp20/alpha crystallin family protein	*Methylococcus capsulatus*
38596	1245	92.0	$4.0E^{-36}$	WP017366029	hypothetical protein	*Methylococcus capsulatus*
15731	1228	87.0	$6.0E^{-38}$	WP086090963	cold-shock protein	*Pseudorhodoplanes sinuspersici*
12627	1224	63.6	$4.0E^{-157}$	WP014889689	methane monooxygenase/ammonia monooxygenase subunit B	*Methylocystis sp.* SC2
38972	1189	70.0	$3.0E^{-175}$	WP010960194	sel1 repeat family protein	*Methylococcus capsulatus*
37455	1185	96.0	$1.0E^{-120}$	WP010961369	hypothetical protein	*Methylococcus capsulatus*

Gene	TPM (avg)	% identity	e-value	Accession	Identity	Taxonomy
38597	1183	54.5	$4.3E^{-15}$	WP011478703	DUF466 domain-containing protein	*Methylobacillus flagellatus* KT
33682	1165	83.0	$5.0E^{-31}$	WP003666108	type I restriction enzyme M protein	*Nitrosomonas ureae*
37263	1163	80.0	$3.0E^{-16}$	WP096451135	DUF4102 domain-containing protein	*Thauera sp.* K11
32038	1155	98.0	$4.0E^{-164}$	WP010961100	cell division protein FtsH	*Methylococcus capsulatus*
36123	1129	63.9	$3.5E^{-57}$	ABE07269	NAD(P) transhydrogenase subunit alpha	*Escherichia coli* UTI89
34482	1097	64.4	$3.5E^{-125}$	WP005372671	methanol oxidation system protein MoxJ	*Methylomicrobium album* BG8
36292	1090	83.0	0	WP010962287	outer membrane protein MopB	*Methylococcus capsulatus*
34577	1088	84.0	$1.0E^{-32}$	WP010960648	bacterioferritin-associated ferredoxin	*Methylococcus capsulatus*
39181	1081	86.0	$2.0E^{-73}$	SCC95225	transposase	*Thiomonas sp.* X19
33683	1058	53.0	$5.0E^{-41}$	OQY67211	hypothetical protein	*Polyangiaceae* bacterium UTPRO1
32713	1028	89.0	$1.0E^{-91}$	WP010960984	Hsp20/alpha crystallin family protein	*Methylococcus capsulatus*
39890	1002	80.0	$4.0E^{-31}$	WP017365281	hypothetical protein	*Methylococcus capsulatus*

3.3.4 GDS1 methane metabolism

In GDS1 samples, transcripts encoding both particulate and soluble forms of methane monooxygenase were expressed, along with multiple methanol dehydrogenase enzymes (Figure 3.3). Methylamine oxidation to formaldehyde was possible via methylamine dehydrogenase (KEGG Orthology number K15229/ Enzyme Commission number EC 1.4.9.1), but while trimethylamine could be oxidised by trimethylamine dehydrogenase (K00317/EC 1.5.8.2), no transcripts encoding the enzymes capable of oxidising the resulting dimethylamine were detected. Transcripts encoding the key enzymes required for methanogenesis, including methyl-coenzyme M reductase (K00399/EC 2.8.4.1) heterodisulfide reductase (K08264/EC 1.8.98.1) and tetrahydromethanopterin S-methyltransferase (K00577/EC 2.1.1.86), were not detected.

Methylotrophs encode a variety of different 'modules' for the oxidation and removal of formaldehyde [41], which is formed by methanol dehydrogenase, methylamine dehydrogenase and enzymes involved in oxidation of halomethanes or methylated sulfur species, and is usually toxic even in low concentrations [36]. Transcripts for multiple potential mechanisms for formaldehyde oxidation were expressed by the GDS1 community, including glutathione-dependent formaldehyde dehydrogenases, and tetrahydrofolate- and tetrahydromethanopterin linked pathways. However, transcripts for a glutathione-independent formaldehyde dehydrogenase for the formation of formate, or for a membrane-associated quinoprotein formaldehyde dehydrogenase, isolated from *M. capsulatus* and reported to be the major formaldehyde-oxidising enzyme in this strain during pMMO expression [339], were not detected in this study.

Methanotrophs are able to assimilate carbon via either the serine cycle, the ribulose monophosphate (RuMP) cycle, or by assimilating carbon dioxide through the Calvin-Benson-Bassham (CBB) cycle [41]. All genes encoding enzymes involved in the RuMP (Figure 3.3) and CBB cycles were identified in GDS1 transcripts, but the serine cycle pathway was not complete. Two key modules were not detected in transcripts (Figure 3.3); K00830, which represents both EC 2.6.1.45 (serine to hydroxypyruvate) and EC 2.6.1.44 (glycoxylate to pyruvate); and K08692, which represents malate-CoA ligase (EC 6.2.1.9).

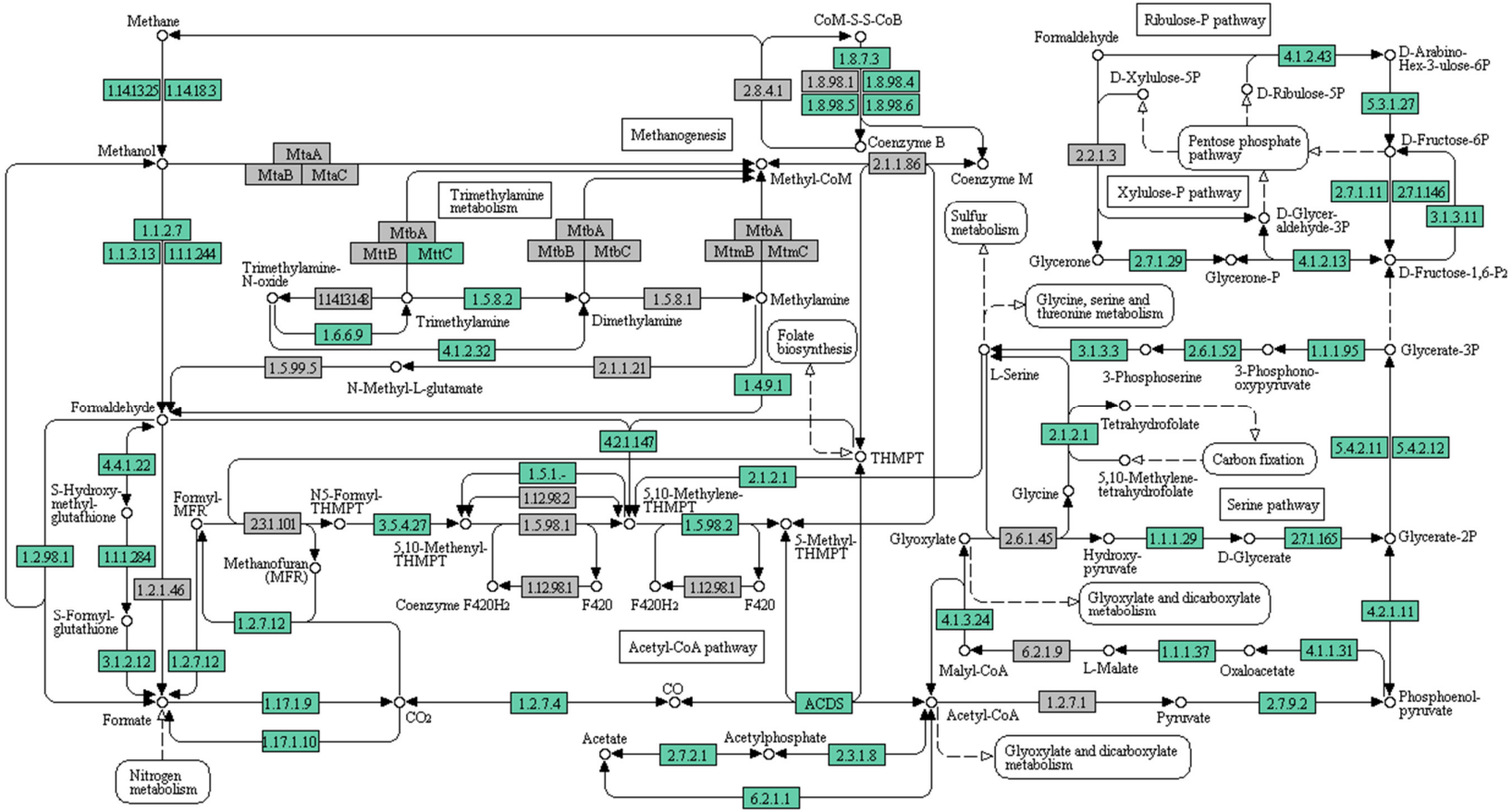

Figure 3.3 Golden Springs GDS1 gene expression in the context of KEGG methane metabolism pathways. Green boxes indicate enzymes identified from transcripts, grey boxes indicate enzymes not identified. Metabolism map copyright Kanehisa Laboratories. See xxi-xxii for gene abbreviations.

3.3.5 GDS1 oxidative phosphorylation

Oxidative phosphorylation is the process of the regeneration of ATP mediated by the electron transport chain (ETC) in aerobic organisms. Reducing equivalents obtained from substrates (electrons and protons) flow from donors with a negative redox potential to acceptors with a more positive redox potential, coupled to the synthesis of ATP from ADP and P*i* [56]. The components of the ETC are membrane-bound, and the enzyme ATP synthase uses the electrochemical gradient across the membrane created by the migration of protons to synthesise ATP.

In the GDS1 samples, genes encoding complete ETC complexes I-V were expressed. For Complex I, genes for all NADH: ubiquinone oxidoreductase subunits were detected (NuoABCDEFGHIJKLMN), but only one subunit of the NAD(P)H-quinone oxidoreductase complex (NdhD) (Figure 3.4). For complex II, genes encoding the bacterial/archaeal succinate dehydrogenase complex (Sdh) subunits A-D were detected, but none of the genes encoding for subunits of the fumarate reductase enzyme. Genes for all three subunits of a ubiquinol cytochrome *c* reductase for Complex III were detected (iron-sulfur, cytochrome *b* and cytochrome *c*1 subunits).

The GDS1 community expressed several genes encoding for the cytochrome *c* oxidase Complex IV. Transcripts of genes encoding for a complete cytochrome *bd* complex were detected (CydABX), but genes encoding subunit IV of the cbb_3-type oxidase was not found, nor genes encoding subunits CyoA or CyoE of heme o synthase. Finally, the ATPase (Complex V) detected in the GDS1 transcripts was of the F-type (AtpABCDEFH), although the gamma subunit could not be distinguished, and no genes encoding sub-units of the V/A type (ATPVABCDEFG/HIK) were identified.

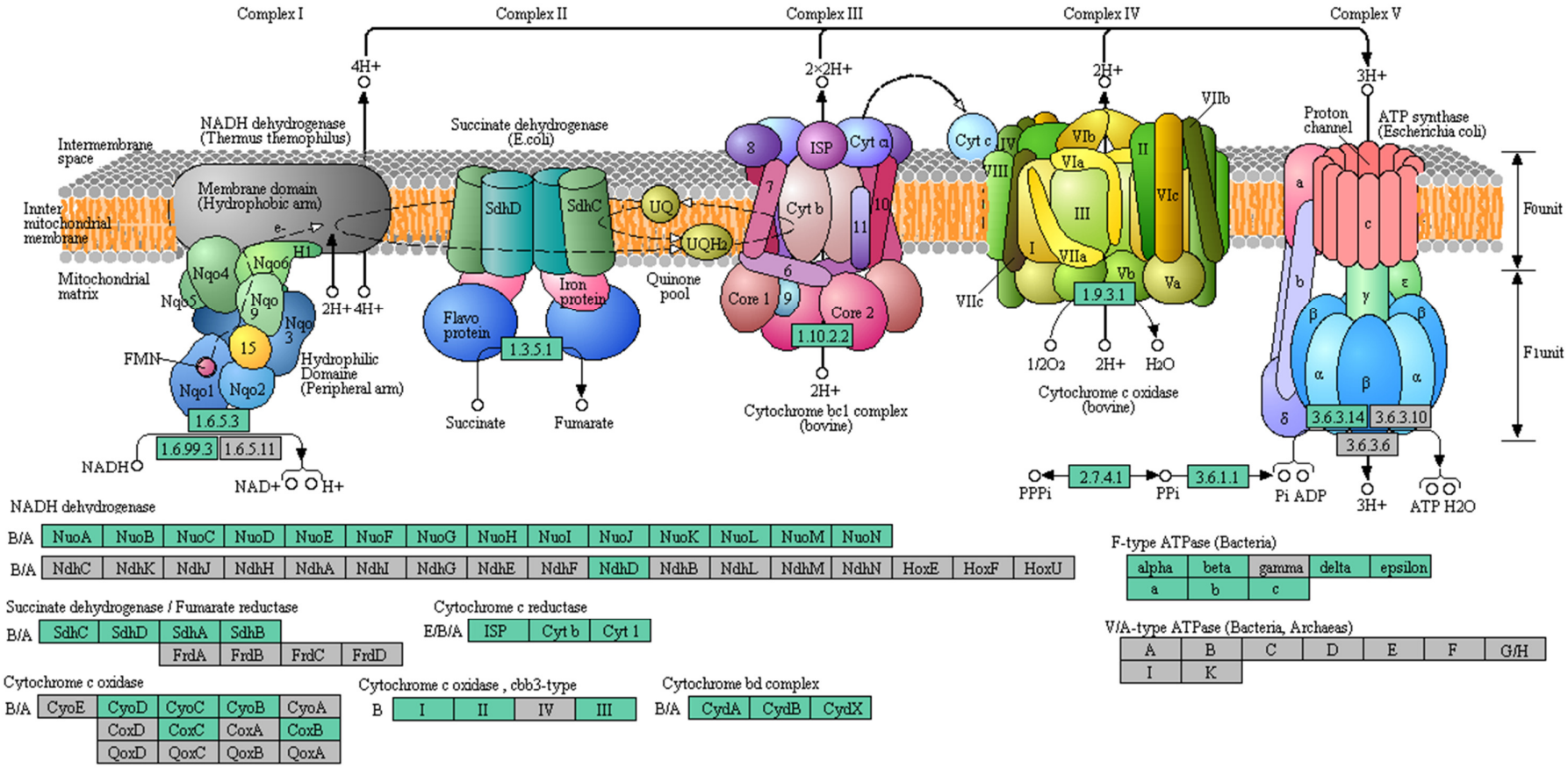

Figure 3.4 GDS1 gene expression in the context of the KEGG oxidative phosphorylation pathways. Green boxes indicate enzymes identified from transcripts, grey boxes indicate enzymes not identified. Metabolism map copyright Kanehisa Laboratories. See xxi-xxii for gene abbreviations.

3.3.6 GDS1 nitrogen metabolism

The GDS1 community was capable of both dissimilatory and assimilatory nitrate reduction to ammonia using multiple pathways (Figure 3.5); genes encoding the NarGHJI (K00370), NapAB (K02567) and NasAB (K00372) forms of nitrate reductases (EC 1.7.99.-) were all detected. Nitrite could be converted to ammonia by various forms of nitrite reductase, with either NADH (NirBD, K00362), cytochrome-*c*552 (NrfAH, K03385), NAD(P)H (NIT-6, K17877) or ferredoxin (NirA, K00366) as co-factors. However, genes encoding NO-forming nitrite reductase (NirK, K00368, or NirS, K15864) were not detected, indicating that denitrification from nitrate to nitrogen was not occurring at the time of sampling.

In addition, the GDS1 community was not performing complete nitrification from ammonia to nitrate at the time of sampling, or transcripts were not detected. Although few ammonia monooxygenase transcripts were identified (average 1,309 transcripts per million), there was a high proportion of genes encoding methane monooxygenase that were expressed (average 205,264 transcripts per million), and this enzyme is also capable of oxidising ammonia, although with no energy gain to methanotrophs [204]. The hydroxylamine produced by this process could then be catalysed to nitrite using hydroxylamine dehydrogenase (Hao, K10535), but genes encoding nitrite oxidoreductase (NxrAB), which converts nitrite to nitrate, were not identified.

Nitrogen could be converted to ammonia through the activity of a molybdenum-iron nitrogenase (NifDKH, K02586), but *anfHDGK* genes encoding an iron-only nitrogenase were not detected. None of the genes encoding enzymes required for anaerobic ammonium oxidation (anammox) were expressed by the GDS1 community.

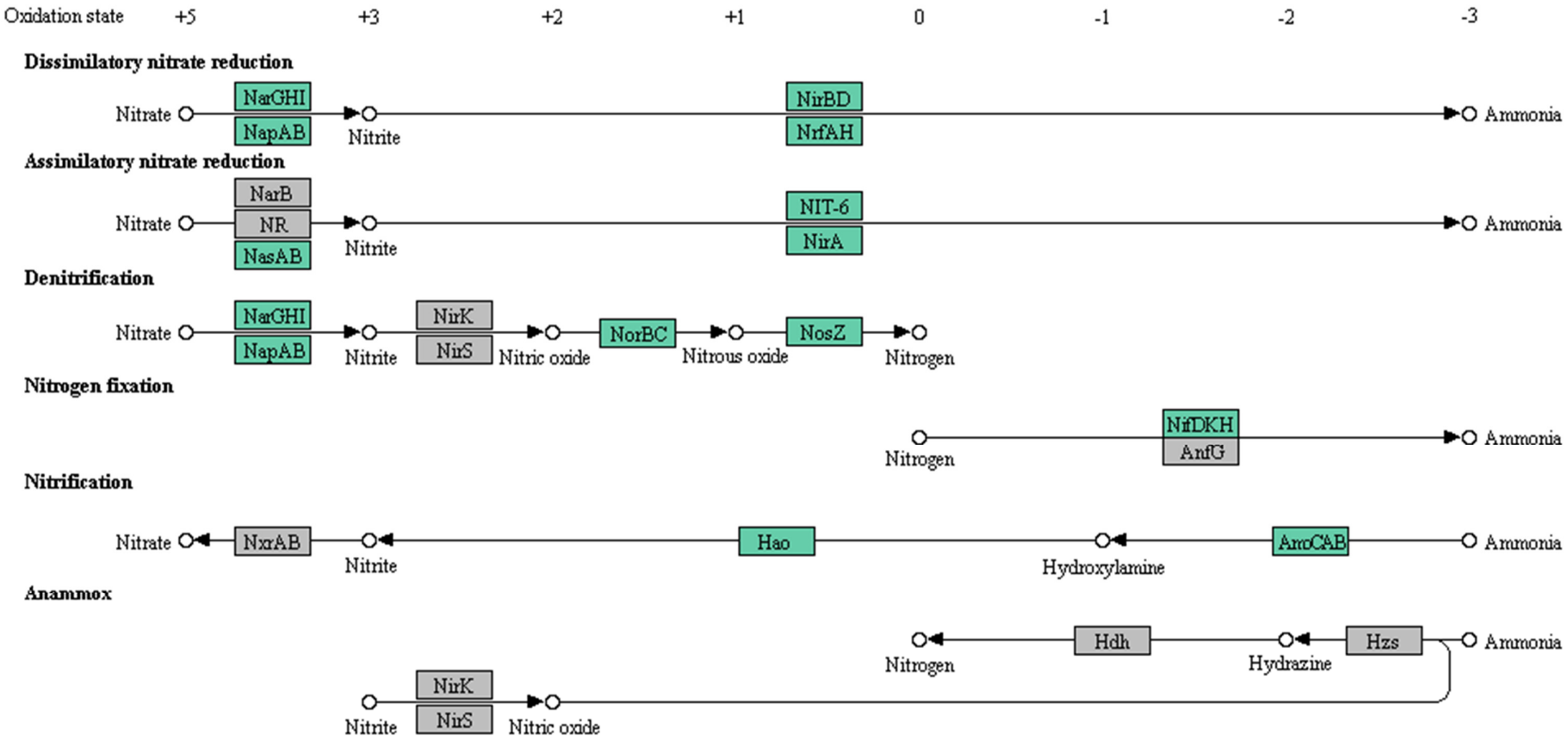

Figure 3.5 GDS1 gene expression in the context of the KEGG nitrogen metabolism pathways. Green boxes indicate enzymes identified from transcripts, grey boxes indicate enzymes not identified. Metabolism map copyright Kanehisa Laboratories. See xxi-xxii for gene abbreviations.

3.3.7 Tokaanu sample 7 (TOK7) replicates

A total of 32.2 Gb trimmed and quality checked reads from three biological replicates (10.73 ± 1.47 Gb/sample) were co-assembled using Trinity [327, 328]. The TOK7 assembly contained 80,528 clusters, which were predicted to include 108,009 genes [329]. Sequences were clustered at 85 % nucleotide sequence identity and a single representative sequence from each cluster was retained (82,693 predicted genes). Using the BLASTx programme from NCBI [333], 64,412 proteins with significant alignments to the translated predicted genes (based on an Expect or e-value of < 0.01) were identified (77.9 %).

3.3.8 TOK7 highly expressed genes

Gene expression was quantified by matching trimmed sequencing reads against the Trinity assembly made from concatenated reads across all three biological replicates. The most highly expressed genes, with an average of > 1000 transcripts per million (TPM) across all three TOK7 biological replicates, are shown in Table 3.5. The full set of transcripts, with their expression across the replicates and their BLASTx annotations, is available in Extended Data Set 6.

The biological replicates showed similar expression patterns; 48.1 % of the transcripts were identified in all three replicates, although all of the transcripts that were only found in one or two of the replicates had less than 110 TPM each. The most highly expressed genes were again classified as from methanotrophs, with 22 of the top 30 transcripts assigned to strains from *Methylococcaceae* (Table 3.5). However, there were only 109 transcripts in total from methanotrophs (0.2 %), including 16 with a top BLASTx hit from *Methylocystis* or *Methylosinus*.

The remaining transcripts included genes encoding for proteins classified as *Pseudomonas* (*Gammaproteobacteria*, 7.8%), *Anaeromyxobacter* (*Deltaproteobacteria*, 5.2 %), *Streptomyces* (*Actinobacteria*, 5.2 %), *Mycobacterium* (*Actinobacteria*, 5.0 %), and *Rhodopseudomonas* (*Alphaproteobacteria*, 5.0 %).

The most highly expressed gene in all three replicates encoded a pyrroloquinoline quinone (PQQ) precursor peptide, PqqA, which comprised up to 5.8 % of the

transcripts. PQQ is a co-factor in a number of bacterial dehydrogenases [340], of which the methanol dehydrogenases encoded by *mxaF* and *xoxF* and found in all methylotrophs [42] are the best characterised [341]. PQQ-dependent dehydrogenases (methanol/ethanol family) were also abundant in the TOK7 transcripts (Table 3.5) with up to 3,977 TPM in the TOK7-C sample. Methane monooxygenase transcripts comprised between 0.9 and 1.8 % of the total transcripts.

Other highly expressed genes included those encoding RNA-binding proteins, and both 30S and 50S ribosomal proteins, essential for translation of mRNA to proteins. However, some RNA proteins, such as those in the Hfq family, regulate stress responses to misfolded proteins and heat stress [342], and it is difficult to determine the function of the RNA-binding proteins expressed by the TOK7 community, based on the available annotation within the NCBI database. A substantial number of other transcripts were also related to stress responses: HU family DNA-binding proteins, which specifically recognise damaged DNA [343]; cold-shock proteins, which also regulate tolerance to oxidative, starvation, pH and ethanol stress [344]; Hsp20, which acts as a protein chaperone during heat stress [345]; and proteins involved in defence against oxidative damage, including superoxide dismutase, peroxiredoxin, and thiol reductase thioredoxin. Another abundant set of transcripts were those for carbon storage regulators, a type of RNA-binding proteins that are involved in post-transcriptional regulation by binding to mRNA and altering translation [346]. Carbon storage regulators are also involved in a wide variety of cellular processes, including controlling metabolic pathways [347], repressing biofilm formation [348] and regulating motility [349], and have been identified as essential for infection by *Borrelia burgdorferi* [350].

Table 3.5 Most abundant transcripts from TOK7 biological replicates. Transcripts that had an average TPM (transcripts per million) > 1000 across three biological replicates are shown. Identity is based on a BLASTx search using the NCBI non-redundant (nr) database. Taxonomy is derived from the BLASTx protein sequence with the most significant similarity, and may not be accurate.

Gene	TPM (avg)	% identity	e-value	Accession	Identity	Taxonomy
40193	44756.4	96.0	$1.0E^{-08}$	WP077731218	pyrroloquinoline quinone precursor peptide PqqA	*Methylocaldum*
39757	14696.4	86.0	$2.0E^{-41}$	KXJ40929	RNA-binding protein	*Methylothermaceae* bacteria B42
39638	12183.9	98.0	$3.0E^{-20}$	KXJ41919	carbon storage regulator	*Methylothermaceae* bacteria B42
22578	12164.6	82.0	$3.0E^{-46}$	WP022948003	HU family DNA-binding protein	*Methylohalobius crimeensis*
14796	7729.3	92.0	$6.0E^{-36}$	WP089399015	cold-shock protein	*Noviherbaspirillum humi*
51290	7158.6	72.0	$1.0E^{-38}$	WP022948549	hypothetical protein	*Methylohalobius crimeensis*
39720	7130.7	83.0	$6.0E^{-13}$	EDN70857	30S ribosomal protein S19	*Beggiatoa sp.* PS
22535	6690.8	77.0	$5.0E^{-27}$	KXJ39747	hypothetical protein AXA67_11835	*Methylothermaceae* bacteria B42
44286	6380.8	76.0	$1.0E^{-40}$	WP022948894	30S ribosomal protein S16	*Methylohalobius crimeensis*
38267	6023.0	93.0	$5.0E^{-124}$	BAJ21968	3-hexulose-6-phosphate synthase	*Methylothermus subterraneus*
51498	5505.7	64.0	$2.0E^{-57}$	WP022947508	Hsp20/alpha crystallin family protein	*Methylohalobius crimeensis*
38266	5437.4	94.0	$2.0E^{-120}$	BAJ21969	6-phospho-3-hexuloisomerase	*Methylothermus subterraneus*
22546	5195.5	96.0	$1.0E^{-31}$	WP045224233	acyl carrier protein	*Methyloterricola oryzae*
38287	4957.3	65.7	0	BAE86886	methane monooxygenase protein B	*Methylomicrobium japanense*
38285	4316.5	78.7	$1.4E^{-147}$	AAD43965	particulate methane monooxygenase	*Methylococcus capsulatus* str. Bath
51217	4248.2	89.0	$1.0E^{-48}$	KXJ40623	50S ribosomal protein L27	*Methylothermaceae* bacteria B42
39613	3672.7	84.0	$6.0E^{-107}$	WP022948752	superoxide dismutase	*Methylohalobius crimeensis*
39561	3644.3	77.0	$4.0E^{-84}$	WP022950180	peptidylprolyl isomerase	*Methylohalobius crimeensis*

Gene	TPM (avg)	% identity	e-value	Accession	Identity	Taxonomy
51220	3589.8	80.0	$2.0E^{-34}$	WP022949566	30S ribosomal protein S20	*Methylohalobius crimeensis*
40154	3575.4	61.0	$6.0E^{-44}$	ABX77934	conserved hypothetical protein, 23S rRNA intervening sequence region	*Coxiella burnetii* RSA 331
51216	3499.5	77.0	$2.0E^{-37}$	WP022949562	50S ribosomal protein L21	*Methylohalobius crimeensis*
100785	3371.1	90.0	$8.0E^{-05}$	GAM74922	ATP synthase alpha chain	*Vibrio*
23254	3266.9	71.0	$4.0E^{-20}$	WP022947738	DUF1631 domain-containing protein	*Methylohalobius crimeensis*
38286	3145.2	79.3	$3.0E^{-137}$	AAB49821	particulate methane monooxygenase	*Methylococcus capsulatus* str. Bath
52979	2912.8	89.0	0	WP026596301	PQQ-dependent dehydrogenase, methanol/ethanol	*Methylohalobius crimeensis*
22551	2793.3	92.0	$1.0E^{-24}$	KXJ39714	50S ribosomal protein L32	*Methylothermaceae* bacteria B42
63826	2498.0	69.0	$2.0E^{-30}$	WP090829651	DUF2188 domain-containing protein	*Nitrosovibrio tenuis*
39715	2465.9	66.2	$1.2E^{-34}$	WP011494643	30S ribosomal protein S17	*Shewanella denitrificans*
60009	2451.6	63.8	$3.6E^{-25}$	WP014331580	cold-shock protein	*Sinorhizobium*
40164	2433.1	78.8	$2.1E^{-40}$	WP003095657	RNA-binding protein Hfq	*Pseudomonas*
39832	2364.9	66.7	$9.8E^{-55}$	WP001280776	thiol reductase thioredoxin	*Proteobacteria*
17946	2350.1	83.3	$3.9E^{-02}$	EAS50136	hypothetical protein SI859A1_01496	*Aurantimonas manganoxydans*
38430	2324.6	87.0	$1.0E^{-132}$	WP022946976	peroxiredoxin	*Methylohalobius crimeensis*
44475	2320.5	86.0	$8.0E^{-77}$	WP010961620	cytochrome c	*Methylococcus capsulatus*
44435	2160.0	67.4	$5.4E^{-42}$	WP011422641	co-chaperone GroES	*Anaeromyxobacter*
35669	2114.1	81.8	$1.6E^{-34}$	WP011311367	cold-shock protein	*Thiobacillus denitrificans*
37142	2082.4	81.8	$5.4E^{-21}$	WP011467202	30S ribosomal protein S21	*Saccharophagus degradans*
15657	2058.3	80.0	$3.6E^{-32}$	WP011959870	50S ribosomal protein L28	*Psychrobacter sp.* PRwf-1
44561	1967.2	59.1	$3.8E^{-19}$	EAS77841	cytochrome c554	*Vibrio alginolyticus* 12G01

Gene	TPM (avg)	% identity	e-value	Accession	Identity	Taxonomy
51587	1905.2	73.3	$9.4E^{-36}$	WP015466189	30S ribosomal protein S19	*Psychromonas sp.* CNPT3
22517	1864.9	69.5	$4.0E^{-63}$	WP000829823	30S ribosomal protein S9	*Vibrio*
38254	1860.5	62.0	$3.6E^{-39}$	WP011468840	DUF1244 domain-containing protein	*Saccharophagus degradans*
30116	1822.6	78.0	0	WP011310676	fructose-bisphosphate aldolase class II	*Thiobacillus denitrificans*
3709	1813.0	55.3	$2.3E^{-13}$	WP006228351	glycerol-3-phosphate 1-O-acyltransferase PlsY	*Photobacterium profundum*
38258	1772.9	60.7	$5.6E^{-12}$	WP006230688	preprotein translocase subunit SecG	*Photobacterium profundum*
39703	1715.4	75.4	$8.6E^{-69}$	WP001029684	30S ribosomal protein S11	*Proteobacteria*
39678	1713.8	86.3	$3.9E^{-74}$	WP000201237	30S ribosomal protein S12	*Vibrio*
38451	1703.6	53.4	$6.5E^{-24}$	AAL17787	hypothetical protein	*Rhizobium leguminosarum bv. trifolii*
51195	1693.8	33.0	$3.0E^{-07}$	WP062274947	hypothetical protein	*Marichromatium gracile*
38608	1636.8	100	$6.0E^{-45}$	KXJ41997	translation initiation factor IF-1	*Methylothermaceae* bacteria B42
39700	1622.5	76.7	$1.3E^{-55}$	WP003255451	50S ribosomal protein L17	*Pseudomonas*
59255	1599.6	76.0	$1.0E^{-75}$	WP022948298	membrane protein	*Methylohalobius crimeensis*
44618	1571.5	79.0	$4.0E^{-42}$	KXJ40541	acetyltransferase	*Methylothermaceae* bacteria B42
39681	1568.5	69.0	$2.3E^{-33}$	WP011467406	50S ribosomal protein L7/L12	*Saccharophagus degradans*
40350	1521.3	52.3	$9.2E^{-15}$	WP007292277	hypothetical protein	*delta proteobacterium* MLMS-1
39711	1460.3	61.4	$3.1E^{-41}$	WP007233013	30S ribosomal protein S14	*gamma proteobacterium* HTCC2207
39719	1457.2	72.5	$2.5E^{-51}$	WP011467447	50S ribosomal protein L22	*Saccharophagus degradans*
51764	1426.0	58.2	$2.9E^{-73}$	WP011312427	N-(5'-phosphoribosyl) anthranilate isomerase	*Thiobacillus denitrificans*
51273	1333.1	66.0	$3.0E^{-28}$	WP026596486	prepilin-type cleavage/methylation domain-containing protein	*Methylohalobius crimeensis*
39702	1330.0	70.1	$1.4E^{-75}$	WP000135216	30S ribosomal protein S4	*Vibrio*

Gene	TPM (avg)	% identity	e-value	Accession	Identity	Taxonomy
51522	1281.7	53.7	$1.2E^{-126}$	WP003151768	aminotransferase	*Pseudomonas aeruginosa*
39842	1267.5	71.4	0	WP011468282	NADH:ubiquinone reductase (Na(+)-transporting)	*Saccharophagus degradans*
44283	1243.5	77.4	$1.0E^{-59}$	WP011312888	50S ribosomal protein L19	*Thiobacillus denitrificans*
15683	1233.1	60.0	$2.0E^{-31}$	WP051149774	dihydrolipoyllysine-residue acetyltransferase	*Methylohalobius crimeensis*
22610	1208.2	65.0	$2.0E^{-31}$	WP022947998	copper chaperone	*Methylohalobius crimeensis*
37923	1194.1	57.8	$2.8E^{-20}$	WP007291910	50S ribosomal protein L35	*delta proteobacterium* MLMS-1
18970	1185.8	70.0	$1.0E^{-72}$	KXJ40693	hypothetical protein AXA67_08610	*Methylothermaceae* bacteria B42
39710	1176.8	67.9	$4.9E^{-59}$	WP006052216	30S ribosomal protein S8	*Burkholderiaceae*
39764	1158.0	71.0	$1.0E^{-54}$	KXJ40255	hypothetical protein AXA67_10365	*Methylothermaceae* bacteria B42
37969	1151.9	59.7	$1.2E^{-98}$	WP007232013	30S ribosomal protein S2	*gamma proteobacterium* HTCC2207
51586	1111.2	63.7	$3.7E^{-54}$	WP011312617	30S ribosomal protein S6	*Thiobacillus denitrificans*
44282	1098.4	53.3	$1.4E^{-24}$	WP011312889	methylated-DNA-[protein]-cysteine S-methyltransferase	*Thiobacillus denitrificans*
44462	1095.1	55.9	$2.2E^{-08}$	WP011453216	exodeoxyribonuclease VII small subunit	*Jannaschia sp.* CCS1
28704	1088.8	72.0	$3.0E^{-24}$	WP018289817	YgiT-type zinc finger domain-containing protein	*Verrucomicrobia sp.* 3C
39714	1066.0	84.4	$7.7E^{-71}$	WP011494644	50S ribosomal protein L14	*Shewanella*
44501	1049.9	69.0	$4.0E^{-44}$	WP022949643	ribonuclease P protein component	*Methylohalobius crimeensis*
40418	1004.1	89.0	$1.0E^{-74}$	WP077385540	IS607 family transposase	*Mycobacterium tuberculosis*

3.3.9 TOK7 methane metabolism

Genes encoding both particulate and soluble forms of methane monooxygenase were expressed in the TOK7 samples (Figure 3.6), and methanol dehydrogenase with PQQ as a-cofactor (EC 1.1.2.7). Formaldehyde could be oxidised via S-(hydroxymethyl) glutathione synthase (K03396/EC 4.4.1.22), a formaldehyde activating enzyme (K10713/EC 4.2.1.147) for the tetrahydromethanopterin pathway, or by 3-hexulose-6-phosphate synthase (K08093/EC 4.1.2.43) for the RuMP pathway. Carbon assimilation within the TOK7 community may also be achieved via the CBB cycle, as all genes for this pathway were identified from the assembly. In contrast, the serine cycle for carbon assimilation was not complete, as genes encoding malate-CoA ligase (K08692/EC 6.2.1.9), malyl-CoA lyase (K08691/EC 4.1.3.24) and an alanine/serine transaminase (K00830/EC 2.6.1.44 or 2.6.1.45 or 2.6.1.51) were all absent from the transcripts. No genes encoding enzymes for the oxidation of mono-, di- or trimethylamine were found in the TOK7 transcripts, and the only evidence for methanogenesis were genes encoding two subunits (of six) of heterodisulfide reductase (EC 1.8.7.3).

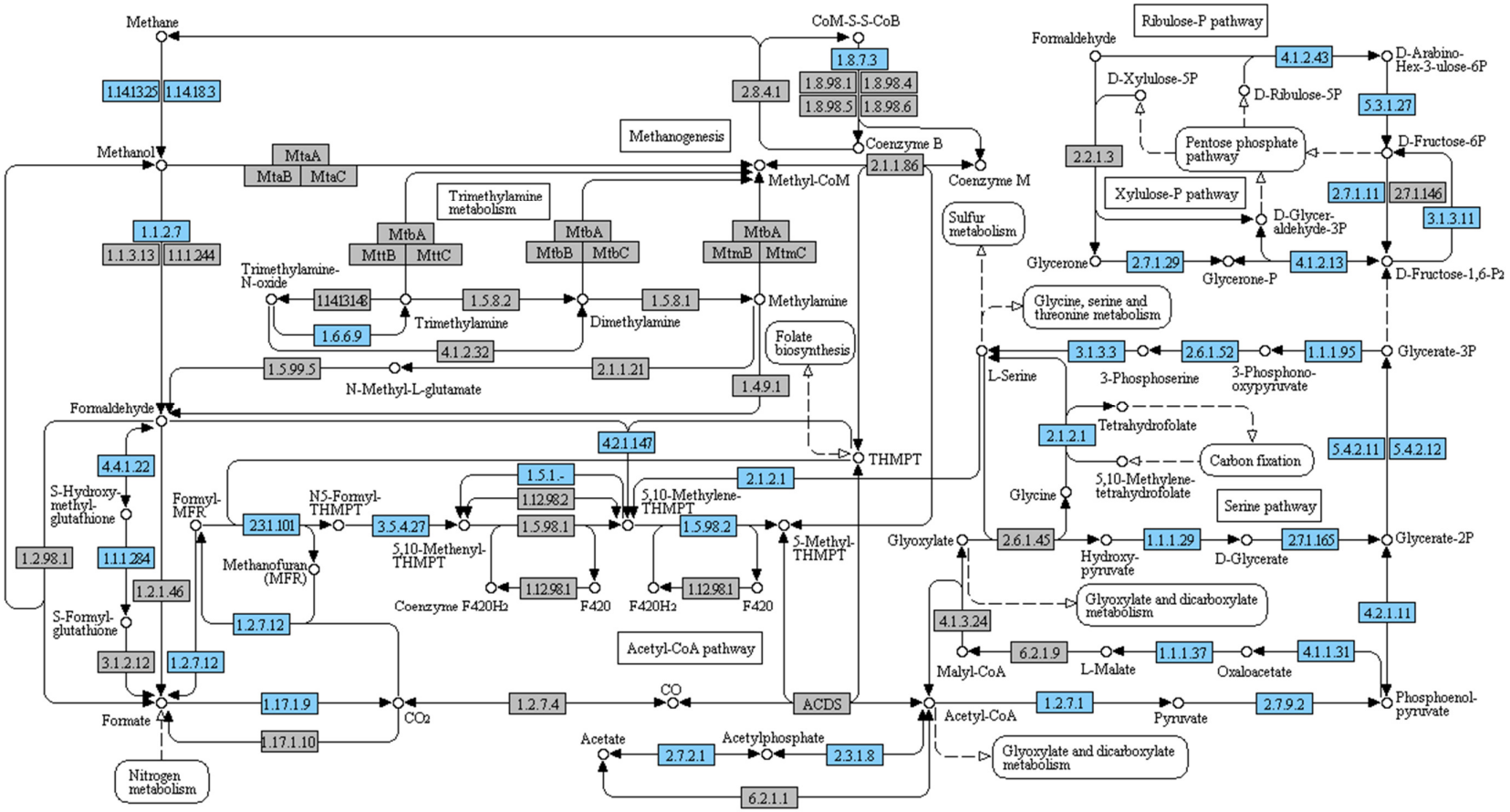

Figure 3.6 TOK7 gene expression in the context of the KEGG methane metabolism pathways. Blue boxes indicate enzymes identified from transcripts, grey boxes indicate enzymes not identified. Metabolism map copyright Kanehisa Laboratories. See xxi-xxii for gene abbreviations.

3.3.10 TOK7 oxidative phosphorylation

The electron transport chain in the TOK7 community could not be fully identified from the transcripts. For Complex I, genes encoding all subunits of NADH-quinone oxidoreductase (EC 1.6.5.3) were expressed with the exception of NuoE (Figure 3.7), and genes encoding for 4/14 NAD(P)H-quinone oxidoreductase (EC 1.6.5.3) subunits were also identified. Genes encoding succinate dehydrogenase (EC 1.3.5.1) were identified within the TOK7 transcripts, as well as cytochrome *c* reductase (EC 1.10.2.-). For respiratory complexes IV and V, the enzymes used are not immediately obvious. While the TOK7 community expressed multiple genes encoding cytochrome *c* oxidase subunits, none of these complexes were complete. Transcripts encoding genes for subunits CydA and CydB from cytochrome *bd* oxidase were identified, but not CydX. The CydX subunit is encoded by a short gene within the operon but has only recently been identified as essential for cytochrome *bd* oxidase activity [351], and protein homologs may not be annotated as such within the NCBI database. Genes that encoded the cbb_3-type cytochrome *c* oxidase (II and IV), heme o synthase (D), and the Cox/COX cytochrome *c* oxidases (A and D, COX15) were also not detected. Neither an F-type (EC 3.6.3.14) or a V/A-type (3.6.3.10) ATPase were completely detected within the TOK7 metatranscriptomes; genes encoding 4/8 F-type subunits and 4/9 V/A-type subunits were detected (Figure 3.7).

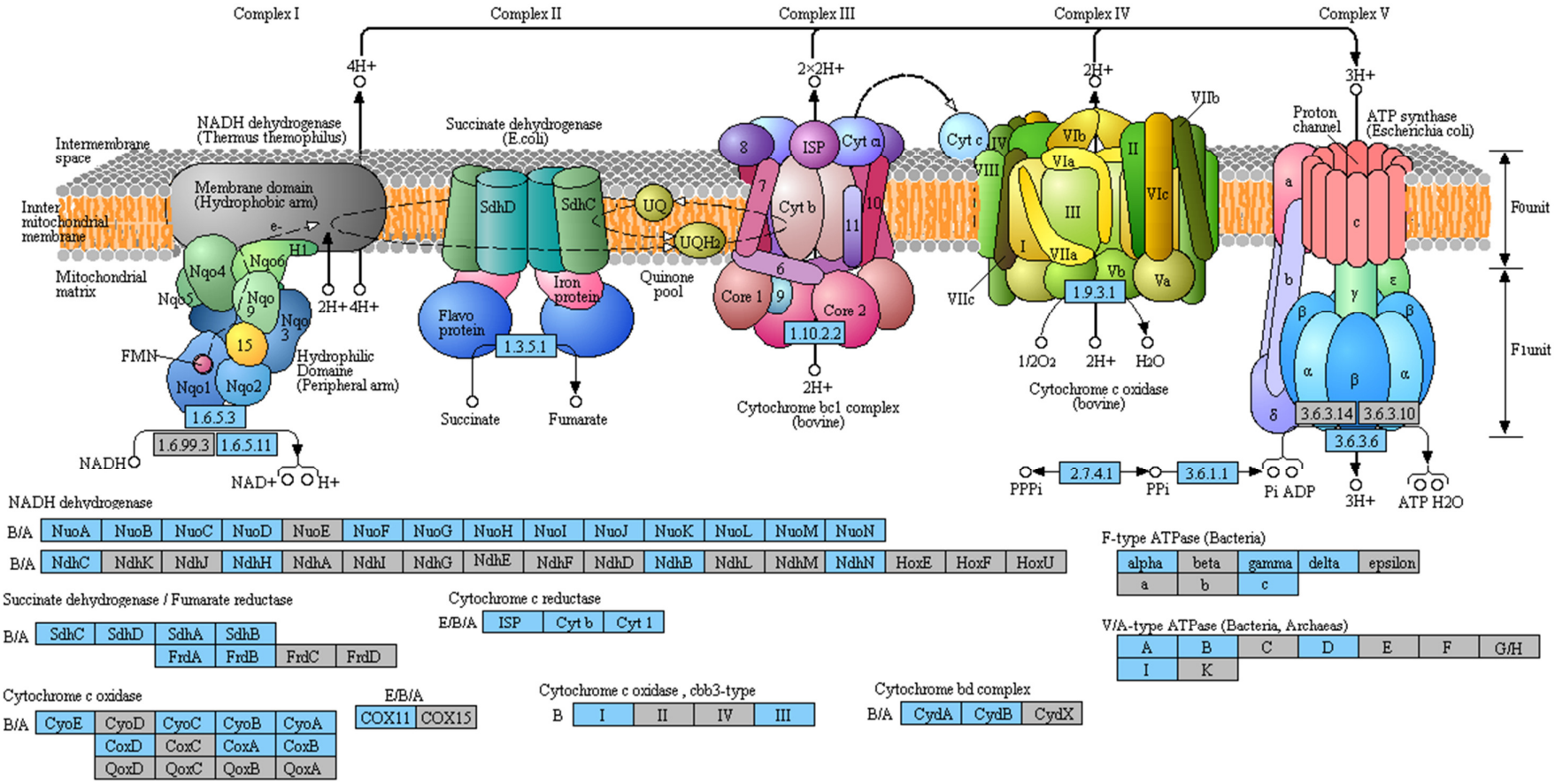

Figure 3.7 TOK7 gene expression in the context of the KEGG oxidative phosphorylation pathways. Blue boxes indicate enzymes identified from transcripts, grey boxes indicate enzymes not identified. Metabolism map copyright Kanehisa Laboratories. See xxi-xxii for gene abbreviations.

3.3.11 TOK7 nitrogen metabolism

The TOK7 community expressed *narGHI* genes for dissimilatory nitrate reduction to nitrite, and could convert this nitrite to ammonia through either NirBD (K00362/EC 1.7.1.15) or NfrAH (K03385/EC 1.7.2.2) nitrite reductases (Figure 3.8). Genes encoding both NirB (K00362) and NrfA (K03385) nitrite reductases were identified in the transcripts. The community was also capable of assimilatory nitrate reduction using NAD(P)H nitrate reductase (K10534) or the NasAB (K00372) nitrate reductase, and converting the resultant nitrite to ammonia using nitrite reductases NIT-6 (K17877) or NirA (K00366), which use NAD(P)H or ferredoxin, respectively, as co-factors.

The metabolic pathways for the denitrification of nitrate to nitrogen via nitric and nitrous oxides were not completely expressed, as the presence of genes encoding NorBC (nitric oxide reductase, K04561) were not detected, although other genes in this pathway for nitrate, nitrite and nitrous oxide reduction were expressed. No genes for the fixation of nitrogen to ammonia (*nifDKH* or *anfHDGK*) were expressed. Genes encoding ammonia monooxygenase were detected in the transcripts (average 1.0 transcripts per million), in addition to methane monooxygenase (average 7,203.5 transcripts per million), which are both capable of oxidising ammonia to hydroxylamine. However, genes encoding hydroxylamine reductase (Hao, K10535) and nitrite oxidoreductase (NxrAB, K00370) were not detected in the transcriptome. Genes encoding enzymes associated with the anaerobic oxidation of ammonium (anammox) could not be identified from TOK7 transcripts (hydrazine synthase, EC 1.7.52.7, or hydrazine dehydrogenase, EC 1.7.2.8).

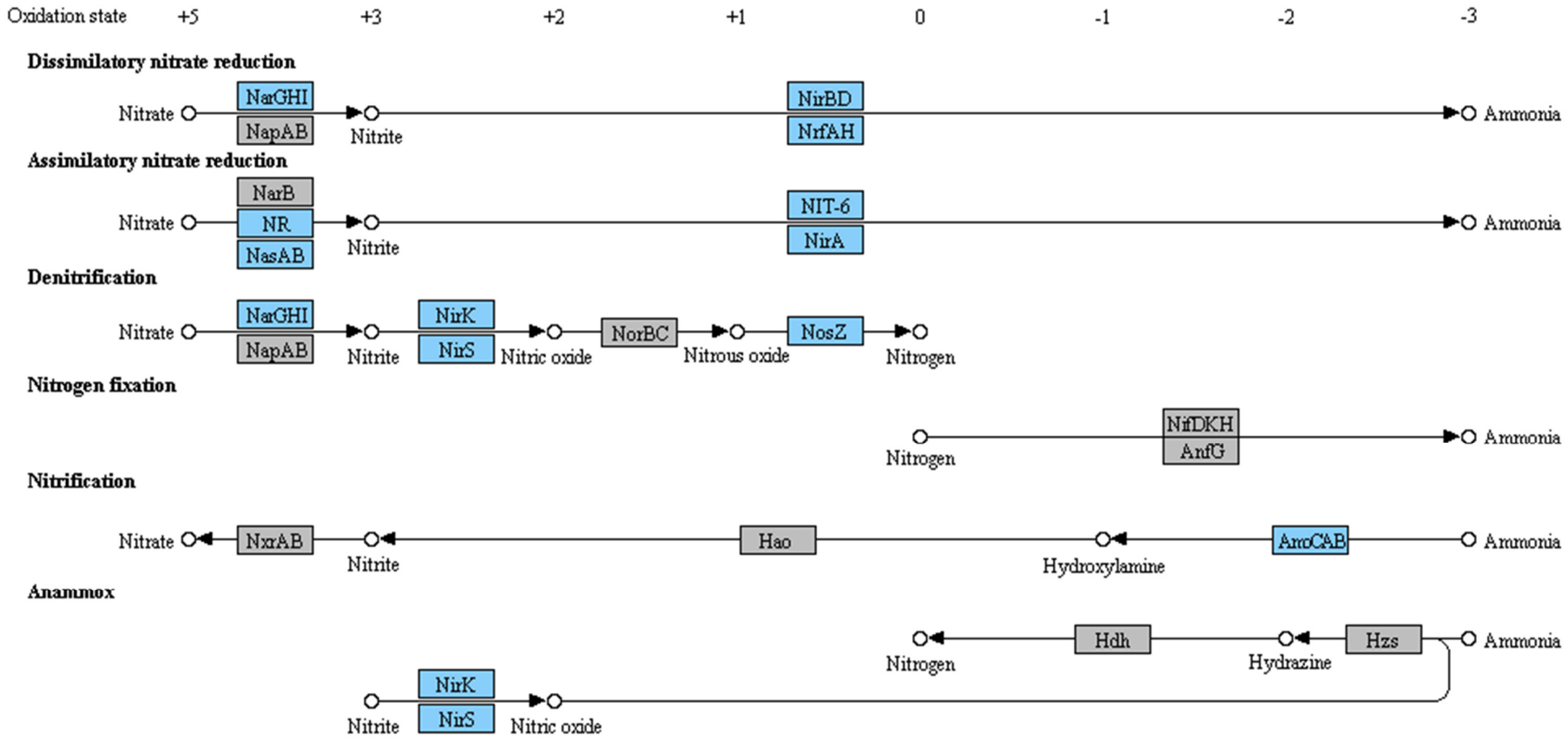

Figure 3.8 TOK7 gene expression in the context of KEGG nitrogen metabolism pathways. Blue boxes indicate enzymes identified from transcripts, grey boxes indicate enzymes not identified. Metabolism map copyright Kanehisa Laboratories. See xxi-xxii for gene abbreviations.

3.3.12 Comparison of GDS1 and TOK7

A comparison of the most abundant transcripts from the GDS1 and TOK7 enrichments is shown in Figure 3.9. GDS1 samples, which displayed an average methane oxidation rate of 478 µmoles/hour at the point of sampling, showed an abundance of methane monooxygenase (average 205,264 TPM) and methanol dehydrogenase transcripts (average 6,842 TPM). These were in much lower abundance in the TOK7 samples (7,203 TPM and 3,652 TPM, respectively), which correlates with the slower rate of methane oxidation of 208.5 µmoles/hour in TOK7 (Appendix 7.7). However, the TOK7 samples expressed an abundance of genes encoding pyrroloquinoline quinone (PQQ) precursors, which could be for the synthesis of methanol dehydrogenases that require PQQ as a co-factor.

TOK7 samples expressed a high number of transcripts of genes encoding 30S and 50S ribosomal proteins and a translation initiation factor, indicating high translation activity, in addition to peptidylprolyl isomerase, which is required for correct folding of newly synthesised proteins [352]. Although these transcripts were also identified in the GDS1 samples, they were at least four-fold more highly expressed in the TOK7 enrichment over the GDS1 enrichment microcosms. Both GDS1 and TOK7 samples expressed an abundance of transcripts for acyl carrier proteins, which are involved in the biosynthesis of fatty acids as well as other lipids, co-factors and signalling molecules [353], and a range of genes for response to various stresses, including cold-shock, heat-shock and oxidative stress. A peptidylprolyl isomerase from *Thermococcus* was induced by cold-shock when temperatures dropped below the optimum for growth [354].

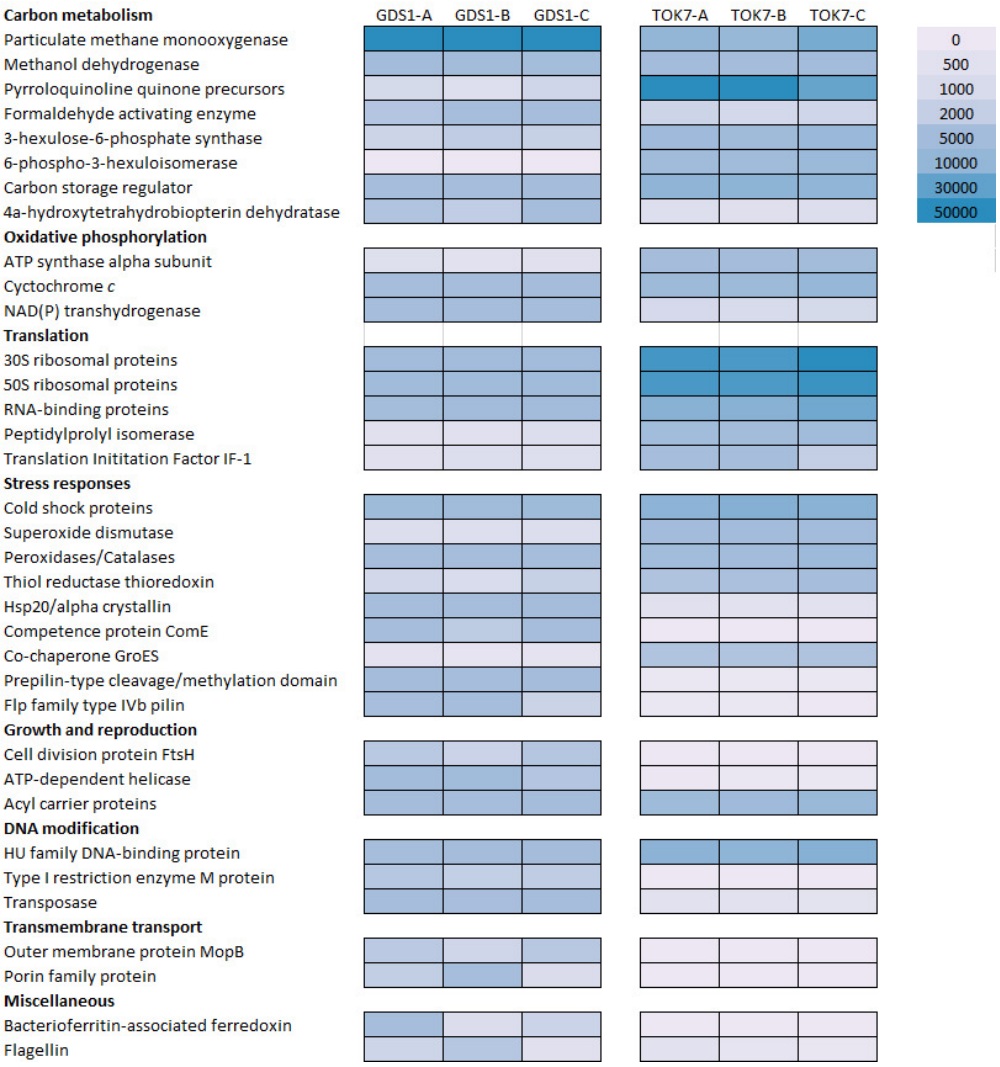

Figure 3.9 Heat map of highly expressed transcripts from GDS1 and TOK7 communities. Abundances are based on the total number of transcripts with annotations indicating the same protein e.g. the number of methane monooxygenase transcripts was determined by combining abundances for "methane monooxygenase", "particulate methane monoxygenase subunit", "methane monooxygenase protein B", "particulate methane monooxygenase subunit PmoC3" and "particulate methane monooxygenase 27 kDa subunit". A full list of the sequence identities combined can be found in Extended Data Set 6.

3.4 Discussion

The three aims of this chapter were to create geothermal enrichment microcosms, to quantify rates of methane oxidation by the microcosms, and to conduct metatranscriptomics on a selection of methane-oxidising microcosms. More than 70 enrichment microcosms were created using the original geothermal samples and a variety of culture media, with 22 oxidising methane, with a maximum rate of 24.5 µmol/day. However, the ability of an enrichment microcosm to oxidise methane was not predictable by any obvious factor, such as the methane oxidation rate of the original sample, or even the proportion of known methanotrophs identified through 16S rRNA sequencing of the sample. For example, the sample from Orakei Korako, OKO2, oxidised methane at a rate of 17.4 µmol/g/day (Table 2.1), but no methane oxidation was observed with enrichment microcosms made with two different media. 16S rRNA gene sequences from this microcosm contained no known methanotrophs, but the sequences were dominated by *Bathyarchaeota* (65.4 % of total sequences), and it has been speculated that members of this phylum perform anaerobic dissimilatory methane oxidation [19]. In this case, the aerobic atmosphere of the enrichment microcosms may have inhibited growth, whereas the original soil microcosm could have contained sufficient anaerobic microenvironments to maintain anaerobic methane oxidation.

Similarly, two samples from Tikitere, TKT67 and TKT68 oxidised methane at 9.4 and 7.1 µmol/g/day respectively, but no oxidation was observed in media. 16S rRNA gene sequences from these samples also had high abundances of *Bathyarchaeota* (10.0 % and 10.2 %, respectively), but also high numbers of *Thaumarchaeota* reads (18.0 % and 18.9 %, respectively). Although few members of this phylum have yet been cultivated, those that have been are all known aerobic ammonia-oxidisers [355-358], and the ammonia monooxygenase enzyme is capable of also oxidising methane, although with no energy gain to the host [204]. *Bathyarchaeota* or *Thaumarchaeota* were also prevalent in five of the other microcosms which did not continue to oxidise methane in media; Tokaanu TOK15 (0.1 % and 29.7 %, respectively); Waimangu WAM36 (5.2 % and 17.5 %); Whakarewarewa WHV15 (20.8 % and 0.5 %); Waikite WKT45 (0.3 % and 13.5 %); and Wairakei Thermal Valley WTV4 (68.0 % and 9.0 %). 16S rRNA gene sequences from known aerobic methanotrophs comprised very low

proportions of each microcosm, and anaerobic methane-oxidisers such as ANME or *Methylomirabilis* were not detected at all.

The two final microcosms which did not continue oxidising methane were Loop Road LPR14 and Whakarewarewa WHV13. The 16S rRNA gene sequences of LPR14 were dominated by *Sulfolobacea*e reads (91.0 %), which grow via sulfur oxidation, but *Methylacidiphilum* reads also made up 2.7 % of the total, suggesting that these aerobic methanotrophs were responsible for the observed methane oxidation. However, the microcosm did not oxidise methane when inoculated into V4 medium, which was previously used to culture *M. infernorum*, and this may have been due to the availability of soluble methane during the transition into liquid media. Initial observations of methane oxidation within geothermal soils (Section 2.3.2) were assessed on soils only, whereas the enrichment microcosms in this chapter were a mix of the initial geothermal soils amended with liquid medium. Thus, while all samples were given the same headspace (containing approximately 10 % v/v CH_4), methane diffuses through water 10,000 times slower than through air [191], and methane solubility markedly decreases with increasing temperature [359]. It therefore would be logical that methane diffusion into the medium would have been limited in high temperature microcosms compared to the lower temperature microcosms and/or the original microcosms. This may explain why the Loop Road LPR14 enrichment microcosm, and other samples incubated at 75 °C, showed limited methane oxidising capabilities (only 33 % of samples above 75 °C showed substantial methane oxidation), while all of the samples incubated at 60 °C or below showed methane-oxidising activity, with the exception of TKT68 (50 °C) as mentioned above. Increasing the concentration of methane in the headspace, or increasing the overall headspace pressure to force more methane to dissolve in the media, may have alleviated this issue.

The microorganisms responsible for the initial methane oxidation of the Whakarewarewa WHV13 sample are unknown, although the high incubation temperature (75 °C) may have caused the lack of methane oxidation observed with the enrichment culture. 16S rRNA reads were dominated by the families *Aquificaceae* (45.7 %) and *Desulfurococcaceae* (16.6 %), as well as other

uncultured *Thermoprotei* (21.6 %), while *Bathyarchaeota* and *Thaumarchaeota* reads comprised just 0.1 % each of the total. 0.4 % of reads were classified as *Methylacidiphilum*, but the pH of the original sample was pH 8.7, far higher than the known growth range for these strains (pH 0.8 – 6.0) [14, 43]. No anaerobic methane oxidisers were identified.

Another factor that may have inhibited the growth of methanotrophs (or ammonia oxidisers) is the lack of required specific growth factors not commonly used in standard culture media. *Methylacidiphilum* species require micromolar concentrations of rare earth elements (REE) as co-factors for their methanol dehydrogenases [42], although these were thought for a number of years to be biologically inert [341] (these were present in the V4 culture medium used in this study). Similarly, ammonia-oxidisers from *Thaumarchaeota* are often grown in medium containing selenite and tungstate [360, 361], which were not added to media in this study, and cultured under static conditions in the dark, which may have affected their growth and co-oxidation of methane.

Three of the methane-oxidising enrichment microcosms were selected for metatranscriptomic analysis, based on the presence of methanotrophs predicted by 16S rRNA gene sequencing; Ngatamariki NGM89 (*Methylacidiphilum*), Tokaanu TOK7 (*Methylothermus*), and Golden Springs GDS1 (*Methylococcaceae* that were not assigned as *Methylothermus*). Unfortunately, RNA was only successfully extracted from GDS1 and TOK7. This may have been due to the presence of high concentrations of humic acids in the NGM89 microcosm, which inhibit detection and amplification of nucleic acids [308], or of clay minerals that can adsorb RNA [308].

Both GDS1 and TOK7 samples contained active methanotrophs, with abundant transcripts corresponding to methane monooxygenase and methanol dehydrogenase from both *Methylococcaceae* (Type I methanotrophs) and *Methylocystaceae* (Type II). Soluble methane monooxygenase from *Methylomicrobium* were also identified in both sets of microcosms, but at very low levels of expression, which is consistent with inhibition of the *mmo* operon caused by amended copper added as part of the culture media [77].

It should be noted that taxonomic assignments based on community protein transcripts should be assessed with some caution, as BLASTx alignment with the e-value closest to zero may not reflect community composition exactly. Protein domains may be highly conserved across taxa or there may be variability within families [337]. In addition, the heuristic BLAST algorithms represent a trade-off between speed and sensitivity [362, 363] and may fail to detect some distant relationships between sequences [337]. Thus, it is not surprising that a comparison of the GDS1 16S rRNA gene sequence taxonomies of the geothermal soil microcosm (Extended Data Set 3) did not reflect the BLASTx taxonomies in this chapter. For example, OTUs from the original sample were dominated by *Pseudomonas* (46.9 % of total normalised reads), and with no OTU reads affiliated to *Rhodopseudomonas*, *Aurantimonas*, *Novosphingobium*, *Streptomyces* or *Mycobacterium*, yet community protein transcripts in analysis suggested these strains were highly active. Conversely, *Flavobacterium* did appear in the 16S rRNA gene sequences, but comprised only 75 transcript reads (0.05 %). Many of these inconsistencies may stem from the association bias within the NCBI database that favours just four phyla (*Proteobacteria, Actinobacteria*, *Bacteroidetes*, and *Firmicutes*) [309]; approximately 90 % of all isolated strains are affiliated to one of these phyla and therefore have a higher proportion of characterised proteins within the database. Metatranscriptomic analysis is also biased towards microorganisms within the community with a higher rate of transcription [364].

The *Methylocystaceae* OTUs in GDS1 comprised 4.9 % of all reads, although no reads classified as *Methylocystis* were found in the original sample, and some transcripts were identified as such. Protein products of the genes expressed in the GDS1 community may share significant homology with proteins from Type II methanotrophs from *Methylocystaceae,* in the same manner as the proteins classified as *Alphaproteobacteria, Actinobacteria* and *Bacteroidetes* strains. Another explanation for this observation is that there may have been a very small number of these microbes in the sample that were missed by the original sequencing, perhaps due to extraction or amplification bias, but that have been sufficiently enriched with methane as the sole energy source to become highly active.

Similarly, TOK7 transcripts were primarily identified as *Pseudomonas, Anaeromyxobacter*, *Streptomyces*, *Mycobacterium*, and *Rhodopseudomonas*, which did not reflect the community sequenced from the original geothermal sample, which contained six *Pseudomonas* OTUs from 149,400 normalised reads, and none from any of the other genera listed above. The TOK7 soil sample was dominated by OTUs assigned to *Methylacidiphilum* (18.0 % of normalised reads), *Methylothermus* (11.2 %), *Thermus* (7.5 %), and *Sulfolobus* (3.6 %). No BLASTx hits were assigned to *Methylacidiphilum* or *Sulfolobus*, and only 12 to *Methylothermus* (0.02 %) and 310 to *Thermus* (0.5 %).

Both GDS1 and TOK7 transcripts contained sequences for the complete oxidation of methane, using either the RuMP or CBB cycle for carbon assimilation, but the serine cycle was not complete; malate-CoA ligase and serine-glycoxylate transaminase were absent in both samples, in addition to malyl-CoA lyase that was not identified in TOK7 transcripts. There were also critical genes in the oxidative phosphorylation pathways for which transcripts could not be identified, including the gamma subunit of an F-type ATPase in the GDS1 transcriptome, and the *nuoE* gene for a NADH dehydrogenase subunit within the TOK7 transcriptome. There are multiple reasons why transcripts of genes essential for ATP synthesis were not found in this study. The mRNA extraction process, with subsequent cDNA synthesis by random hexamers and PCR enrichment, may introduce bias with some transcripts not extracted or amplified; transcripts for specific genes may have been removed during the filtering process to remove poor quality or short sequences; and the heuristic model method used to predict genes (hidden Markov model) may have missed some sequences. In addition, clustering predicted genes at 90 % similarity for GDS1 and at 85 % for TOK7 (to reduce the complexity of the transcriptome for further analysis), may have meant that transcripts of genes with similar sequences were combined incorrectly.

In the nitrogen metabolism pathways, both GDS1 and TOK7 communities were capable of both dissimilatory and assimilatory nitrate reduction, but key denitrification transcripts were not identified: *nirK* or *NirS* in GDS1, to convert nitrite to nitric oxide, and *norBC* in TOK7, to convert nitric oxide to nitrogen. In this case, the short half-life of mRNA may mean that it is not possible to detect

ephemeral transcription of specific genes [365], if these are present in the genomes of the community.

Both sets of microcosms had a high of abundance of transcripts for carbon metabolism, particularly methane monooxygenase in GDS1 replicates and methanol dehydrogenase precursors in TOK7. Highly expressed genes in both microcosms included a large number that were classified as stress responses. Transcripts from all samples contained between 11,283 and 18,008 TPM cold-shock proteins, which may be related to the effect of centrifugation at 10 °C at the end of the experiment, possibly before RNAlater had penetrated through all the cells. Alternatively, cold-shock proteins may be expressed in response to a variety of other environmental stresses, including starvation or alcohol concentrations [344], which could be caused by rapid methane oxidation and production of methanol by the highly active methanotrophs within the community.

There were some notable differences between the microcosms in terms of highly expressed genes. In the GDS1 replicates, there was an abundance of transcripts related to DNA modification including restriction enzymes and transposase, and *comE*, which encodes proteins involved in the uptake of DNA as well as pilus synthesis and protein secretion [366]. The high proportion of transcripts for pilin and prepilin proteins in these replicates may indicate that community members involved in DNA uptake or conjugation, although pili are also involved in cell adherence and biofilm modulation [367].

TOK7 replicates expressed a higher abundance of genes related to translation, including 30S and 50S ribosomal proteins, peptidylprolyl isomerase and translation initiation factors. In addition, co-chaperone *GroES* was expressed more highly in these microcosms than in GDS1 replicates. This gene encodes a chaperonin that is required for protein folding and assembly, and is induced under heat-shock or other stress conditions [368].

3.5 Conclusions

Methane oxidation was observed in 22 enrichment microcosms made from geothermal soil or sediment samples inoculated into a range of media. Methane

oxidation rates were not correlated with the rate of methane oxidation observed with the original microcosm, and were not predicted by 16S rRNA gene sequencing. The reduction in the number of enrichment microcosms oxidising methane > 60 °C, compared to the number of original microcosms, may be significant. The decrease in solubility of both methane and oxygen as temperatures increase may constrain the growth of thermophilic methane-oxidising bacteria in aqueous solutions, and thermophilic methanotrophy may be restricted to moist soils with high gas diffusion.

Metatranscriptomics has elucidated many of the metabolic pathways used by the GDS1 and TOK7 communities, but use of stable isotope probing (SIP) may have given more focused results. The addition of ^{13}C-methane to the headspace, and sequencing of labelled RNA, would have targeted methane oxidisers and reduced the number of transcripts from non-methylotrophic microbes [163]. However, this would not have given information about co-operative behaviour [316] or interactions with heterotrophs [317], although in practice this was difficult to determine, given the high proportion of transcripts classified as genera not identified in the original 16S rRNA sequences and probably over-represented in the NCBI database. Methanotrophs outside of the four major phyla that constitute NCBI protein databases (*Proteobacteria, Actinobacteria*, *Bacteroidetes*, and *Firmicutes*), such as *Methylacidiphilum* strains or other novel genera, were unlikely to be detected.

The next stage of this study is to attempt isolation of methanotrophs from the methane-oxidising enrichment cultures, and if successful, to characterise the strains in terms of their physiology and phylogeny.

4. Isolation and Characterisation of Methanotrophs

4.1 Introduction

Aerobic methane-oxidising bacteria play a significant role in the global carbon cycle by acting as a sink for methane released through biogenic and abiotic processes. Wetlands, which include swamps and bogs, are the largest source of methane, releasing up to 284 Tg CH_4 annually [4], and methanotrophic communities have been extensively studied in these environments.

Geological sources of methane, including the oceans, can release up to 75 Tg CH_4 each year [4], and geothermal areas are important ecosystems for methanotrophs, with several thermotolerant [64, 273] and thermophilic [47, 57, 58] strains of *Gammaproteobacteria* and *Verrucomicrobia* isolated from hot springs or geothermal soils. Several molecular studies have also highlighted the presence of methanotrophs in geothermal areas [122, 139, 236, 237], using the *pmoA* gene, which encodes for a subunit of the particulate methane monooxygenase enzyme found in almost all known methanotrophs. The primers used are based on the sequences of cultured strains, and there is a high degree of divergence within these sequences [112, 115, 117]. The existence of methanotrophs from the phylum *Verrucomicrobia* was unknown until 2007, when three groups almost simultaneously isolated novel strains for which standard PCR primers were unable to amplify *pmoA* sequences [14, 43, 55].

However, the detection of methanotrophs within these soils must be considered conservatively as the presence of extracellular or relic DNA in soils [285] may over-estimate the abundance of methanotroph populations. OTUs most similar to *Methylacidiphilum* were found in all 59 geothermal soil samples initially collected and assessed in this research (Section 2.3.8), yet included environmental conditions (particularly pH or temperatures) outside of the growth range for these strains [47]. Culture-based investigations are therefore vital in order to understand not only the prevalence of specific microbes, but also their physiology, their role in their environment and their interactions with other organisms.

In the previous chapter, microcosms were established to demonstrate methane oxidation, and for establishing enrichments for metatranscriptomic analysis of communities to identify methanotroph taxonomies and putative methane oxidation pathways. This work, combined with the community diversity analysis (chapter two), clearly demonstrate active and potentially novel thermophilic methanotrophic communities are present within geothermal soils in the TVZ. In this chapter, I aim to enrich, isolate and characterise thermophilic methanotrophs from soils shown to support active thermophilic methanotrophic communities to better elucidate the conditions under which these methanotrophs operate. Thus, the aims of this chapter are to i) isolate methanotrophs from the enrichment microcosms established in chapter three, and ii) to characterise these isolates in terms of their growth temperature and pH ranges, preferred carbon and nitrogen sources, rates of methane oxidation and the presence or absence of specific functional genes.

4.2 Methods

4.2.1 Sampling and enrichment

Sampling locations, methods and enrichment procedures are outlined in chapters two and three. Briefly, 32 soil or sediment microcosms exhibiting methane oxidation were split and transferred into vials containing 40 ml sterile media. Each sample was then tested for methane oxidation in a modified NMS media (Appendix 7.4) and at least one other medium, depending on the measured pH of the sample and the putative methanotrophs within the sample as determined by 16S rRNA gene sequencing (Table 3.1). The media chosen were: NMS [214], dNMS [320], ANMS [57], mmj [62], or V4 [14]. For media composition, see Appendix 7.4. All media was autoclaved at 122 °C and 15 PSI for 20 minutes. A gas mixture, consisting of 80 % CH_4, 15 % CO_2 and 5 % O_2 (all v/v), was injected into the sample vial air headspace through a sterile filter resulting in final gas headspace concentrations of approximately (v/v) 10 % CH_4, 1 % CO_2 and 22 % O_2 (approximately 7-20 kPa). Vials were incubated in rotary shakers at close to *in situ* sample temperatures and the headspace was sampled at regular intervals to quantify methane oxidation using GCs equipped with either a Flame Ionisation Detector (Peak Performer 1, Peak Laboratories, CA) or a Thermal Conductivity Detector (Micro-GC, Agilent, CA).

4.2.2 Isolation

Isolation of methanotrophs was attempted from all 22 enrichment microcosms that became visibly turbid after incubation and where methane oxidation was observed via headspace sampling and quantification. Enrichment cultures were transferred to fresh media (1:10 v/v) and incubated under the same conditions (Table 4.1). After at least three passages with concurrent methane oxidation, the enrichments were serially-diluted to extinction. In some instances, antibiotics such as monensin (30 µg/ml), which specifically target Gram-positive microorganisms, were used to remove contaminating bacterial species in mixed cultures. The resultant cultures were checked for axenic purity via phase-contrast microscopy (Eclipse Ni; Nikon, Tokyo, Japan), the absence of growth of heterotrophs on complex media, and sequencing of the 16S rRNA gene. Unless otherwise stated, all axenic cultures generated via this strategy were cultivated for characterisation in an air headspace with the addition of approximately (v/v) 8 % CH_4 and 0.08 % CO_2, with shaking at 170 r.p.m., for all physiological tests.

Table 4.1 Cultivation conditions for enrichment microcosms that demonstrated methane oxidation.

Source	Source nomenclature	Media	Media pH	Incubation temperature (°C)	Enrichment oxidation rate µmol/day
Golden Springs	GDS1	NMS	6.8	37	24.49
	GDS2	NMS	6.8	37	22.68
Loop Road	LPR16	V4	1.5	70	4.56
	LPR17	mNMS	1.5	60	1.18
Ngatamariki	NGM89	mNMS*	3.0	60	5.54
	NGM91	ANMS	6.8	60	10.64
	NGM91R	mNMS	6.8	60	2.33
Te Kopia	TKA8	mNMS	5.0	75	1.32
	TKA9	mNMS	4.2	70	2.82

Source	Source nomenclature	Media	Media pH	Incubation temperature (°C)	Enrichment oxidation rate µmol/day
	TKA13	mNMS	4.0	70	5.18
	TKA15	mNMS	5.0	70	1.09
	TKA16	mNMS	5.0	70	1.82
Tokaanu	TOK7	ANMS	6.8	60	3.48
	TOK10	ANMS	6.8	60	7.67
	TOK12	ANMS	8.0	60	8.88
	TOK17	mNMS	7.5	60	5.98
Waipahihi	WAP11	ANMS	6.8	46	4.30
Whakarewarewa Village	WHV12	mNMS*	3.0	60	6.54
	WHV16	mNMS	5.5	60	0.47
	WHV18	mNMS	2.5	50	2.23
Wairakei Thermal Valley	WTV1	mNMS	4.0	70	2.29
	WTV2	mNMS	8.0	75	2.40

*When the taxonomy of the strain isolated from these samples was determined, the medium was switched to V4 [29] at pH 3.0 for improved growth.

Methanotroph isolate characterisation

4.2.3 Genomic DNA extraction

Cells grown under standard conditions were collected in mid-exponential growth phase via centrifugation. Two millilitres of cell suspension were centrifuged for 10 minutes at 22,000 x *g* in a Gyrozen 1730R centrifuge (Seoul, Korea). The supernatant was discarded, and the cell pellet resuspended in 180 µl of a Tris-HCl buffer containing 20 mM Tris/HCl, 2 mM EDTA, 1 % (v/v) Triton X-100 and 20 mg/ml lysozyme (pH 8.0) (AppliChem, MO), and 25 µl proteinase K (Macherey-Nagel GmbH and Co., Düren, Germany). The buffer-cell suspension was heated to 55 °C for 2 hours using a microplate thermoshaker (500 r.p.m., Hangzhou Allshen Instruments, Hangzhou, China). DNA was extracted using the

NucleoSpin Tissue kit (Macherey-Nagel) according to the manufacturer's instructions and eluted with 2 x 40 µl of elution buffer (5 mM Tris-HCl, pH 8).

4.2.4 Sequencing of 16S rRNA and methane monooxygenase genes

PCR was carried out in 50 µl reaction volumes in 200 µl tubes containing 100 µM dNTPs, 0.5 µM primers and 1U Intron i-Taq™. The final concentration of $MgCl_2$ was 1.5 mM. DNA extracts from cultures were used at final concentrations of 10 – 50 ng/reaction. PCR amplifications were performed using a T100 thermal cycler (Bio-Rad, Hercules, CA). The 16S rRNA gene was amplified using the universal bacterial primers 9f (originally named fD1) and 1492r (rP1) [369]. Particulate methane monooxygenase genes were targeted using the forward primer A189b [370] with one of the reverse primers A650 [120], mb661 [370], or A682 [93]. The primer pair mmoXA and mmoXB [371] were used to amplify the soluble methane monooxygenase *mmoX* gene. PCR reactions that produced a product of the expected size (~1,400 bp for the 16S rRNA gene, ~500 bp for *pmoA* and ~1200 bp for *mmoX*) were cleaned using the NucleoSpin Gel and PCR Clean-up kit (Macherey-Nagel). The resulting products were subsequently sequenced by Macrogen Inc. (South Korea) via the Sanger Sequencing method.

4.2.5 Phylogenetic analysis

The near-full length 16S rRNA gene sequences were manually checked for quality. Closely-related strains were determined by conducting a pair-wise similarity assessment of the isolate 16S rRNA gene sequences using BLAST (discontiguous megablast search) [333] in the NCBI portal. The 16S rRNA gene sequences from the isolates and closely related strains and phylotypes were aligned (all retrieved sequences were > 1338 bp in length) using the CLUSTAL W algorithm in MEGA7 [126]. Phylogenetic distances were inferred by using the Maximum Likelihood methodology [124] based on the Jukes-Cantor model [372]. The consensus tree was inferred from 1000 bootstrap replications. Initial tree(s) for the heuristic search were obtained automatically by applying Neighbour-Joining and BioNJ algorithms to a matrix of pairwise distances estimated using the Maximum Composite Likelihood [127] approach, and then selecting the topology with superior log likelihood value.

The *pmoA* sequences from the isolates (all sequences were > 448 bp in length) and *mmoX* sequences (> 1140 bp) were aligned with sequences obtained from the GenBank database, as above, in MEGA7 [126]. Derived amino acids were determined via MEGA7 and used to construct phylogenetic trees using the Maximum Likelihood method based on the JTT matrix-based model [373]. The consensus tree was inferred from 1000 bootstrap replications. Initial trees(s) for the heuristic search were obtained automatically by applying Neighbour-Joining and BioNJ algorithms to a matrix of pairwise distances estimated using a JTT model, and then selecting the topology with superior log likelihood value.

Phenotypic characterisation

4.2.6 Temperature ranges and optima

Cells were grown in their respective cultivation media (Table 4.1) in 18 mm (dia.) anaerobic tubes sealed with gas-tight butyl rubber stoppers. The tubes were incubated in duplicate in a Temperature Gradient Incubator (Terratec Corporation, Hobart, Australia), initially set to a Δ 40 °C gradient (± 20 °C initial sample temperature) and agitated at 70 oscillations per minute. OD_{600} was measured daily using an adaptor (Perkin-Elmer, Waltham, MA) that allowed the tubes to be directly inserted into a Halo Vis-10 spectrophotometer (Dynamica Scientific, Newport Pagnell, UK) without subsampling cultures. The optimum temperature for growth was estimated based on the fastest growth rate and the highest OD obtained for each strain.

4.2.7 pH ranges and optima

For all pH experiments, tests were conducted in triplicate using 18 mm (dia.) anaerobic tubes sealed with gas-tight butyl rubber stoppers, under initial cultivation conditions (Table 4.1). Buffers were used to control pH in some experiments (detailed below). All pH measurements were calibrated and measured at room temperature (20 °C) using a model 320 HI11310 pH probe (Hanna Instruments, RI), before and after autoclaving (prior to inoculation), and after the growth experiment was terminated. An additional non-inoculated control for each growth medium pH was included to measure abiotic pH shifts during incubation. Cell growth was followed daily via spectrophotometer (OD_{600}) as described in section 4.2.6.

The buffers used for the determination of pH range and optima varied depending on the medium and isolate taxonomy and are described forthwith: GDS1.7 and GDS2.4 were tested in NMS medium with the addition of either 60 mM Tris(hydroxymethyl)aminomethane (Tris) buffer (pH 6.8-9.5) or 30 mM phosphate-citrate buffer (pH 3.0-6.8). The pH of the medium was tested after addition of the buffer and adjusted, if necessary, with 0.1 M H_2SO_4 or 0.1 M NaOH, before autoclaving.

NGM89.1 and WHV12.1 were tested in V4 medium, and WAP11.3 in ANMS medium, without the addition of buffer, as described in the original description papers for the closest related strains [14, 70]. Media showed a marked difference between the set and observed pH's when maintained at elevated temperatures, due to the dissociation of the potassium dihydrogen phosphate within the media [374]. To combat this, the pH measurements were calibrated at 60 °C (for NGM89.1) or 50 °C (for WAP11.3 and WHV12.1), before autoclaving, using the temperature sensor incorporated within the Hanna pH probe. The pH of both inoculated and non-inoculated tubes was tested again at these temperatures, and at 20 °C at the conclusion of the experiments.

4.2.8 Maximum growth rates under optimal conditions

Isolates were cultured in 500 ml Schott bottles containing 250 ml of growth media and sealed with rubber stoppers. Cultures were incubated at their optimal temperature and pH as previously determined. The headspaces consisted of air with the addition of approximately 8 % (v/v) CH_4 and 0.08 % (v/v) CO_2. For each isolate, four replicate bottles were incubated at close to optimal temperature, one with 4 % (v/v) acetylene added to the headspace to inhibit the activity of methane monooxygenase. Three control (non-inoculated) bottles were incubated at the same temperature. The headspace composition and OD_{600} of all bottles was measured at regular intervals of up to every four hours, depending on the strain being tested, until all the methane was consumed in the inoculated bottles.

4.2.9 Substrate utilisation

Substrate utilisation tests were performed using media in 18 mm (dia.) anaerobic tubes sealed with gas-tight butyl rubber septa. Methanol (up to 2.5 % v/v), ethanol

(0.025 % v/v), formaldehyde (0.025 % v/v), methylamine (0.05 % v/v), or trimethylamine (0.05 % v/v) were aseptically passaged via a sterile 0.22 µm syringe filter to sterilised media. Other substrates tested (sodium acetate, trisodium citrate, sodium formate, malic acid, sodium pyruvate, sodium succinate, fructose, glucose, sucrose, xylose, glycerol, and mannitol) were added to the growth medium at a concentration of 0.1 % (w/v) prior to sterilisation. Growth was tested on each substrate in triplicate, with an additional non-inoculated control to check the pH of the medium. Two positive controls with 5 % (v/v) CH_4 and one negative control with no carbon source were inoculated with the same inoculum volume; to confirm viability and to account for any observed growth due to substrate carry-over with the inoculum, respectively. Although hydrogen oxidation has been observed in several methanotrophs [34, 35, 228, 229], this energy source was not investigated in this study, as this will be the focus of the next chapter.

4.2.10 Nitrogen source determination

The nitrogen sources for each of the isolates were tested by incubating cultures with either N_2, urea, NO_3, NH_4^+, methylamine or peptides (peptone and YE), with approximately 3 % (v/v) CH_4 added to the headspace of test vials. Initially, dinitrogen gas (N_2) was tested as a sole N-source by incubating strains in 20 ml serum vials containing a modified version of each media minus its stipulated N-source e.g. KNO_3 or NH_4Cl. Isolates that showed weak growth were passaged once into identical N_2-only medium. Where N_2-fixation was observed via growth (increase in OD_{600}) in N-free media, cultures were further tested using an 80:20 (v/v) argon:oxygen headspace. Where NO_3 or NH_4^+ were tested as N-sources, their final medium concentrations were made up to reflect the molar concentration of the N source in the standard growth medium (Appendix 7.4). Methylamine was tested as a nitrogen source by adding 0.05 % (v/v) to N-free media; potential toxicity to the culture was checked via a positive control containing both methylamine (0.05 % v/v) and a nitrogen source (NH_4Cl or KNO_3), as used in the standard culture media. Urea was tested as a nitrogen source and for toxicity in the same manner as methylamine at a concentration of 0.05 g/l. Peptone and yeast extract were separately tested as nitrogen sources by adding 0.01 g/l respectively to otherwise N-free media.

4.2.11 Physiological tests

To determine the effects of acetylene as an inhibitor of methane-oxidising activity, 4 % (v/v) acetylene was added via a sterile 0.22 µm syringe filter to the headspace of duplicate Schott bottles containing cultures in early exponential phase. Positive controls inoculated at the same time, and with the same CH_4-in-air headspace but no acetylene, were incubated in triplicate.

The tolerance of isolates to heat in excess of their T_{max} was determined by heating aliquots of cell suspension at 70, 80 and 90 °C for 10 minutes, cooling these rapidly on ice, then transferring the aliquots into fresh medium at optimal pH and incubating at optimal temperature for three weeks. Strains with a maximum growth temperature of less than 50 or 60 °C were also heat-shocked for 10 minutes at these temperatures. Desiccation resistance was tested by spreading cultures on sterile glass slides and allowing these to dry before storage at room temperature in a sealed 50 ml centrifuge tube on a laboratory bench. Dried preparations were resuspended in optimal medium after 3, 7, 10, 14 and 21 days.

Cells were tested for viability following cryostorage by centrifuging 2 ml of culture for ten minutes at 22,000 x *g* in a 1730R centrifuge (Gyrozen) and resuspending in either standard culture media or Tryptic Soy Broth (TSB) (adjusted to pH 3.0 for some strains), with the addition of either 5 % DMSO or 10 % glycerol, before freezing at -80 °C. Cells were tested for viability after two months of storage at -80 °C by inoculating 0.2 ml of culture, defrosted at 4 °C, into 8 ml of optimal media and incubating at optimal temperature with 10 % (v/v) CH_4 in the headspace for up to six weeks. The headspace composition and OD_{600} of all bottles was measured at regular intervals.

4.2.12 Antibiotic resistance and sensitivity

Isolates were tested for their susceptibility to various antibiotics. The antibiotics tested (ampicillin, erythromycin, kanamycin, monensin, nalidixic acid, polymyxin B, tetracycline, and vancomycin) were chosen for their range of mechanisms of action, and where possible, their stability at temperatures greater than 50 °C (Table 4.2).

Antibiotic resistance tests were performed by inoculating strains (10 % v/v) into standard growth media in 18 mm (dia.) anaerobic tubes sealed with gas-tight butyl rubber septa. Cultures were incubated at 37 °C (GDS1.7, GDS2.4) or 46 °C (NGM89.1, WAP11.3, WHV12.1) to reduce thermal degradation of the antibiotics. Antibiotics were added via a sterile 0.22 µm syringe filter to sterilised media, to a final concentration of 3 µg/ml. All tests were performed in triplicate and the OD at 600 nm was measured daily for five days. Isolates that showed resistance to an antibiotic at a concentration of 3 µg/ml (growth equivalent to an increase in OD_{600} of > 0.04) were then tested with the same antibiotic at a higher final concentration of 30 µg/ml. The toxicity of the nalidixic acid (30 mg/ml) diluent, NaOH (final concentrations 30 µM or 300 µM) was also checked by growing cells in medium with the addition of NaOH without the nalidixic acid. All other stock solutions were diluted in RO water, except for monensin, which was dissolved in methanol that can be used as a growth substrate by methanotrophs. Cells grown in the absence of antibiotics were used as positive controls.

Table 4.2 Mechanisms of action of selected antibiotics stable above 50 °C.

Antibiotic	Susceptible microorganisms	Target	Stability at 50 °C
Ampicillin	Gram-positive and Gram-negative bacteria	Transpeptidase; cell wall synthesis	Some loss of potency; better at lower pH
Erythromycin	Aerobic, Gram-negative bacteria, some mycobacteria, some Gram-positive bacteria	50S ribosomal subunits; peptide translocation and protein synthesis	Stable
Kanamycin	Gram-negative bacteria	30S ribosomal subunits; translation	Stable
Monensin	Gram-positive bacteria	Divalent cations; internal pH	Slight increase in potency
Nalidixic acid	Gram-negative bacteria	DNA gyrase or topoisomerase; DNA replication	Not known
Polymyxin B	Gram-negative bacteria	Lipopolysaccharide (LPS); membrane permeability	Slight increase in potency
Tetracycline	Gram-positive and Gram-negative bacteria	30S ribosomal subunits; protein synthesis	Some loss of potency
Vancomycin	Gram-positive bacteria	N-acetylglucosamine (NAG)/ N-acetylmuramic acid (NAM); cell wall synthesis	Stable

Information obtained from [375-377].

4.2.13 Phospholipid fatty acid analysis

Cells were grown to late-exponential phase under standard conditions (Table 4.1) with 15 % (v/v) methane and then harvested by centrifugation at 16,000 x *g* for 40 minutes in a 1736R centrifuge (Gyrozen). The supernatant was discarded and the cell pellet was couriered to Callaghan Innovation (Wellington, New Zealand) where the fatty acid content was determined [378]. Briefly, this process involved using a base reagent (NaOH in methanol), toluene, and an acidic reagent (HCl in methanol), sequentially, to catalyse the methylation of fatty acids to fatty acid methyl esters (FAME). FAME were dissolved in hexane or trimethylchlorosilane (TMCS) and analysed by GC-MS. Individual peaks of FAME were identified by comparison with standards of FAME and by equivalent chain length (ECL) values [379].

4.3 Results

Methane oxidation was observed in 22 of the enrichment cultures (Table 3.3), but for most of the microcosms, this trait was not sustained during multiple passages into fresh medium. Methanotrophs were isolated from five of the enrichment cultures (Table 4.3), and phylogenetic and phenotypic characterisation was carried out on these five isolates.

In addition, methane oxidation was maintained in an enrichment culture from the Tokaanu sample TOK7 for more than two years, but a methanotroph could not be obtained in an axenic culture despite repeated efforts to purify (e.g. dilution series, incubation across a temperature gradient, and the addition of antibiotics including ampicillin, monensin, polymyxin B and vancomycin). The enrichment culture formed a stable community of two or three morphologies; roughly 75 % of the cells were large cocci, approximately 1.5 µm in diameter, and short and long rods, approximately 1 to 1.5 µm wide by 1.5 to 4 µm long, formed the remainder of the community. Both cocci and rods were present in cultures between 42-63 °C, with maximum optical density observed at 48-57 °C. DNA was extracted from the community and amplification of a *pmoA* gene indicated that the community included a strain with 89 % nucleotide sequence identity to *Methylothermus subterraneous*. The identity of the other community members was not determined.

Table 4.3 Summary of methanotrophic enrichment source samples and the resulting isolate/consortium nomenclature.

Location	Nomenclature	Culture
Golden Springs	GDS1.7	axenic
	GDS2.4	axenic
Ngatamariki	NGM89.1	axenic
Tokaanu	TOK7	mixed
Waipahihi	WAP11.3	axenic
Whakarewarewa Village	WHV12.1	axenic

Characterisation of Golden Springs strain GDS1.7

4.3.1 GDS1.7 Phylogenetic analysis

The near-full length (1,338 bp) 16S rRNA gene sequence of strain GDS1.7 was assessed via pair-wise sequence analysis and was found to be related to strains and environmental clones related to those in genus *Methylocystis*. The most closely related cultivated strain was a *Methylocystis* species (KS8a, 99 % sequence identity) isolated from freshwater lake sediments in Israel (Accession number AJ458493) (Figure 4.1). In addition, three environmental clones detected in studies on American and Russian peat bogs (HQ844543, 99 %; FR720614, 99 %, respectively) and a soil from China (JX576012, 99 %) had similar 16S rRNA gene sequence similarities, as did the closest described strain *Methylocystis echinoides* (NR025544, 99 %).

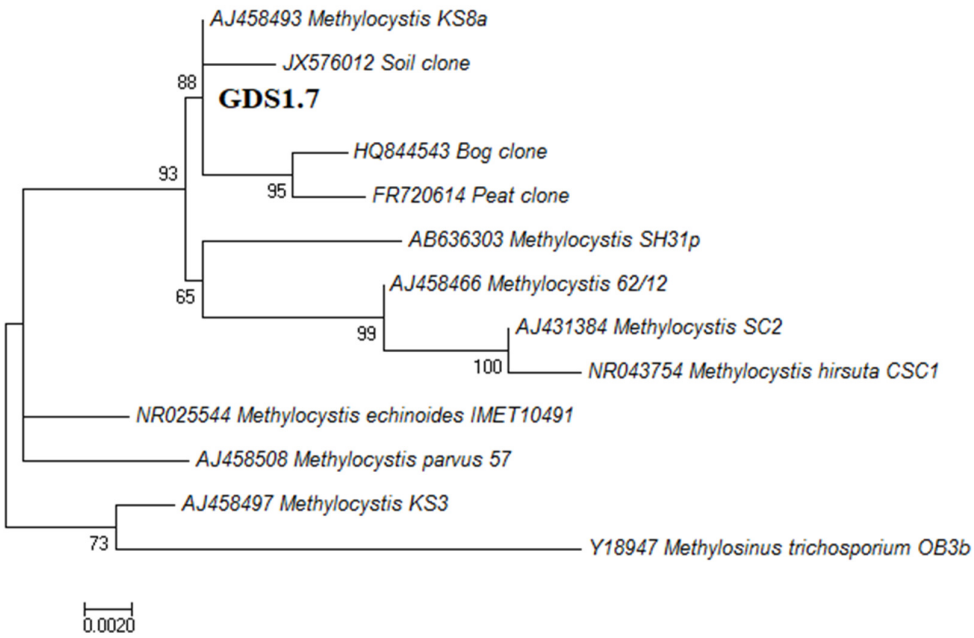

Figure 4.1 Maximum likelihood 16S rRNA gene sequence phylogeny of GDS1.7
The tree shows the phylogenetic relationships between isolate GDS1.7, closely related methanotrophic isolates, and clonal sequences detected in environmental samples. Bootstrap values > 50 % are shown at the branch nodes (1000 replicates). The scale bar represents 0.002 nucleotide substitutions per site.

The inferred PmoA protein amino acid sequence of *Methylocystis* GDS1.7 was identical to the MMO encoded by *Methylocystis* strain KS3, (AJ459033, 100 % amino acid sequence identity) (Figure 4.2), isolated from the same lake in Israel as KS8a. The PmoA protein sequences from both *Methylocystis* strains GDS1.7 and KS3 were more distantly related to other *Methylocystis* PmoA sequences in the NCBI database. *Methylocystis* KS8a (AJ459035) showed 99 % nucleotide sequence identity to the GDS1.7 sequence, while *Methylocystis echinoides* (AJ45900) was only 98 % similar. PCR primers for *mmoX* (the gene for the alpha component of soluble methane monooxygenase) failed to amplify an *mmoX* product from DNA extracted from GDS1.7 cultures.

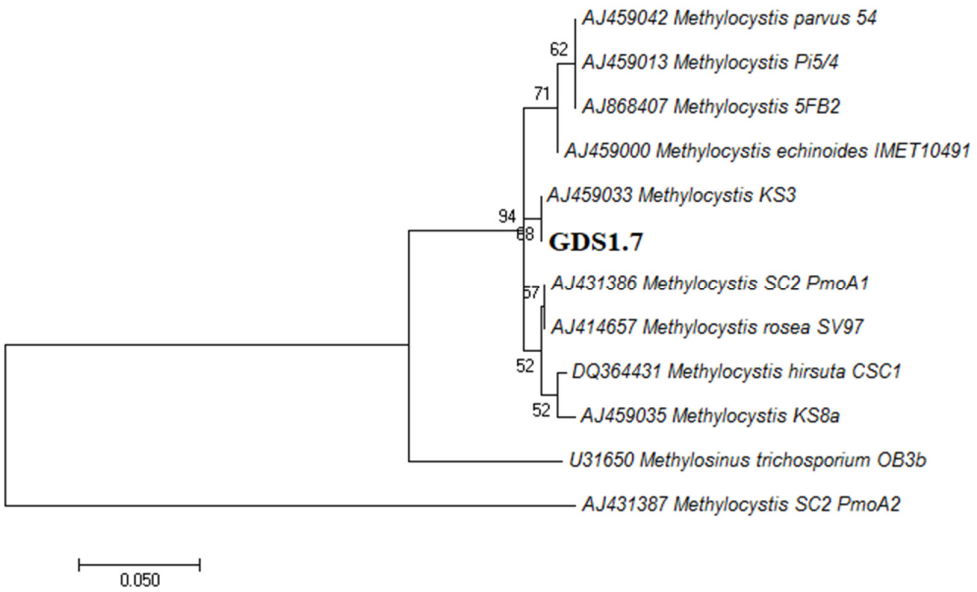

Figure 4.2 Maximum likelihood PmoA sequence phylogeny of GDS1.7 The tree shows the phylogenetic relationships between isolate GDS1.7 and closely related methanotrophic isolates, based on the inferred amino acid sequence of PmoA. Bootstrap values > 50 % are shown at the branch nodes (1000 replicates). The scale bar represents 0.05 nucleotide substitutions per site.

4.3.2 Methylocystis GDS1.7 cultivation and general characteristics

Enrichment cultures of *Methylocystis* GDS1.7 were initially mixed containing cells with motile rod, and non-motile vibrioid, morphologies. Multiple rounds of serial dilutions to extinction, with supplementation of 30 µg/ml monensin, were required to isolate the non-motile *Methylocystis* GDS1.7 strain. *Methylocystis* GDS1.7 cells had a vibrioid morphology, were approximately 0.8 µm wide by 2-4 µm long and grew between pH 5.0-9.2 (optimum pH 5.8). No growth was observed at pH 4.6 or below, or at pH 9.3 or above. Cells grew between 20-43 °C (optimum 36 °C), but growth was not observed at 18 °C or below, or at 46 °C or above. The generation time was 12.5 hours at optimum pH and temperature. The addition of 4 % acetylene to the headspace of cultures completely inhibited methane oxidation and growth of *Methylocystis* GDS1.7. The methane oxidation rate under ideal conditions (pH 6.0, 36 °C) was 47.6 µmoles/hour.

4.3.3 Methylocystis GDS1.7 phenotypic characteristics

Methylocystis GDS1.7 was able to grow using methane or methanol as an energy source only. It could tolerate up to 2.0 % (v/v) methanol in the growth medium, but concentrations of 2.5 % (v/v) inhibited growth. No growth was observed using ethanol, formaldehyde, methylamine, trimethylamine, sodium acetate, trisodium citrate, sodium formate, malic acid, sodium pyruvate, sodium succinate, fructose, glucose, sucrose, xylose, glycerol, or mannitol as substrates. Cultures could utilise either NH_4Cl or KNO_3 as nitrogen sources, but not N_2, methylamine, urea, peptone, or yeast extract.

Methylocystis GDS1.7 was able to tolerate desiccation for up to 3 days but could not be revived following 7 days desiccation. Cell viability was not maintained when cultures were exposed to temperatures > 50 °C. Cells could be revived from storage at -80 °C when Tryptic Soy Broth (TSB) was used but not in instances where NMS was used for a storage medium. The addition of either 5 % (v/v) DMSO or 10 % (v/v) glycerol as a cryo-protectant to TSB maintained cell viability at -80 °C. *Methylocystis* GDS1.7 growth was not inhibited by the addition of ampicillin, monensin, polymyxin B and vancomycin at either 3 or 30 µg/ml to growth medium. However, cells were sensitive to 3 µg/ml erythromycin, kanamycin, nalidixic acid and tetracycline. The principal fatty acids of *Methylocystis* GDS1.7 cells grown to exponential phase in NMS media (pH 6.0) at 37 °C, with 15 % (v/v) methane in the headspace were 18:1ω8c and 18:1ω7c (Table 4.4).

Table 4.4 Cellular phospholipid fatty acid profiles of *Methylocystis* GDS1.7.

Individual fatty acid distribution presented in weight % of total fatty acids.

Fatty acids	Composition
16:0	0.6
16:1ω7c	1.2
18:0	0.5
18:1ω8c	67.6
18:1ω7c	19.8
18:2	9.6

PLFA nomenclature is used according to Guckert [380]. ω, aliphatic end of molecule; c, *cis*. The position of the double bond was not determined for 18:2 fatty acids.

A summary of the phenotypic characteristics of *Methylocystis* GDS1.7 and those of phylogenetically related methanotrophs can be found in Table 4.5.

Table 4.5 Characteristics of *Methylocystis* GDS1.7 and phylogenetically related methanotrophs. Strains: 1, GDS1.7 (this study); 2, *M. parvus* [44-46, 214]; 3, *M. echinoides* [45, 46, 381]; 4, *M. hirsuta* [382]. +, Positive; -, negative; ND, not determined. Traits where data is only available for GDS1.7 are not shown.

Strain	**1**	**2**	**3**	**4**
16S rRNA gene sequence similarity with *Methylocystis* GDS1.7				
	-	99 %	99 %	99 %
Cell morphology				
Shape	Vibrioid	Coccobacillus	Coccobacillus, rod	Dumbbell
Width (μm)	0.8	0.3-0.5	0.6	0.3-0.6
Length (μm)	2-4	0.5-1.5	0.8-1.2	0.7-1.0
pH for growth				
Range	5.0-9.2	5.0-9.0	6.0-9.0	ND
Optimum	5.8	ND	6.5-7.5	7.0
Temperature for growth				
Range (°C)	20-43	~20-37	~20-37	ND
Optimum (°C)	36	~30	28-33	30
Generation time	12.5 hr	ND	6-7 hr	ND
Growth on methanol (v/v)				
0.1 %	+	-	+	+
1 %	+	-	-	ND
Nitrogen sources				
N_2	-	ND	+	+
KNO_3	+	+	+	+
NH_4Cl	+	ND	+	ND
Methylamine	-	-	-	ND
YE	-	+	+	ND
Desiccation resistance	3 days	7 days	-	ND
Heat resistance	-	ND	-	-
Major fatty acids	18:1ω8c, 18:1ω7c	18:1ω8c, 18:1ω7c	18:1ω8c, 18:1ω7c	ND

4.3.4 GDS2.4 phylogenetic analysis

Using 16S rRNA gene sequence pairwise identity, the strain GDS2.4 was found to be closely related to *Methylococcus* strains. The 1,403 bp sequence shared 100 % nucleotide identity with the corresponding sequence from *Methylococcus capsulatus* Bath (AE017282), and was closely related to other *M. capsulatus* strains, Cla (JN166980, 99 %), and Texas (NR042183, 99 %) (Figure 4.3). Similar 16S rRNA gene sequence similarities were found with an environmental clone detected in bagasse (HM362450, 99 %).

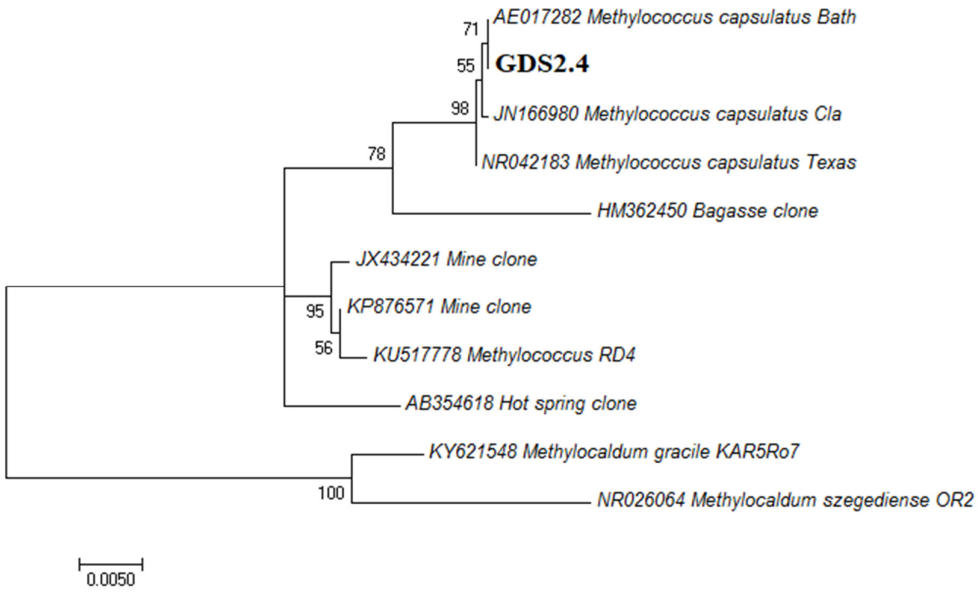

Figure 4.3 Maximum likelihood 16S rRNA gene sequence phylogeny of GDS2.4
The tree shows the phylogenetic relationships between isolate GDS2.4, closely related methanotrophic isolates, and clonal sequences detected in environmental samples. Bootstrap values > 50 % are shown at the branch nodes (1000 replicates). The scale bar represents 0.005 nucleotide substitutions per site.

The inferred amino acid sequence of the PmoA protein showed that GDS2.4 had high pairwise similarity with *M. capsulatus* Bath (AE017282, 98 % amino acid identity), but the protein sequence was slightly more closely related to *Methylomonas methanica* (FJ713037, 99 %) (Figure 4.4).

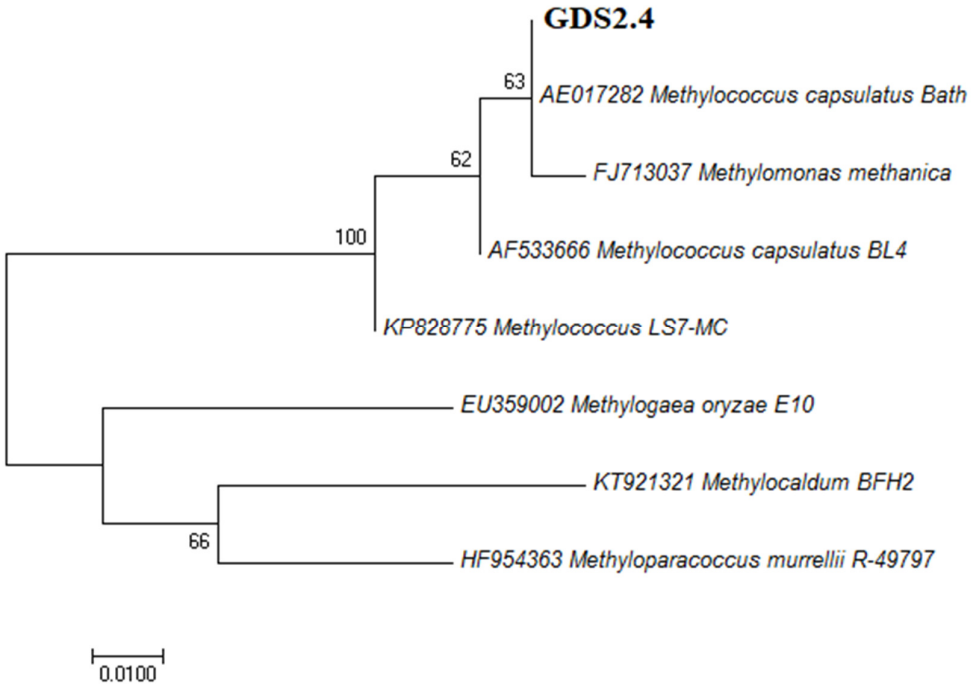

Figure 4.4 Maximum likelihood PmoA sequence phylogeny of GDS2.4 The tree shows the phylogenetic relationships between isolate GDS2.4 and closely related methanotrophic isolates, based on the inferred amino acid sequence of PmoA. Bootstrap values > 50 % are shown at the branch nodes (1000 replicates). The scale bar represents 0.01 nucleotide substitutions per site.

The MmoX sequence from GDS2.4 again confirmed the close phylogenetic relationship with *M. capsulatus* Bath (M90050, 100 % nucleotide sequence identity), and a similar relationship was found with an environmental clone sampled from an acidic fen in Germany (FR726170, 100 %) (Figure 4.5). An *mmoX* sequence for the *M. capsulatus* strains Cla, Texas and BL4 was not available in the NCBI database.

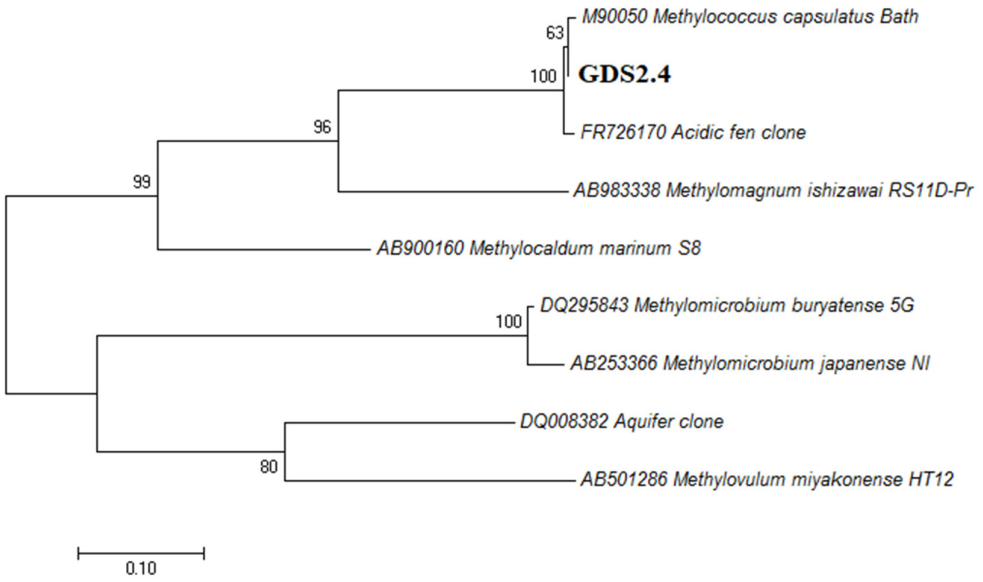

Figure 4.5 Maximum likelihood MmoX sequence phylogeny of GDS2.4 The tree shows the phylogenetic relationships between isolate GDS2.4, closely related methanotrophic isolates, and environmental clones, based on the inferred amino acid sequence of MmoX. Bootstrap values > 50 % are shown at the branch nodes (1000 replicates). The scale bar represents 0.1 nucleotide substitutions per site.

4.3.5 Methylococcus GDS2.4 cultivation and general characteristics

Enrichment cultures of *Methylococcus* GDS2.4 were initially mixed, with a large proportion of coccoid cells and far fewer tiny, highly motile rods. The non-motile, coccoid strain *Methylococcus* GDS2.4 was isolated through multiple rounds of serial dilution and the addition of 30 µg/ml monensin to cultures. *Methylococcus* GDS2.4 cells were approximately 0.8-2.0 µm in diameter, and were usually seen in pairs, while single cells and tetrads were less common. Cultures grew between 27-49 °C (optimum 40 °C) and pH 5.6-8.7 (optimum pH 6.8), but growth was not observed at 24 or 50 °C, or at pH 5.4 or 8.9. The doubling time was 8.4 hours. The methane oxidation rate under optimal conditions (37 °C, pH 6.8) was 87.8 µmoles/hr. Acetylene in the headspace (4 %, v/v) completely inhibited growth of *Methylococcus* GDS2.4 cultures.

4.3.6 Methylococcus GDS2.4 phenotypic characteristics

Methylococcus GDS2.4 could grow using methane or methanol as energy sources only, and could tolerate up to 0.5 % (v/v) methanol in growth media. Concentrations of methanol of 0.6 % (v/v) or higher inhibited growth. No growth was observed using ethanol, formaldehyde, methylamine, trimethylamine, sodium acetate, trisodium citrate, sodium formate, malic acid, sodium pyruvate, sodium succinate, fructose, glucose, sucrose, xylose, glycerol, or mannitol as energy sources. Cultures could utilise either NH_4Cl or KNO_3 as nitrogen sources, but not N_2, methylamine, urea, or peptides.

Methylococcus GDS2.4 cells could not tolerate desiccation, but could withstand heat-shock at up to 90 °C for ten minutes. Cells could only be revived from -80 °C storage if frozen in TSB medium with the addition of either 5 % DMSO or 10 % glycerol. *Methylococcus* GDS2.4 was resistant to a final concentration of 30 µg/ml of the antibiotics monensin or vancomycin added to growth medium, and sensitive to 3 µg/ml erythromycin, kanamycin, nalidixic acid and tetracycline. The response to ampicillin and polymyxin B was dosage-dependent; *Methylococcus* GDS2.4 cells were resistant to 3 µg/ml, but sensitive to 30 µg/ml of both antibiotics added to growth medium.

The major fatty acids in cells grown to exponential phase under optimal conditions (37 °C, pH 6.8) with 15 % (v/v) methane in the headspace were 16:0, 16:1ω7c, 16:1ω6c and 16:1ω5c (Table 4.6).

Table 4.6 Cellular phospholipid fatty acid profiles of *Methylococcus* GDS2.4.

Individual fatty acids distribution presented in weight % of total fatty acids.

Fatty acid	Composition
14:0	6.4
15:0	0.3
16:0	36.5
16:1ω5c	13.4
16:1ω6c	13.6
16:1ω7c	19.9
17:1	7.4
18:0	0.3
18:1	0.3

PLFA nomenclature is used according to Guckert [380]. ω, aliphatic end of molecule; c, *cis*. The position of the double bond was not determined for 17:1 fatty acids.

A summary of these results and a comparison to closely related methanotroph strains is presented in Table 4.7.

Table 4.7 Characteristics of *Methylococcus* GDS2.4 and phylogenetically related methanotrophs. Strains: 1, GDS2.4 (this study); 2, *Methylococcus capsulatus* [44, 45, 64]; 3, *Methylococcus thermophilus* [60, 293]; 4, *Methylocaldum szegediense* [58]. +, Positive; -, negative; ND, not determined. Traits where data is only available for GDS2.4 are not shown.

Strain	1	2	3	4
16S rRNA gene sequence similarity with *Methylococcus* GDS2.4				
	-	100 %	94 %	92 %
Cell morphology				
Shape	Coccoid	Coccoid	Coccoid	Rod/ pleomorphic
Width (μm)	0.8-2.0	0.8-1.0	0.5-1.0	1.0-1.2
Length (μm)	0.8-2.0	1.0-1.5	1.0-1.5	1.2-1.5
pH for growth				
Range	5.6-8.7	5.5-8.5	5.5-9.0	ND
Optimum	7.0	ND	ND	ND
Temperature for growth				
Range (°C)	27-49	28-50	37-62	37-62
Optimum (°C)	40	37	50-56	55
Generation time	8.4 hr	3.5-5.0 hr	ND	ND
Growth on methanol (v/v)				
0.1 %	+	+	-	-
Growth on other carbon sources				
Formate	-	+	-	-
Methylamine	-	+	-	-
Nitrogen sources				
N_2	-	+	+	-
NO_3	+	+	+	+
NH_4	+	+	+	ND
Methylamine	-	+	+	ND
YE	-	+	+	ND
Desiccation resistance	-	-	-	-
Heat resistance	+	-	-	+
Major fatty acids	16:0, 16:1ω7c	16:0, 16:1ω7c	16:0, 16:1ω7c	ND

4.3.7 NGM89.1 phylogenetic analysis

The near full length (1,395 bp) 16S rRNA gene sequence from NGM89.1 showed the strain was closely related to the *Methylacidiphilum* species *infernorum* (AM900833, 99 % nucleotide sequence identity) and RTK17.1 (LN998017, 99 %), which were isolated from geothermal soils in New Zealand. A clone from a hot spring in China (KM221310, 98 %) was also closely related to the NGM89.1 sequence (Figure 4.6).

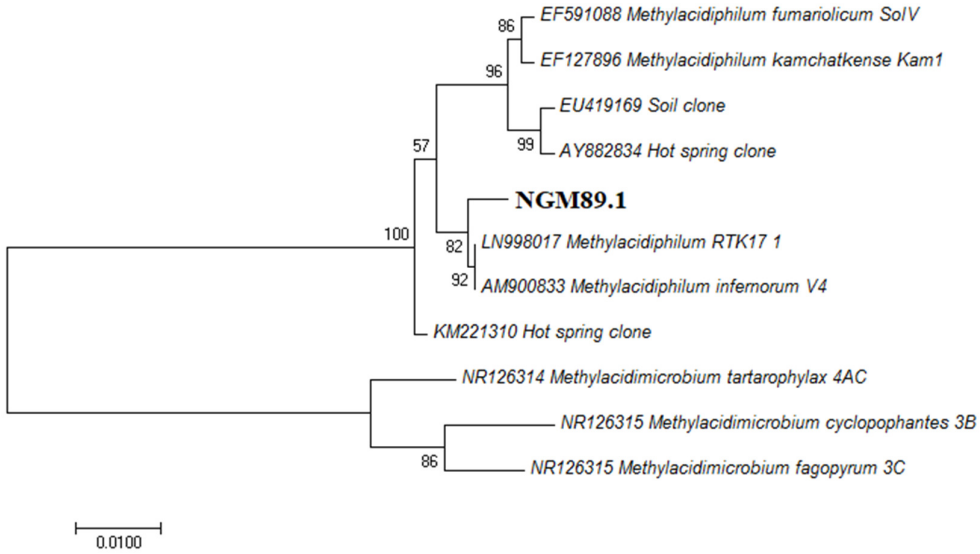

Figure 4.6 Maximum likelihood 16S rRNA gene sequence phylogeny of NGM89.1 The tree shows the phylogenetic relationships between isolate NGM89.1, closely related methanotrophic isolates and clonal sequences detected in environmental samples. Bootstrap values > 50 % are shown at the branch nodes (1000 replicates). The scale bar represents 0.01 nucleotide substitutions per site.

The inferred amino acid sequence of the PmoA protein from NGM89.1 was most closely related to the PmoA1 proteins from *Methylacidiphilum infernorum* (EU223859, 99 % nucleotide sequence identity) and *Methylacidiphilum* sp. RTK17.1 (KU509368, 99 %) (Figure 4.7). PCR primers for *mmoX* (for soluble methane monooxygenase) did not amplify a product from DNA from NGM89.1.

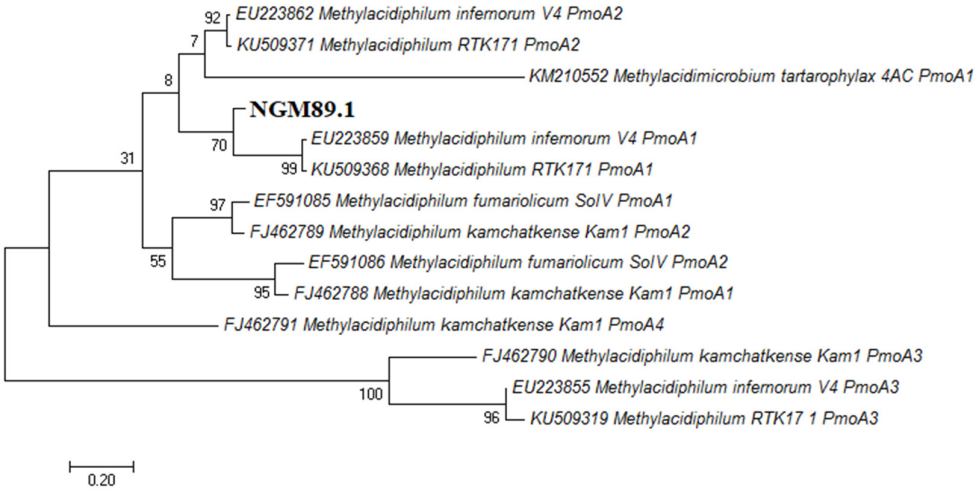

Figure 4.7 Maximum likelihood PmoA sequence phylogeny of NGM89.1 The tree shows the phylogenetic relationships between isolate NGM89.1 and closely related methanotrophic isolates, based on the inferred amino acid sequence of PmoA. Bootstrap values are shown at the branch nodes (1000 replicates). The scale bar represents 0.2 nucleotide substitutions per site.

4.3.8 Methylacidiphilum NGM89.1 cultivation and general characteristics

Enrichment cultures of *Methylacidiphilum* NGM89.1 initially had very low levels of *Alicyclobacillus* spores, which were very rarely seen under the microscope, but that germinated during substrate or nitrogen tests when carbohydrates, yeast extract or peptone were added to media. These required multiple rounds of serial dilutions using 1:20 (v/v) inocula to remove the contaminants and to isolate the *Methylacidiphilum* NGM89.1 strain. Cells were non-motile, short rods, approximately 0.8 µm wide by 1.6-2.4 µm long, which grew between 40-66 °C (optimum 53-60 °C), but not at 38 or 67 °C. Growth was observed between pH 2.1-5.8 (optimum pH 2.5-5.0), but not at pH 2.0 or 6.0. The generation time was 17.7 hours. The methane oxidation rate at 62 °C was 27.3 µmoles/hour and was completely inhibited by the addition of 4 % (v/v) acetylene to the headspace.

4.3.9 Methylacidiphilum NGM89.1 phenotypic characteristics

Methylacidiphilum NGM89.1 was able to grow using methane or methanol as sole energy sources only. It could tolerate up to 0.3 % (v/v) methanol in the culture medium but concentrations of 0.4 % (v/v) or above of methanol in culture

medium inhibited cell growth. Cells could not grow using ethanol, formaldehyde, methylamine, trimethylamine, sodium acetate, trisodium citrate, sodium formate, malic acid, sodium pyruvate, sodium succinate, fructose, glucose, sucrose, xylose, glycerol or mannitol as sole energy sources. *Methylacidiphilum* NGM89.1 could utilise NH_4Cl as a nitrogen source, but was unable to use KNO_3, N_2, urea, methylamine, or peptides.

Methylacidiphilum NGM89.1 cells were unable to tolerate desiccation or heat-shock, and could only be revived from freezing at -80 °C if stored in TSB medium with either 5 % (v/v) DMSO or 10 % (v/v) glycerol as cryo-protectants. *Methylacidiphilum* NGM89.1 was resistant to a final concentration of 30 µg/ml of the antibiotics monensin, polymyxin B and vancomycin added to growth medium, but was sensitive to 3 µg/ml of erythromycin, kanamycin or nalidixic acid. *Methylacidiphilum* NGM89.1 could tolerate a final concentration of 3, but not 30, µg/ml of ampicillin and tetracycline. Cells grown to exponential phase under optimal conditions (60 °C, pH 3.0) with 15 % (v/v) methane in the headspace were dominated by the saturated fatty acids 18:0, *a*15:0, *i*14:0, and 16:0 (Table 4.8).

Table 4.8 Cellular phospholipid fatty acid profiles of *Methylacidiphilum* NGM89.1. Individual fatty acids distribution presented in weight % of total fatty acids.

Fatty acid	Composition
*i*14:0	11.7
14:0	11.6
*i*15:0	2.0
*a*15:0	15.5
*i*16:0	4.0
16:0	12.8
*a*17:0	10.9
17:0	0.6
*i*18:0	0.5
18:0	40.0

PLFA nomenclature is used according to Guckert [380]: *a*, anteiso; *i,* iso.

A summary of the phenotypic characteristics of *Methylacidiphilum* NGM89.1 and those of phylogenetically related methanotrophs can be found in Table 4.9.

Table 4.9 Characteristics of *Methylacidiphilum* NGM89.1 and phylogenetically related methanotrophs. Strains: 1, NGM89.1 (this study); 2, *M. infernorum* [14, 47]; 3, *M. fumariolicum* [43, 47]; 4, *M. kamchatkense* [47, 55]. +, Positive; -, negative; ND, not determined. Traits where data is only available for NGM89.1 are not shown.

Strain	1	2	3	4
16S rRNA gene sequence similarity with *Methylacidiphilum* NGM89.1				
	-	99 %	99 %	99 %
Cell morphology				
Shape	Rods	Rods	Rods	Rods
Width (μm)	0.8	0.3-0.5	0.4-0.6	0.5-0.7
Length (μm)	1.6-2.4	1.0-4.0	0.8-2.0	0.8-1.0
pH for growth				
Range	2.1-5.8	1.0-6.0	0.8-5.8	2.0-5.0
Optimum	2.5-5.0	2.0-2.5	2.0	3.5
Temperature for growth				
Range (°C)	40-66	40-60	40-65	37-60
Optimum (°C)	53-60	60	55	55
Generation time	18 hr	18 hr	10 hr	38 hr
Growth on methanol (v/v)				
0.1 %	+	+	+	+
1 %	-	ND	+	-
Nitrogen sources				
N_2	-	+	-	+
NO_3	-	ND	+	+
NH_4	+	+	+	+
Major fatty acids	18:0, *a*15:0	18:0, 16:0	18:0, *a*15:0	*a*15:0, *i*14:0

4.3.10 WAP11.3 phylogenetic analysis

The near-full length (1,403 bp) 16S rRNA gene sequence from WAP11.3 was analysed through pairwise similarity and was found to be related to strains and environmental clones from the genus *Methylocaldum*. The most closely related strain was *Methylocaldum* BFH2 (KP828774, 99 % nucleotide sequence identity) that was isolated from a soil in Bangladesh (Figure 4.8). The WAP11.3 16S rRNA gene also shared 99 % sequence similarity with environmental clones from bagasse (HM362534) and landfill soil (AF215633).

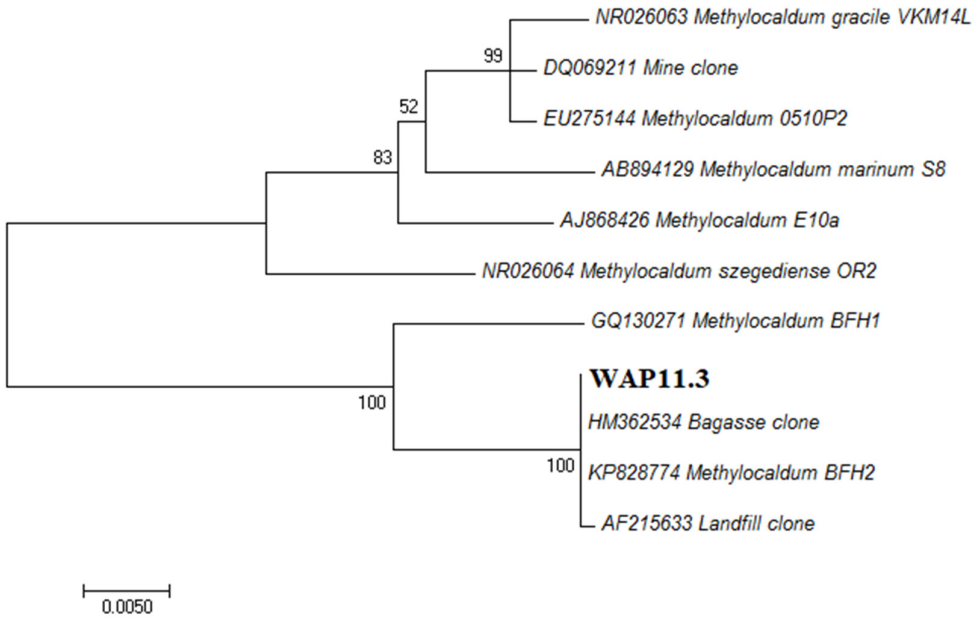

Figure 4.8 Maximum likelihood 16S rRNA gene sequence phylogeny of WAP11.3 The tree shows the phylogenetic relationships between isolate WAP11.3, closely related methanotrophic isolates, and clonal sequences detected in environmental samples. Bootstrap values > 50 % are shown at the branch nodes (1000 replicates). The scale bar represents 0.005 nucleotide substitutions per site.

The inferred amino acid sequence of the PmoA protein also showed a close phylogenetic relationship between WAP11.3 and *Methylocaldum* BFH2 (KT921321, 99 % amino acid sequence identity) (Figure 4.9). There was also an association with *Methylosoma* strain TFB (GQ130273, 99 %) and *Methylocaldum* BFH1 (GQ130270,98 %). PCR primers for *mmoX* (soluble methane monooxygenase) did not amplify a product from DNA from WAP11.3.

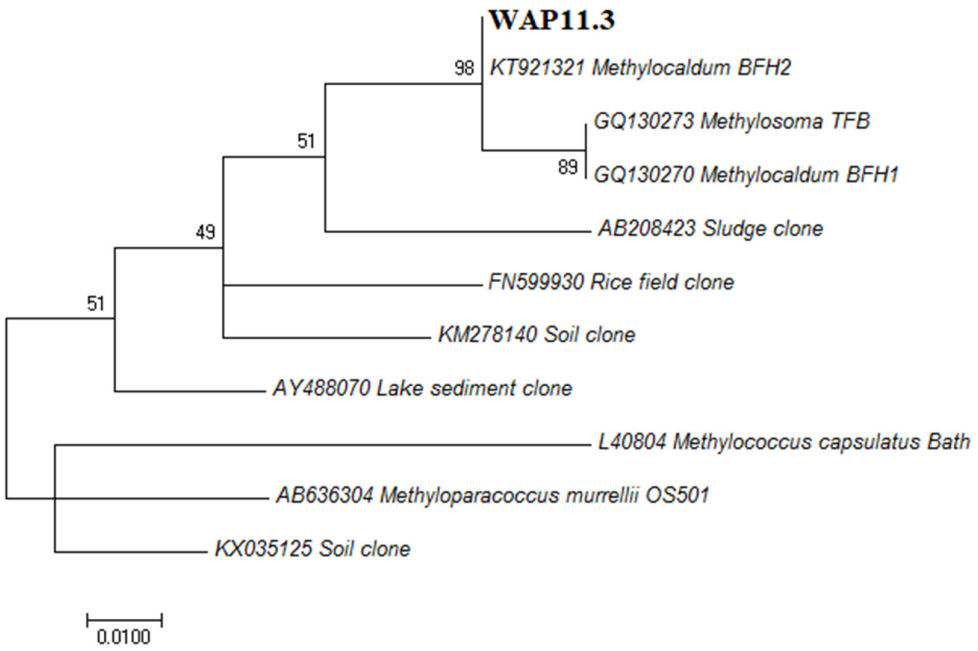

Figure 4.9 Maximum likelihood PmoA sequence phylogeny of WAP11.3 The tree shows the phylogenetic relationships between isolate WAP11.3, closely related methanotrophic isolates, and environmental clones based on the inferred amino acid sequence of PmoA. Bootstrap values > 50 % are shown at the branch nodes (1000 replicates). The scale bar represents 0.01 nucleotide substitutions per site.

4.3.11 Methylocaldum WAP11.3 cultivation and general characteristics

Methylocaldum WAP11.3 cells were non-motile, coccoid, approximately 1.6-2.0 µm wide by 1.6-2.8 µm long and were usually found in pairs. Cells grew between 39-59 °C (optimum 49-56 °C), and between pH 4.3-7.4 (optimum pH 5.6-6.5). No growth was observed at 37 or 62 °C, or at pH 4.2 or 7.6. Cells took 27.2 hours to double in number. The methane oxidation rate under optimal conditions (52 °C,

pH 6) was 23.9 µmoles/hour. The addition of 4 % acetylene to the headspace of cultures completely inhibited methane oxidation and growth of *Methylocaldum* WAP11.3.

4.3.12 Methylocaldum WAP11.3 phenotypic characteristics

Methylocaldum WAP11.3 grew on methane and methanol as sole energy sources, and could tolerate up 0.4 % (v/v) methanol in the growth medium. Concentrations of 0.5 % (v/v) methanol inhibited growth. Cells could not grow using ethanol, formaldehyde, methylamine, trimethylamine, sodium acetate, trisodium citrate, sodium formate, malic acid, sodium pyruvate, sodium succinate, fructose, glucose, sucrose, xylose, glycerol or mannitol as sole energy sources. *Methylocaldum* WAP11.3 could utilise NH_4Cl, KNO_3 or peptone as nitrogen sources, but not methylamine, urea or yeast extract.

Methylocaldum WAP11.3 could tolerate heat-shock for ten minutes at either 70 or 80 °C, but not 90 °C, but did not tolerate desiccation. Cells were only able to be revived from storage at -80 °C when frozen in Tryptic Soy Broth (TSB) and not in ANMS standard cultivation medium, although both 5 % DMSO or 10 % glycerol served as cryo-protectants.

Methylocaldum WAP11.3 was resistant to a final concentration of 30 µg/ml of the antibiotics monensin, nalidixic acid and vancomycin added to growth medium, and sensitive to 3 µg/ml of erythromycin or kanamycin. The strain was resistant to a final concentration of 3 µg/ml, but sensitive to 30 µg/ml, of ampicillin, polymyxin B and tetracycline. The fatty acid profile of *Methylocaldum* WAP11.3 cells grown to exponential phase under optimal conditions (50 °C, pH 6.0) with 15 % (v/v) methane in the headspace showed that this strain was dominated by 16 carbon fatty acids, 16:0 and 16:1ω7c (Table 4.10).

Table 4.10 Cellular phospholipid fatty acid profiles of *Methylocaldum* WAP11.3.

Individual fatty acids distribution presented in weight % of total fatty acids.

Fatty acid	Composition
16:0	55.0
16:1ω7c	33.7
17:0*cyc*	11.3

PLFA nomenclature is used according to Guckert [380]: ω, aliphatic end of molecule; c, *cis*; *cyc*, cyclopropyl fatty acid.

A summary of the phenotypic characteristics of *Methylocaldum* WAP11.3 and those of phylogenetically related methanotrophs can be found in Table 4.11.

Table 4.11 Characteristics of *Methylocaldum* WAP11.3 and phylogenetically related methanotrophs. Strains: 1, WAP11.3 (this study); 2, *Methylocaldum* BFH2 [70] 3, *Methylocaldum* BFH1 [70]; 4, *M. szegediense* [58]. +, Positive; -, negative; ND, not determined. Amp, ampicillin; Ery, erythromycin; Kan, kanamycin; Nal, nalidixic acid; Tet, tetracycline. Traits where data is only available for WAP11.3 are not shown.

Strain	**1**	**2**	**3**	**4**
16S rRNA gene sequence similarity with *Methylocaldum* WAP11.3				
	-	99 %	99 %	95 %
Cell morphology				
Shape	Coccoid	Coccoid	Coccoid	Pleomorphic
Width (μm)	1.6-2.0	1.0-1.3	1.0-1.3	1.0-1.2
Length (μm)	1.6-2.4	1.0-2.0	1.0-2.0	1.2-1.5
pH for growth				
Range	4.3-7.4	4.5-7.5	4.2-7.5	ND
Optimum	5.6-6.5	5.7-6.2	5.5-6.0	ND
Temperature for growth				
Range (°C)	39-59	30-60	30-60	37-62
Optimum (°C)	49-56	51-55	51-55	55
Generation time	27 hr	19 hr	21 hr	ND
Growth on methanol (v/v)				
0.1 %	+	+	+	-
Nitrogen sources				
N_2	-	+	+	-
KNO_3	+	+	+	+
NH_4Cl	+	+	+	-
Desiccation resistance	-	ND	ND	-
Heat resistance	+	ND	ND	+
Antibiotic sensitivity	Amp, Ery, Kan, Tet	Amp, Ery, Kan, Nal, Tet	Amp, Ery, Kan, Nal, Tet	ND
Major fatty acids	16:0, 16:1ω7c	ND	16:0, 17:0*cyc*	ND

4.3.13 WHV12.1 phylogenetic analysis

The near full length (1,391 bp) 16S rRNA gene sequence from WHV12.1 was found to be closely related to *Methylacidiphilum* strains, via pairwise sequence analysis. The closest cultured strains were *M. infernorum* (AM900833) and *Methylacidiphilum* sp. RTK17.1 (LN998017), which both shared 100 % nucleotide sequence identity with the WHV12.1 sequence (Figure 4.10). In addition, an environmental clone sampled from a hot spring in China (KM221310) also shared 99 % nucleotide sequence identity with WHV12.1.

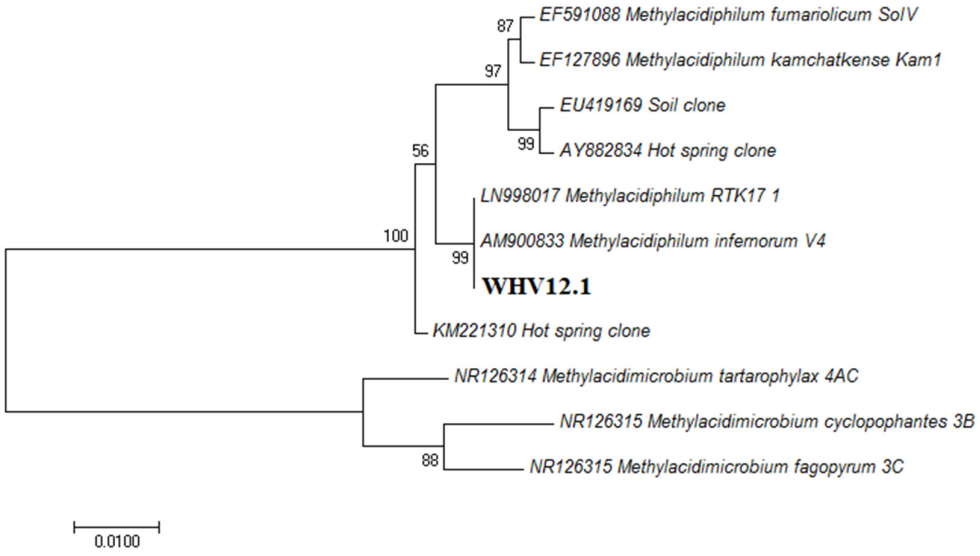

Figure 4.10 Maximum likelihood 16S rRNA gene sequence phylogeny of WHV12.1 The tree shows the phylogenetic relationships between isolate WHV12.1, closely related methanotrophic isolates, and clonal sequences detected in environmental samples. Bootstrap values > 50 % are shown at the branch nodes (1000 replicates). The scale bar represents 0.01 nucleotide substitutions per site.

The inferred amino acid sequence of the PmoA protein from WHV12.1 also showed a close phylogenetic relationship to *Methylacidiphilum* (Figure 4.11); the PmoA2 sequence from the species RTK17.1 (KU509371) shared 99 % amino acid sequence identity with PmoA from WHV12.1, while the M. *infernorum* sequence (EU223862) shared 89 % amino acid sequence similarity. PCR primers for *mmoX*

(soluble methane monooxygenase) did not amplify a product from DNA from WHV12.1.

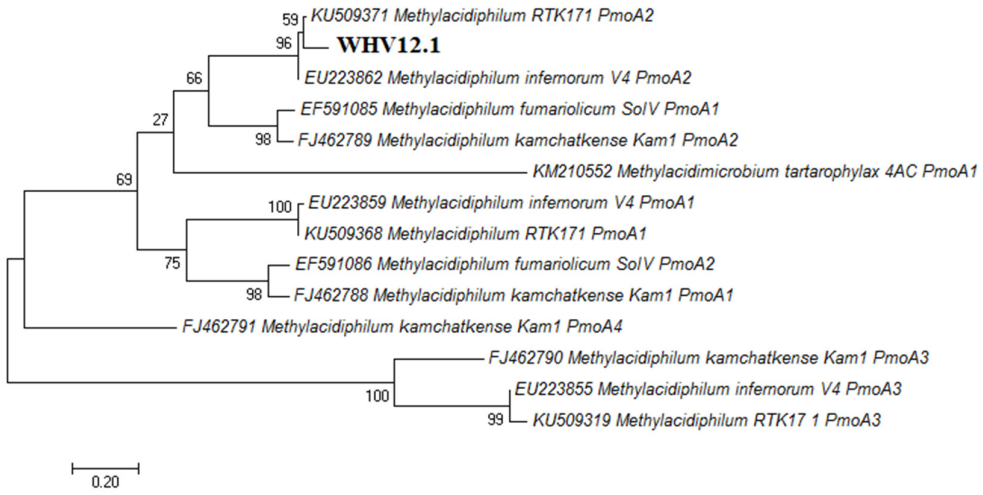

Figure 4.11 Maximum likelihood PmoA sequence phylogeny of WHV12.1 The tree shows the phylogenetic relationships between isolate WHV12.1 and closely related methanotrophic isolates, based on the inferred amino acid sequence of PmoA. Bootstrap values are shown at the branch nodes (1000 replicates). The scale bar represents 0.2 nucleotide substitutions per site.

4.3.14 Methylacidiphilum WHV12.1 cultivation and general characteristics

Cultures of *Methylacidiphilum* WHV12.1 had very low levels of *Alicyclobacillus* spores, which were very rarely seen under the microscope, but that germinated when testing growth on complex media, or when adding peptides to standard V4 culture medium. Multiple rounds of serial dilutions using 1:20 (v/v) inocula were required to isolate the *Methylacidiphilum* WHV12.1 strain. Cells were non-motile short rods, approximately 0.8 µm wide by 1.6-2.4 µm long, which grew between 34-62 °C (optimum 52-58). Growth was not observed at 32 or 64 °C. *Methylacidiphilum* WHV12.1 was capable of growth between pH 1.1-5.4 (optimum pH 3.5-5.3), but growth was not observed at pH 1.0 or 5.5. The generation time was 12.7 hours, and the methane oxidation rate at 52 °C was 25.9 µmoles/hour. The addition of 4 % (v/v) acetylene to the headspace of cultures completely inhibited methane oxidation and growth.

4.3.15 Methylacidiphilum WHV12.1 phenotypic characteristics

Methylacidiphilum WHV12.1 was able to use methane or methanol for energy only. It tolerated 0.3 % (v/v) methanol in the growth medium, but a concentration of 0.4 % (v/v), methanol in the medium inhibited growth. *Methylacidiphilum* WHV12.1 cells could not grow using ethanol, formaldehyde, methylamine, trimethylamine, sodium acetate, trisodium citrate, sodium formate, malic acid, sodium pyruvate, sodium succinate, fructose, glucose, sucrose, xylose, glycerol or mannitol as energy sources. Cells could utilise dinitrogen gas, NH_4Cl or KNO_3 as nitrogen sources, but not methylamine, urea or peptides.

Methylacidiphilum WHV12.1 was not resistant to desiccation or heat-shock, and could only be revived from –80 °C if frozen in TSB medium with either 5 % (v/v) DMSO or 10 % (v/v) glycerol as cryo-protectants. *Methylacidiphilum* WHV12.1 was resistant to a final concentration of 30 µg/ml of the antibiotics ampicillin, kanamycin, monensin, polymyxin B and vancomycin added to growth medium, but sensitive to 3 µg/ml of nalidixic acid. Cells were sensitive to a final concentration of 30 µg/ml of erythromycin and tetracycline but resistant to the lower dose of these antibiotics. Fatty acids of cells grown to exponential phase under optimal conditions (50 °C, pH 3.0) with 15 % (v/v) methane in the headspace were primarily 18:0, *ai*15:0, *i*14:0, and 16:0 (Table 4.12).

Table 4.12 Cellular phospholipid fatty acid profiles of *Methylacidiphilum* WHV12.1. Individual fatty acids distribution presented in weight % of total fatty acids.

Fatty acid	Composition
*i*14:0	16.6
14:0	6.6
*i*15:0	2.4
*a*15:0	21.2
*i*16:0	2.8
16:0	14.6
*i*17:0	0.3
*a*17:0	0.8
17:0	0.4
*i*18:0	0.4
18:0	28.6
18:1ω9c	5.0

PLFA nomenclature is used according to Guckert [380]: ω, aliphatic end of molecule; c, *cis*; a, anteiso; i, iso.

A summary of the phenotypic characteristics of *Methylacidiphilum* WHV12.1 and those of phylogenetically related methanotrophs can be found in Table 4.13.

Table 4.13 Characteristics of *Methylacidiphilum* WHV12.1 and phylogenetically related methanotrophs. Strains: 1, WHV12.1 (this study); 2, *M. infernorum* [14, 47]; 3, *M. fumariolicum* [43, 47]; 4, *M. kamchatkense* [47, 55]. +, Positive; -, negative; ND, not determined. Traits where data is only available for WHV12.1 are not shown.

Strain	1	2	3	4
16S rRNA gene sequence similarity with *Methylacidiphilum* WHV12.1				
	-	100 %	98 %	98 %
Cell morphology				
Shape	Rods	Rods	Rods	Rods
Width (μm)	0.8	0.3-0.5	0.4-0.6	0.5-0.7
Length (μm)	1.6-2.4	1.0-4.0	0.8-2.0	0.8-1.0
pH for growth				
Range	1.1-5.4	1.0-6.0	0.8-5.8	2.0-5.0
Optimum	3.5-5.3	2.0-2.5	2.0	3.5
Temperature for growth				
Range (°C)	34-62	40-60	40-65	37-60
Optimum (°C)	52-58	60	55	55
Generation time	13 hr	18 hr	10 hr	38 hr
Growth on methanol (v/v)				
0.1 %	+	+	+	+
1 %	-	ND	+	-
Nitrogen sources				
N_2	+	+	-	+
NO_3	+	ND	+	+
NH_4	+	+	+	+
Major fatty acids	18:0, *a*15:0	18:0, 16:0	18:0, *a*15:0	*a*15:0, *i*14:0

The results of the phenotypic characterisation of the methanotroph strains isolated in this study are summarised in Table 4.14. The results of the antibiotic susceptibility tests are summarised in Table 4.15.

Table 4.14 Physiological properties of the methanotroph strains.

Characteristics	**Isolates**				
	GDS1.7	**GDS2.4**	**NGM89.1**	**WAP11.3**	**WHV12.1**
Genus	*Methylo-cystis*	*Methylo-coccus*	*Methyl-acidiphilum*	*Methylo-caldum*	*Methyl-acidiphilum*
Cell morphology					
Shape	Vibrioid	Coccoid	Rod	Coccoid	Rod
Motility	No	No	No	No	No
Width (μm)	0.8	0.8	0.8	1.6-2.0	0.8
Length (μm)	2.0-2.4	2.0	1.6-2.4	1.6-2.4	1.6-2.4
pH for growth					
Range	5.0-9.2	5.6-8.7	2.1-5.8	4.3-7.4	1.1-5.4
Optimum	5.8	6.8	2.5-5.0	5.6-6.5	3.5-5.3
Temperature for growth (°C)					
Range	20-43	27-49	40-66	39-59	34-62
Optimum	36	40	53-62	49-56	52-58
Generation time					
	12.5 hr	8.4 hr	17.7 hr	27.2 hr	12.7 hr
Methane oxidation rate (μmoles/hr)					
	47.6	87.8	27.3	23.9	25.9
Methanol tolerated (%, v/v)					
	2.0	0.5	0.3	0.4	0.3
Nitrogen sources					
	NH_4Cl, KNO_3	NH_4Cl, KNO_3	NH_4Cl	NH_4Cl, KNO_3, peptone	N_2, NH_4Cl, KNO_3
Resistant to:					
Desiccation	3 days	No	No	No	No
Heat-shock	No	90 °C	No	70-80 °C	No
Major fatty acids (> 10 %)					
	18:1ω8c, 18:1ω7c	16:0, 16:1ω7c, 16:1ω6c, 16:1ω5c	18:0, *a*15:0, 16:0, *i*14:0, 14:0	16:0, 16:1ω7c, 17:0*cyc*	18:0, *a*15:0, *i*14:0, 16:0

Resistance to desiccation is defined as presence of viable cells after rehydration after the listed number of days. Resistance to heat shock is defined as presence of viable cells after exposure to the temperature shown for 10 minutes.

Table 4.15 Summary table of the antibiotic sensitivities of the methanotrophs. Strains are shown as resistant (R) to the highest concentration tested (µg/ml), or the concentration to which they were sensitive (S). Green boxes highlight resistance to the higher concentration of antibiotic tested (30 µg/ml); red boxes highlight sensitivity to the lower concentration tested (3 µg/ml).

Strain	GDS1.7	GDS2.4	NGM89.1	WAP11.3	WHV12.1
Genus	*Methylo-cystis*	*Methylo-coccus*	*Methyl-acidiphilum*	*Methylo-caldum*	*Methyl-acidiphilum*
Ampicillin	R (30)	S (30)	S (30)	S (30)	R (30)
Erythromycin	S (3)	S (3)	S (3)	S (3)	S (30)
Kanamycin	S (3)	S (3)	S (3)	S (3)	R (30)
Monensin	R (30)	R (30)	R (30)	R (30)	R (30)
Nalidixic acid	S (3)	S (3)	S (3)	R (30)	S (3)
Polymyxin B	R (30)	S (30)	R (30)	S (30)	R (30)
Tetracycline	S (3)	S (3)	S (30)	S (30)	S (30)
Vancomycin	R (30)	R (30)	R (30)	R (30)	R (30)

4.4 Discussion

The isolation of microbes, and culture-based investigations, are essential to understand the phenotypic characteristics of microorganisms, rather than simply their genetic potential. The aim of this chapter was to isolate and characterise thermophilic methanotrophs from geothermal microcosms. Isolation of thermophilic methanotrophs was attempted from 22 enrichment cultures established in chapter three that demonstrated methane oxidation. Six of the enrichment microcosms continued to oxidise methane over a prolonged period; GDS1 and GDS2 from Golden Springs, NGM89 from Ngatamariki, TOK7 from Tokaanu, WAP11 from Waipahihi and WHV12 from Whakarewarewa, and from these, five methanotrophs were obtained as axenic cultures.

For most of the consortia, methane oxidation was not sustained over multiple passages into fresh media. One reason for this observation may be that an environmental parameter essential for the growth of specific microorganisms was not replicated in the laboratory setting. This could include incubation temperature,

pH, oxygen or methane concentrations or an unknown aspect of the environment [108]. The enrichment media used may also have lacked a crucial growth factor; for example, lanthanides are essential in micromolar concentrations for the growth of *M. fumariolicum* [136] as a co-factor in a XoxF methanol dehydrogenase enzyme that is widespread in many environments [137]. Similar growth factors could have been present in geothermal samples but diluted to concentrations lower than those required to support growth during the sub-culturing process.

Phylogenetic analysis of DNA from the successful isolation attempts using both 16S rRNA and *pmoA* or *mmoX* gene sequences indicated that the isolates were members of the genera *Methylocystis* (GDS1.7) (*Alphaproteobacteria*), *Methylococcus* (GDS2.4) and *Methylocaldum* (WAP11.3) (*Gammaproteobacteria*) and *Methylacidiphilum* (NGM89.1 and WHV12.1) (*Verrucomicrobia*). The strains obtained in axenic culture were not always representative of the dominant species identified through sequencing of the 16S rRNA gene from chapter two. For example, in the first Golden Springs sample, GDS1, *Methylacidiphilum* comprised 8.7 % of the total sequences, with a much smaller proportion assigned to *Methylococcus* (0.4 %). A substantial number of other reads were identified only as far as family level, to *Methylococcaceae* (4.5 %). *Methylacidiphilum* was not targeted for isolation as the sample was of circumneutral pH and the presence of relic DNA [285] was suspected, but the NMS media chosen to enrich *Methylococcus* strains instead sustained a *Methylocystis* strain from this sample, which was not identified at all in the Illumina sequencing data. Similarly, sequencing reads from the Waipahihi WAP11 sample identified very few methanotrophs; 0.5 % *Methylacidiphilum*, and less than 0.01 % of reads affiliated to *Methylothermus* and *Methylocystis*. The *Methylocaldum* strain isolated from this sample was not detected. These results may be an indication of biases during the DNA extraction, PCR amplification or sequencing processes, or as a result of the inherent difficulties of laboratory-based cultivation, and highlights that classical cultivation techniques rarely select for the dominant and ecologically most active member of a community.

Conversely, sequencing of the geothermal samples NGM89 (Ngatamariki) and WHV12 (Whakarewarewa Village) indicated that both contained a high

proportion of *Methylacidiphilum*; 60.7 % and 50.6 % of total reads respectively. A *Methylacidiphilum* strain appeared to be rapidly isolated from both samples but these were mixed cultures with very low abundance of *Alicyclobacillus* spores. Both samples had only four reads assigned to *Alicyclobacillus*, which may reflect the difficulty in extracting DNA from spores [383], rather than their true prevalence in the environment.

However, in GDS2 from Golden Springs, 1.5 % of the 16S rRNA gene sequencing reads were affiliated with *Methylococcaceae*, with 0.1 % assigned to *Methylococcus*, which corresponds with the successful isolation of a *Methylococcus* strain from this sample. Similarly, the sequencing of 16S rRNA genes from the Tokaanu TOK7 sample indicated a high proportion of reads assigned to *Methylothermus* (11.2 %), a genus that was enriched in the methane-oxidising microcosm, although an axenic culture was not obtained.

A more diverse range of methanotrophs may have been cultivated if a range of different media, altering environmental parameters, or alternate methods had been used. Miniaturised extinction culturing (parallel dilution-to-extinction cultures using microtiter plates, following an initial enrichment step) [384] is efficient for the isolation of methanotrophs from a variety of environments. However, most of these strains were identified as *Methylomonas*, which may be selected for from multiple environmental strains using this method. Diffusion chambers, which allow nutrients and growth factors, but not cells, to pass between co-cultures, have been successfully used to isolate previously 'unculturable' bacteria, including methylotrophs [385, 386], while metatranscriptomics have been used to identify the growth substrates of a leech symbiont, leading to isolation [387].

Several of the methanotrophs in this study had a close association with one or more "satellite" microbes after multiple passages to fresh medium and serial dilutions. The presence of heterotrophs within methanotrophic co-cultures stimulates methane oxidation [317], and there is presumably a cooperative interaction between the methanotrophs and their associated microbes, perhaps by providing a specific growth factor [388], or by removing potentially inhibitory

compounds such as methanol or formaldehyde that are produced during the methane oxidation process [389].

Four of the methanotrophs isolated during this study were thermophiles, with optimum temperatures for growth > 40 °C, as defined in chapter one, while one isolate (GDS1.7) was thermotolerant, with a maximum growth temperature of 43 °C. The procedures used were designed to target high-temperature strains, but many of the enrichment microcosms incubated at 60 °C and above did not oxidise methane, or stopped doing so after being passaged into fresh (liquid) medium. One reason for this may be the low solubility of methane in water [206], or the presence of oxygen; anaerobic or microaerophilic strains responsible for methane oxidation that were able to survive within the soil or sediment microcosms may not have been able to withstand higher levels of oxygen dissolved in enrichment media that was constantly shaken.

Phenotypic characterisation of the isolates showed that, in general, the results were consistent with the known physiological traits of closely related strains (Table 4.5, Table 4.7, Table 4.9, Table 4.11, Table 4.13). In some instances, the most closely related strain has not been fully described in the literature, and trait comparisons have been made using a more distantly related strain. For this study these are defined as *Methylocystis* GDS1.7 and *M. echinoides* [381], and *Methylacidiphilum* NGM89.1 and WHV12.1, which are compared not only to the isolate *M. infernorum*, but also to *M. fumariolicum* and *M. kamchatkense* [47].

Temperature ranges of the isolates were comparable with those of closely related strains with the exception of *Methylacidiphilum* WHV12.1; this strain was about to grow at temperatures as low as 34 °C although the previous lowest known growth temperature for a strain from this genus was *M. kamchatkense*, which can grow at 37 °C [55]. Similarly, pH ranges of the isolates were almost identical to those described in the literature for similar strains. There was a slight difference with the *Methylacidiphilum* strain WHV12.1, which could grow at pH as low as 1.1 while *M. infernorum* grows only at pH 1.5 and above, but the more distantly related strain *M. fumariolicum* is able to grow at pH 0.8 [47].

The novel strains were all obligate methanotrophs, able to utilise only methane and methanol for energy, which is consistent with the majority of described strains. Some facultative species have been described within the *Alphaproteobacteria*; *Methylocystis bryophila* and *Methylocapsa aurea* cells can use acetate [27, 28], while *Methylocella* species can use acetate, malate, pyruvate, succinate, and ethanol [30], but *Methylocystis* GDS1.7 was unable to use any complex, multicarbon substrates. The addition of 4 % (v/v) acetylene to the headspace of cultures completely inhibited methane oxidation and growth of all of the strains, possibly through inhibition of pMMO [46] as previously demonstrated in *Methylocaldum* BFH2 [70] and *M. infernorum* [47].

The PmoA of *Methylacidiphilum* NGM89.1, based on inferred amino acid sequence, was most similar to PmoA1 of *M. infernorum* and *Methylacidiphilum* sp. RTK17.1, whereas the PmoA of *Methylacidiphilum* WHV12.1 was more similar to PmoA2 from the same strains. This may reflect bias introduced during the PCR process, as several methanotrophs including *M. infernorum* encode multiple *pmoCAB* operons [54, 241], and the standard primers used in this study may not amplify all sequences equally. Genome sequencing of the isolates would enable identification of duplicate operons, and allow better resolution of the phylogenetic relationship between these strains.

The methanol tolerance of the novel strains was generally similar to that of described strains. *Methylocystis* GDS1.7 grew in the presence of up to 2 % (v/v) methanol in growth media, while the close relative *M. echinoides* grew with 0.1 % (v/v), but not 1.0 % (v/v) [381]. However, *Methylocystis parvus* was adapted to grow with 4 % (v/v) methanol in culture medium over a period of weeks [390]. *Methylococcus* GDS2.4 grew with up to 0.5 % (v/v) methanol in the culture medium but the methanol tolerance of *M. capsulatus* beyond 0.1 % (v/v) [44] has not been reported. *Methylacidiphilum* strains NGM89.1 and WHV12.1, and *Methylocaldum* WAP11.3 showed similar methanol tolerances to those described for related strains [47, 70].

All isolates were able to use NH_4Cl as a nitrogen source, and all except *Methylacidiphilum* NGM89.1 could also utilise nitrate, which is fairly consistent

with the literature; *M. infernorum* has not been tested on nitrate but the genome contains genes for assimilatory nitrate reduction [391], and *M. fumariolicum* is able to use nitrate as a source of nitrogen [43]. Nitrogen fixation, or growth in N-free media, has been observed with *M. echinoides* [45], *M. capsulatus* [45], *Methylocaldum* BFH2 [70] and *M. infernorum* [47], but the only novel strain from this study that was able to use dinitrogen gas as a nitrogen source was *Methylacidiphilum* WHV12.1. However, the oxic atmosphere used in these experiments may have inhibited nitrogenase activity [106].

Physiological tests on the isolates indicated their levels of resistance to sub-optimal conditions, but the novel strains do not appear to display many adaptations to fluctuating environmental conditions. None of the strains isolated during this study produced cysts or spores, often formed during periods of methane starvation [214, 240, 381], or used multi-carbon substrates [27, 30], but hydrogen oxidation, as reported for several methanotrophs [34, 35, 228, 229], was not investigated in this chapter.

Methylocaldum WAP11.3 and *Methylococcus* GDS2.4 showed resistance to heat-shock at 80 and 90 °C respectively, but neither *Methylocaldum* BFH2 or *M. capsulatus* are heat-resistant [45, 70]. This may be an adaptation to fluctuating temperatures. The Waipahihi (WAP) site is periodically covered with lake water much colder than the geothermal water rising from below the sample site, which could create a selective pressure on microorganisms from this environment. The thermotolerant isolate *Methylocystis* GDS1.7 has a maximum temperature for growth of 42 °C and was not viable after heat-shock at 50 °C, despite being isolated from an enrichment microcosm initially incubated at 50 °C. Given that this strain did not produce cysts or spores, its survival at elevated temperatures is noteworthy. Overexpression of the DNA chaperone proteins GroEL/GroES in *Escherichia coli* leads to adaptation, over time, to temperatures up to 3 °C greater than normal T_{max} [392]. Alternatively, the presence of NaCl increases heat tolerance in *Burkholderia* [393], suggesting attributes of the original environmental sample could be responsible for the *Methylocystis* GDS1.7 result.

Trehalose is accumulated by a variety of bacteria in response to various stresses, including heat, high osmolarity and desiccation [394-396], but in yeast, it is the expression of trehalose-6-phosphate synthase (TPS), rather than trehalose itself, which is responsible for both thermal tolerance and resistance to desiccation [397]. *Methylocystis* GDS1.7 was the only strain in this study able to be revived after three days of desiccation, and given that TPS was expressed at low levels in the GDS1 enrichment microcosm (Extended Data Set 6) and has been identified in the genomes of *Methylocystis* species Rockwell and LW5 [391], TPS expression is another potential method of gradual stress tolerance in this strain.

All isolates were only able to be revived from storage at -80 °C when frozen in Tryptic Soy Broth (TSB) (adjusted to pH 3.0 for *Methylacidiphilum strains*) and not in their standard cultivation media, although either 5 % (v/v) DMSO or 10 % (v/v) glycerol served as cryo-protectants. Most type I methanotrophs [293], including *Methylogaea,* [234], *Methylomonas* and *Methylovulum* species [398], cannot be revived from cryostorage, and freezing may induce a viable but non-culturable state in methanotrophs [399]. Preservation of cells in a ten-fold dilution of TSB with the addition of 1 % (v/v) trehalose, using either 5 % (v/v) DMSO or 15 % (v/v) glycerol, enabled revival of *Methylocystis parvus*, *Methylococcus capsulatus* and *Methylocaldum gracile* from storage both at -80 °C and in liquid nitrogen [399].

Although antibiotic sensitivities are not routinely reported for methanotrophs, or many other non-pathogenic strains, resistance to anti-microbials may be important in their natural environment, as thermophilic fungi [400] and bacteria [401, 402] release bacteriostatic or microbicidal compounds that could affect the survival or fitness of strains. The activity of antimicrobial agents tested against the methanotrophic isolates in this study (Table 4.15) was generally consistent with what has been described for similar strains.

All strains were resistant to the antibiotics monensin and vancomycin, consistent with being Gram-negative, as are all known methanotrophs [45, 47]. Monensin alters the internal pH of the cell and disrupts cell processes [376] but is unable to pass through Gram-negative cell membranes, meaning that resistance is intrinsic,

as with vancomycin, which prevents cell wall synthesis [375]. Conversely, most of the isolated strains were sensitive to 3 μg/ml erythromycin, kanamycin, and nalidixic acid, except for *Methylocaldum* WAP11.3 and *Methylacidiphilum* WHV12.1 (Table 4.15). *Methylocaldum* BFH2 [70] and *Methylococcus* species [403] are sensitive to erythromycin and kanamycin, but in contrast to *Methylocaldum* WAP11.3, BFH2 was also sensitive to nalidixic acid.

The macrolide antibiotic erythromycin binds reversibly to 50S ribosomal subunits, preventing binding of tRNA and inhibiting peptide translocation and protein synthesis [404], but genes for macrolide efflux proteins and erythromycin resistance methylase were not found in published *Methylocaldum* or *Methylacidiphilum* genomes, and resistance may be due to a multi-drug efflux pump, which were identified in the *Methylocaldum szegediense* and *Methylacidiphilum infernorum* genomes [391]. Nalidixic acid binds reversibly to DNA complexed with DNA gyrase in Gram-negative bacteria, blocking DNA replication [375]. Resistance may be conferred again through efflux pumps, or through mutations in DNA gyrase, alterations to membrane permeability, or through the expression of plasmid-encoded proteins that bind to and protect DNA gyrase from inhibition [405].

Methylacidiphilum WHV12.1 was resistant to kanamycin, an aminoglycoside synthesised by common soil organisms such as *Streptomyces* species [406], which binds to 30S ribosomal subunits and gives rise to substantial amounts of mistranslation [375]. The action of aminoglycosides in *Pseudomonas* strains is inhibited by low pH [407], but as both *Methylacidiphilum* strains were tested in V4 medium at pH 3.0 and only NGM89.1 was sensitive, this inhibition does not appear to be exhibited under these conditions. Resistance to kanamycin can be conferred by aminoglycoside-modifying enzymes that modify the antibiotic so that ribosomal binding is impaired, through efflux pumps, or by alterations in membrane permeability through mechanisms as yet unknown [408]. Aminoglycoside-modifying enzymes are often encoded on plasmids and are also associated with transposable elements, suggesting that lateral gene transfer may have occurred in the WHV12.1 population but not the NGM89.1 community.

In this study, *Methylocystis* GDS1.7 and *Methylacidiphilum* WHV12.1 showed resistance to 30 μg/ml of ampicillin, a semi-synthetic β-lactam antibiotic that inhibits transpeptidase in cell wall synthesis [375]. Antibiotics with similar structures are synthesised by thermophilic *Bacillus* [409] as well as by a range of other bacteria and fungi [410]. Resistance could be conferred by the activity of one or more members of a broad family of enzymes that hydrolyse the β-lactam ring [411], which have been identified in multiple *Methylocystis* and *Methylacidiphilum* genomes [391]. All strains were resistant to at least 3 μg/ml polymyxin B (Table 4.15), which interacts with lipopolysaccharide (LPS) in the membranes of Gram-negative bacteria, altering membrane permeability [375]. There are several known mechanisms for resistance: efflux pumps, complete loss of lipopolysaccharide, or LPS modifications resulting in a positive charge on the LPS that reduces binding to polymyxins [412]. LPS modifications can compromise the integrity of cell membranes, which may explain why most of the strains tested were only resistant to low concentrations (3 μg/ml).

Finally, *Methylocystis* GDS1.7 and *Methylococcus* GDS2.4 were sensitive to 3 μg/ml of tetracycline, consistent with previous results [70, 403], while *Methylocaldum* WAP11.3 and *Methylacidiphilum* NGM89.1 and WHV12.1 were sensitive only to 30 μg/ml of the antibiotic (Table 4.15). Tetracycline binds reversibly to 30S subunits and blocks the attachment of charged aminoacyl-tRNA, inhibiting protein synthesis [375]. Partial resistance could be caused by low levels of expression of efflux pumps or Ribosomal Protection Proteins (RPP) [413, 414], and has been reported for the gammaproteobacterium *Aeromonas* sp. ARM81 [415] and for *Blastopirellula marina* [416, 417], a member of the *Planctomycetes-Verrucomicrobia-Chlamydiae* (PVC) superphylum.

The fatty acid composition of cell membranes from the methanotrophs were consistent with described strains. The major fatty acids of *Methylocystis* GDS1.7 (18:1ω8c and 18:1ω7c) and *Methylococcus* GDS2.4 (16:0 and 16:1ω7c) were identical to those of *Methylocystis parvus* and *Methylococcus capsulatus*, respectively [45]. The fatty acid composition of *Methylocaldum* WAP11.3 was very similar to *Methylocaldum* BFH2; dominated by 16:0 (54 % of the total fatty acids in each strain), and with high amounts of 17:0 *cyc* (11.3 and 26.3 %,

respectively) and 16:1ω7c (33.7 and 13.8 %, respectively). BFH2 also contained minor amounts (< 1 %) of 12 other fatty acids that were not detected in WAP11.3.

The fatty acid composition of both *Methylacidiphilum* NGM89.1 and WHV12.1 was almost entirely comprised of saturated fatty acids, mainly 18:0, *a*15:0, *i*14:0, 16:0 and 14:0. These also dominate the fatty acids of *M. infernorum*, *M. fumariolicum* and *M. kamchatkense* [47] although the proportions vary between the strains. Increases in cultivation temperature of specific bacteria leads to an alteration in fatty acid composition, from branched to straight chain, and with an increase in chain length e.g. [87, 418, 419]. This may explain why the fatty acid composition of *Methylacidiphilum* NGM89.1, cultivated at 60 °C, consisted of more 18:0 than *Methylacidiphilum* WHV12.1, grown at 50 °C (40 % and 28.6 % of total fatty acids, respectively).

4.5 Conclusions

Methanotrophs are ubiquitous in geothermal soils within the Taupō Volcanic Zone, and methane-oxidising bacteria were isolated and characterised from five geothermal enrichment microcosms during this study, although none could be considered new species, using the similarity cut-off of < 97% 16S rRNA gene sequence for species differentiation. As well as targeting a group of bacteria with very specific nutritional needs and a wide range of published data on their growth requirements, this study has highlighted the difficulty in isolating methanotrophs from geothermal samples. Sequencing of the 16S rRNA gene was inadequate at predicting if geothermal samples would oxidise methane under laboratory conditions, or if methanotrophs could be isolated from these samples. Using media that was designed to culture specific methanotrophs was not sufficient to isolate strains that had been identified as present in the original sample via 16S rRNA gene sequencing.

The isolated methanotrophs were similar in their phenotypic characteristics to previously described strains. Of note was the lack of adaptations to changing environmental conditions; no isolates produced spores or cysts, only *Methylocystis* GDS1.7 showed limited resistance to desiccation, and only *Methylococcus* GDS2.4 and *Methylocaldum* WAP11.3 showed resistance to heat-

shock. No isolates were capable of using multi-carbon substrates in the absence of methane. However, several described methanotrophs, including *Methylococcus capsulatus* [229] and *Methylacidiphilum* sp. RTK17.1 [34, 35] are capable of oxidising hydrogen, and this may be a survival strategy during periods of methane starvation or other sub-optimal conditions. The next stage of this study is to determine if hydrogen oxidation is observed within the methanotrophs, and if this contributes to their survival or persistence.

5. H_2 oxidation by methanotrophs and its possible implications for survival at elevated temperatures

5.1 Introduction

Microbial communities often alternate between a state of growth and a metabolically-inactive (dormant) state due to fluctuations in their natural environment [51]. Methanotrophic ecosystems are particularly dynamic, with fluctuating conditions that may include periods of oxygen or methane starvation, or changes in temperature, pH, and water availability [420, 421]. Depth profiles of soils, including geothermal environments, indicate that temperature and methane partial pressures correlate with depth, while partial pressures of oxygen are inversely correlated to depth [14, 35, 422], and suggest that disturbances in the soil profile can adversely affect local growth conditions.

Methanotrophs in both soils and sediments may be frequently exposed to temperature change due to geothermal activity, hypoxic/anoxic conditions or changes in methane availability [188, 447], and respond to these dynamic events by inducing one of several advantageous persistence strategies, for example by producing cysts or spores under these conditions [214]. Methanotrophs have traditionally been described as obligate C1 compound specialists, deriving energy exclusively from the oxidation of methane, methanol, and in certain cases methylated amines and halomethanes [46]. However, some methanotrophs from *Alphaproteobacteria* utilise acetate, pyruvate, succinate, malate, ethanol and various alkanes [27, 28, 30, 31], which imparts a selective advantage over other methanotrophs during periods of methane starvation, and may allow methane oxidation at atmospheric concentrations [423]. *Methylococcus*, *Methylomicrobium* and *Methylacidiphilum* strains accumulate intracellular glycogen that can be utilised as an energy source in the absence of methane [448-450].

A handful of methanotroph species oxidise hydrogen in a respiratory-linked process during hypoxic growth [34, 35, 227]. Hydrogen has been suggested as the universal energy source for long-term survival of microorganisms, due to its ubiquitous presence in the troposphere, a high environmental permeability, the ability to readily diffuse into cells, and a low activation energy (the minimum energy required to start a chemical reaction –Equation 1)[222]. The maintenance

energy needed for survival, as cells repair the effects of depurination of DNA and racemization of amino acids, is much less than the requirement for growth or cell division, or other maintenance activities such as osmoregulation or for shifts in metabolic pathways [424]. These low energy requirements make hydrogen an ideal candidate to serve in this role.

Equation 1

$H_{2(g)} + 0.5O_{2(g)} \leftrightarrow H_2O_{(l)}$ ΔG_r^0 = -237 kJ mol^{-1} at 25 °C [207]

The metabolic energy gained through the oxidation of atmospheric hydrogen (~0.5 ppmv) is sufficient to maintain microbial populations in forest and agricultural soils [425], as well as oligotrophic geothermal [224] and Antarctic soils [426]. In geothermal systems, molecular hydrogen is readily available [427, 428] and may be derived from small amounts of H_2O dissolved in minerals, released from igneous rocks such as andesite [282] and basalt [429], as well as from volcanic gases from the oxidation of the mineral magnetite to haematite [430]. Hydrogen is also produced by a wide variety of *Bacteria* and *Archaea*, either to remove excess reducing power by evolving molecular hydrogen [431], through the action of nitrogenase enzymes (Equation 2) [432] or via photosynthesis [433].

Equation 2

$N_2 + 8H^+ + 8e^- \rightarrow 2NH_3 + H_2$ ΔG_r^0 = -33.2 kJ mol^{-1} at 25 °C [434]

Hydrogen metabolism is often a dominant theme among organisms from geothermal environments [435-437], and may have been one of the earliest metabolisms to evolve [438]. Hydrogenases, a physiologically diverse class of enzymes that catalyse the reversible oxidation of H_2 to protons, have been identified in all published methanotroph genomes [226]; therefore suggesting hydrogen oxidation may also be important for methanotrophs in geothermal areas. Hydrogenases identified in methanotroph genomes all belong to the [NiFe]-family, named for the metal content of the H_2-binding site [35]. These can be

classified further into 22 groups based on phylogeny, structure, predicted function, and regulatory components; groups 1a to 1h (membrane-bound H_2-uptake hydrogenases), 2a to 2d (cytosolic H_2-uptake hydrogenases), 3a to 3d (cytosolic bidirectional hydrogenases), and 4a to 4f (membrane-bound H_2-evolving hydrogenases) [226], although the latter group has not been identified in methanotroph genomes [35]. Each group is characterised by two conserved amino acid motifs (L1 and L2) that coordinate binding of cysteine ligands to the [NiFe]-centre [226, 439]. These motifs can be used to confirm the identity of putative hydrogenase sequences (Table 5.1).

Table 5.1 Conserved amino acid residues surrounding cysteine ligands of selected groups of [NiFe]-hydrogenases identified in methanotroph genomes. Data taken from [226].

Group	L1 motif	L2 motif
1d	xxRICGVCTxxH	SFDPCLACxxH
1h/5	TSRICGICGDNH	SFDPCLPCGVH
2b	xPRICGICSxSQ	SFDPCMVCTVH
3b	xxRICxxCxxxx	xxDPCISCxxH
3d	xxRxCGICPVSH	xxDPCLSCxTH

Despite the prevalence of hydrogenases encoded in methanotroph genomes, few reports have sought to describe the physiological role of hydrogen metabolism in methanotrophic bacteria. In *Methylosinus trichosporium* OB3b, hydrogen provides reducing power for both sMMO and pMMO activity [227, 228] possibly by regenerating intracellular NADH. The strain encodes four hydrogenases; two uptake hydrogenases from groups 1d and 1h/5, as well as a regulatory, histidine-kinase linked hydrogenase from group 2b, and a bidirectional, NADP-coupled hydrogenase from the 3b family [35]. It is uncertain which enzymes are responsible for the constitutive and inducible uptake of molecular hydrogen that have been observed in this strain [227]. Cultivation of this strain in nitrate-deficient media induces nitrogenase activity leading to the production of intracellular hydrogen [227].

Methylococcus capsulatus Bath encodes two constitutive hydrogenases; one soluble (group 3d) and one respiratory-linked, membrane-bound (group 1d). Group 3d [NiFe]-hydrogenases drive both sMMO and pMMO activity under low and near-atmospheric levels of oxygen [229], and the expression of the group 1d [NiFe]-hydrogenase could be linked to oxygen availability [440]. Methanotrophy in microaerophilic niches can be significant, particularly in sediments [188, 218], and the simultaneous oxidation of methane and hydrogen (mixotrophy) may be one method to cope with both oxygen and methane starvation.

Of the verrucomicrobial methanotrophs, both *Methylacidiphilum fumariolicum* SolV and *Methylacidiphilum* sp. RTK17.1 express oxygen-sensitive (group 3b) and oxygen-tolerant (group 1d) hydrogenases that are used not only to provide reductant for pMMO, but also to support carbon dioxide fixation and provide respiratory energy under microoxic conditions (less than 1% oxygen) [34, 35]. Transcriptional upregulation of the group 1d hydrogenase of *M. fumariolicum* has been demonstrated in response to low oxygen [34]. Further, as soil temperatures in geothermal areas typically increase with depth [14, 35, 422], and the mechanisms utilised by methanotrophs to persist at elevated temperatures are not known (other than through the production of spores and cysts [214]), it is possible the extra respiratory energy provided from hydrogen oxidation may benefit cell survival. In partial support of this, in cultures of *M. capsulatus*, an increase in incubation temperature, from 45 to 57 °C, resulted in a small observable increase in hydrogen-driven pMMO activity [229].

Finally, hydrogen metabolism may also be important to the survival of methanotrophic bacteria in fully oxic niches. A recent study of forest soils and farmland showed significant decreases in methane oxidation when soils were exposed to high partial pressures of hydrogen [441]. Although the microbes responsible for hydrogen oxidation were not definitively identified, this could indicate methanotrophs in methane-starvation conditions switching to hydrogen oxidation under atmospheric levels of oxygen.

This study aims to determine if the oxidation of hydrogen is used by the methanotrophs isolated from geothermal habitats in chapter four as a means of

survival and persistence during exposure to elevated temperatures. Some methanotrophs make resting stage or dormant morphotypes such as cysts and exospores, which are resistant to desiccation and/or heat [45, 214]. However, none of the isolates from this study displayed cyst or exospore formation, and therefore are likely to require alternative strategies to survive exposure to sub-optimal conditions.

My aims for this chapter are i) to determine if the methanotrophs in this study encode [NiFe]-hydrogenases; ii) to determine if the methanotrophs oxidise hydrogen, under atmospheric or microaerophilic levels of oxygen; iii) if hydrogen oxidation is observed, to determine if hydrogen metabolism influences either volumes of methane oxidised or growth yields; and iv) to determine if hydrogen oxidation is utilised as a method of survival during exposure to elevated temperatures.

5.2 Methods

Table 5.2 Methanotroph strains studied in this chapter.

Sample site	Isolate	Genus	T_{min}	T_{opt}	T_{max}
Golden Springs	GDS1.7	*Methylocystis*	20	36	43
Golden Springs	GDS2.4	*Methylococcus*	27	40	49
Ngatamariki	NGM89.1	*Methylacidiphilum*	40	53-62	66
Whakarewarewa	WHV12.1	*Methylacidiphilum*	34	52-58	62
Waipahihi	WAP11.3	*Methylocaldum*	39	49-56	59

Primer design and PCR for [NiFe]-hydrogenases within isolates

Hydrogenases encoded within methanotroph genomes are all [NiFe]-containing enzymes [226]. On the basis of their phylogeny [35], strains likely to encode hydrogenases homologous to enzymes present within methanotrophs from this study were selected (Table 5.3). Nucleotide sequences encoding the relevant methanotroph hydrogenases were retrieved from the National Center for Biotechnology Information (NCBI) database [442]. Retrieved sequences were classified into hydrogenase groupings via translation to amino acid sequences and confirmation of the presence of conserved L1 and L2 motifs (Table 5.1) [226].

PCR primers targeting the [NiFe]-hydrogenase large subunit were designed using Primer3 ([443], v2.3.4) within the software Geneious (Biomatters, v8.1.6). Annealing temperatures were chosen based on the predicted T_m of each primer within a pair (Table 5.4).

Table 5.3 Classification of [NiFe]-hydrogenases identified in genomes of methanotroph strains, from the same genera as the strains from this study. Data taken from [35].

	Predicted presence and type of [NiFe] hydrogenase				
	1d	1h/5	2b	3b	3d
Genus	Uptake	Uptake	Regulatory	Bidirectional	Bidirectional
Methylocystis	Y	Y	Y	Y	N
Methylococcus	Y	N	N	N	Y
Methylacidiphilum	Y	Y	N	Y	N
Methylocaldum	Y	N	N	Y	N

Table 5.4 PCR primers targeting the large subunit of [NiFe]-hydrogenases. Degenerate primers follow the IUPAC code.

Group	Genera	Primer name	Sequence	Tm (°C)	Annealing temperature (°C)	Amplicon size (bp)
1d	*Methylocystis*	Cystis_hyd_1d_301F	GAG AAC GCC AAT TCG ATC CGC	58.9	57	1165
		Cystis_hyd_1d_1466R	TTC TCG ACA TTG GCG GTC	55.1		
1d	*Methylacidiphilum*	Verr_hyd_1d_773F	AGY CAG CTC AAC TTR GTC TC	54.3	55	896
		Verr_hyd_1d_1669R	AGA AGR GAG GCC TCA AAA GC	56.1		
1d	*Methylocaldum, Methylococcus*	Gamma_hyd_1d_208F	GCC TTC ACC GAA CGG ATC T	57.4	56	301-1354
		Gamma_hyd_1d_316F	ATC CGC AAC ATC ATG CAG C	56.5		
		Gamma_hyd_1d_511F	AAG AAG TTC GTC GAG AGC GG	57.0		
		Gamma_hyd_1d_812R	ATG AAC TCG ATG GTC TGG TCG	56.7		
		Gamma_hyd_1d_1562R	CCG TCC TTG ATC TTG ATC CA	54.3		
1h/5	*Methylocystis*	Alpha_hyd_1h_408F	CGA TTT CTG CGA GCA GAT GG	56.3	56	1299
		Alpha_hyd_1h_1707R	GCG CAT GAT GTC GAT GCC	57.4		
1h/5	*Methylacidiphilum*	Hyd_1h_429F	TGC GAR MAR ATG GTC AAG G	54.3	52	1354
		Hyd_1h_1783R	ABA TAC ATA TGC ACM CCY G	50.9		
2b	*Methylocystis*	Hyd_2b_183F	GCA TTT GCT CGG TCT CGC	57.2	55	1133
		Hyd_2b_1316R	GGC GCG ATG ATC TGA TAG	52.9		
3b	*Methylocaldum, Methylocystis*	Hyd_3b_215F	CCS GTM GCC TAT CAG ATG AG	55.6	54	1067
		Hyd_3b_1282R	CAS GGR TCG TAA TTG CG	52.3		
3b	*Methylocaldum*	Caldum_hyd_3b_381F	CCC GGA GAT GGC AAA GGA TT	57.6	58	289
		Caldum_hyd_3b_670R	GGT ATT CGG AGG GAT GCC TG	57.6		
3b	*Methylacidiphilum*	Verr_hyd_3b_368F	TCT TTC TYC ATG CTC CCG G	55.8	53	794
		Verr_hyd_3b_1162R	AAR CAG GTK GGA GGA AC	51.9		
3d	*Methylococcus*	Coccus_hyd_3d_6F	CGA CCA TCT SGA RAC CGC	57.2	57	1260
		Coccus_hyd_3d_1266R	GTT STG GGT GGT GGA GAC G	58.2		

PCR was carried out in 50 µl reaction volumes in 200 µl tubes containing 100 µM dNTPs, 0.5 µM primers, 1U i-Taq (iNtRON Biotechnology, South Korea) and 7 µl of an enhancer solution (2.7 M betaine, 0.2 M trehalose, 6.7 mM DTT, 0.055 mg ml^{-1} BSA and 0.067 % DMSO). The final concentration of $MgCl_2$ was 1.5 mM. Each of the three Gamma_hyd_1d forward primers (Table 5.4) were tested in combination with both Gamma_hyd_1d reverse primers, in separate PCR reactions. Duplicate DNA extracts from methanotroph strains were used at final concentrations of 10 – 50 ng/reaction. PCR amplifications were performed using a T100 thermal cycler (Bio-Rad, Hercules, CA). The PCR conditions were as follows: 94 °C for 5 minutes; 30 cycles consisting of 94 °C for 45 seconds, the selected annealing temperature for 60 seconds and 72 °C for 90 seconds; and a final extension step at 72 °C for 5 minutes. PCR reactions that amplified a product of the expected size were purified using the NucleoSpin Gel and PCR Clean-up kit (Macherey-Nagel), before being sequenced by Macrogen Inc. (South Korea).

Hydrogenase gene sequences retrieved from the methanotroph isolates via PCR (all sequences were > 776 bp in length) were manually checked for quality, and closely-related strains to the isolates were determined by subjecting the sequences to a discontiguous megablast search [333]. The inferred amino acid sequences from the isolates were aligned with sequences obtained from the GenBank database of closely related strains and phylotypes, using the CLUSTALW algorithm in MEGA7 [126]. Phylogenetic trees of the derived amino acid sequences were constructed using the Maximum Likelihood method based on the JTT matrix-based model [373]. The tree topology was determined by 1000 bootstrap replications. Initial trees(s) for the heuristic search were obtained automatically by applying Neighbour-Join and BioNJ algorithms [124] to a matrix of pairwise distances estimated using a JTT model [373], and then selecting the topology with superior log likelihood value.

5.2.1 Hydrogen oxidation by isolates

Initial hydrogen oxidation tests were performed using media in 18 mm (dia.) anaerobic tubes sealed with butyl rubber septa, at optimal pH and temperatures for each isolate (Table 4.1). Basal salt media for each isolate was prepared as described in section 3.2.1. Four duplicate tubes were set up for each of six

conditions (Table 5.5) to test if hydrogen oxidation enhanced growth (as determined by an increase in maximum OD_{600}) or µmoles of methane oxidised (determined by FID), compared to controls. All cultures were tested under atmospheric (22 % v/v) or low (8 % v/v) oxygen conditions. Cell cultures were also prepared to see if strains were capable of strictly hydrogenotrophic growth (H_2/CO_2) in air in the absence of methane. Tubes with low oxygen were vacuumed and flushed with nitrogen a minimum of three times before the final addition of nitrogen to match the pressure in tubes with an air headspace (approximately 7-8 kPa). Four sets of tubes had methane added by sterile injection of a gas mixture consisting of 85 % CH_4, 10 % CO_2 and 5 % O_2 (v/v) into the headspace to final concentrations as shown in Table 5.5. As necessary, hydrogen was added to a final concentration of 0.02 % (v/v).

Table 5.5 Headspace compositions for initial hydrogen oxidation tests of methanotrophs. The six conditions are labelled A-F for ease of identification in the results section.

Tube ID		Final approximate headspace concentration (% v/v)			
		CH_4	CO_2	H_2	O_2
A	-ve growth control (air)	0	0.04	0	21
B	+ve growth control	8	0.8	0	22
C	H_2 test, atmospheric O_2	8	0.8	0.02	22
D	Hydrogenotrophic growth in air	0	0.04	0.02	21
E	Low oxygen control	8	0.8	0	8
F	H_2 test, low O_2	8	0.8	0.02	8

Headspace pressure was quantified before gas sampling using a XP2i digital pressure gauge (Crystal Engineering Corporation, CA), following vigorous shaking to ensure even dispersal of low-density hydrogen and methane. Initial headspaces of each tube were analysed by Peak Performer 1 Gas Analyzers (Peak Laboratories, CA) equipped with a flame ionization detector (FID) for CH_4 or a Reducing Compound Photometer (RCP) for H_2, and a Micro-GC (Agilent, CA) equipped with a thermal conductivity detector (TCD) for O_2, CO_2, and N_2.

Headspaces were then monitored daily using the FID and RCP. OD_{600} was measured daily via a Halo Vis-10 spectrophotometer (Dynamica Scientific, Newport Pagnell, UK) using a custom adaptor (Perkin-Elmer, Waltham, MA) that permits cell growth to be directly observed (without sampling). Where appropriate, Student's *t*-tests (two-tailed) were performed to determine if there were significant (p-value < 0.05) differences in cell growth (OD_{600}), or µmoles of methane oxidised, between cultures with and without hydrogen added to the headspace.

5.2.2 Hydrogen oxidation within isolates across a temperature gradient in the presence of atmospheric oxygen concentrations

Methanotroph isolates that were positive for observed hydrogen oxidation under atmospheric oxygen were next subjected to incubation across a temperature gradient to determine if hydrogen oxidation was temperature dependent. Initial tests with atmospheric oxygen were performed in anaerobic tubes sealed with butyl rubber septa, incubated in a Temperature Gradient Incubator (Terratec Corporation, Hobart, Australia) set from the T_{min} for growth to 3 °C greater than the T_{max} of each strain tested. Paired cultures, on either side of the gradient incubator, had methane added by sterile injection (4 ml) of a custom gas mixture consisting of 85 % CH_4, 10 % CO_2 and 5 % O_2 (all v/v) into the headspace to yield final headspace concentrations of approximately 8 % CH_4, 0.8 % CO_2 and 22 % O_2. One of each paired culture next had H_2 added to a final headspace concentration of approximately 0.02 %. Headspace concentrations of cultures and uninoculated controls were analysed daily by GC equipped with RCP and FID detectors as described above. Cell growth was determined by OD_{600} measurements daily, as before.

5.2.3 Hydrogen oxidation within isolates across a temperature gradient in the presence of low oxygen concentrations

Methanotroph isolates that were positive for hydrogen oxidation under low oxygen conditions were next incubated across a temperature gradient that ranged from the optimum temperature for growth, to 10 °C greater than the maximum temperature for growth. Paired cultures were prepared in anaerobic tubes as described previously. In this instance, however, all tubes were flushed with

nitrogen for 20 minutes to ensure a final concentration of O_2 of approximately 3 % prior to the addition of custom gas mixes to yield final CH_4:CO_2:H_2 headspace concentrations of approximately 8 %, 0.8 % and 0.02 % (v/v) respectively.

5.2.4 Hydrogen oxidation within isolates and survival at elevated temperatures

To determine if hydrogen oxidation contributed to the survival of methanotrophs at elevated temperatures, cultures from temperature gradient experiments were subjected to Most Probable Number (MPN) determination [444] to estimate the viable number of cells present following incubation. Paired methanotroph 'test' cultures selected for MPN determination were first incubated for eight days at the optimum growth temperature, 2 °C < the maximum growth temperature, and both 2 °C and 10 °C > the maximum growth temperature. Next, tubes were inoculated (in triplicate) with a 1:10, 1:100, 1: 1,000 and 1: 10,000 dilution of the 'test' culture and incubated at their respective optimum growth temperature for 14 days. OD_{600} was measured at regular intervals, and an increase in OD_{600} of > 0.02 from baseline was considered growth. At the end of the incubation period, the summed number of tubes that displayed a positive growth result was used to calculate viable numbers in the original culture, using three consecutive dilutions (either 1:10 to 1:1,000 or 1:100 to 1:10,000) and MPN tables from the US Department of Agriculture [444].

Results

5.2.5 PCR for [NiFe]-hydrogenases within isolates

To determine if the methanotrophs isolated in chapter four encoded [NiFe]-hydrogenases, specific PCR primers were designed for the large subunit of various hydrogenase groups. PCR was carried out with DNA from each methanotroph using primers specific to the predicted hydrogenase groups encoded by phylogenetically similar strains. The phylogenetic relationships of all hydrogenase gene sequences amplified by PCR were confirmed by constructing a Maximum Likelihood tree from inferred amino acid sequences (Figure 5.1).

Methylocystis GDS1.7

Methylocystis strains closely related to GDS1.7 encode group 1d, group 1h/5, group 3b (*M. parvus, Methylocystis* SC2) and group 2b [NiFe]- hydrogenases (*Methylocystis* SC2) [35] and thus PCR primers were designed to probe for the presence of these hydrogenase types. Primers targeting group 3b hydrogenases (Hyd_3b_215F/Hyd_3b_1282R) amplified *Methylocystis GDS1.7* DNA to yield a PCR product of the expected ~1000 bp. This amplicon was subsequently sequenced and found to have 73 % nucleotide sequence identity to a nickel-dependent hydrogenase found in the *Methylocystis* SC2 genome (Accession number HE956757). The inferred amino acid sequence of the SC2 hydrogenase product was checked for consensus motifs to confirm the identity of a group 3b (NADP-coupled bidirectional) hydrogenase. Unfortunately, none of the other primer sets targeting *Methylocystis* hydrogenases (Table 5.4) were successful in amplifying *Methylocystis* GDS1.7 DNA, despite each primer set yielding a product of the correct size with DNA from *Methylocystis* SC2 with 99 % sequence identity to the hydrogenases from this species.

Methylococcus GDS2.4

Methylococcus capsulatus encodes [NiFe]-hydrogenases from groups 1d and 3d [35]. Primers targeting the group 1d hydrogenase (Gamma_1d_hyd_208F/ Gamma_hyd_1d_1562R) amplified *Methylococcus* GDS2.4 DNA to yield a PCR product of approximately 1300 bp. The sequenced amplicon fragment was found to have 94 % nucleotide sequence identity to the *hup*-type hydrogenase (group 1d) from *M. capsulatus* (AY032955). Primers targeting the group 3d hydrogenase

(Coccus_hyd_3d_6F/Coccus_hyd_3d_1266R) amplified *Methylococcus* GDS2.4 DNA with a PCR product of the expected size (1300 bp). The PCR product was sequenced and found to share 93 % nucleotide sequence identity with the β-subunit of a NAD-reducing hydrogenase (type 3d) from the *M. capsulatus* genome (AE017282). The inferred amino acid of the PCR product was checked for consensus motifs to confirm the identity of the type 3d hydrogenase (Appendix 7.8).

Methylacidiphilum NGM89.1

Methylacidiphilum species encode hydrogenases from groups 1d and 3b, and 1h/5 (*M. fumariolicum* and *M. kamchatkensis* only) [35]. Primers for the 3b hydrogenase large subunit gene (Verr_hyd_3b_368F/Verr_hyd_3b_1162R), amplified DNA extracted from *Methylacidiphilum* NGM89.1 cultures, yielding PCR products of approximately 800 bp. These products had 97 % nucleotide sequence identity to the large subunit of the NADP-coupled cytosolic bidirectional (3b) hydrogenase of *Methylacidiphilum* sp. RTK17.1 (KU509473). No PCR products were detected using primers designed to target either group 1d or group 1h/5 hydrogenases.

Methylacidiphilum WHV12.1

Primers targeting the group 1d and 3b hydrogenases (Verr_hyd_1d_773F/ Verr_hyd_1d_1669R; Verr_hyd_3b_368F/ Verr_hyd_3b_1162R) amplified DNA extracted from *Methylacidiphilum* WHV12.1 cultures; yielding PCR products of the expected sizes (~ 900 and 800 bp, respectively). The group 1d PCR product displayed 97 % nucleotide sequence identity to the large subunit of the oxygen-tolerant membrane-bound (group 1d) hydrogenase of *Methylacidiphilum* RTK17.1 (KU509386), while the group 3b PCR product was 99 % identical to the large subunit of the NADP-coupled cytosolic bidirectional (3b) hydrogenase of *Methylacidiphilum* sp. RTK17.1 (KU509473).

Methylocaldum WAP11.3

Methylocaldum szegediense, which is closely related to *Methylocaldum* WAP11.3, encodes hydrogenases from the 1d and 3b groups [35]. Multiple primer sets, designed using the group 1d hydrogenase gene sequences from *M.*

szegediense and *M. capsulatus* (Gamma_hyd_1d_208F or 316F or 511F with 812R or 1562R), amplified *Methylococcus* GDS2.4 DNA but were unable to amplify *Methylocaldum* WAP11.3 DNA. Neither primers for the group 3b hydrogenase, designed using the gene sequence from *M. szegediense* as a template (Caldum_hyd_3b381F/670R), or using the consensus sequence derived from the *M. szegediense* sequence aligned to the group 3b sequences of four *Methylocystis* species (Hyd_3b_215F/ 1282R), were successful in amplifying DNA from *Methylocaldum* WAP11.3.

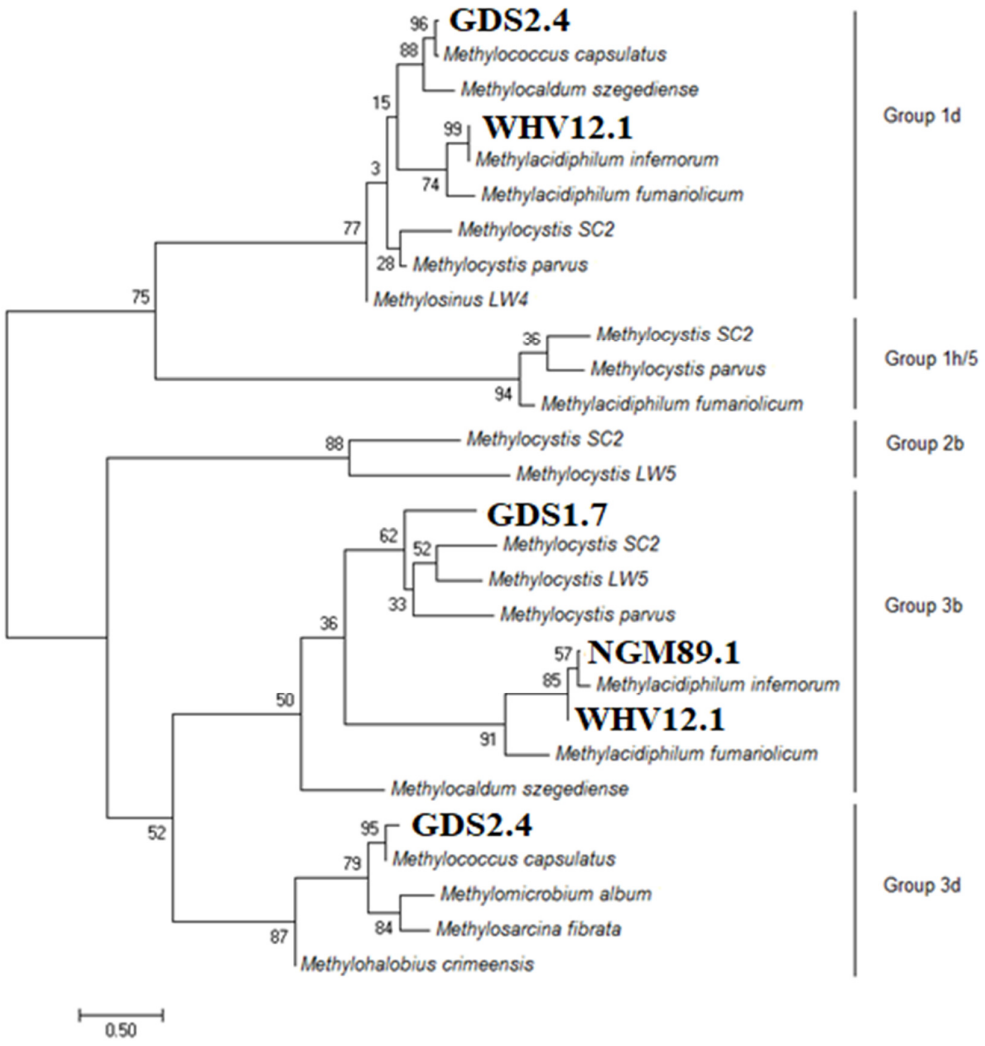

Figure 5.1 Phylogenetic relationships between [Ni-Fe]- hydrogenases of the isolates and known methanotroph species. Sequences were derived from PCR amplification (isolates and described species) or whole genome sequencing (described species only). Inferred amino acid sequences were used to construct the phylogenetic tree. The percentage of trees in which the associated taxa clustered together in the bootstrap test (1000 replicates) are shown next to the branches. Evolutionary analyses were conducted in MEGA7 [126]. The scale bar represents 0.5 nucleotide substitutions per site.

Initial hydrogen oxidation tests of isolates

Following the identification and characterisation of hydrogenase types within the methanotroph isolates, the effect of hydrogen on cell growth and methane gas oxidation was investigated. As anticipated from the expected presence of a group 1d respiratory [NiFe]-hydrogenase, which exhibit oxygen-dependent transcriptional regulation [35], in *Methylocystis* GDS1.7 cultures, hydrogen oxidation significantly increased (two-tailed Student's *t*-test, $p = 0.032$) in response to reduced O_2 availability in the headspace (Figure 5.2B). Low levels of hydrogen oxidation (of atmospheric hydrogen) occurred with 22 % oxygen (Figure 5.2B, treatments A and B), and this increased under low oxygen conditions (Figure 5.2B, treatments E). When compared to cultures with no hydrogen added into the headspace, however, *Methylocystis* GDS1.7 cultures with both methane and hydrogen added did not display a significant difference (Student's *t*-test, $p > 0.05$) in either quantity of methane oxidised (Figure 5.2A) or observed maximal growth (OD_{600}, Figure 5.2C).

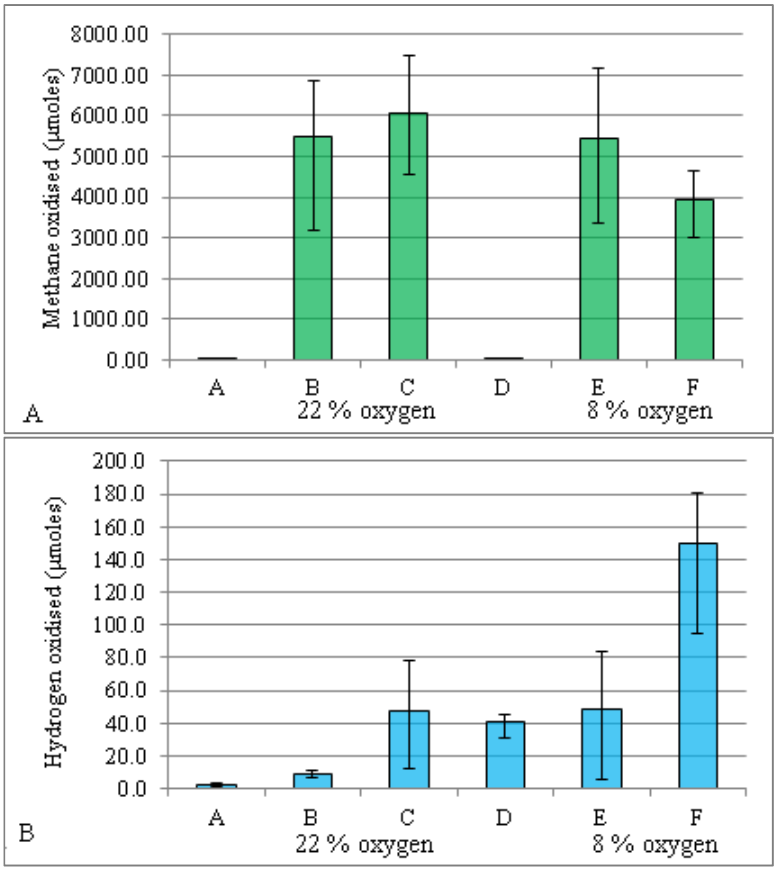

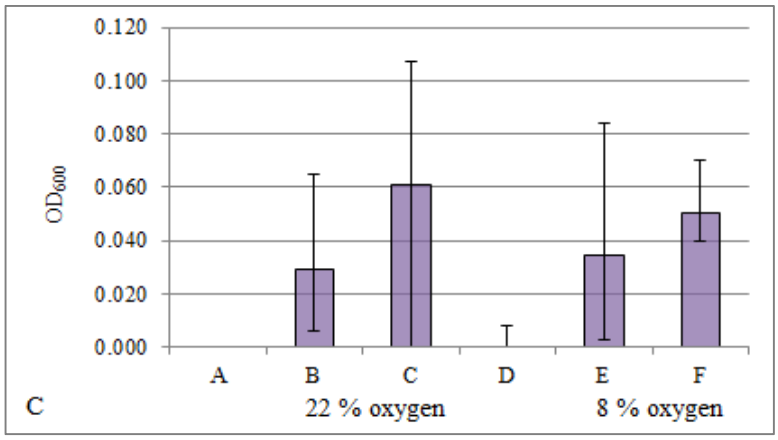

Figure 5.2 Effect of hydrogen on growth and consumption of methane gas in *Methylocystis* GDS1.7 cultures. The average µmoles of methane gas (panel A) and hydrogen gas (panel B) oxidised, and average maximum increase in OD_{600} (panel C), following 72 hours incubation at 37 °C. **A**, No added methane or hydrogen (22 % O_2); **B**, 8 % methane, no added hydrogen (22 % O_2); **C**, 8 % methane + 0.02 % hydrogen (22 % O_2); **D**, No added methane, 0.02 % hydrogen (22 % O_2); **E**, 8 % methane, no added hydrogen (8 % O_2); **F**, 8 % methane + 0.02 % hydrogen (8 % O_2) (all v/v). Error bars represent maximum and minimum values measured in four duplicate cultures.

In contrast to *Methylocystis* GDS1.7, cultures of *Methylococcus* GDS2.4 with both methane and hydrogen added into the headspace displayed a greater maximum growth (via OD_{600}) than cultures with methane alone (Figure 5.3); however, this result was only significant in low oxygen conditions (low O_2 students *t*-test, $p = 0.031$, compared to atmospheric O_2 students *t*-test, $p=0.317$). There was no significant difference in the quantity of methane oxidised when hydrogen was added to the headspace, either under atmospheric or low oxygen conditions.

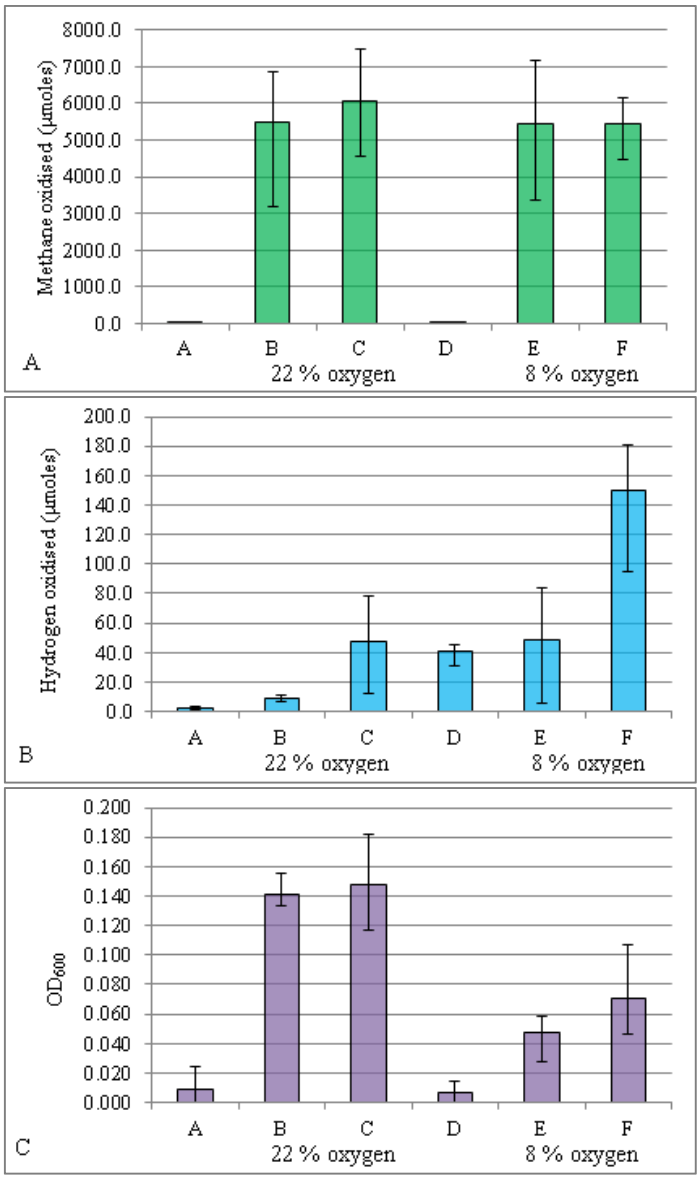

Figure 5.3 Effect of hydrogen on growth of *Methylococcus* GDS2.4 cultures.
The average µmoles of methane gas (panel A) and hydrogen gas (panel B) oxidised, and average maximum increase in OD_{600} (panel C) following 72 hours incubation at 37 °C. **A**, No added methane or hydrogen (22 % O_2); **B**, 8 % methane, no added hydrogen (22 % O_2); **C**, 8 % methane + 0.02 % hydrogen (22 % O_2); **D**, No added methane, 0.02 % hydrogen (22 % O_2); **E**, 8 % methane, no added hydrogen (8 % O_2); **F**, 8 % methane + 0.02 % hydrogen (8 % O_2) (all v/v). Error bars represent maximum and minimum values measured in four duplicate cultures.

Methylacidiphilum NGM89.1 cultures oxidised hydrogen under both atmospheric and low (8 %, v/v) oxygen conditions (Figure 5.4B). With 22 % (v/v) oxygen in the headspace, cultures showed both a slight increase in the total µmoles of

methane oxidised and the maximum OD_{600} value observed (Figure 5.4A and C). In contrast, under low oxygen conditions the maximum optical density was slightly lower in cultures with hydrogen added to the headspace, although more µmoles of methane were oxidised than in cultures without hydrogen.

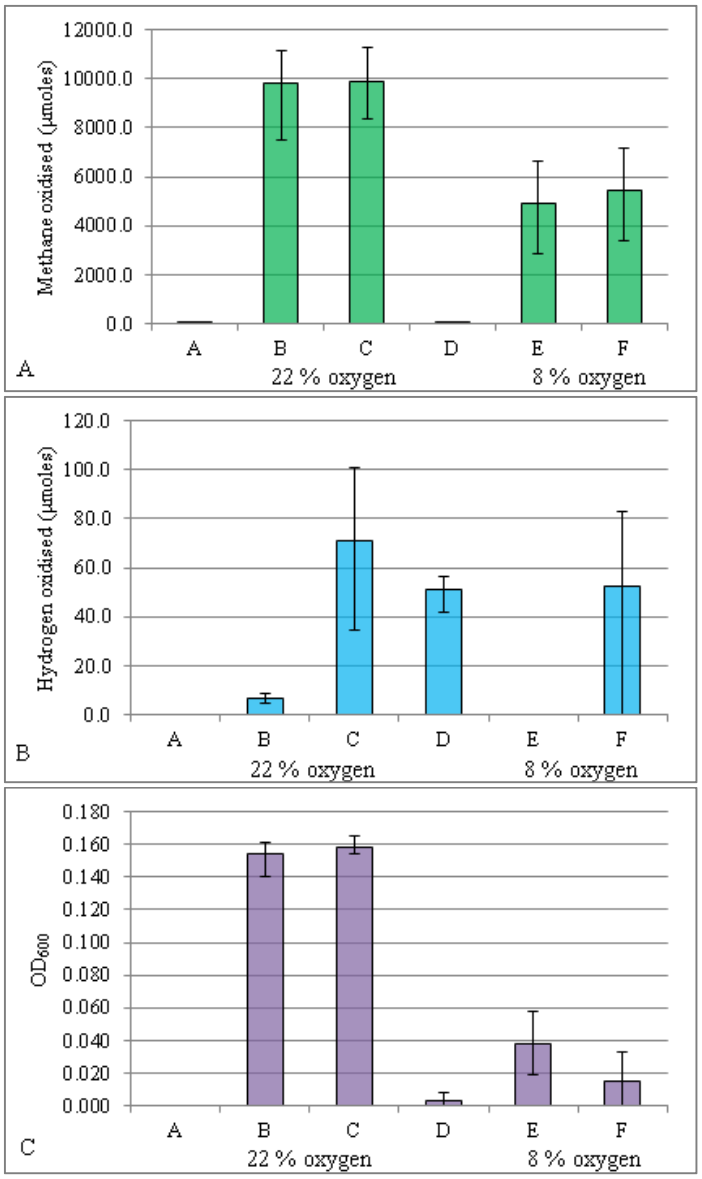

Figure 5.4 Effect of hydrogen on growth and consumption of methane gas in *Methylacidiphilum* NGM89.1 cultures. The average µmoles of methane (panel A) and hydrogen (panel B) oxidised, and average maximum increase in OD_{600} (panel C), following 96 hours incubation at 60 °C from four replicates. **A**, No added methane or hydrogen (22 % O_2); **B**, 8 % methane, no added hydrogen (22 % O_2); **C**, 8 % methane + 0.02 % hydrogen (22 % O_2); **D**, No added methane, 0.02 % hydrogen (22 % O_2); **E**, 8 % methane, no added hydrogen (8 % O_2); **F**, 8 % methane + 0.02 % hydrogen (8 % O_2) (all v/v). Error bars represent maximum and minimum values measured.

Cultures of *Methylacidiphilum* WHV12.1 oxidised very little hydrogen under either atmospheric or low oxygen conditions. Cell growth (OD_{600}) was slightly, but not significantly, reduced in cultures with hydrogen added to the headspace (Figure 5.5C), and methane oxidation slightly reduced only under 8 % (v/v) oxygen conditions (Figure 5.5A).

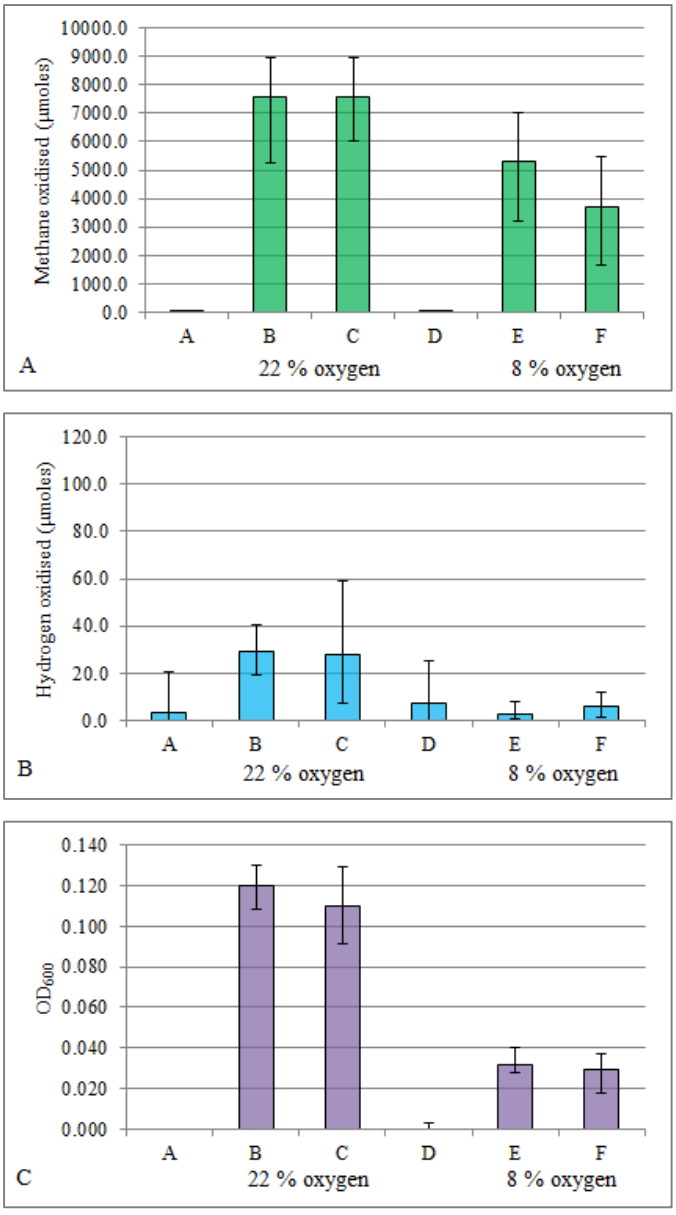

(facing page) **Figure 5.5 Effect of hydrogen on growth and consumption of methane gas in *Methylacidiphilum* WHV12.1 cultures.** The average µmoles of methane gas (panel A) and hydrogen gas (panel B) oxidised, and average maximum increase in OD_{600} (panel C), following 72 hours incubation at 50 °C from four replicate cultures. A, No added methane or hydrogen (22 % O_2); B, 8 % methane, no added hydrogen (22 % O_2); C, 8 % methane + 0.02 % hydrogen (22 % O_2); D, No added methane, 0.02 % hydrogen (22 % O_2); E, 8 % methane, no added hydrogen (8 % O_2); F, 8 % methane + 0.02 % hydrogen (8 % O_2) (all v/v). Error bars represent maximum and minimum values measured.

Consistent with the absence of detectable PCR amplicons targeting relevant hydrogenase types, cultures of *Methylocaldum* WAP11.3 oxidised very low volumes of hydrogen in the presence of methane under conditions of either atmospheric (22 % v/v) or reduced (8 % v/v) oxygen availability. In both oxic and low oxygen (in the absence of hydrogen) cultures, the production of up to 60 µmoles of hydrogen was observed following 96 hours of incubation. Neither the quantity of methane consumed nor cell growth (OD_{600}) were affected by the presence of hydrogen (Figure 5.6).

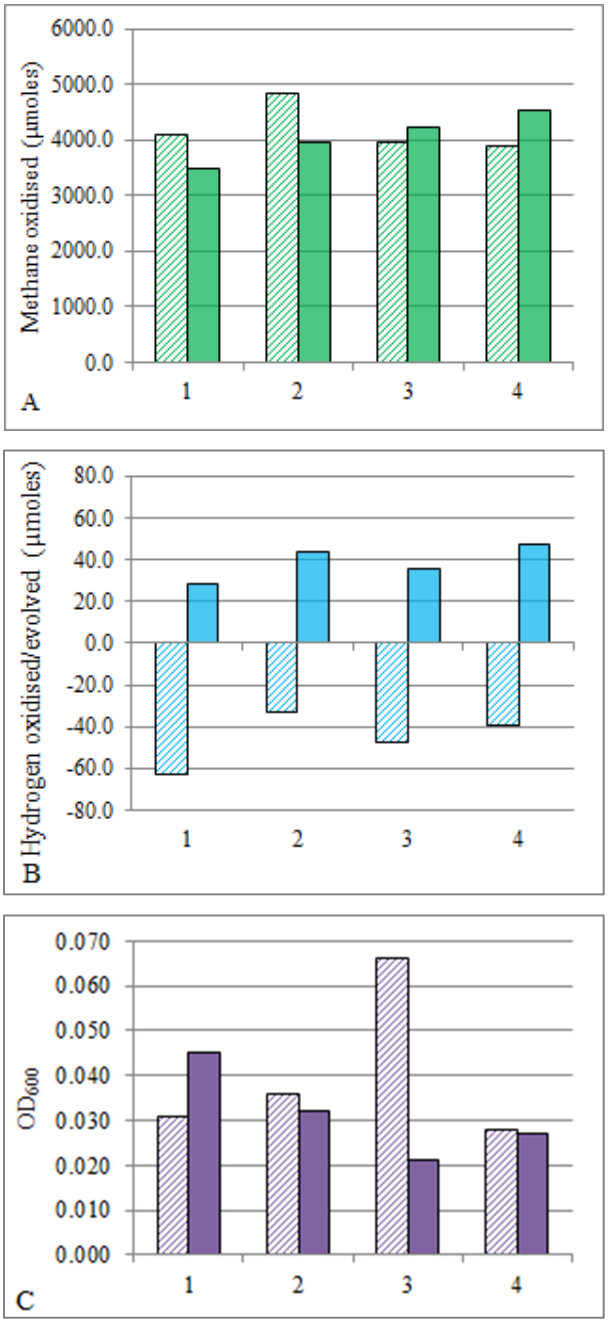

(facing page) **Figure 5.6 Effect of hydrogen on growth and consumption of methane gas in *Methylocaldum* WAP11.3 cultures.** The µmoles of methane (panel A), or hydrogen (panel B) oxidised/evolved, and maximum OD_{600} observed (panel C), following 96 hours incubation at 46 °C. Each column (1-4) represents a single measurement of a culture following 96 hours incubation with 8 % O_2 and 8 % CH_4 in the headspace (all v/v). Solid bars, cultures with 0.02 % (v/v) hydrogen in the headspace; hatched bars, cultures with no hydrogen in headspace.

In summary, hydrogen oxidation was observed in three methanotrophs; *Methylocystis* GDS1.7, *Methylococcus* GDS2.4 and *Methylacidiphilum* NGM89.1 oxidised hydrogen in addition to methane under oxic conditions (Table 5.6), and *Methylococcus* GDS2.4 and *Methylacidiphilum* NGM89.1 additionally oxidised hydrogen under low O_2 conditions (8 % v/v). Hydrogenotrophic growth (increase in OD_{600}) was not observed in any of the five strains under oxic conditions, although this may be due to the experimental conditions chosen, as both *M. fumariolicum* and *Methylacidiphilum* sp. RTK17.1 display hydrogenotrophic growth only under hypoxic conditions (< 1.5 % (v/v) oxygen [34, 35]).

Table 5.6 Summary of effect of hydrogen on all methanotroph cultures. ↑, increase; ↓, decrease. An asterisk (*) indicates that an effect was significant (Student's *t*-test, $p < 0.05$).

		GDS 1.7	**GDS 2.4**	**NGM 89.1**	**WAP 11.3**	**WHV 12.1**
	H_2 oxidation (atmospheric O_2)	Y	Y	Y	N	N
	H_2 oxidation (low O_2)	N	Y	Y	N	N
	Hydrogenotrophic growth	N	N	N	N	N
High O_2	Effect on OD_{600}	none	↑	↑	none	↓
	Effect on CH_4 oxidation	↑	none	↑	none	none
Low O_2	Effect on OD_{600}	none	↑*	↓	↓	↓
	Effect on CH_4 oxidation	↓	↑	↑	none	↓

5.2.6 Hydrogen oxidation within isolates across a temperature gradient in the presence of atmospheric oxygen concentrations

Soil temperatures in geothermal areas increase with depth [14, 35, 422], and the ability of methanotrophs to respond to these changes or to persist at elevated temperatures is not known, other than through the production of spores and cysts [214]. To determine if hydrogen oxidation could influence survival of methanotrophs at elevated temperatures (> T_{max}), methanotroph strains that had demonstrated an ability to oxidise hydrogen at optimum growth temperatures (*Methylocystis* GDS1.7, *Methylococcus* GDS2.4 and *Methylacidiphilum* NGM89.1), were next incubated with or without hydrogen across a temperature gradient that spanned their known growth range to 3 °C greater than T_{max}. Initial experiments were performed with oxygen at a concentration of 22 % (v/v), which is comparable to atmospheric levels.

The maximum µmoles of methane oxidised in *Methylocystis* GDS1.7 was observed in cultures incubated at close to the optimum known growth temperature (36 °C) of this strain. Observations of methane oxidation declined sharply at temperatures greater than T_{max} (43 °C) (Figure 5.7A). The addition of hydrogen to the headspace did not significantly affect the observed quantity of methane oxidised. Cultures showed a low quantity of hydrogen oxidised, which reached a maximum at 41 °C, but this then declined as the temperature increased beyond the T_{max} growth temperature (Figure 5.7B).

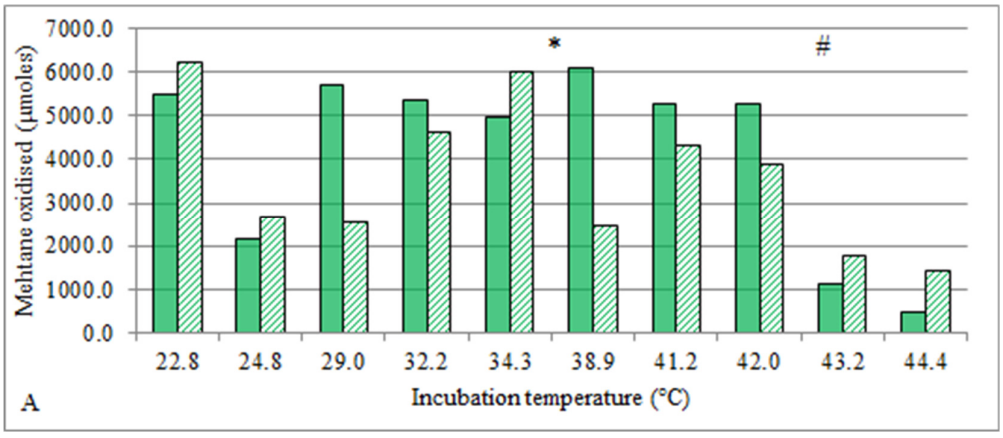

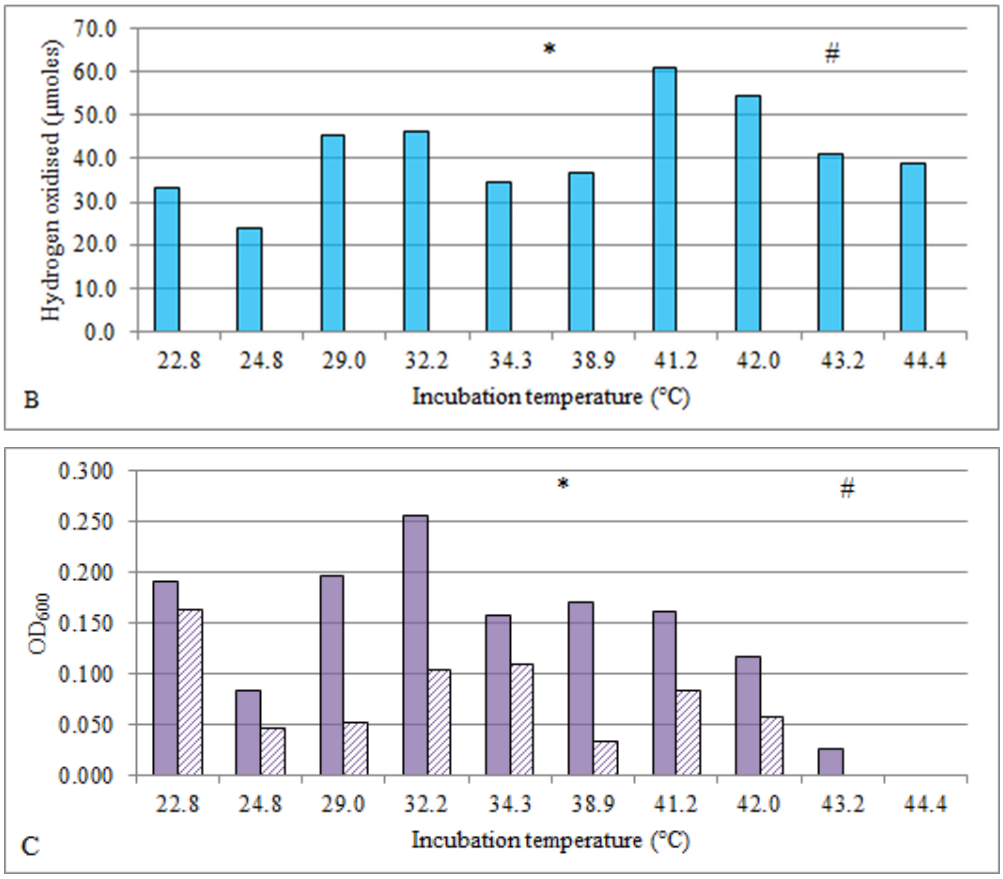

Figure 5.7 Gas oxidation in cultures of *Methylocystis* GDS1.7 incubated across a gradient of temperatures with atmospheric oxygen concentrations. Panel A, methane oxidation; panel B, hydrogen oxidation; panel C, OD_{600}. Initial headspace concentrations of methane and hydrogen were 8 % and 0.02 % (v/v), respectively. Each bar represents a single culture. Temperatures indicate the average incubation temperature of the paired tubes. Cultures were incubated for four days. Solid bars, cultures with both methane and hydrogen in the headspace; hatched bars, cultures with no hydrogen in headspace. The optimum growth temperature (*) and maximum growth temperature (#) for this strain are shown.

Profiles of both methane oxidation and hydrogen oxidation in cultures of *Methylococcus* GDS2.4 were relatively constant between 30 and 45 °C (Figure 5.8). The addition of hydrogen to the headspace did not affect the quantity of methane oxidised nor increase cell growth (O_{D600}) in this experiment. As with *Methylocystis* GDS1.7, hydrogen continued to be oxidised by the culture beyond the strain's growth T_{max}.

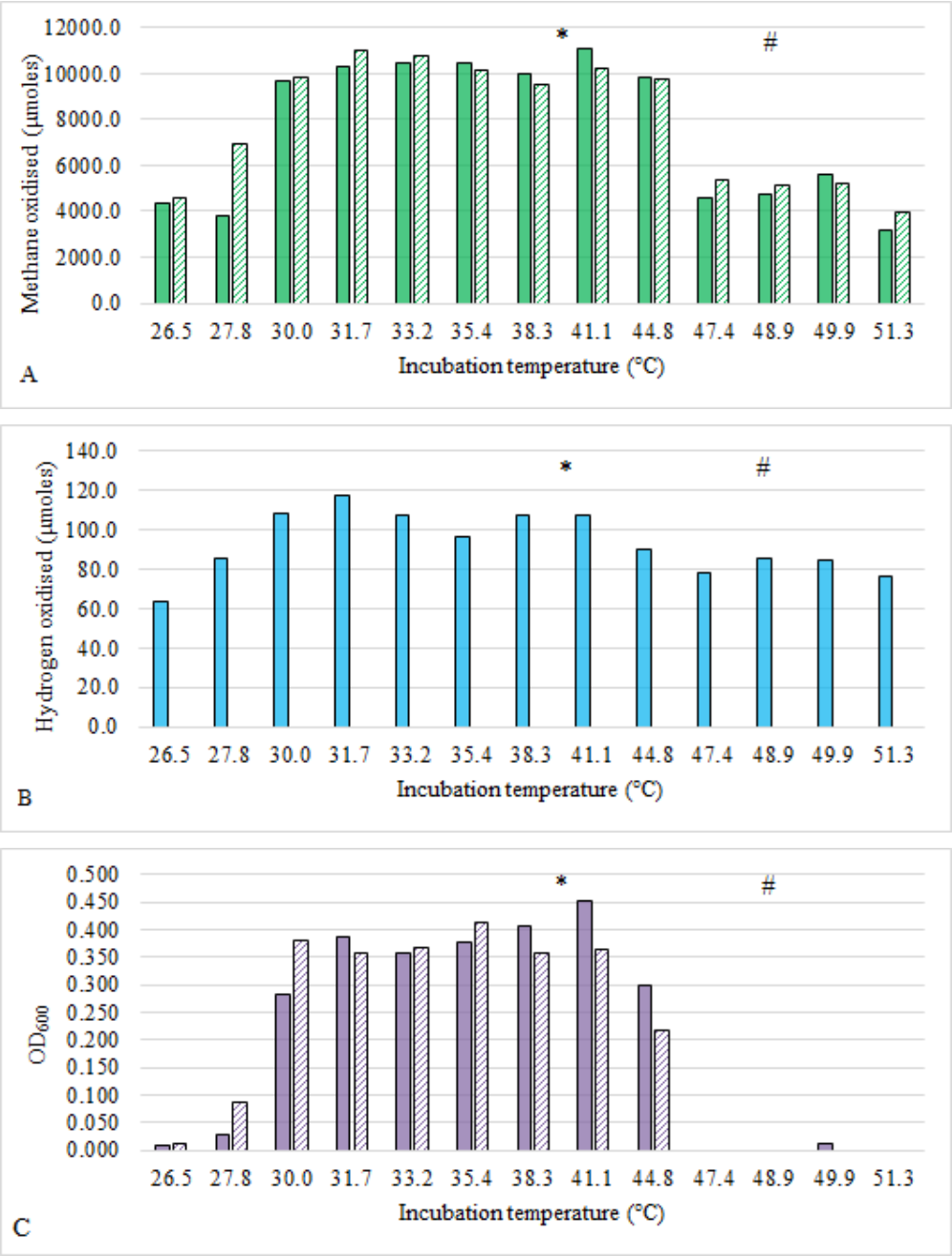

Figure 5.8 Gas oxidation in cultures of *Methylococcus* GDS2.4 incubated across a gradient of temperatures with atmospheric oxygen concentrations. Panel A, methane oxidation; panel B, hydrogen oxidation; panel C, OD_{600}. Initial headspace concentrations of methane and hydrogen were 8 % and 0.02 % (v/v), respectively. Each bar represents an individual tube culture. Temperatures indicate the average incubation temperature of the paired tubes. Cultures were incubated for six days. Solid bars, cultures with both methane and hydrogen in the headspace; hatched bars, cultures with no hydrogen in headspace. The optimum growth temperature (*) and maximum growth temperature (#) for this strain are shown.

Cultures of *Methylacidiphilum* NGM89.1 showed the maximum μmoles of methane oxidised were in tubes at the optimum growth temperatures of 53–60 °C, and the quantity of methane oxidised then declined with increasing temperature (Figure 5.9A). The addition of hydrogen significantly increased the amount of methane oxidised (Student's *t*-test, $p = 0.005$). There was a steady increase in the amount of hydrogen oxidation from 300 to 834 μmoles as the temperature increased, up to the maximum temperature tested at 69 °C (Figure 5.9B).

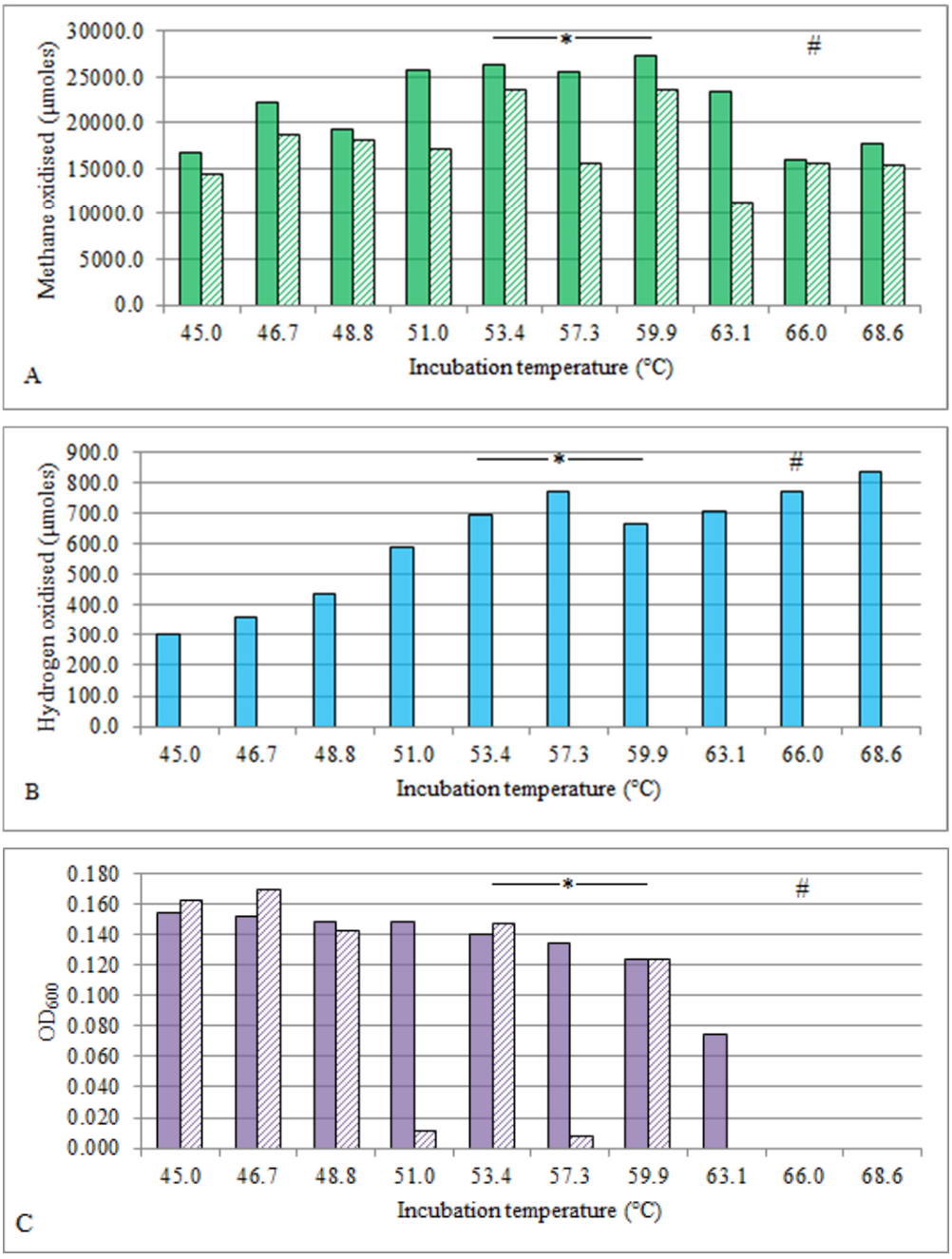

Figure 5.9 Gas oxidation in cultures of *Methylacidiphilum* NGM89.1 incubated across a gradient of temperatures with atmospheric oxygen concentrations. Panel A, methane oxidation; panel B, hydrogen oxidation; panel C, OD_{600}. Initial headspace concentrations of methane and hydrogen were 8 % and 0.02 % (v/v), respectively. Each bar represents an individual tube culture. Temperatures indicate the average incubation temperature of the paired tubes. Cultures were incubated for six days. Solid bars, cultures with both methane and hydrogen in the headspace; hatched bars, cultures with no hydrogen. The optimum growth temperature (*) and maximum growth temperature (#) for this strain are shown.

5.2.7 Hydrogen oxidation by isolates across a temperature gradient in the presence of low oxygen concentrations

The two methanotroph strains that displayed hydrogen oxidation under oxygen-limiting conditions, *Methylococcu*s GDS2.4 and *Methylacidiphilum* NGM89.1, were additionally tested over a temperature gradient, as described previously, but in the presence of low oxygen concentrations (approximately 3 % (v/v) O_2) in the headspace. Methane oxidation, hydrogen oxidation and growth were only detected in cultures of *Methylococcus* GDS2.4 at the four lowest temperatures tested (39.7 – 43.8 °C) (Figure 5.10A and B), despite the T_{max} for this strain previously shown to be 49 °C under atmospheric oxygen conditions. At temperatures ≥ 47.5 °C, methane and hydrogen oxidation rates were not significantly different to gas loss in control tubes via sampling (Student's *t*-test, $p = 0.26$).

Methylacidiphilum strain NGM89.1 cultures showed an increase in the rate of hydrogen oxidation as the temperature increased from 58.7 °C (approximately T_{opt}) to 76.3 °C (> T_{max}) (Figure 5.11A). While the observed rates of hydrogen oxidation were significantly different between tubes incubated below and above the T_{max} (Student's *t*-test, p=0.035), rates of observed methane oxidation remained almost constant (Figure 5.11A). Growth was observed in cultures incubated at temperatures between 58.7 °C and 63.6 °C, but the maximum OD_{600} reached was much less than in previous experiments in an atmospheric oxygen headspace (Figure 5.11B).

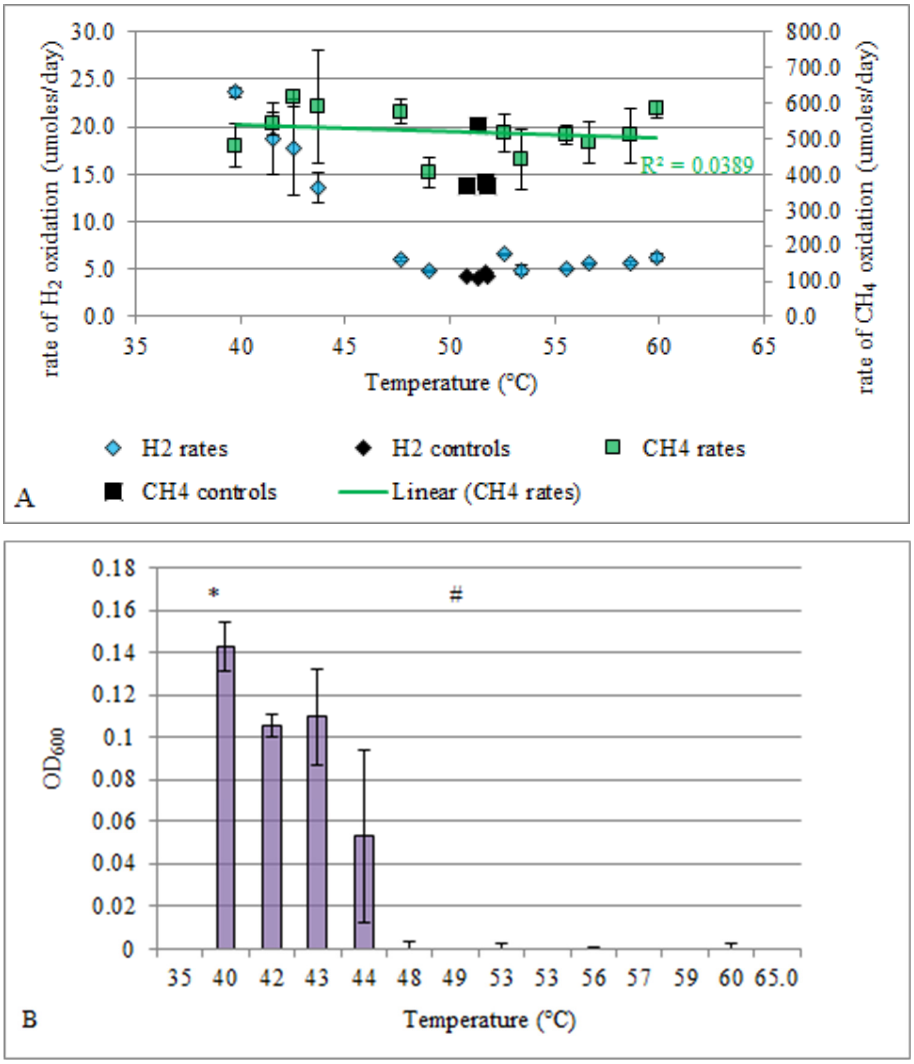

Figure 5.10 Gas oxidation in cultures of *Methylococcus* GDS2.4 incubated across a temperature gradient with low oxygen concentrations for ten days. Panel A, gas oxidation: Blue diamonds, rates of hydrogen oxidation; black diamonds, rates of hydrogen loss from controls; green squares, rates of methane oxidation; black squares, rates of methane loss from controls. Data points represent the average of biological duplicates, with error bars indicating minimum and maximum measured values. Temperatures indicate the average incubation temperature of the paired tubes. Trendlines with linear regression are shown for hydrogen (blue line) and methane (green line). Panel B, growth of cultures: Bars indicate averages of the maximum OD_{600} reached in paired cultures. Error bars represent maximum and minimum values measured. The optimum (*) and maximum (#) growth temperature for this strain are shown.

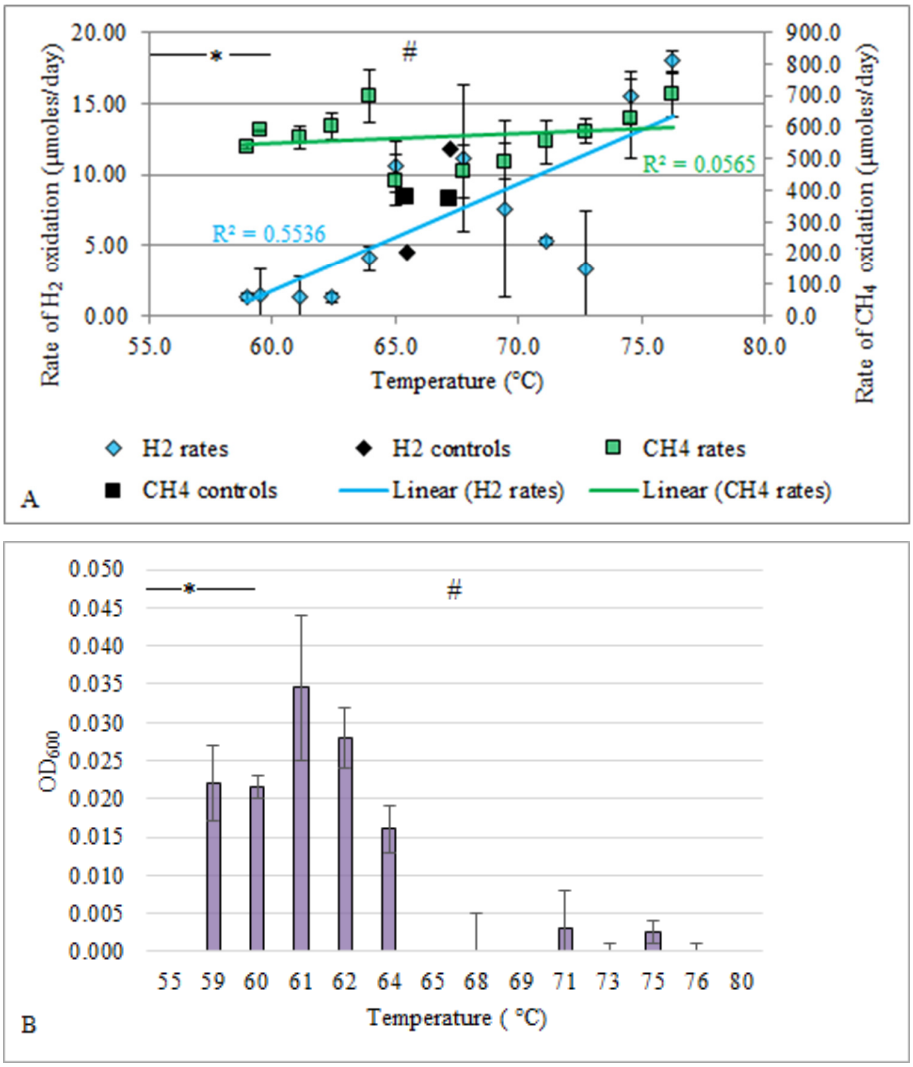

Figure 5.11 Gas oxidation in cultures of *Methylacidiphilum* NGM89.1 incubated across a temperature gradient with low oxygen concentrations over seven days. Panel A, gas oxidation: Blue diamonds, rates of hydrogen oxidation; black diamonds, rates of hydrogen loss from controls; green squares, rates of methane oxidation; black squares, rates of methane loss from controls. Data points represent the average of biological duplicates, with error bars indicating minimum and maximum measured values. Temperatures indicate the average incubation temperature of the paired tubes. Trendlines with linear regression are shown for hydrogen (blue line) and methane (green line). Panel B, growth of cultures: Bars indicate averages of the maximum OD_{600} reached in paired cultures. Error bars represent maximum and minimum values measured. The optimum (*) and maximum (#) growth temperature for this strain are shown.

5.2.8 Estimates of viable cells using Most Probable Number (MPN)

Finally, to determine if the observed increase in hydrogen oxidation rate at temperatures > T_{max} increased survival of *Methylacidiphilum* NGM89.1 cells, eight duplicates from the gradient incubator experiment were subjected to the Most Probable Number procedure to estimate numbers of viable cells following incubation. Tubes selected were duplicates that had been incubated at ~ optimum growth temperature (59 °C), ~2 °C below the maximum growth temperature (64 °C), ~2 °C above the maximum growth temperature (68 °C), and ~10 °C above the maximum growth temperature (76 °C). Duplicate tubes from opposite sides of the gradient incubator had approximately, but not exactly, equal incubation temperatures. These were serially diluted to 1:10,000 in triplicate and incubated at ~optimum temperature (60 °C) for two weeks.

Under low oxygen conditions, *Methylacidiphilum* NGM89.1 cultures did not display a high maximal OD_{600} following seven days incubation (maximum 0.044 increase above baseline), while negative control tubes decreased slightly below baseline levels. The threshold for growth of MPN cultures was therefore determined to be an increase in OD_{600} of more than 0.02 above baseline. MPN tubes from cultures grown at close to the optimum temperature (58.7 and 59.2 °C) showed viable cells were present in the 1:10, 1:100 and 1: 1,000 dilutions. Unfortunately, the 1: 10,000 dilutions of the sample from 58.7 °C were lost, but none of the three 1: 10,000 dilutions of the duplicate tube incubated at 59.2 °C showed viable cells, indicating that there were between 11 and 24 viable cells/ml in these tubes (Table 5.7). Cultures originally incubated at approximately 2 °C below the T_{max} (63.6 and 64.3 °C) were estimated to have between 7.5 and 9.3 viable cells per ml.

For cultures originally incubated above the T_{max} for *Methylacidiphilum* NGM89.1, MPN tubes down to the 1:10,000 dilution from the 67.6 °C culture grew, with an estimated 21 viable cells/ml in the original tube, but only one of the 1:10 dilution tubes from the culture incubated at 68.0 °C showed viability, despite this original culture having much higher rates of both methane and hydrogen oxidation than the culture on the other side of the gradient incubator that was at a slightly lower temperature (Table 5.7). None of the tubes originally incubated at 10 °C greater

than the maximum growth temperature displayed viable cells via MPN analysis. This finding contradicts the observation that up to 4637 µmoles of methane and 116 µmoles of hydrogen were oxidised in these cultures during the seven-day incubation period in the temperature gradient incubator. This could indicate that the enzymes responsible are capable of gas oxidation in a cell-free state i.e. when no longer attached to a living cell [445, 446], or that the MPN experiment, as performed, is not an adequate methodology to evaluate the viability of methanotrophic bacteria.

Table 5.7 Estimates of numbers of viable *Methylacidiphilum* NGM89.1 cells after gradient temperature incubation with low oxygen atmosphere for seven days. Initial headspace concentrations of methane and hydrogen were 8 % and 0.1 % (v/v), respectively. OD_{600} was measured after two weeks incubation at optimum temperature (60 °C). Green shading indicates the three consecutive dilutions used to estimate numbers of cells using the MPN methodology. ND, not determined.

	Dilution				
	1:10	1:100	1:1,000	1:10,000	
Incubation temperature (°C)	Number of tubes positive for growth				Most probable number (cells/ml)
~ optimum					
58.7	3	3	2	ND	11
59.2	3	3	3	0	24
~ 2 °C below T_{max}					
63.6	3	3	2	0	9.3
64.3	3	3	1	1	7.5
~ 2 °C above T_{max}					
67.6	3	3	2	2	21
68.0	1	0	0	0	0.036
~ 10 °C above T_{max}					
76.0	0	0	0	0	<0.03
76.5	0	0	0	0	<0.03

5.3 Discussion

In geothermally heated soils, where gas flux (including methane, carbon dioxide, and hydrogen) may be correlated to temperature and soil depth [14, 35, 422] and inversely related to oxygen availability, it seems plausible methanotrophs are likely to have developed strategies to survive changing conditions caused by soil disturbances (e.g. hypoxia) or increased geothermal activity (e.g. temperature). The purpose of this study was therefore to determine whether the methanotrophs from chapter four encoded [NiFe]-hydrogenases and, if so, to determine whether hydrogen oxidation was constitutive or oxygen dependent, and whether hydrogen metabolism influenced maximum OD_{600} or contributed to survival at elevated temperatures (> T_{max}).

Hydrogenase-specific PCR on the isolates indicated that several of the strains encoded genes for hydrogenase enzymes similar to those identified within related genera. *Methylocystis* GDS1.7 encodes a group 3b (NADP-linked, bidirectional) [Ni-Fe]-hydrogenase but does not appear to encode the group 1d, 1h/5 or 2b [NiFe]-hydrogenases characteristic of other *Methylocystis* strains [35]. The absence of amplification with hydrogenase-specific PCR primers indicates there is either significant sequence divergence between the hydrogenases in *Methylocystis* GDS1.7 and its closest relatives, preventing primer annealing, or that the strain has lost the ability to derive respiratory energy from molecular hydrogen, possibly due to a lack of selection pressure to retain this capability in its natural environment. In contrast, *Methylococcus* GDS2.4 encodes both a group 1d (membrane-bound H_2-uptake) hydrogenase and a group 3d (cytosolic bidirectional) hydrogenase.

Methylacidiphilum NGM89.1 was found to encode a NADP-dependent cytosolic group 3b [NiFe]-hydrogenase but does not appear to encode either the membrane-bound group 1d or 1h/5 [NiFe]-uptake hydrogenases, as predicted from related strains [35]. The lack of amplification with the specific primers may again indicate sequence divergence. PCR targeting hydrogenase genes using a range of different primers did not amplify DNA from *Methylocaldum* WAP11.3, while *Methylacidiphilum* WHV12.1 encoded group 1d and group 3b [NiFe]-hydrogenases, as predicted from related strains [35].

Hydrogen oxidation was observed in three of the five methanotrophs isolated in chapter four. *Methylocystis* GDS1.7, *Methylococcus* GDS2.4 and *Methylacidiphilum* NGM89.1 oxidised hydrogen in the presence of methane under oxic conditions. Although strictly hydrogenotrophic growth (increase in OD_{600}) was not observed in any of the strains, in comparison to cultures grown with methane alone, supplementation with hydrogen increased either the maximum observed OD_{600} (*Methylococcus* GDS2.4, *Methylacidiphilum* NGM89.1), or the total µmoles of methane oxidised (GDS1.7, NGM89.1), over the course of the experiment. Hydrogen can provide reductant to pMMO and sMMO activity in *M. capsulatus* [229], and improve growth of *Methylacidiphilum* sp. RTK17.1 [35].

In simulated oxic/anoxic boundary conditions (8 % O_2, v/v), hydrogen oxidation was observed in two strains, *Methylococcus* GDS2.4 and *Methylacidiphilum* NGM89.1. Hydrogen metabolism was found to significantly increase the maximum optical density of *Methylococcus* GDS2.4 cultures at 37 °C, but was not found to influence growth (OD_{600}) or µmoles of methane oxidised in *Methylacidiphilum* NGM89.1 cultures at 60 °C. As aerobic methanotrophy requires oxygen both as a substrate for methane oxidation and as a terminal electron acceptor for respiration [451], the oxidation of hydrogen likely serves as a more readily metabolizable source of energy during periods of hypoxia. Despite hydrogenotrophic growth being reported in the Calvin-Benson-Bassham pathway-utilising verrucomicrobial methanotrophs (*Methylacidiphilum fumariolicum* and *Methylacidiphilum* sp. RTK17.1) under microaerophilic (< 1.5 % O_2, v/v) growth conditions [34, 35], no hydrogen-dependent growth was observed in *Methylacidiphilum* NGM89.1. Further, the group 3b (NADP-linked, bidirectional) [Ni-Fe]-hydrogenase encoded by *Methylocystis* GDS1.7 is oxygen-tolerant [452, 453] but may also be induced by low oxygen conditions [223], or active in anaerobic conditions [453]. It is interesting, therefore, that no hydrogen oxidation was observed by this strain under low oxygen conditions.

Methylococcus GDS2.4 encodes both group 1d and 3d [NiFe]-hydrogenases, and either of the hydrogenases could have been responsible for the oxidation of hydrogen observed with atmospheric and low oxygen in the headspace. These enzymes are oxygen-tolerant [226, 454], and the membrane-bound hydrogenase

of *Methylococcus capsulatus* was constitutively expressed with between 0 and 15 % (v/v) oxygen in the headspace [229]. Under low oxygen conditions, the 3d [NiFe]-hydrogenase may be used to support CO_2 fixation through the Calvin-Benson-Bassham cycle [95] by supplying reducing equivalents from hydrogen [454].

Methylocaldum WAP11.3 was not observed to oxidise hydrogen, but hydrogen production of up to 60 µmoles was observed under low oxygen (8 %, v/v) conditions. Despite an absence of detectable hydrogenase genes (via PCR), the genome of *Methylocaldum szegediense* encodes both group 3b and group 1d [NiFe]-hydrogenases [35], and there may be a similar hydrogenases produced by *Methylocaldum* WAP11.3 with nucleotide sequences significantly different to that of *M. szegediense* to prevent PCR amplification. Alternatively, nitrogenase activity could be responsible for H_2 evolution (Equation 2), as observed in *Methylosinus trichosporium* [227] and the alphaproteobacterium *Rhodopseudomonas palustris* [455]. Nitrogen fixation is inhibited in *Methylococcus capsulatus* at high oxygen concentrations [456] and the presence of a similarly oxygen-sensitive nitrogenase in *Methylocaldum* WAP11.3 could explain this result.

Despite *Methylacidiphilum* WHV12.1 encoding the large sub-units of both group 1d and group 3b [NiFe]-hydrogenases, hydrogen oxidation was not observed under oxic nor hypoxic growth conditions. Many [NiFe]-hydrogenases are inactivated by high oxygen concentrations [439], but this seems unlikely when hydrogen oxidation with atmospheric oxygen was observed in *Methylacidiphilum* NGM89.1, which encoded a 3b [NiFe]-hydrogenase where the large subunit shared 97 % nucleotide identity with that of the *Methylacidiphilum* WHV12.1 sequence. There may be other reasons for the lack of hydrogenase activity observed with *Methylacidiphilum* WHV12.1; mutations, the absence of other genes within the hydrogenase operon, or differences in expression of maturation proteins essential for hydrogenase biosynthesis [457].

As temperature in geothermal areas generally increases with soil depth [14, 35], and can be correlated with hydrogen concentrations [35], the final aim of this

chapter was to investigate whether the respiratory energy gained through hydrogen oxidation promoted the persistence of methanotroph isolates during exposure to elevated (sub-optimal) growth temperatures. Under oxic conditions, observations of both hydrogen and methane oxidation were constrained to the temperature range for growth for moderate thermophiles *Methylocystis* GDS1.7 and *Methylococcus* GDS2.4. In comparison, for the thermophile *Methylacidiphilum* NGM89.1, hydrogen oxidation rates steadily increased with increasing incubation temperature up to a maximum value of 138 µmoles/day at 69 °C; a value 3 °C greater than the observed Tmax. Contrasting this, methane oxidation in *Methylacidiphilum* NGM89.1 declined at temperatures greater than the optimum for growth.

Under hypoxic growth conditions (3 % O_2, v/v), a consistent rate of methane oxidation was observed (~520 µmol/day) in batch cultures of *Methylococcus* GDS2.4 over the entire temperature range tested, up to a maximum of 60 °C. Growth and hydrogen oxidation, however, was only observed at temperatures up to 44 °C (T_{max} 49 °C). It is possible loss of hydrogen oxidation activity may limit growth of this strain at elevated temperatures. Alternatively, the strain may be using the energy derived from methane oxidation for processes other than growth, such as cell maintenance or the production of intracellular storage polymers [448] or protein [458].

In hypoxic cultures of *Methylacidiphilum* NGM89.1, there was a slight increase in methane oxidation rate (537 to 702 µmol/hour) over the temperature range measured (59 to 76 °C), but there was a significant increase in hydrogen oxidation rates (Student's t-test, *p*-value = 0.005) up to 10 °C greater than the T_{max} for this strain (66 °C). Growth of cells and a corresponding increase in optical density only occurred at < 64 °C, which again suggests that the strain uses energy for non-growth mechanisms. Previous studies on *M. fumariolicum* have shown this species is capable of synthesising large volumes of intracellular glycogen under nitrogen-limiting conditions (up to 36 % of total dry weight [450]). During these experiments, the authors report decreasing optical density despite cell numbers remaining relatively constant. The synthesis of storage molecules, protein or biopolymers [459] could explain the observed lack of growth in

Methylacidiphilum NGM89.1 cultures, which were still clearly oxidising hydrogen at elevated temperatures, and should be investigated further.

Finally, in an attempt to ascertain whether observations of hydrogen oxidation contributed to survival, Most Probable Number tests were performed on cultures of *Methylacidiphilum* NGM89.1 that were actively oxidising hydrogen (Figure 5.11A). Results indicate that increasing rates of hydrogen oxidation (in association with elevated growth temperatures) do not improve cell viability. Cultures that had previously been incubated at 67.6 °C displayed a comparable number of viable cells to cultures incubated at 59.2 °C, but very few viable cells from the culture that had been incubated at 68.0 °C. No viable cells were found in cultures at 76.0 or 76.5 °C. Small variations in temperature over the course of an experiment (usually less than 1 °C) have previously been observed with the temperature gradient incubator used in this study, which could mean that cells were incubated at temperatures slightly lower than set, but no growth (increase in OD_{600}) was observed during the initial incubation temperature.

Future work could include another method to determine cell viability, such as flow cytometry using live/dead stain [399], which may give more accurate results than MPN tests. Consumption of glycogen in *M. fumariolicum* is associated with increased viability of cells during periods of methane starvation [450], but if *Methylacidiphilum* NGM89.1 produced a similar storage molecule during incubation at elevated temperatures, this did not appear to increase cell survival and viability at 10 °C above the known maximum temperature for growth.

5.4 Conclusions

There is a great deal of variation in the types of hydrogenases encoded by methanotrophs; not only between genera but also within species. Genome sequencing (or better still, transcriptomic analysis under different conditions) of each of the methanotroph isolates described in this study would help to further elucidate the connections between hydrogenase regulation and the hydrogen oxidation activity observed in this study. Nevertheless, hydrogen oxidation was observed in three isolates under oxic conditions, and in two under low oxygen conditions. *Methylocystis* GDS1.7, *Methylococcus* GDS2.4 and

Methylacidiphilum NGM89.1 appear to co-oxidise hydrogen and methane, in a manner similar to the mixotrophic strategy employed by *Methylacidiphilum* sp. RTK17.1 [35], and this may be important in their natural environment when subjected to variations in methane and oxygen availability.

The association between hydrogen oxidation and elevated temperatures remains unclear. Hydrogen increases with depth in geothermal soils as temperature also increases [35], but only the thermophile *Methylacidiphilum* NGM89.1 displayed an increase in hydrogen oxidation with increasing temperature, under both oxygen-replete and oxygen-limiting conditions. Hydrogen oxidation did not appear to be linked to survival at elevated temperatures, based on MPN analysis, although there may be other factors, such as nitrogen limitation [450], increased oxygen limitation [34], or methane starvation [35], which interact with hydrogen oxidation to affect fitness and viability. Further experiments, controlling for each of these variables, are necessary to determine the role, if any, of hydrogen oxidation during survival in sub-optimal conditions.

6. Thesis Summary, Conclusions and Future Directions

Methanotrophs play an important role in the global methane cycle by oxidising the majority of biogenic methane produced each year. Low temperature environments, such as wetlands and paddy fields, have been extensively characterised in terms of their methane-oxidising communities, but there has been little research on geothermal fields, which are high-methane, high-temperature environments.

The central hypothesis of this thesis was that thermophilic methanotrophs are present and active in the Taupo Volcanic Zone of New Zealand and could be detected, and their community structure and activity described, using a combination of culture-independent and cultivation-dependent techniques. The first stage was to quantify methane oxidation under laboratory conditions within geothermal microcosms, in addition to carrying out a 16S rRNA gene sequence survey to identify putative methanotrophs.

Methane oxidation was observed in 31 of the 58 sample microcosms across a wide range of incubation pH and temperature. While this metabolism appears to be significant in geothermal areas, rates of methane oxidation did not necessarily correlate with environmental factors, such as temperature, pH or *in situ* methane concentrations. This may be due to the relatively small numbers of samples taken for each category, and further sampling, including expanding the survey area to include more geothermal fields, including those in other countries, or other high-temperature, high-methane environments such as gas fields [6] or oil reservoirs [7] may be necessary. Different environments are likely to harbour different microbial communities, and an increased sampling depth, together with the measurement of a wide variety of physicochemical parameters such as in the 1000 Springs project [247] may help to elucidate the links between the variables that drive methanotrophic activities at elevated temperatures. In addition, temporal sampling at some of the sites could indicate the influence of changing environmental conditions such as rainfall or gas flux [12].

Microbial diversity was high within the majority of the geothermal microcosms; with many taxa previously isolated from geothermal ecosystems and few

ubiquitous genera detected. 16S rRNA gene sequencing was sometimes inadequate at predicting methane oxidation within microcosms; with some actively oxidising methane despite the absence of known methanotrophs, and others not oxidising methane despite the retrieval of *Methylacidiphilum* 16S rRNA gene sequences in high proportions. Some of these samples were from environments outside the known temperature and pH ranges for described strains, suggesting the presence of either non-viable cells or extracellular DNA, which may have come from the environment sampled or from laboratory contamination. The use of propidium monazide to bind and remove relic DNA during sequencing efforts would enable identification of links between community structure and viability of cells, while sequencing blanks or mock communities would allow more robust analysis of microbial taxonomy within geothermal samples. The survey results highlighted the importance of using culture-based techniques to confirm metabolic capabilities inferred through DNA sequencing. This may be achieved by using metagenomic approaches, but it is difficult to reconstruct complete genomes for lower-abundance members of a microbial community [460], and targeting specific metabolic guilds through the use of stable isotope probing [307, 461] would be a good way to filter and identify active methanotrophs. DNA-SIP can require long incubation times, leading to the labelling of cross-feeders [154]], which can be overcome by the use of RNA-SIP instead. However, the difficulty in extracting RNA from geothermal soils may constrain the use of this technique [308]. SIP experiments are likely to be labour intensive, as while proteobacterial methanotrophs readily assimilate $^{13}C\text{-}CH_4$, verrucomicrobial methanotrophs require the addition of $^{13}C\text{-}CO_2$ [26], and other autotrophs present in the sample may make results more ambiguous.

Elucidating the role of *Bathyarchaeota* in methane cycling is also an area for future work. Reads affiliated to this phylum dominated the 16S rRNA gene sequences from the Orakei Korako OKO2 and Wairakei Thermal Valley WTV4 microcosms that both oxidised methane rapidly but contained very few known aerobic methanotrophs (13 and 954 of 149,400 reads, respectively). As these microcosms did not oxidise methane when in liquid media, it would be intriguing to investigate if members of *Bathyarchaeota* are indeed capable of anaerobic methane oxidation [19] or methylotrophic methanogenesis [20], and under what

conditions. Other methane-oxidising samples with few known methanotrophs were dominated by uncultured *Thaumarchaeota*, *Thermoprotei* (*Crenarchaeota*) or *Aquificaceae* (*Aquificae*) and it is unclear what role, if any, these taxa play in methane metabolism. Stable isotope probing would again be a useful technique for these issues, with RNA-SIP being the preferred choice to identify active methanotrophic community members [164]. In addition, oligotyping of the sequences to analyse exact sequence variants could be used in conjunction with metagenome assembly to correlate specific uncultured taxa with their function [364].

The next objective of the study was to investigate enrichment microcosms made from the geothermal samples in terms of methane oxidation rates, and the community structure and function of microcosms actively oxidising methane. Methane oxidation was observed in 22 enrichment microcosms at temperatures of up to 75 °C. In enrichment microcosms that did not continue to oxidise methane, methanotrophs present in the original sample may have required alternative media, or the presence of helper organisms to provide specific growth factors or remove toxic metabolites. For example, cultured members of *Thaumarchaeota* are known ammonia oxidisers, which express an ammonia monooxygenase enzyme that will also oxidise methane, although with no energy gain to the host [204]. These archaea are generally cultured in the presence of tungstate, which is an essential trace metal for at least some members of *Thermococcales* (*Euryarchaeota*) [462], and the lack of tungstate in the culture media used in this study may have prevented growth and continual methane oxidation in liquid phase. The decreased solubility of gases at high temperature may also constrain growth in liquid media, and experiments with increased headspace pressure or concentrations may alleviate this issue.

Metatranscriptomic analysis was performed on two of the enrichment microcosms, although RNA could not be extracted from the more thermophilic Ngatamariki NGM89 microcosm, possibly due to the presence of humic acids or clay minerals [308]. In future work, multiple extraction methods in parallel may overcome the difficulties in retrieving RNA from environmental samples. Transcripts from the Golden Springs GDS1 microcosm and the Tokaanu TOK7

microcosm indicated that methanotrophs were highly active in both; however, stress response associated transcripts were also abundant, suggesting enrichment conditions in these microcosms were not optimal. Although only methane and nitrogen metabolism and oxidative phosphorylation pathways were examined in this study, further investigation would be required to identify genes expressed during various kinds of stress, including the biosynthesis of osmo- or thermo-protectants.

Community structure of the enrichment microcosms was difficult to determine, as the taxonomy of BLASTx results for transcripts indicated the majority of proteins identified were from genera not detected in the original 16S rRNA gene sequences from the microcosms. Future studies should include parallel sequencing of both mRNA and either rRNA or DNA in order to reconcile population taxonomy. The uneven representation of phyla across the NCBI databases means that newer taxonomic assignment pipelines, such as the Metagenomes Rapid Annotations using Subsystems Technology (MG-RAST) server [463] that compares annotations from multiple databases, will aid in better taxonomy as more metagenomic data is deposited.

The third aim of this study was to isolate and characterise thermophilic methanotrophs from the geothermal enrichment microcosms. Although there is a great deal of literature on the growth requirements for select methanotroph species, this study has highlighted some of the difficulties inherent in cultivating this guild of bacteria. Methane oxidation was not sustained throughout the passaging of many microcosms; suggesting the possible dilution of either an essential growth factor or of cooperative neighbours. Improved cultivation approaches could include the use of diffusion chambers that allow physical separation of cells while allowing the passage of nutrients [108]. Metagenomics or metatranscriptomics could also be used to rationally inform media design and cultivation parameters. Chemical analysis of a sub-sample of each microcosm taken during future sampling may assist in determining, and replicating, essential trace elements for thermophilic methanotrophy. Although multiple media types were used for all samples in this study, this could be built upon to encompass the "culturomics" approach used in recent animal microbiome studies [464, 465].

This method involves high throughput cultivation by subjecting each sample to multiple culture conditions, including altering temperatures, atmosphere or using thermal shock and preincubation [465].

Nevertheless, thermophilic and thermotolerant methanotrophs were isolated from five geothermal enrichment microcosms and displayed similar phenotypic characteristics to previously described strains. The isolates exhibited few signs of adaptation to changing environmental conditions, such as resistance to heat-shock or desiccation, although each demonstrated resistance to multiple antibiotics that may be synthesised by bacteria or fungi *in situ*. Genome sequencing of the isolates would enable identification of essential pathways for survival encoded by each strain. This would then enable the design of qPCR primers for example, which could be used in conjunction with electron microscopy during experimental procedures such as wetting and drying regimes.

The final objective of this study was to investigate hydrogen oxidation by the methanotrophic isolates. Genes for [NiFe]-hydrogenase subunits were amplified from four of the isolates using PCR, but given the sequence variation within groups, genome sequencing of the isolates is necessary to clarify the presence/absence and completeness of specific [NiFe]-hydrogenase operons. Transcriptome sequencing under a range of environmental conditions, including a range of oxygen concentrations, would establish links between genome sequences and functional activity. Hydrogen oxidation was observed in parallel with methane oxidation in three of the methanotroph isolates, suggesting these strains co-utilise the respiratory energy gained through the oxidation of both these gases. One thermophilic isolate showed an increase in hydrogen oxidation with increasing temperatures, but this was not a common feature of all three hydrogen-oxidising methanotrophs and the association between hydrogen oxidation and elevated temperatures remains unclear. Further experiments under a variety of sub-optimal conditions are needed in order to determine if hydrogen oxidation is linked to survival during other conditions such as desiccation or methane starvation. These could be combined with cell counts and electron microscopy to determine if, for example, hydrogen oxidation is used to drive the production of storage granules rather than cell division and growth.

Culture-independent and cultivation studies have shown methanotrophs to be both prolific and highly active within geothermal soils and sediments in the Taupō Volcanic Zone. Methanotrophs from these environments have been successfully isolated and characterised, adding to our knowledge both of their physiology and their ecological role.

References

1. Forster, P., et al., *Changes in atmospheric constituents and in radiative forcing*, in *Climate Change 2007: The Physical Science Basis. Contribution of Working Group I to the Fourth Assessment Report of the Intergovernmental Panel on Climate Change*, Solomon, S., et al., Editors. 2007, IPCC. p. 129-234.
2. Myhre, G., et al., *Contribution of working group I to the fifth assessment report of the Intergovernmental Panel on Climate Change*, in *Climate Change 2013: The Physical Science Basis*, Stocker, T.F., et al., Editors. 2013, IPCC. p. 1535 pp.
3. Conrad, R., *The global methane cycle: Recent advances in understanding the microbial processes involved.* Environmental Microbiology Reports, 2009. **1** (5): p. 285-292.
4. Ciais, P., et al., *Contribution of working group I to the fifth assessment report of the Intergovernmental Panel on Climate Change* in *Climate Change 2013: The Physical Science Basis*, Stocker, T.F., et al., Editors. 2013, IPCC. p. 1535 pp.
5. Etiope, G., *Mud volcanoes and microseepage: The forgotten geophysical components of atmospheric methane budget.* Ann. Geophys., 2005. **48** (1): p. 1-7.
6. Mochimaru, H., et al., *Microbial diversity and methanogenic potential in a high temperature natural gas field in Japan.* Extremophiles, 2007. **11** (3): p. 453-461.
7. Nazina, T.N., et al., *Microbiological investigations of high-temperature horizons of the Kongdian petroleum reservoir in connection with field trial of a biotechnology for enhancement of oil recovery.* Microbiology, 2007. **76** (3): p. 287-296.
8. Magnabosco, C., et al., *Comparisons of the composition and biogeographic distribution of the bacterial communities occupying South African thermal springs with those inhabiting deep subsurface fracture water.* Frontiers in Microbiology, 2014. **5**.
9. Engle, M.A., et al., *Gas emissions, minerals, and tars associated with three coal fires, Powder River Basin, USA.* Science of The Total Environment, 2012. **420**: p. 146-159.
10. Etiope, G. and Klusman, R.W., *Geologic emissions of methane to the atmosphere.* Chemosphere, 2002. **49** (8): p. 777-789.
11. Giggenbach, W.F., *Variations in the chemical and isotopic composition of fluids discharged from the Taupo Volcanic Zone, New Zealand.* J. Volcanol. Geotherm. Res., 1995. **68** (1-3): p. 89-116.
12. Cardellini, C., et al., *Accumulation chamber measurements of methane fluxes: Application to volcanic-geothermal areas and landfills.* Appl. Geochem., 2003. **18** (1): p. 45-54.
13. Reeburgh, W.S., *Global methane biogeochemistry*, in *Treatise on Geochemistry, Vol 4: The Atmosphere*, Holland, H.D. and Turekian, K.K., Editors. 2003, Elsevier. p. 1-25.
14. Dunfield, P.F., et al., *Methane oxidation by an extremely acidophilic bacterium of the phylum Verrucomicrobia.* Nature, 2007. **450** (7171): p. 879-882.
15. Beal, E.J., House, C.H., and Orphan, V.J., *Manganese- and iron-dependent marine methane oxidation.* Science, 2009. **325** (5937): p. 184-7.

16. Milucka, J., et al., *Zero-valent sulphur is a key intermediate in marine methane oxidation.* Nature, 2012. **491** (7425): p. 541-546.
17. Haroon, M.F., et al., *Anaerobic oxidation of methane coupled to nitrate reduction in a novel archaeal lineage.* Nature, 2013. **500** (7464): p. 567-570.
18. Cui, M., et al., *Anaerobic oxidation of methane: An "active" microbial process.* MicrobiologyOpen, 2015. **4** (1): p. 1-11.
19. Biddle, J.F., et al., *Heterotrophic Archaea dominate sedimentary subsurface ecosystems off Peru.* P Natl Acad Sci USA, 2006. **103** (10): p. 3846-3851.
20. Evans, P.N., et al., *Methane metabolism in the archaeal phylum Bathyarchaeota revealed by genome-centric metagenomics.* Science, 2015. **350** (6259): p. 434-438.
21. Vanwonterghem, I., et al., *Methylotrophic methanogenesis discovered in the archaeal phylum Verstraetearchaeota.* Nature Microbiology, 2016. **1**: p. 16170.
22. Ettwig, K.F., et al., *Nitrite-driven anaerobic methane oxidation by oxygenic bacteria.* Nature, 2010. **464** (7288): p. 543-8.
23. Timmers, P.H.A., et al., *Reverse methanogenesis and respiration in methanotrophic Archaea.* Archaea, 2017. **2017**: p. 22.
24. Ding, J., et al., *New primers for detecting and quantifying denitrifying anaerobic methane oxidation archaea in different ecological niches.* Appl Microbiol Biot, 2015. **99** (22): p. 9805-9812.
25. Khadem, A.F., et al., *Autotrophic methanotrophy in Verrucomicrobia: Methylacidiphilum fumariolicum SolV uses the Calvin-Benson-Bassham cycle for carbon dioxide fixation.* J Bacteriol, 2011. **193** (17): p. 4438-4446.
26. Sharp, C.E., Stott, M.B., and Dunfield, P.F., *Detection of autotrophic verrucomicrobial methanotrophs in a geothermal environment using stable isotope probing.* Frontiers in Microbiology, 2012. **3**.
27. Dunfield, P.F., et al., *Methylocapsa aurea sp. nov., a facultative methanotroph possessing a particulate methane monooxygenase, and emended description of the genus Methylocapsa.* International Journal of Systematic and Evolutionary Microbiology, 2010. **60** (11): p. 2659-2664.
28. Belova, S.E., et al., *Methylocystis bryophila sp. nov., a facultatively methanotrophic bacterium from acidic Sphagnum peat, and emended description of the genus Methylocystis (ex Whittenbury et al. 1970) Bowman et al. 1993.* International Journal of Systematic and Evolutionary Microbiology, 2013. **63** (Pt 3): p. 1096-1104.
29. Dunfield, P.F. and Dedysh, S.N., *Methylocella: A gourmand among methanotrophs.* Trends in Microbiology, 2014. **22** (7): p. 368-369.
30. Dedysh, S.N., Knief, C., and Dunfield, P.F., *Methylocella species are facultatively methanotrophic.* J Bacteriol, 2005. **187** (13): p. 4665-4670.
31. Crombie, A.T. and Murrell, J.C., *Trace-gas metabolic versatility of the facultative methanotroph Methylocella silvestris.* Nature, 2014. **510**: p. 148-151.
32. van Beilen, J.W.A., et al., *Distinct effects of sorbic acid and acetic acid on the electrophysiology and metabolism of Bacillus subtilis.* Appl Environ Microb, 2014. **80** (19): p. 5918-5926.

33. Aston, J.E., et al., *Toxicity of select organic acids to the slightly thermophilic acidophile Acidithiobacillus caldus.* Environmental Toxicology and Chemistry, 2009. **28** (2): p. 279-286.
34. Mohammadi, S., et al., *Methylacidiphilum fumariolicum SolV, a thermoacidophilic `Knallgas' methanotroph with both an oxygen-sensitive and -insensitive hydrogenase.* The ISME Journal, 2017. **11** (4): p. 945-958.
35. Carere, C.R., et al., *Mixotrophy drives niche expansion of verrucomicrobial methanotrophs.* The ISME Journal, 2017. **11** (11): p. 2599-2610.
36. Chistoserdova, L. and Lidstrom, M.E., *Aerobic Methylotrophic Prokaryotes*, in *The Prokaryotes*, Rosenberg, E., et al., Editors. 2013, Springer-Verlag: Berlin. p. 267-285.
37. Antony, C.P., et al., *Active methylotrophs in the sediments of Lonar Lake, a saline and alkaline ecosystem formed by meteor impact.* The ISME Journal, 2010. **4** (11): p. 1470-1480.
38. Anders, H., et al., *Thermoflavifilum aggregans gen. nov., sp. nov., a thermophilic and slightly halophilic filamentous bacterium from the phylum Bacteroidetes.* International Journal of Systematic and Evolutionary Microbiology, 2014. **64** (4): p. 1264-1270.
39. King, C.E. and King, G.M., *Description of Thermogemmatispora carboxidivorans sp. nov., a carbon-monoxide-oxidizing member of the class Ktedonobacteria isolated from a geothermally heated biofilm, and analysis of carbon monoxide oxidation by members of the class Ktedonobacteria.* International Journal of Systematic and Evolutionary Microbiology, 2014. **64** (4): p. 1244-1251.
40. Miroshnichenko, M.L., et al., *Vulcanithermus mediatlanticus gen. nov., sp. nov., a novel member of the family Thermaceae from a deep-sea hot vent.* International Journal of Systematic and Evolutionary Microbiology, 2003. **53** (4): p. 1143-1148.
41. Chistoserdova, L., *Modularity of methylotrophy, revisited.* Environmental Microbiology, 2011. **13** (10): p. 2603-2622.
42. Keltjens, J., et al., *PQQ-dependent methanol dehydrogenases: rare-earth elements make a difference.* Appl Microbiol Biot, 2014. **98** (14): p. 6163-6183.
43. Pol, A., et al., *Methanotrophy below pH 1 by a new Verrucomicrobia species.* Nature, 2007. **450** (7171): p. 874-878.
44. Whittenbury, R., Phillips, K.C., and Wilkinson, J.F., *Enrichment, isolation and some properties of methane-utilizing bacteria.* Journal of General Microbiology, 1970. **61** (2): p. 205-218.
45. Bowman, J.P., et al., *Revised taxonomy of the methanotrophs: Description of Methylobacter gen. nov., emendation of Methylococcus, validation of Methylosinus and Methylocystis species, and a proposal that the family Methylococcaceae includes only the group I methanotrophs.* International Journal of Systematic Bacteriology, 1993. **44** (2): p. 375.
46. Hanson, R.S. and Hanson, T.E., *Methanotrophic bacteria.* Microbiological Reviews, 1996. **60** (2): p. 439-71.
47. Op den Camp, H.J.M., et al., *Environmental, genomic and taxonomic perspectives on methanotrophic Verrucomicrobia.* Environmental Microbiology Reports, 2009. **1** (5): p. 293-306.

48. Nazaries, L., et al., *Methane, microbes and models: Fundamental understanding of the soil methane cycle for future predictions.* Environmental Microbiology, 2013. **15** (9): p. 2395-2417.
49. Tavormina, P.L., et al., *Methyloprofundus sedimenti gen. nov., sp. nov., an obligate methanotroph from ocean sediment belonging to the Deep Sea 1 clade of marine methanotrophs.* International Journal of Systematic and Evolutionary Microbiology, 2014. **65**: p. 251-259.
50. Stoecker, K., et al., *Cohn's Crenothrix is a filamentous methane oxidizer with an unusual methane monooxygenase.* P Natl Acad Sci USA, 2006. **103** (7): p. 2363-2367.
51. Roslev, P. and King, G.M., *Aerobic and anaerobic starvation metabolism in methanotrophic bacteria.* Appl Environ Microb, 1995. **61** (4): p. 1563-70.
52. Cai, Y., et al., *Conventional methanotrophs are responsible for atmospheric methane oxidation in paddy soils.* Nat. Commun., 2016. **7**.
53. Graham, D.W., et al., *Factors Affecting Competition between Type I and Type II Methanotrophs in Two-Organism, Continuous-Flow Reactors.* Microbial Ecology, 1993. **25** (1): p. 1-17.
54. Hou, S., et al., *Complete genome sequence of the extremely acidophilic methanotroph isolate V4, Methylacidiphilum infernorum, a representative of the bacterial phylum Verrucomicrobia.* Biol. Direct, 2008. **3**.
55. Islam, T., et al., *Methane oxidation at 55°C and pH 2 by a thermoacidophilic bacterium belonging to the Verrucomicrobia phylum.* P Natl Acad Sci USA, 2008. **105** (1): p. 300-304.
56. Schlegel, H.G., *General Microbiology*. Seventh ed. 1992, Cambridge: Cambridge University Press.
57. Tsubota, J., et al., *Methylothermus thermalis gen. nov., sp. nov., a novel moderately thermophilic obligate methanotroph from a hot spring in Japan.* International Journal of Systematic and Evolutionary Microbiology, 2005. **55** (5): p. 1877-1884.
58. Bodrossy, L., et al., *Analysis of 16S rRNA and methane monooxygenase gene sequences reveals a novel group of thermotolerant and thermophilic methanotrophs, Methylocaldum gen. nov.* Archives of Microbiology, 1997. **168** (6): p. 493-503.
59. Bodrossy, L., et al., *A novel thermophilic methane-oxidising γ-Proteobacterium.* FEMS Microbiology Letters, 1999. **170** (2): p. 335-341.
60. Malashenko, Y.R., et al., *Thermophilic and thermotolerant bacteria assimilating methane* Microbiology, 1975. **44** (5): p. 855-862.
61. Tsypenzhapova, I.S., et al., *A new thermotolerant aerobic methanotroph from a thermal spring in Buryatia.* Microbiology, 2007. **76** (1): p. 118-121.
62. Hirayama, H., et al., *Methylothermus subterraneus sp. nov., a moderately thermophilic methanotroph isolated from a terrestrial subsurface hot aquifer.* International Journal of Systematic and Evolutionary Microbiology, 2011. **61** (11): p. 2646-2653.
63. Hirayama, H., et al., *Methylomarinovum caldicuralii gen. nov., sp. nov., a moderately thermophilic methanotroph isolated from a shallow submarine hydrothermal system, and proposal of the family Methylothermaceae fam. nov.* International Journal of Systematic and Evolutionary Microbiology, 2014. **64**: p. 989-999.

64. Foster, J.W. and Davis, R.H., *A methane-dependent coccus, with notes on classification and nomenclature of obligate, methane-utilizing bacteria.* J Bacteriol, 1966. **91** (5): p. 1924-1931.
65. Romanovskaya, V.A., Malashenko Yu, R., and Bogachenko, V.N., *Corrected diagnoses of genera and species of methane assimilating bacteria.* Microbiology, 1978. **47** (1): p. 120-130.
66. Takeuchi, M., et al., *Methylocaldum marinum sp. nov., a novel thermotolerant methane oxidizing bacterium isolated from marine sediments.* International Journal of Systematic and Evolutionary Microbiology, 2014. **64**: p. 3240-3246.
67. Jäckel, U., Thummes, K., and Kämpfer, P., *Thermophilic methane production and oxidation in compost.* FEMS Microbiology Ecology, 2005. **52** (2): p. 175-184.
68. Eshinimaev, B.T., et al., *New thermophilic methanotrophs of the genus Methylocaldum.* Microbiology, 2004. **73** (4): p. 448-456.
69. Dvoryanchikova, E.N., et al., *Molecular detection of methanotrophic bacteria in the hot springs of the Uzon caldera, Kamchatka.* Microbiology, 2011. **80** (6): p. 867-869.
70. Islam, T., et al., *Acid-tolerant moderately thermophilic methanotrophs of the class Gammaproteobacteria isolated from tropical topsoil with methane seeps.* Frontiers in Microbiology, 2016. **7**.
71. Tamas, I., et al., *The (d)evolution of methanotrophy in the Beijerinckiaceae -a comparative genomics analysis.* The ISME Journal, 2014. **8** (2).
72. Cook, S.A. and Shiemke, A.K., *Evidence that a type-2 NADH:quinone oxidoreductase mediates electron transfer to particulate methane monooxygenase in Methylococcus capsulatus.* Archives of Biochemistry and Biophysics, 2002. **398** (1): p. 32-40.
73. Lawton, T.J. and Rosenzweig, A.C., *Methane-oxidizing enzymes: An upstream problem in biological gas-to-liquids conversion.* Journal of the American Chemical Society, 2016. **138** (30): p. 9327-9340.
74. DiSpirito, A.A., et al., *Methanobactin and the link between copper and bacterial methane oxidation.* Microbiology and Molecular Biology Reviews, 2016. **80** (2): p. 387-409.
75. Lee, S.W., et al., *Mixed pollutant degradation by Methylosinus trichosporium OB3b expressing either soluble or particulate methane monooxygenase: Can the tortoise beat the hare?* Appl Environ Microb, 2006. **72** (12): p. 7503-7509.
76. Ho, A., et al., *Conceptualizing functional traits and ecological characteristics of methane-oxidizing bacteria as life strategies.* Environmental Microbiology Reports, 2013. **5** (3): p. 335-345.
77. Semrau, J.D., et al., *Methanobactin and MmoD work in concert to act as the "copper-switch" in methanotrophs.* Environmental Microbiology, 2013. **15** (11): p. 3077-3086.
78. Semrau, J.D., DiSpirito, A.A., and Yoon, S., *Methanotrophs and copper.* FEMS Microbiology Reviews, 2010. **34** (4): p. 496-531.
79. Colby, J., Stirling, D.I., and Dalton, H., *The soluble methane mono oxygenase of Methylococcus capsulatus (Bath). Its ability to oxygenate n-alkanes, n-alkenes, ethers, and alicyclic, aromatic and heterocyclic compounds.* Biochemical Journal, 1977. **165** (2): p. 395-402.

80. Dalton, H., *Ammonia oxidation by the methane oxidising bacterium Methylococcus capsulatus strain Bath.* Archives of Microbiology, 1977. **114** (3): p. 273-279.
81. Jiang, H., et al., *Methanotrophs: Multifunctional bacteria with promising applications in environmental bioengineering.* Biochemical Engineering Journal, 2010. **49** (3): p. 277-288.
82. Yoon, S., et al., *Constitutive expression of pMMO by Methylocystis strain SB2 when grown on multi-carbon substrates: Implications for biodegradation of chlorinated ethenes.* Environmental Microbiology Reports, 2011. **3** (2): p. 182-188.
83. Semprini, L., et al., *A field evaluation of in-situ biodegradation of chlorinated ethenes: Part 2, results of biostimulation and biotransformation experiments.* Groundwater, 1990. **28** (5): p. 715-727.
84. Sutfin, J.A. and Ramey, D., *In situ biological treatment of TCE-impacted soil and groundwater: Demonstration results.* Environmental Progress, 1997. **16** (4): p. 287-296.
85. Medvedkova, K.A., Khmelenina, V.N., and Trotsenko, Y.A., *Sucrose as a factor of thermal adaptation of the thermophilic methanotroph Methylocaldum szegediense O-12.* Microbiology, 2007. **76** (4): p. 500-502.
86. Kumar, S., Tsai, C.J., and Nussinov, R., *Factors enhancing protein thermostability.* Protein Engineering, 2000. **13**.
87. Pond, J.L. and Langworthy, T.A., *Effect of growth temperature on the long-chain diols and fatty acids of Thermomicrobium roseum.* J Bacteriol, 1987. **169** (3): p. 1328-1330.
88. Oshima, T., *Unique polyamines produced by an extreme thermophile, Thermus thermophilus.* Amino Acids, 2007. **33** (2): p. 367-372.
89. d'Avó, A.F., et al., *A unique pool of compatible solutes in Rhodopirellula baltica, member of the deep-branching phylum Planctomycetes.* PLoS ONE, 2013. **8** (6).
90. Salvador, M., et al., *Contribution of RpoS to metabolic efficiency and ectoines synthesis during the osmo- and heat-stress response in the halophilic bacterium Chromohalobacter salexigens.* Environ Microbiol Reports, 2015. **7** (2): p. 301-311.
91. Bowman, J.P., et al., *Methylomonas fodinarum sp. nov. and Methylomonas aurantiaca sp. nov.: Two closely related type I obligate methanotrophs.* Systematic and Applied Microbiology, 1990. **13** (3): p. 279-287.
92. Bodrossy, L., et al., *Heat-tolerant methanotrophic bacteria from the hot water effluent of a natural gas field.* Appl Environ Microb, 1995. **61** (10): p. 3549-3555.
93. Holmes, A.J., et al., *Evidence that particulate methane monooxygenase and ammonia monooxygenase may be evolutionarily related.* FEMS Microbiology Letters, 1995. **132** (3): p. 203-208.
94. Whitaker, W.B., et al., *Synthetic methylotrophy: Engineering the production of biofuels and chemicals based on the biology of aerobic methanol utilization.* Current Opinion in Biotechnology, 2015. **33**: p. 165-175.
95. Ward, N., et al., *Genomic insights into methanotrophy: The complete genome sequence of Methylococcus capsulatus (Bath).* PloS Biol., 2004. **2** (10).

96. Chen, Y., et al., *Complete genome sequence of the aerobic facultative methanotroph Methylocella silvestris BL2.* J Bacteriol, 2010. **192** (14): p. 3840-3841.
97. Miller, S.R., McGuirl, M.A., and Carvey, D., *The evolution of RuBisCO stability at the thermal limit of photoautotrophy.* Mol. Biol. Evol., 2013. **30** (4): p. 752-760.
98. Maeda, N., et al., *The unique pentagonal structure of an archaeal Rubisco is essential for its high thermostability.* J Biol Chem, 2002. **277** (35): p. 31656-31662.
99. Medvedkova, K.A., et al., *Antioxidant systems of moderately thermophilic methanotrophs Methylocaldum szegediense and Methylococcus capsulatus.* Microbiology, 2009. **78** (6): p. 670-677.
100. Elvert, M. and Niemann, H., *Occurrence of unusual steroids and hopanoids derived from aerobic methanotrophs at an active marine mud volcano.* Organic Geochemistry, 2008. **39** (2): p. 167-177.
101. Lamb, D.C., et al., *Lanosterol biosynthesis in the prokaryote Methylococcus capsulatus: Insight into the evolution of sterol biosynthesis.* Mol. Biol. Evol., 2007. **24** (8): p. 1714-1721.
102. Caron, B., Mark, A.E., and Poger, D., *Some like it hot: The effect of sterols and hopanoids on lipid ordering at high temperature.* J. Phys. Chem. Lett., 2014. **5** (22): p. 3953-3957.
103. Tian, B., et al., *Evaluation of the antioxidant effects of carotenoids from Deinococcus radiodurans through targeted mutagenesis, chemiluminescence, and DNA damage analyses.* Biochimica et Biophysica Acta - General Subjects, 2007. **1770** (6): p. 902-911.
104. Rottem, S. and Markowitz, O., *Carotenoids act as reinforcers of the Acholeplasma laidlawii lipid bilayer.* J Bacteriol, 1979. **140** (3): p. 944-948.
105. Han, D., Link, H., and Liesack, W., *Response of Methylocystis sp. strain SC2 to salt stress: Physiology, global transcriptome, and amino acid profiles.* Appl Environ Microb, 2017. **83** (20).
106. Khadem, A.F., et al., *Metabolic regulation of "Ca. Methylacidiphilum fumariolicum" soIV cells grown under different nitrogen and oxygen limitations.* Frontiers in Microbiology, 2012. **3**.
107. Rappé, M.S. and Giovannoni, S.J., *The Uncultured Microbial Majority.* Annual Reviews Microbiology, 2003. **57**: p. 369-394.
108. Stewart, E.J., *Growing unculturable bacteria.* J Bacteriol, 2012. **194** (16): p. 4151-4160.
109. Pace, N.R., *Mapping the Tree of Life: Progress and prospects.* Microbiology and Molecular Biology Reviews, 2009. **73** (4): p. 565-576.
110. Lynch, M.D.J. and Neufeld, J.D., *Ecology and exploration of the rare biosphere.* Nature Reviews Microbiology, 2015. **13** (4): p. 217-229.
111. Semrau, J.D., et al., *Particulate methane monooxygenase genes in methanotrophs.* J Bacteriol, 1995. **177** (11): p. 3071-3079.
112. Baani, M. and Liesack, W., *Two isozymes of particulate methane monooxygenase with different methane oxidation kinetics are found in Methylocystis sp. strain SC2.* P Natl Acad Sci USA, 2008. **105** (29): p. 10203-10208.
113. Dam, B., et al., *Ammonium induces differential expression of methane and nitrogen metabolism-related genes in Methylocystis sp. strain SC2.* Environmental Microbiology, 2014. **16** (10): p. 3115-3127.

114. Erikstad, H.A., et al., *Differential expression of particulate methane monooxygenase genes in the verrucomicrobial methanotroph 'Methylacidiphilum kamchatkense' Kam1.* Extremophiles, 2012. **16** (3): p. 405-409.
115. Tavormina, P.L., et al., *A novel family of functional operons encoding methane/ammonia monooxygenase-related proteins in gammaproteobacterial methanotrophs.* Environmental Microbiology Reports, 2011. **3** (1): p. 91-100.
116. Hakemian, A.S. and Rosenzweig, A.C., *The biochemistry of methane oxidation.* Annual Review of Biochemistry 2007. **76**: p. 223-241.
117. Oswald, K., et al., *Crenothrix are major methane consumers in stratified lakes.* The ISME Journal, 2017. **11**: p. 2124-2140.
118. Redmond, M.C., Valentine, D.L., and Sessions, A.L., *Identification of novel methane-, ethane-, and propane-oxidizing bacteria at marine hydrocarbon seeps by stable isotope probing.* Appl Environ Microb, 2010. **76** (19): p. 6412-6422.
119. Kolb, S., et al., *Quantitative detection of methanotrophs in soil by novel pmoA-targeted real-time PCR Assays.* Appl Environ Microb, 2003. **69** (5): p. 2423-2429.
120. Bourne, D.G., McDonald, I.R., and Murrell, J.C., *Comparison of pmoA PCR primer sets as tools for investigating methanotroph diversity in three Danish soils.* Appl Environ Microb, 2001. **67** (9): p. 3802-3809.
121. Lüke, C. and Frenzel, P., *Potential of pmoA amplicon pyrosequencing for methanotroph diversity studies.* Appl Environ Microb, 2011. **77** (17): p. 6305-6309.
122. Sharp, C.E., et al., *Distribution and diversity of Verrucomicrobia methanotrophs in geothermal and acidic environments.* Environmental Microbiology, 2014. **16** (6): p. 1867-1878.
123. Luesken, F.A., et al., *pmoA primers for detection of anaerobic methanotrophs.* Appl Environ Microb, 2011. **77** (11): p. 3877-3880.
124. Saitou, N. and Nei, M., *The neighbor-joining method: a new method for reconstructing phylogenetic trees.* Mol. Biol. Evol., 1987. **4** (4): p. 406-425.
125. Zuckerkandl, E. and Pauling, L., *Evolutionary divergence and convergence in proteins*, in *Evolving Genes and Proteins* Bryson, V. and Vogel, H.J., Editors. 1965, Academic Press: New York. p. 97-166.
126. Kumar, S., Stecher, G., and Tamura, K., *MEGA7: Molecular Evolutionary Genetics Analysis version 7.0 for bigger datasets.* Mol. Biol. Evol., 2016. **33** (7): p. 1870-1874.
127. Tamura, K., Nei, M., and Kumar, S., *Prospects for inferring very large phylogenies by using the neighbor-joining method.* P Natl Acad Sci USA, 2004. **101** (30): p. 11030-11035.
128. Semrau, J.D., diSpirito, A.A., and Vuilleumier, S., *Facultative methanotrophy: False leads, true results, and suggestions for future research.* FEMS Microbiology Letters, 2011. **323** (1): p. 1-12.
129. McDonald, I.R., et al., *Molecular ecology techniques for the study of aerobic methanotrophs.* Appl Environ Microb, 2008. **74** (5): p. 1305-1315.
130. McDonald, I.R., Kenna, E.M., and Murrell, J.C., *Detection of methanotrophic bacteria in environmental samples with the PCR.* Appl Environ Microb, 1995. **61** (1): p. 116-21.

131. Liebner, S. and Svenning, M.M., *Environmental transcription of mmoX by methane-oxidizing Proteobacteria in a subarctic palsa peatland.* Appl Environ Microb, 2013. **79** (2): p. 701-706.
132. Holmes, A.J., Owens, N.J.P., and Murrell, J.C., *Detection of novel marine methanotrophs using phylogenetic and functional gene probes after methane enrichment.* Microbiology, 1995. **141** (8): p. 1947-1955.
133. Rahman, M.T., et al., *Environmental distribution and abundance of the facultative methanotroph Methylocella.* The ISME Journal, 2011. **5** (6): p. 1061-1066.
134. Lau, E., et al., *The methanol dehydrogenase gene, mxaF, as a functional and phylogenetic marker for proteobacterial methanotrophs in natural environments.* Plos One, 2013. **8** (2).
135. Schmidt, S., et al., *Functional investigation of methanol dehydrogenase-like protein XoxF in Methylobacterium extorquens AM1.* Microbiology, 2010. **156** (8): p. 2575-2586.
136. Pol, A., et al., *Rare earth metals are essential for methanotrophic life in volcanic mudpots.* Environmental Microbiology, 2013. **16** (1): p. 255-264.
137. Taubert, M., et al., *xoxF encoding an alternative methanol dehydrogenase is widespread in coastal marine environments.* Environmental Microbiology, 2015. **17** (10): p. 3937-3948.
138. Inagaki, F., et al., *Distribution and phylogenetic diversity of the subsurface microbial community in a Japanese epithermal gold mine.* Extremophiles, 2003. **7** (4): p. 307-317.
139. Gagliano, A.L., et al., *Methanotrophic activity and diversity of methanotrophs in volcanic geothermal soils at Pantelleria (Italy).* Biogeosciences, 2014. **11** (20): p. 5865-5875.
140. Nercessian, O., et al., *Diversity of functional genes of methanogens, methanotrophs and sulfate reducers in deep-sea hydrothermal environments.* Environmental Microbiology, 2005. **7** (1): p. 118-132.
141. Kizilova, A.K., et al., *Methane oxidation activity and diversity of aerobic methanotrophs in pH-neutral and semi-neutral thermal springs of the Kunashir Island, Russian Far East.* Extremophiles, 2014. **18** (2): p. 207-218.
142. Holler, T., et al., *Thermophilic anaerobic oxidation of methane by marine microbial consortia.* The ISME Journal, 2011. **5** (12): p. 1946-1956.
143. Bonch-Osmolovskaya, E.A., et al., *Radioisotopic, culture-based, and oligonucleotide microchip analyses of thermophilic microbial communities in a continental high-temperature petroleum reservoir.* Appl Environ Microb, 2003. **69** (10): p. 6143-6151.
144. Li, H., et al., *Molecular phylogenetic diversity of the microbial community associated with a high-temperature petroleum reservoir at an offshore oilfield.* FEMS Microbiology Ecology, 2007. **60** (1): p. 74-84.
145. Orphan, V.J., et al., *Culture-dependent and culture-independent characterization of microbial assemblages associated with high-temperature petroleum reservoirs.* Appl Environ Microb, 2000. **66** (2): p. 700-711.
146. Kolb, S., et al., *Abundance and activity of uncultured methanotrophic bacteria involved in the consumption of atmospheric methane in two forest soils.* Environmental Microbiology, 2005. **7** (8): p. 1150-1161.

147. Chen, Y., et al., *Identification of active methanotrophs in a landfill cover soil through detection of expression of 16S rRNA and functional genes.* Environmental Microbiology, 2007. **9** (11): p. 2855-2869.
148. Chen, Y., et al., *Diversity of the active methanotrophic community in acidic peatlands as assessed by mRNA and SIP-PLFA analyses.* Environmental Microbiology, 2008. **10** (2): p. 446-459.
149. Csáki, R., et al., *Genes involved in the copper-dependent regulation of soluble methane monooxygenase of Methylococcus capsulatus (Bath): Cloning, sequencing and mutational analysis.* Microbiology, 2003. **149** (7): p. 1785-1795.
150. Theisen, A.R., et al., *Regulation of methane oxidation in the facultative methanotroph Methylocella silvestris BL2.* Molecular Microbiology, 2005. **58** (3): p. 682-692.
151. Luesken, F.A., et al., *Effect of oxygen on the anaerobic methanotroph 'Candidatus Methylomirabilis oxyfera': kinetic and transcriptional analysis.* Environmental Microbiology, 2012. **14** (4): p. 1024-1034.
152. Lesniewski, R.A., et al., *The metatranscriptome of a deep-sea hydrothermal plume is dominated by water column methanotrophs and lithotrophs.* The ISME Journal, 2012. **6** (12): p. 2257-2268.
153. Boschker, H.T.S., et al., *Direct linking of microbial populations to specific biogeochemical processes by ^{13}C-labelling of biomarkers.* Nature, 1998. **392** (6678): p. 801-804.
154. Radajewski, S., et al., *Stable-isotope probing as a tool in microbial ecology.* Nature, 2000. **403** (6770): p. 646-649.
155. Lueders, T., et al., *Stable isotope probing of rRNA and DNA reveals a dynamic methylotroph community and trophic interactions with fungi and protozoa in oxic rice field soil.* Environmental Microbiology, 2004. **6** (1): p. 60-72.
156. Whiteley, A.S., et al., *RNA stable-isotope probing.* Nature Protocols, 2007. **2** (4): p. 838-844.
157. von Bergen, M., et al., *Insights from quantitative metaproteomics and protein-stable isotope probing into microbial ecology.* The ISME Journal, 2013. **7** (10): p. 1877-1885.
158. Borek, E. and Rittenberg, D., *Anomalous growth of microorganisms produced by changes in isotopes in their environment.* P Natl Acad Sci USA, 1960. **46** (6): p. 777-782.
159. Han, B., et al., *Diversity and activity of methanotrophs in alkaline soil from a Chinese coal mine.* FEMS Microbiology Ecology, 2009. **70** (2): p. 196-207.
160. Martineau, C., Whyte, L.G., and Greer, C.W., *Stable isotope probing analysis of the diversity and activity of Methanotrophic bacteria in soils from the Canadian high Arctic.* Applied and Environmental Microbiology, 2010. **76** (17): p. 5773-5784.
161. Saidi-Mehrabad, A., et al., *Methanotrophic bacteria in oilsands tailings ponds of northern Alberta.* The ISME Journal, 2013. **7** (5): p. 908-921.
162. Esson, K.C., et al., *Alpha-and gammaproteobacterial methanotrophs codominate the active methane-oxidizing communities in an acidic boreal peat bog.* Appl Environ Microb, 2016. **82** (8): p. 2363-2371.

163. Dumont, M.G., Pommerenke, B., and Casper, P., *Using stable isotope probing to obtain a targeted metatranscriptome of aerobic methanotrophs in lake sediment.* Environmental Microbiology Reports, 2013. **5** (5): p. 757-764.
164. Manefield, M., et al., *RNA stable isotope probing, a novel means of linking microbial community function to phylogeny.* Appl Environ Microb, 2002. **68** (11): p. 5367-5373.
165. Rasigraf, O., et al., *Autotrophic carbon dioxide fixation via the Calvin-Benson-Bassham cycle by the denitrifying methanotroph Candidatus "Methylomirabilis oxyfera".* Appl Environ Microb, 2014. **80** (8): p. 2451-2460.
166. Holmes, A.J., et al., *Characterization of methanotrophic bacterial populations in soils showing atmospheric methane uptake.* Appl Environ Microb, 1999. **65** (8): p. 3312-3318.
167. Roslev, P. and Iversen, N., *Radioactive fingerprinting of microorganisms that oxidize atmospheric methane in different soils.* Appl Environ Microb, 1999. **65** (9): p. 4064-4070.
168. Gainutdinova, E.A., et al., *Aerobic methanotrophic communities in the bottom sediments of Lake Baikal.* Microbiology, 2005. **74** (4): p. 486-494.
169. Zelenkina, T.S., et al., *Aerobic methanotrophs from the coastal thermal springs of Lake Baikal.* Microbiology, 2009. **78** (4): p. 492-497.
170. Roslev, P., Iversen, N., and Henriksen, K., *Oxidation and assimilation of atmospheric methane by soil methane oxidizers.* Appl Environ Microb, 1997. **63** (3): p. 874-880.
171. Lee, N., et al., *Combination of fluorescent in situ hybridization and microautoradiography - A new tool for structure-function analyses in microbial ecology.* Appl Environ Microb, 1999. **65** (3): p. 1289-1297.
172. Stiehl-Braun, P.A., et al., *Effects of N fertilizers and liming on the micro-scale distribution of soil methane assimilation in the long-term Park Grass experiment at Rothamsted.* Soil Biology and Biochemistry, 2011. **43** (5): p. 1034-1041.
173. Krause, S., et al., *Compositional and functional stability of aerobic methane consuming communities in drained and rewetted peat meadows.* FEMS Microbiology Ecology, 2015. **91** (11).
174. Boetius, A., et al., *A marine microbial consortium apparently mediating anaerobic oxidation methane.* Nature, 2000. **407** (6804): p. 623-626.
175. Orphan, V.J., et al., *Multiple archaeal groups mediate methane oxidation in anoxic cold seep sediments.* P Natl Acad Sci USA, 2002. **99** (11): p. 7663-7668.
176. Orphan, V.J., et al., *Methane-consuming archaea revealed by directly coupled isotopic and phylogenetic analysis.* Science, 2001. **293** (5529): p. 484-487.
177. Boschker, H.T.S. and Middelburg, J.J., *Stable isotopes and biomarkers in microbial ecology.* FEMS Microbiology Ecology, 2002. **40** (2): p. 85-95.
178. Pelz, O., et al., *Use of isotopic and molecular techniques to link toluene degradation in denitrifying aquifer microcosms to specific microbial populations.* Archives of Microbiology, 2001. **175** (4): p. 270-281.
179. Johnsen, A.R., et al., *Linking of microorganisms to phenanthrene metabolism in soil by analysis of ^{13}C-labeled cell lipids.* Appl Environ Microb, 2002. **68** (12): p. 6106-6113.

180. Fierer, N. and Jackson, R.B., *The diversity and biogeography of soil bacterial communities.* P Natl Acad Sci USA, 2006. **103** (3): p. 626-631.
181. Sharp, C.E., et al., *Humboldt's spa: microbial diversity is controlled by temperature in geothermal environments.* The ISME Journal, 2014.
182. Ramirez, K.S., et al., *Biogeographic patterns in below-ground diversity in New York City's Central Park are similar to those observed globally.* Proc. R. Soc. B Biol. Sci., 2014. **281** (1795).
183. Saari, A., et al., *Methane oxidation in soil profiles of Dutch and Finnish coniferous forests with different soil texture and atmospheric nitrogen deposition.* Soil Biology and Biochemistry, 1997. **29** (11–12): p. 1625-1632.
184. Bender, M. and Conrad, R., *Effect of CH_4 concentrations and soil conditions on the induction of CH_4 oxidation activity.* Soil Biology and Biochemistry, 1995. **27** (12): p. 1517-1527.
185. Gebert, J., Groengroeft, A., and Pfeiffer, E.-M., *Relevance of soil physical properties for the microbial oxidation of methane in landfill covers.* Soil Biology and Biochemistry, 2011. **43** (9): p. 1759-1767.
186. Sass, R.L., et al., *Methane emissions from rice fields: effect of soil properties.* Global Biogeochemical Cycles, 1994. **8** (2): p. 135-140.
187. Singh, J.S., et al., *Effect of soil nitrogen, carbon and moisture on methane uptake by dry tropical forest soils.* Plant Soil, 1997. **196** (1): p. 115-121.
188. Blees, J., et al., *Micro-aerobic bacterial methane oxidation in the chemocline and anoxic water column of deep south-Alpine Lake Lugano (Switzerland).* Limnology and Oceanography, 2014. **59** (2): p. 311-324.
189. Henneberger, R., et al., *Field-scale tracking of active methane-oxidizing communities in a landfill-cover soil reveals spatial and seasonal variability.* Environmental Microbiology, 2014. **17**: p. 1721-1737.
190. Adamsen, A.P.S. and King, G.M., *Methane consumption in temperate and subarctic forest soils: Rates, vertical zonation, and responses to water and nitrogen.* Appl Environ Microb, 1993. **59** (2): p. 485-490.
191. Castro, M.S., et al., *Factors controlling atmospheric methane consumption by temperate forest soils.* Global Biogeochemical Cycles, 1995. **9** (1): p. 1-10.
192. Price, S.J., et al., *Environmental and chemical factors regulating methane oxidation in a New Zealand forest soil.* Aust. J. Soil Res., 2004. **42** (7): p. 767-776.
193. Whalen, S.C., Reeburgh, W.S., and Sandbeck, K.A., *Rapid methane oxidation in a landfill cover soil.* Appl Environ Microb, 1990. **56** (11): p. 3405-3411.
194. Cai, Z. and Yan, X., *Kinetic model for methane oxidation by paddy soil as affected by temperature, moisture and N addition.* Soil Biology and Biochemistry, 1999. **31** (5): p. 715-725.
195. West, A.E. and Schmidt, S.K., *Acetate stimulates atmospheric CH_4 oxidation by an alpine tundra soil.* Soil Biology and Biochemistry, 1999. **31** (12): p. 1649-1655.
196. Harriss, R.C., Sebacher, D.I., and Day Jr, F.P., *Methane flux in the Great Dismal Swamp.* Nature, 1982. **297** (5868): p. 673-674.
197. Kelley, C.A., Martens, C.S., and Ussler, W.I.I., *Methane dynamics across a tidally flooded riverbank margin.* Limnology and Oceanography, 1995. **40** (6): p. 1112-1129.

198. Melling, L., Hatano, R., and Kah, J.G., *Methane fluxes from three ecosystems in tropical peatland of Sarawak, Malaysia.* Soil Biology and Biochemistry, 2005. **37** (8): p. 1445-1453.
199. Jensen, S., et al., *Diversity in methane enrichments from agricultural soil revealed by DGGE separation of PCR amplified 16S rDNA fragments.* FEMS Microbiology Ecology, 1998. **26** (1): p. 17-26.
200. Hu, A. and Lu, Y., *The differential effects of ammonium and nitrate on methanotrophs in rice field soil.* Soil Biology and Biochemistry, 2015. **85**: p. 31-38.
201. Zhang, X., et al., *Effects of ammonium on the activity and community of methanotrophs in landfill biocover soils.* Systematic and Applied Microbiology, 2014. **37** (4): p. 296-304.
202. Noll, M., Frenzel, P., and Conrad, R., *Selective stimulation of type I methanotrophs in a rice paddy soil by urea fertilization revealed by RNA-based stable isotope probing.* FEMS Microbiology Ecology, 2008. **65** (1): p. 125-132.
203. Lee, S.W., et al., *Effect of nutrient and selective inhibitor amendments on methane oxidation, nitrous oxide production, and key gene presence and expression in landfill cover soils: Characterization of the role of methanotrophs, nitrifiers, and denitrifiers.* Appl Microbiol Biot, 2009. **85** (2): p. 389-403.
204. Bédard, C. and Knowles, R., *Physiology, biochemistry, and specific inhibitors of CH_4, NH_4^+, and CO oxidation by methanotrophs and nitrifiers.* Microbiological Reviews, 1989. **53** (1): p. 68-84.
205. Schnell, S. and King, G.M., *Mechanistic analysis of ammonium inhibition of atmospheric methane consumption in forest soils.* Appl Environ Microb, 1994. **60** (10): p. 3514-3521.
206. Duan, Z., et al., *The prediction of methane solubility in natural waters to high ionic strength from 0 to 250 °C and from 0 to 1600 bar.* Geochim. Cosmochim. Acta, 1992. **56** (4): p. 1451-1460.
207. Amend, J.P. and Shock, E.L., *Energetics of overall metabolic reactions of thermophilic and hyperthermophilic Archaea and Bacteria.* FEMS Microbiology Reviews, 2001. **25** (2): p. 175-243.
208. Geng, M. and Duan, Z., *Prediction of oxygen solubility in pure water and brines up to high temperatures and pressures.* Geochim. Cosmochim. Acta, 2010. **74** (19): p. 5631-5640.
209. King, G.M. and Adamsen, A.P.S., *Effects of temperature on methane consumption in a forest soil and in pure cultures of the methanotroph Methylomonas rubra.* Appl Environ Microb, 1992. **58** (9): p. 2758-2763.
210. Striegl, R.G., et al., *Consumption of atmospheric methane by desert soils.* Nature, 1992. **357** (6374): p. 145-147.
211. Bradford, M.A., et al., *Role of CH4 oxidation, production and transport in forest soil CH4 flux.* Soil Biol. Biochem., 2001. **33** (12-13): p. 1625-1631.
212. Chan, A.S.K. and Parkin, T.B., *Methane oxidation and production activity in soils from natural and agricultural ecosystems.* Journal of Environmental Quality, 2001. **30** (6): p. 1896-903.
213. Jensen, S., Priemé, A., and Bakken, L., *Methanol improves methane uptake in starved methanotrophic microorganisms.* Applied and Environmental Microbiology, 1998. **64** (3): p. 1143-1146.

214. Whittenbury, R., Davies, S.L., and Davey, J.F., *Exospores and cysts formed by methane-utilizing bacteria.* Microbiology, 1970. **61** (2): p. 219-226.
215. Dunfield, P.F. and Conrad, R., *Starvation alters the apparent half-saturation constant for methane in the type II methanotroph Methylocystis strain LR1.* Appl Environ Microb, 2000. **66** (9): p. 4136-4138.
216. Reim, A., et al., *One millimetre makes the difference: high-resolution analysis of methane-oxidizing bacteria and their specific activity at the oxic–anoxic interface in a flooded paddy soil.* The ISME Journal, 2012. **6**: p. 2128.
217. Chu, K.-H. and Alvarez-Cohen, L., *Evaluation of toxic effects of aeration and trichloroethylene oxidation on methanotrophic bacteria grown with different nitrogen sources.* Appl Environ Microb, 1999. **65** (2): p. 766-772.
218. Hernandez, M.E., et al., *Oxygen availability is a major factor in determining the composition of microbial communities involved in methane oxidation.* PeerJ, 2015. **3**: p. e801.
219. Kits, K.D., Klotz, M.G., and Stein, L.Y., *Methane oxidation coupled to nitrate reduction under hypoxia by the Gammaproteobacterium Methylomonas denitrificans, sp. nov. type strain FJG1.* Environmental Microbiology, 2015. **17**: p. 3219-3232.
220. Dam, B., et al., *Genome analysis coupled with physiological studies reveals a diverse nitrogen metabolism in Methylocystis sp. strain SC2.* Plos One, 2013. **8** (10).
221. Costa, C., et al., *The effect of oxygen on methanol oxidation by an obligate methanotrophic bacterium studied by in vivo ^{13}C nuclear magnetic resonance spectroscopy.* Journal of Industrial Microbiology and Biotechnology, 2001. **26** (1-2): p. 9-14.
222. Morita, R.Y., *Is H_2 the universal energy source for long-term survival?* Microbial Ecology, 1999. **38** (4): p. 307-320.
223. Greening, C., et al., *Persistence of the dominant soil phylum Acidobacteria by trace gas scavenging.* P Natl Acad Sci USA, 2015. **112** (33): p. 10497–10502.
224. Greening, C., et al., *A soil actinobacterium scavenges atmospheric H_2 using two membrane-associated, oxygen-dependent [NiFe] hydrogenases.* P Natl Acad Sci USA, 2014. **111** (11): p. 4257-4261.
225. Lenz, O., et al., *H_2 conversion in the presence of O_2 as performed by the membrane-bound [NiFe]-hydrogenase of Ralstonia eutropha.* ChemPhysChem, 2010. **11** (6): p. 1107-1119.
226. Greening, C., et al., *Genomic and metagenomic surveys of hydrogenase distribution indicate H_2 is a widely utilised energy source for microbial growth and survival.* The ISME Journal, 2015.
227. Chen, Y.P. and Yoch, D.C., *Regulation of two nickel-requiring (inducible and constitutive) hydrogenases and their coupling to nitrogenase in Methylosinus trichosporium OB3b.* J Bacteriol, 1987. **169** (10): p. 4778-4783.
228. Shah, N.N., et al., *Batch cultivation of Methylosinus trichosporium OB3B: IV. Production of hydrogen-driven soluble or particulate methane monooxygenase activity.* Biotechnology and Bioengineering, 1995. **45** (3): p. 229-238.

229. Hanczár, T., et al., *Detection and localization of two hydrogenases in Methylococcus capsulatus (Bath) and their potential role in methane metabolism.* Archives of Microbiology, 2002. **177** (2): p. 167-172.
230. Lieberman, R.L. and Rosenzweig, A.C., *Biological methane oxidation: Regulation, biochemistry, and active site structure of particulate methane monooxygenase.* Crit. Rev. Biochem. Mol. Biol., 2004. **39** (3): p. 147-164.
231. Kaasalainen, H. and Stefánsson, A., *The chemistry of trace elements in surface geothermal waters and steam, Iceland.* Chem. Geol., 2012. **330-331**: p. 60-85.
232. Tyler, G., *Rare earth elements in soil and plant systems - A review.* Plant Soil, 2004. **267** (1-2): p. 191-206.
233. Danilova, O.V., et al., *Methylomonas paludis sp. nov., the first acid-tolerant member of the genus Methylomonas, from an acidic wetland.* International Journal of Systematic and Evolutionary Microbiology, 2013. **63** (6): p. 2282-2289.
234. Geymonat, E., Ferrando, L., and Tarlera, S.E., *Methylogaea oryzae gen. nov., sp. nov., a mesophilic methanotroph isolated from a rice paddy field.* International Journal of Systematic and Evolutionary Microbiology, 2011. **61** (11): p. 2568-2572.
235. Henneberger, R., et al., *Field-scale labelling and activity quantification of methane-oxidizing bacteria in a landfill-cover soil.* FEMS Microbiology Ecology, 2013. **83** (2): p. 392-401.
236. Kizilova, A.K., et al., *Investigation of the methanotrophic communities of the hot springs of the Uzon caldera, Kamchatka, by molecular ecological techniques.* Microbiology, 2012. **81** (5): p. 606-613.
237. Sharp, C.E., et al., *Methanotrophic bacteria in warm geothermal spring sediments identified using stable isotope probing.* FEMS Microbiology Ecology, 2014. **90**: p. 92-102.
238. Castaldi, S. and Tedesco, D., *Methane production and consumption in an active volcanic environment of Southern Italy.* Chemosphere, 2005. **58** (2): p. 131-139.
239. Vigliotta, G., et al., *Clonothrix fusca Roze 1896, a filamentous, sheathed, methanotrophic γ-Proteobacterium.* Appl Environ Microb, 2007. **73** (11): p. 3556-3565.
240. Dunfield, P.F., et al., *Isolation of a Methylocystis strain containing a novel pmoA-like gene.* FEMS Microbiology Ecology, 2002. **41** (1): p. 17-26.
241. Yimga, M.T., et al., *Wide distribution of a novel pmoA-like gene copy among type II methanotrophs, and its expression in Methylocystis strain SC2.* Appl Environ Microb, 2003. **69** (9): p. 5593-5602.
242. Vekeman, B., et al., *New Methyloceanibacter diversity from North Sea sediments includes methanotroph containing solely the soluble methane monooxygenase.* Environmental Microbiology, 2016. **18** (12): p. 4523-4536.
243. Caporaso, J.G., et al., *Global patterns of 16S rRNA diversity at a depth of millions of sequences per sample.* P Natl Acad Sci USA, 2011. **108 Suppl 1**: p. 4516-22.
244. Whitman, W.B., Coleman, D.C., and Wiebe, W.J., *Prokaryotes: The unseen majority.* P Natl Acad Sci USA, 1998. **95** (12): p. 6578-6583.

245. Ramsing, N. and Gundersen, J., *Seawater and gases. Tabulated physical parameters of interest to people working with microsensors in marine systems*. 1994, Max Planck Institute for Marine Microbiology, Bremen, Germany
246. Castro, M.S., et al., *Soil moisture as a predictor of methane uptake by temperate forest soils.* CAN. J. FOR. RES., 1994. **24** (9): p. 1805-1810.
247. *One Thousand Springs: The microbiology of geothermal hotsprings in New Zealand*. 2013 27/8/14]; Available from: http://1000springs.org.nz/.
248. Dumbleton, M.J., *The British soil classification system for engineering purposes: its development and relation to other comparable systems.* UK Transport & Road Research Laboratory, Laboratory Report, 1981 (LR 1030).
249. Andrews, S. FastQC: A quality control tool for high throughput sequence data. 2010. Available online at http://www.bioinformatics.babraham.ac.uk/projects/fastqc/
250. Edgar, R.C., *Search and clustering orders of magnitude faster than BLAST.* Bioinformatics, 2010. **26** (19): p. 2460-2461.
251. Schloss, P.D., et al., *Introducing mothur: Open-source, platform-independent, community-supported software for describing and comparing microbial communities.* Appl Environ Microb, 2009. **75** (23): p. 7537-7541.
252. Caporaso, J.G., et al., *QIIME allows analysis of high-throughput community sequencing data.* Nat. Methods, 2010. **7** (5): p. 335-336.
253. Wang, Q., et al., *Naïve Bayesian classifier for rapid assignment of rRNA sequences into the new bacterial taxonomy.* Appl Environ Microb, 2007. **73** (16): p. 5261-5267.
254. Quast, C., et al., *The SILVA ribosomal RNA gene database project: Improved data processing and web-based tools.* Nucleic Acids Research, 2013. **41** (D1): p. D590-D596.
255. Corteselli, E.M., Aitken, M.D., and Singleton, D.R., *Description of Immundisolibacter cernigliae gen. nov., sp. nov., a high-molecular-weight polycyclic aromatic hydrocarbon-degrading bacterium within the class Gammaproteobacteria, and proposal of Immundisolibacterales ord. nov. and Immundisolibacteraceae fam. nov.* International Journal of Systematic and Evolutionary Microbiology, 2016. **67** (4): p. 925-931.
256. Teramoto, M., Yagyu, K.-i., and Nishijima, M., *Perspicuibacter marinus gen. nov., sp. nov., a semi-transparent bacterium isolated from surface seawater, and description of Arenicellaceae fam. nov. and Arenicellales ord. nov.* International Journal of Systematic and Evolutionary Microbiology, 2015. **65** (2): p. 353-358.
257. Chao, A., *Nonparametric estimation of the number of classes in a population.* Scandinavian Journal of Statistics, 1984. **11** (4): p. 265-270.
258. Shannon, C.E. and Weaver, W., *The Mathematical Theory of Communication*. 1963: University of Illinois Press.
259. Simpson, E.H., *Measurement of diversity.* Nature, 1949. **163** (4148): p. 688.
260. Lozupone, C.A., et al., *Quantitative and qualitative β diversity measures lead to different insights into factors that structure microbial communities.* Appl Environ Microb, 2007. **73** (5): p. 1576-1585.
261. Mantel, N., *The detection of disease clustering and a generalized regression approach.* Cancer Res, 1967. **27**: p. 209-220.

262. McDonald, A.I., *Handbook of Biological Statistics*. 3rd. ed. 2014, Baltimore, Maryland: Sparky House Publishing.
263. Anderson, M.J., *A new method for non-parametric multivariate analysis of variance.* Austral Ecology, 2001. **26** (1): p. 32-46.
264. Anderson, M.J. and Walsh, D.C.I., *PERMANOVA, ANOSIM, and the Mantel test in the face of heterogeneous dispersions: What null hypothesis are you testing?* Ecol. Monogr., 2013. **83** (4): p. 557-574.
265. Fagerland, M.W. and Sandvik, L., *The Wilcoxon-Mann-Whitney test under scrutiny.* Stat. Med., 2009. **28** (10): p. 1487-1497.
266. Corder, G.W. and Foreman, D.I., *Comparing More Than Two Related Samples: The Friedman Test*, in *Nonparametric Statistics for Non-Statisticians*, Corder, G.W. and Foreman, D.I., Editors. 2011, Wiley: Hoboken, New Jersey.
267. Lozupone, C. and Knight, R., *UniFrac: A new phylogenetic method for comparing microbial communities.* Appl Environ Microb, 2005. **71** (12): p. 8228-8235.
268. Garrity, G.M., Bell, J.A., and Lilburn, T., *The family Pseudomonadaceae*, in *Bergey's Manual of Systematic Bacteriology*, Brenner, D.J., Krieg, N.R., and Staley, J.T., Editors. 2005, Springer: New York. p. 323-411.
269. Imachi, H., et al., *Exilispira thermophila gen. nov., sp. nov., an anaerobic, thermophilic spirochaete isolated from a deep-sea hydrothermal vent chimney.* International Journal of Systematic and Evolutionary Microbiology, 2008. **58** (10): p. 2258-2265.
270. Reysenbach, A.L., et al., *Mesoaciditoga lauensis gen. nov., sp. nov., a moderately thermoacidophilic member of the order Thermotogales from a deep-sea hydrothermal vent.* International Journal of Systematic and Evolutionary Microbiology, 2013. **63** (12): p. 4724-4729.
271. Huber, H. and Stetter, K.O., *The Order Sulfolobales*, in *Bergey's Manual of Systematic Bacteriology*, Boone, D.R. and Castenholz, R.W., Editors. 2001, Springer: New York. p. 198-210.
272. Hanada, S., et al., *Crenotalea thermophila gen. nov., sp. nov., a member of the family Chitinophagaceae isolated from a hot spring*. International Journal of Systematic and Evolutionary Microbiology, 2014. **64** (4): p. 1359-1364.
273. van Teeseling, M.C.F., et al., *Expanding the verrucomicrobial methanotrophic world: Description of three novel species of Methylacidimicrobium gen. nov.* Appl Environ Microb, 2014. **80** (21): p. 6782-6791.
274. Dunfield, P., et al., *Methane production and consumption in temperate and subarctic peat soils: Response to temperature and pH.* Soil Biology and Biochemistry, 1993. **25** (3): p. 321-326.
275. Saari, A., Rinnan, R., and Martikainen, P.J., *Methane oxidation in boreal forest soils: Kinetics and sensitivity to pH and ammonium.* Soil Biology and Biochemistry, 2004. **36** (7): p. 1037-1046.
276. Gardener, M., *Statistics for ecologists using R and Excel*. 2nd ed. 2017, Exeter: Pelagic Publishing.
277. Lee, K.C., et al., *The Chthonomonas calidirosea genome is highly conserved across geographic locations and distinct chemical and microbial environments in New Zealand's Taupō Volcanic Zone.* Appl Environ Microb, 2016. **82** (12): p. 3572-3581.

278. Albuquerque, L. and da Costa, M.S., *The Family Thermaceae*, in *The Prokaryotes - Other Major Lineages of Bacteria and the Archaea*, Rosenberg, E., et al., Editors. 2014, Springer-Verlag: Berlin.
279. Reysenbach, A.L., *Thermoplasmata class.nov.*, in *Bergey's Manual of Systematic Bacteriology*, Boone, D.R. and Castenholz, R.W., Editors. 2001, Springer: New York. p. 335-340.
280. Miroshnichenko, M.L., et al., *Caldimicrobium rimae gen. nov., sp, nov., an extremely thermophilic, facultatively lithoautotrophic, anaerobic bacterium from the Uzon Caldera, Kamchatka.* International Journal of Systematic and Evolutionary Microbiology, 2009. **59** (5): p. 1040-1044.
281. Kojima, H., Umezawa, K., and Fukui, M., *Caldimicrobium thiodismutans sp. nov., a sulfur-disproportionating bacterium isolated from a hot spring, and emended description of the genus Caldimicrobium.* International Journal of Systematic and Evolutionary Microbiology, 2016. **66** (4): p. 1828-1831.
282. Freund, F., Dickinson, J.T., and Cash, M., *Hydrogen in rocks: an energy source for deep microbial communities.* Astrobiology, 2002. **2** (1): p. 83-92.
283. Albers, S.-V. and Siebers, B., *The Family Sulfolobaceae*, in *The Prokaryotes - Other Major Lineages of Bacteria and the Archaea*, Rosenberg, E., et al., Editors. 2014, Springer-Verlag: Berlin.
284. Levy-Booth, D.J., et al., *Cycling of extracellular DNA in the soil environment.* Soil Biology and Biochemistry, 2007. **39** (12): p. 2977-2991.
285. Carini, P., et al., *Relic DNA is abundant in soil and obscures estimates of soil microbial diversity.* Nature Microbiology, 2016. **2**: p. 16242.
286. Nocker, A., et al., *Use of propidium monoazide for live/dead distinction in microbial ecology.* Appl Environ Microb, 2007. **73** (16): p. 5111-5117.
287. Lazar, C.S., et al., *Genomic evidence for distinct carbon substrate preferences and ecological niches of Bathyarchaeota in estuarine sediments.* Environmental Microbiology, 2016. **18** (4): p. 1200-11.
288. Scheller, S., et al., *Artificial electron acceptors decouple archaeal methane oxidation from sulfate reduction.* Science, 2016. **351** (6274): p. 703-707.
289. Kantor, R.S., et al., *Small genomes and sparse metabolisms of sediment-associated bacteria from four candidate phyla.* mBio, 2013. **4** (5).
290. Brown, C.T., et al., *Unusual biology across a group comprising more than 15% of domain Bacteria.* Nature, 2015. **523** (7559): p. 208-211.
291. Nelson, W. and Stegen, J., *The reduced genomes of Parcubacteria (OD1) contain signatures of a symbiotic lifestyle.* Frontiers in Microbiology, 2015. **6** (713).
292. Riis, V., Miethe, D., and Babel, W., *Formate-stimulated oxidation of methanol by Pseudomonas putida 9816.* Bioscience, Biotechnology and Biochemistry, 2003. **67** (4): p. 684-690.
293. Bowman, J., *The Methanotrophs - The families Methylococcaceae and Methylocystaceae*, in *The Prokaryotes*, Falkow, S., et al., Editors. 2006, Springer. p. 266-289.
294. Dedysh, S.N., Haupt, E.S., and Dunfield, P.F., *Emended description of the family Beijerinckiaceae and transfer of the genera Chelatococcus and Camelimonas to the family Chelatococcaceae fam. nov.* International Journal of Systematic and Evolutionary Microbiology, 2016. **66** (8): p. 3177-3182.

295. Vorobev, A.V., et al., *Methyloferula stellata gen. nov., sp. nov., an acidophilic, obligately methanotrophic bacterium that possesses only a soluble methane monooxygenase.* International Journal of Systematic and Evolutionary Microbiology, 2011. **61** (10): p. 2456-2463.
296. Vesty, A., et al., *Evaluating the impact of DNA extraction method on the representation of human oral bacterial and fungal communities.* Plos One, 2017. **12** (1).
297. Acinas, S.G., et al., *PCR-induced sequence artifacts and bias: Insights from comparison of two 16S rRNA clone libraries constructed from the same sample.* Appl Environ Microb, 2005. **71** (12): p. 8966-8969.
298. Fouhy, F., et al., *16S rRNA gene sequencing of mock microbial populations-impact of DNA extraction method, primer choice and sequencing platform.* BMC Microbiology, 2016. **16** (1).
299. Chandler, D.P., Fredrickson, J.K., and Brockman, F.J., *Effect of PCR template concentration on the composition and distribution of total community 16S rDNA clone libraries.* Molecular Ecology, 1997. **6** (5): p. 475-482.
300. Raynaud, X. and Nunan, N., *Spatial Ecology of Bacteria at the Microscale in Soil.* Plos One, 2014. **9** (1): p. e87217.
301. Roesch, L.F.W., et al., *Pyrosequencing enumerates and contrasts soil microbial diversity.* The ISME Journal, 2007. **1** (4): p. 283-290.
302. Edgar, R.C. and Flyvbjerg, H., *Error filtering, pair assembly and error correction for next-generation sequencing reads.* Bioinformatics, 2014. **31** (21): p. 3476-3482.
303. Liu, W.-T., Guo, H., and Wu, J.-H., *Effects of target length on the hybridization efficiency and specificity of rRNA-based oligonucleotide microarrays.* Appl Environ Microb, 2007. **73** (1): p. 73-82.
304. Tourova, T.P., *Copy number of ribosomal operons in prokaryotes and its effect on phylogenetic analyses.* Microbiology, 2003. **72** (4): p. 389-402.
305. Lennon, J.T. and Jones, S.E., *Microbial seed banks: the ecological and evolutionary implications of dormancy.* Nature Reviews Microbiology, 2011. **9**: p. 119.
306. Bhaya, D., et al., *Population level functional diversity in a microbial community revealed by comparative genomic and metagenomic analyses.* ISME Journal, 2007. **1** (8): p. 703-713.
307. Chen, Y. and Murrell, J.C., *When metagenomics meets stable-isotope probing: Progress and perspectives.* Trends in Microbiology, 2010. **18** (4): p. 157-163.
308. Wang, Y., Hayatsu, M., and Fujii, T., *Extraction of bacterial RNA from soil: Challenges and solutions.* Microbes and Environments, 2012. **27** (2): p. 111-121.
309. Rinke, C., et al., *Insights into the phylogeny and coding potential of microbial dark matter.* Nature, 2013. **499** (7459): p. 431-437.
310. Langille, M.G.I., et al., *Predictive functional profiling of microbial communities using 16S rRNA marker gene sequences.* Nat. Biotechnol., 2013. **31** (9): p. 814-821.
311. Bowman, J.S. and Ducklow, H.W., *Microbial communities can be described by metabolic structure: A general framework and application to a seasonally variable, depth-stratified microbial community from the coastal West Antarctic Peninsula.* Plos One, 2015. **10** (8): p. e0135868.

312. Asshauer, K.P., et al., *Tax4Fun: predicting functional profiles from metagenomic 16S rRNA data.* Bioinformatics, 2015. **31** (17): p. 2882-4.
313. Xu, Z., et al., *Which is more important for classifying microbial communities: who's there or what they can do?* The ISME Journal, 2014. **8** (12): p. 2357-2359.
314. The Human Microbiome Project, C., *Structure, function and diversity of the healthy human microbiome.* Nature, 2012. **486**: p. 207.
315. Olins, H.C., et al., *Co-registered geochemistry and metatranscriptomics reveal unexpected distributions of microbial activity within a hydrothermal vent field.* Frontiers in Microbiology, 2017. **8** (1042).
316. Chistoserdova, L., Kalyuzhnaya, M.G., and Lidstrom, M.E., *Cycling single-carbon compounds: From omics to novel concepts: Formerly obscure microbial species emerge as major players in environmental cycling of carbon and nitrogen.* Microbe, 2013. **8** (10): p. 395-400.
317. Ho, A., et al., *The more, the merrier: heterotroph richness stimulates methanotrophic activity.* The ISME Journal, 2014. **8** (1945-1948).
318. Ozsolak, F. and Milos, P.M., *RNA sequencing: advances, challenges and opportunities.* Nature Reviews. Genetics, 2011. **12** (2): p. 87-98.
319. Kalyuzhnaya, M.G., et al., *Classification of halo(alkali)philic and halo(alkali)tolerant methanotrophs provisionally assigned to the genera Methylomicrobium and Methylobacter and emended description of the genus Methylomicrobium.* International Journal of Systematic and Evolutionary Microbiology, 2008. **58** (3): p. 591-596.
320. Dunfield, P.F., et al., *Methylocella silvestris sp. nov., a novel methanotroph isolated from an acidic forest cambisol.* International Journal of Systematic and Evolutionary Microbiology, 2003. **53** (5): p. 1231-1239.
321. Hoefman, S., Heylen, K., and De Vos, P., *Methylomonas lenta sp. nov., a methanotroph isolated from manure and a denitrification tank.* International Journal of Systematic and Evolutionary Microbiology, 2014. **64** (4): p. 1210-1217.
322. Dedysh, S.N., et al., *Methylocystis heyeri sp. nov., a novel type II methanotrophic bacterium possessing 'signature' fatty acids of type I methanotrophs.* International Journal of Systematic and Evolutionary Microbiology, 2007. **57** (3): p. 472-479.
323. Dedysh, S.N., et al., *Methylocapsa palsarum sp. nov., a methanotroph isolated from a sub-Arctic discontinuous permafrost ecosystem.* International Journal of Systematic and Evolutionary Microbiology, 2015. **65** (10): p. 3618-3624.
324. Afgan, E., et al., *The Galaxy platform for accessible, reproducible and collaborative biomedical analyses: 2016 update.* Nucleic Acids Research, 2016. **44** (W1): p. W3-W10.
325. Bolger, A.M., Lohse, M., and Usadel, B., *Trimmomatic: A flexible trimmer for Illumina sequence data.* Bioinformatics, 2014. **30** (15): p. 2114-2120.
326. Gruening, B.A. Galaxy Tool wrappers. 2014. Available online at https://github.com/bgruening/galaxytools
327. Grabherr, M.G., et al., *Full-length transcriptome assembly from RNA-Seq data without a reference genome.* Nat. Biotechnol., 2011. **29** (7): p. 644-652.

328. Haas, B.J., et al., *De novo transcript sequence reconstruction from RNA-seq using the Trinity platform for reference generation and analysis.* Nature Protocols, 2013. **8** (8): p. 1494-1512.
329. Besemer, J. and Borodovsky, M., *Heuristic approach to deriving models for gene finding.* Nucleic Acids Research, 1999. **27** (19): p. 3911-3920.
330. Zhu, W., Lomsadze, A., and Borodovsky, M., *Ab initio gene identification in metagenomic sequences.* Nucleic Acids Research, 2010. **38** (12): p. e132-e132.
331. Khan, A.M. DuplicatesFinder. 2009. Available online at proline.bic.nus.edu.sg/~asif/tools
332. Huang, Y., et al., *CD-HIT Suite: A web server for clustering and comparing biological sequences.* Bioinformatics, 2010. **26** (5): p. 680-682.
333. Altschul, S.F., et al., *Gapped BLAST and PSI-BLAST: A new generation of protein database search programs.* Nucleic Acids Research, 1997. **25** (17): p. 3389-3402.
334. Camacho, C., et al., *BLAST+: Architecture and applications.* BMC Bioinform., 2009. **10**: p. 421.
335. Kanehisa, M., et al., *KEGG as a reference resource for gene and protein annotation.* Nucleic Acids Research, 2016. **44** (Database issue): p. D457-D462.
336. Patro, R., et al., *Salmon provides fast and bias-aware quantification of transcript expression.* Nat. Methods, 2017. **14** (4): p. 417-419.
337. Mount, D.W., *Bioinformatics: Sequence and Genome Analysis*. 2nd ed. 2004, New York: Cold Spring Harbour Laboratory Press.
338. Geer, L.Y., et al., *CDART: Protein homology by domain architecture.* Genome Res., 2002. **12** (10): p. 1619-1623.
339. Zahn, J.A., et al., *Membrane-associated quinoprotein formaldehyde dehydrogenase from Methylococcus capsulatus Bath.* J Bacteriol, 2001. **183** (23): p. 6832-6840.
340. Anthony, C., *Quinoprotein-catalysed reactions.* Biochemical Journal, 1996. **320** (3): p. 697-711.
341. Chistoserdova, L., *Lanthanides: New life metals?* World Journal of Microbiology and Biotechnology, 2016. **32** (8).
342. Guisbert , E., et al., *Hfq modulates the σ^E-mediated envelope stress response and the σ^{32}-mediated cytoplasmic stress response in Escherichia coli.* J Bacteriol, 2007. **189** (5): p. 1963-1973.
343. Balandina, A., Kamashev, D., and Rouviere-Yaniv, J., *The bacterial histone-like protein HU specifically recognizes similar structures in all nucleic acids: DNA, RNA, and their hybrids.* J Biol Chem, 2002. **277** (31): p. 27622-27628.
344. Keto-Timonen, R., et al., *Cold shock proteins: A minireview with special emphasis on Csp-family of Enteropathogenic Yersinia.* Frontiers in Microbiology, 2016. **7**: p. 1151.
345. Bepperling, A., et al., *Alternative bacterial two-component small heat shock protein systems.* P Natl Acad Sci USA, 2012. **109** (50): p. 20407-20412.
346. Romeo, T., Vakulskas, C.A., and Babitzke, P., *Posttranscriptional regulation on a global scale: Form and function of Csr/Rsm systems.* Environmental Microbiology, 2013. **15** (2): p. 313-324.

347. Revelles, O., et al., *The Carbon Storage Regulator (Csr) System Exerts a Nutrient-Specific Control over Central Metabolism in Escherichia coli Strain Nissle 1917.* Plos One, 2013. **8** (6): p. e66386.
348. Pannuri, A., et al., *Translational repression of NhaR, a novel pathway for multi-tier regulation of biofilm circuitry by CsrA.* J Bacteriol, 2012. **194** (1): p. 79-89.
349. Wei, B.L., et al., *Positive regulation of motility and flhDC expression by the RNA-binding protein CsrA of Escherichia coli.* Molecular Microbiology, 2001. **40** (1): p. 245-256.
350. Sze, C.W. and Li, C., *Inactivation of bb0184, which encodes carbon storage regulator A, represses the infectivity of Borrelia burgdorferi.* Infection and Immunity, 2011. **79** (3): p. 1270-1279.
351. VanOrsdel, C.E., et al., *The Escherichia coli CydX protein is a member of the CydAB cytochrome bd oxidase complex and is required for cytochrome bd oxidase activity.* J Bacteriol, 2013. **195** (16): p. 3640-50.
352. Schonbrunner, E.R. and Schmid, F.X., *Peptidyl-prolyl cis-trans isomerase improves the efficiency of protein disulfide isomerase as a catalyst of protein folding.* P Natl Acad Sci USA, 1992. **89** (10): p. 4510-3.
353. Byers, D.M. and Gong, H., *Acyl carrier protein: structure–function relationships in a conserved multifunctional protein family.* Biochemistry and Cell Biology, 2007. **85** (6): p. 649-662.
354. Ideno, A., et al., *FK506-binding protein of the hyperthermophilic archaeum, Thermococcus sp. KS-1, a cold-shock-inducible peptidyl-prolyl cis-trans isomerase with activities to trap and refold denatured proteins.* Biochemical Journal, 2001. **357** (2): p. 465-471.
355. He, J.Z., Hu, H.W., and Zhang, L.M., *Current insights into the autotrophic thaumarchaeal ammonia oxidation in acidic soils.* Soil Biology and Biochemistry, 2012. **55**: p. 146-154.
356. Lebedeva, E.V., et al., *Enrichment and genome sequence of the group I.1a ammonia-oxidizing archaeon "Ca. Nitrosotenuis uzonensis" representing a clade globally distributed in thermal habitats.* Plos One, 2013. **8** (11).
357. Stieglmeier, M., et al., *Nitrososphaera viennensis gen. nov., sp. nov., an aerobic and mesophilic, ammonia-oxidizing archaeon from soil and a member of the archaeal phylum Thaumarchaeota.* International Journal of Systematic and Evolutionary Microbiology, 2014. **64** (8): p. 2738-2752.
358. Jung, M.Y., et al., *Nitrosarchaeum koreense gen. nov., sp. nov., an aerobic and mesophilic, ammonia-oxidizing archaeon member of the phylum Thaumarchaeota isolated from agricultural soil.* International Journal of Systematic and Evolutionary Microbiology, 2018. **68** (10): p. 3084-3095.
359. Duan, Z. and Mao, S., *A thermodynamic model for calculating methane solubility, density and gas phase composition of methane-bearing aqueous fluids from 273 to 523 K and from 1 to 2000 bar.* Geochim. Cosmochim. Acta, 2006. **70** (13): p. 3369-3386.
360. Könneke, M., et al., *Isolation of an autotrophic ammonia-oxidizing marine archaeon.* Nature, 2005. **437** (7058): p. 543-546.
361. Tourna, M., et al., *Nitrososphaera viennensis, an ammonia oxidizing archaeon from soil.* P Natl Acad Sci USA, 2011. **108** (20): p. 8420-8425.
362. Altschul, S.F., et al., *Basic local alignment search tool.* Journal of Molecular Biology, 1990. **215** (3): p. 403-410.
363. Shiryev, S.A., et al., *Improved BLAST searches using longer words for protein seeding.* Bioinformatics, 2007. **23** (21): p. 2949-2951.

364. Knight, R., et al., *Best practices for analysing microbiomes.* Nature Reviews Microbiology, 2018. **16** (7): p. 410-422.
365. Bikel, S., et al., *Combining metagenomics, metatranscriptomics and viromics to explore novel microbial interactions: towards a systems-level understanding of human microbiome.* Computational and Structural Biotechnology Journal, 2015. **13**: p. 390-401.
366. Dubnau, D., *DNA uptake in bacteria.* Annual Review of Microbiology, 1999. **53** (1): p. 217-244.
367. Giltner, C.L., Nguyen, Y., and Burrows, L.L., *Type IV pilin proteins: Versatile molecular modules.* Microbiology and Molecular Biology Reviews, 2012. **76** (4): p. 740-772.
368. Finn, R.D., et al., *InterPro in 2017-beyond protein family and domain annotations.* Nucleic Acids Research, 2017. **45** (D1): p. D190-D199.
369. Weisburg, W.G., et al., *16S ribosomal DNA amplification for phylogenetic study.* J Bacteriol, 1991. **173** (2): p. 697-703.
370. Costello, A.M. and Lidstrom, M.E., *Molecular characterization of functional and phylogenetic genes from natural populations of methanotrophs in lake sediments.* Appl Environ Microb, 1999. **65** (11): p. 5066-5074.
371. Auman, A.J., et al., *Molecular characterization of methanotrophic isolates from freshwater lake sediment.* Appl Environ Microb, 2000. **66** (12): p. 5259-5266.
372. Jukes, T.H. and Cantor, C.R., *Evolution of protein molecules*, in *Mammalian Protein Metabolism*, Munro., H.N., Editor. 1969, Academic Press.: New York. p. pp. 21-132.
373. Jones, D.T., Taylor, W.R., and Thornton, J.M., *The rapid generation of mutation data matrices from protein sequences.* Bioinformatics, 1992. **8** (3): p. 275-282.
374. Bates, R.G., *Revised standard values for pH measurements from 0 to 95 °C.* J. Res. NBS A Phys. Ch., 1962. **66A** (2): p. 179-184.
375. Law, V., et al., *DrugBank 4.0: shedding new light on drug metabolism.* Nucleic Acids Research, 2014. **42** (Database issue): p. D1091-7.
376. Łowicki, D. and Huczyński, A., *Structure and antimicrobial properties of monensin a and its derivatives: Summary of the achievements.* BioMed Research International, 2013. **2013**.
377. Peteranderl, R., Shotts, E.B., and Wiegel, J., *Stability of antibiotics under growth conditions for thermophilic anaerobes.* Appl Environ Microb, 1990. **56** (6): p. 1981-1983.
378. Lagutin, K., et al., *Novel long-chain diol phospholipids from some bacteria belonging to the class Thermomicrobia.* Lipids, 2014: p. 1-9.
379. Stránský, K., et al., *An improved method of characterizing fatty acids by equivalent chain length values.* Journal of High Resolution Chromatography, 1992. **15** (11): p. 730-740.
380. Guckert, J.B., et al., *Phospholipid, ester-linked fatty acid profiles as reproducible assays for changes in prokaryotic community structure of estuarine sediments.* FEMS Microbiology Letters, 1985. **31** (3): p. 147-158.
381. Galchenko, V.F., et al., *Isolation and properties of new strains of obligate methanotrophs.* Microbiology, 1977. **46** (5): p. 890-897.

382. Lindner, A.S., et al., *Methylocystis hirsuta sp. nov., a novel methanotroph isolated from a groundwater aquifer.* International Journal of Systematic and Evolutionary Microbiology, 2007. **57** (8): p. 1891-1900.
383. Sargent, M.G., *A procedure for isolating high quality DNA from spores of Bacillus subtilis 168.* Journal of General Microbiology, 1980. **116** (2): p. 511-514.
384. Hoefman, S., et al., *Miniaturized extinction culturing is the preferred strategy for rapid isolation of fast-growing methane-oxidizing bacteria.* Microbial Biotechnology, 2012. **5** (3): p. 368-378.
385. Kaeberlein, T., Lewis, K., and Epstein, S.S., *Isolating "uncultivable" microorganisms in pure culture in a simulated natural environment.* Science, 2002. **296** (5570): p. 1127-1129.
386. Bollmann, A., Lewis, K., and Epstein, S.S., *Incubation of environmental samples in a diffusion chamber increases the diversity of recovered isolates.* Appl Environ Microb, 2007. **73** (20): p. 6386-6390.
387. Bomar, L., et al., *Directed culturing of microorganisms using metatranscriptomics.* mBio, 2011. **2** (2).
388. Veraart, A.J., et al., *Living apart together—bacterial volatiles influence methanotrophic growth and activity.* The ISME Journal, 2018. **12** (4): p. 1163-1166.
389. Krause, S.M.B., et al., *Lanthanide-dependent cross-feeding of methane-derived carbon is linked by microbial community interactions.* P Natl Acad Sci USA, 2017. **114** (2): p. 358-363.
390. Hou, C.T., Laskin, A.I., and Patel, R.N., *Growth and polysaccharide production by Methylocystis parvus OBBP on methanol.* Appl Environ Microb, 1979. **37** (5): p. 800-804.
391. Markowitz, V.M., et al., *IMG: the integrated microbial genomes database and comparative analysis system.* Nucleic Acids Research, 2012. **40** (D1): p. D115-D122.
392. Rudolph, B., et al., *Evolution of Escherichia coli for growth at high temperatures.* J Biol Chem, 2010. **285** (25): p. 19029-19034.
393. Pumirat, P., et al., *Effects of sodium chloride on heat resistance, oxidative susceptibility, motility, biofilm and plaque formation of Burkholderia pseudomallei.* MicrobiologyOpen, 2017. **6** (4).
394. Reina-Bueno, M., et al., *Role of trehalose in salinity and temperature tolerance in the model halophilic bacterium Chromohalobacter salexigens.* Plos One, 2012. **7** (3).
395. Reina-Bueno, M., et al., *Role of trehalose in heat and desiccation tolerance in the soil bacterium Rhizobium etli.* BMC Microbiology, 2012. **12** (1): p. 207.
396. Zhang, Q. and Yan, T., *Correlation of intracellular trehalose concentration with desiccation resistance of soil Escherichia coli populations.* Appl Environ Microb, 2012. **78** (20): p. 7407-7413.
397. Petitjean, M., et al., *Yeast tolerance to various stresses relies on the trehalose-6P synthase (Tps1) protein, not on trehalose.* J Biol Chem, 2015. **290** (26): p. 16177-16190.
398. Kip, N., et al., *Detection, isolation, and characterization of acidophilic methanotrophs from sphagnum mosses.* Appl Environ Microb, 2011. **77** (16): p. 5643-5654.

399. Hoefman, S., et al., *Survival or revival: Long-term preservation induces a reversible viable but non-culturable state in methane-oxidizing bacteria.* Plos One, 2012. **7** (4).
400. Singh, B., et al., *Thermophilic molds: Biology and applications.* Crit. Rev. Microbiol., 2016. **42** (6): p. 985-1006.
401. Garg, N., et al., *Lantibiotics from Geobacillus thermodenitrificans.* P Natl Acad Sci USA, 2012. **109** (14): p. 5241-5246.
402. Shivlata, L. and Satyanarayana, T., *Thermophilic and alkaliphilic Actinobacteria: Biology and potential applications.* Frontiers in Microbiology, 2015. **6**.
403. Mishra, R.R., et al., *Characterization and evaluation of stress and heavy metal tolerance of some predominant Gram-negative halotolerant bacteria from mangrove soils of Bhitarkanika, Orissa, India.* African Journal of Biotechnology, 2009. **8** (10): p. 2224-2231.
404. Descheemaeker, P., et al., *Macrolide resistance and erythromycin resistance determinants among Belgian Streptococcus pyogenes and Streptococcus pneumoniae isolates.* Journal of Antimicrobial Chemotherapy, 2000. **45** (2): p. 167-173.
405. Jacoby, G.A., *Mechanisms of Resistance to Quinolones.* Clinical Infectious Diseases, 2005. **41** (Supplement_2): p. S120-S126.
406. Kojima, M., Yamada, Y., and Umezawa, H., *Studies on the biosynthesis of kanamycins.* Agricultural and Biological Chemistry, 1968. **32** (4): p. 467-473.
407. Xiong, Y.Q., et al., *Influence of pH on adaptive resistance of Pseudomonas aeruginosa to aminoglycosides and their postantibiotic effects.* Antimicrobial Agents and Chemotherapy, 1996. **40** (1): p. 35-9.
408. Mingeot-Leclercq, M.-P., Glupczynski, Y., and Tulkens, P.M., *Aminoglycosides: Activity and resistance.* Antimicrobial Agents and Chemotherapy, 1999. **43** (4): p. 727-737.
409. Rhazi-Filali, F., et al., *A β-lactamase produced by a thermophilic Bacillus.* FEMS Microbiology Letters, 1996. **140** (1): p. 61-64.
410. Ozcengiz, G. and Demain, A.L., *Recent advances in the biosynthesis of penicillins, cephalosporins and clavams and its regulation.* Biotechnology Advances, 2013. **31** (2): p. 287-311.
411. Bush, K. and Jacoby, G.A., *Updated functional classification of β-lactamases.* Antimicrobial Agents and Chemotherapy, 2010. **54** (3): p. 969-976.
412. Olaitan, A.O., Morand, S., and Rolain, J.-M., *Mechanisms of polymyxin resistance: acquired and intrinsic resistance in bacteria.* Frontiers in Microbiology, 2014. **5** (643).
413. Chopra, I. and Roberts, M., *Tetracycline antibiotics: Mode of action, applications, molecular biology, and epidemiology of bacterial resistance.* Microbiology and Molecular Biology Reviews, 2001. **65** (2): p. 232-260.
414. Connell, S.R., et al., *Ribosomal protection proteins and their mechanism of tetracycline resistance.* Antimicrobial Agents and Chemotherapy, 2003. **47** (12): p. 3675-3681.
415. Adamczuk, M. and Dziewit, L., *Genome-based insights into the resistome and mobilome of multidrug-resistant Aeromonas sp. ARM81 isolated from wastewater.* Archives of Microbiology, 2017. **199** (1): p. 177-183.

416. Schlesner, H., et al., *Taxonomic heterogeneity within the Planctomycetales as derived by DNA-DNA hybridization, description of Rhodopirellula baltica gen. nov., sp. nov., transfer of Perillula marina to the genus Blastopirellula gen. nov. as Blastopirellula marina comb. nov. and emended description of the genus Pirellula.* International Journal of Systematic and Evolutionary Microbiology, 2004. **54** (5): p. 1567-1580.
417. Rivas-Marín, E., et al., *Development of genetic tools for the manipulation of the planctomycetes.* Frontiers in Microbiology, 2016. **7**.
418. Abbas, C.A. and Card, G.L., *The relationships between growth temperature, fatty acid composition and the physical state and fluidity of membrane lipids in Yersinia enterocolitica.* Biochimica et Biophysica Acta - Biomembranes, 1980. **602** (3): p. 469-476.
419. Weerkamp, A. and Heinen, W., *Effect of temperature on the fatty acid composition of the extreme thermophiles, Bacillus caldolyticus and Bacillus caldotenax.* J Bacteriol, 1972. **109** (1): p. 443-446.
420. Börjesson, G. and Svensson, B.H., *Seasonal and diurnal methane emissions from a landfill and their regulation by methane oxidation.* Waste Management & Research, 1997. **15** (1): p. 33-54.
421. Dalal, R.C. and Allen, D.E., *Turner review no. 18. Greenhouse gas fluxes from natural ecosystems.* Aust. J. Bot., 2008. **56** (5): p. 369-407.
422. Sheppard, S.K. and Lloyd, D., *Effects of soil amendment on gas depth profiles in soil monoliths using direct mass spectrometric measurement.* Bioresource Technology, 2002. **84** (1): p. 39-47.
423. Theisen, A.R. and Murrell, J.C., *Facultative methanotrophs revisited.* J Bacteriol, 2005. **187** (13): p. 4303-4305.
424. van Bodegom, P., *Microbial maintenance: A critical review on its quantification.* Microbial Ecology, 2007. **53** (4): p. 513-523.
425. Constant, P., et al., *Streptomycetes contributing to atmospheric molecular hydrogen soil uptake are widespread and encode a putative high-affinity [NiFe]-hydrogenase.* Environmental Microbiology, 2010. **12** (3): p. 821-829.
426. Ji, M., et al., *Atmospheric trace gases support primary production in Antarctic desert surface soil.* Nature, 2017. **552**: p. 400-403.
427. Spear, J.R., et al., *Hydrogen and bioenergetics in the Yellowstone geothermal ecosystem.* P Natl Acad Sci USA, 2005. **102** (7): p. 2555-2560.
428. Hulston, J.R. and McCabe, W.J., *Mass spectrometer measurements in the thermal areas of New Zealand. Part 1. Carbon dioxide and residual gas analyses.* Geochim. Cosmochim. Acta, 1962. **26** (3): p. 383-397.
429. Stevens, T.O. and McKinley, J.P., *Lithoautotrophic microbial ecosystems in deep basalt aquifers.* Science, 1995. **270** (5235): p. 450.
430. Arrhenius, G., *Interaction of ocean-atmosphere with planetary interior.* Advances in Space Research, 1981. **1** (7): p. 37-48.
431. Gray, C.T. and Gest, H., *Biological formation of molecular hydrogen: A "hydrogen valve" facilitates regulation of anaerobic energy metabolism in many microorganisms.* Science, 1965. **148** (3667): p. 186-192.
432. Burris, R.H., *Nitrogenases.* J Biol Chem, 1991. **266** (15): p. 9339-9342.
433. Weber, J., et al., *Biotechnological hydrogen production by photosynthesis.* Engineering in Life Sciences, 2014. **14** (6): p. 592-606.
434. Seefeldt, L.C., et al., *Nitrogenase reduction of carbon-containing compounds.* Biochimica et Biophysica Acta, 2013. **1827** (0): p. 1102-1111.

435. Slobodkin, A.I. and Wiegel, J., *Fe(III) as an electron acceptor for H_2 oxidation in thermophilic anaerobic enrichment cultures from geothermal areas.* Extremophiles, 1997. **1** (2): p. 106-109.
436. Kan, J., et al., *Geochemistry and mixing drive the spatial distribution of free-living archaea and bacteria in Yellowstone Lake.* Frontiers in Microbiology, 2016. **7**.
437. Ward, L., et al., *Microbial community dynamics in Inferno Crater Lake, a thermally fluctuating geothermal spring.* The ISME Journal, 2017. **11** (5): p. 1158-1167.
438. Weiss, M.C., et al., *The physiology and habitat of the last universal common ancestor.* Nature Microbiology, 2016. **1**: p. 16116.
439. Vignais, P.M. and Billoud, B., *Occurrence, classification, and biological function of hydrogenases: An overview.* Chem. Rev., 2007. **107** (10): p. 4206-4272.
440. Csáki, R., et al., *Molecular characterization of structural genes coding for a membrane bound hydrogenase in Methylococcus capsulatus (Bath).* FEMS Microbiology Letters, 2001. **205** (2): p. 203-207.
441. Khdhiri, M., et al., *The tale of a neglected energy source: Elevated hydrogen exposure affects both microbial diversity and function in soil.* Appl Environ Microb, 2017. **83** (11).
442. Pruitt, K.D., Tatusova, T., and Maglott, D.R., *NCBI reference sequences (RefSeq): a curated non-redundant sequence database of genomes, transcripts and proteins.* Nucleic Acids Research, 2007. **35** (Database issue): p. D61-D65.
443. Untergasser, A., et al., *Primer3—new capabilities and interfaces.* Nucleic Acids Research, 2012. **40** (15): p. e115-e115.
444. USDA, *Microbiology Laboratory Guidebook*. 3rd ed. Vol. 1 & 2. 1998: United States Department of Agriculture.
445. Benson, D.R., Arp, D.J., and Burris, R.H., *Cell-free nitrogenase and hydrogenase from actinorhizal root nodules.* Science, 1979. **205** (4407): p. 688-689.
446. Choi, D.W., et al., *The membrane-associated methane monooxygenase (pMMO) and pMMO-NADH:Quinone oxidoreductase complex from Methylococcus capsulatus Bath.* J Bacteriol, 2003. **185** (19): p. 5755-5764.
447. King, G.M., Roslev, P., and Skovgaard, H., *Distribution and rate of methane oxidation in sediments of the Florida Everglades.* Appl Environ Microb, 1990. **56** (9): p. 2902-2911.
448. Linton, J.D. and Cripps, R.E., *The occurrence and identification of intracellular polyglucose storage granules in Methylococcus NCIB 11083 grown in chemostat culture on methane.* Archives of Microbiology, 1978. **117** (1): p. 41-48.
449. Eshinimaev, B.T., et al., *Physiological, biochemical, and cytological characteristics of a haloalkalitolerant methanotroph grown on methanol.* Microbiology, 2002. **71** (5): p. 512-518.
450. Khadem, A.F., et al., *Genomic and physiological analysis of carbon storage in the verrucomicrobial methanotroph "Ca. Methylacidiphilum fumariolicum" SolV.* Frontiers in Microbiology, 2012. **3**.
451. DiSpirito, A.A., et al., *Chapter 7: Respiration in methanotrophs*, in *Respiration in Archaea and Bacteria*, Zannoni, D., Editor. 2004, Springer: AA Dordrecht, The Netherlands. p. pp 149-168.

452. Horch, M., et al., *Probing the active site of an O_2-tolerant NAD^+-reducing [NiFe]-hydrogenase from Ralstonia eutropha H16 by in situ EPR and FTIR spectroscopy.* Angewandte Chemie (International ed. in English), 2010. **49** (43): p. 8026-9.
453. Kwan, P., et al., *The [NiFe]-hydrogenase of Pyrococcus furiosus exhibits a new type of oxygen tolerance.* Journal of the American Chemical Society, 2015. **137** (42): p. 13556-65.
454. Burgdorf, T., et al., *The soluble NAD^+-reducing [NiFe]-hydrogenase from Ralstonia eutropha H16 consists of six subunits and can be specifically activated by NADPH.* J Bacteriol, 2005. **187** (9): p. 3122-3132.
455. Zheng, Y., et al., *A pathway for biological methane production using bacterial iron-only nitrogenase.* Nature Microbiology, 2018. **3**: p. 281-286.
456. Murrell, J.C. and Dalton, H., *Nitrogen fixation in obligate methanotrophs.* Journal of General Microbiology, 1983. **129** (11): p. 3481-3486.
457. Ash, P.A., et al., *Electrochemical and infrared spectroscopic studies provide insight into reactions of the NiFe regulatory hydrogenase from Ralstonia eutropha with O_2 and CO.* J Phys Chem B, 2015. **119** (43): p. 13807-13815.
458. Strong, P.J., et al., *A methanotroph-based biorefinery: Potential scenarios for generating multiple products from a single fermentation.* Bioresource Technology, 2016. **215**: p. 314-323.
459. Strong, P.J., Xie, S., and Clarke, W.P., *Methane as a resource: Can the methanotrophs add value?* Environ. Sci. Technol., 2015. **49** (7): p. 4001-4018.
460. Venter, J.C., et al., *Environmental genome shotgun sequencing of the Sargasso Sea.* Science, 2004. **304** (5667): p. 66-74.
461. Kalyuzhnaya, M.G., et al., *High-resolution metagenomics targets specific functional types in complex microbial communities.* Nat. Biotechnol., 2008. **26** (9): p. 1029-1034.
462. Bini, E., *Archaeal transformation of metals in the environment.* FEMS Microbiology Ecology, 2010. **73** (1): p. 1-16.
463. Meyer, F., et al., *The metagenomics RAST server – a public resource for the automatic phylogenetic and functional analysis of metagenomes.* BMC Bioinform., 2008. **9** (1): p. 386.
464. Zehavi, T., Probst, M., and Mizrahi, I., *Insights into culturomics of the rumen microbiome.* Frontiers in Microbiology, 2018. **9** (1999).
465. Lagier, J.C., et al., *Culture of previously uncultured members of the human gut microbiota by culturomics.* Nature Microbiology, 2016. **1**: p. 16203.
466. Wolin, E.A., Wolin, M.J., and Wolfe, R.S., *Formation of methane by bacterial extracts.* J Biol Chem, 1963. **238** (8): p. 2882-2886.

7. Appendices

7.1 Rates of methane oxidation for geothermal microcosms.

Samples are arranged by decreasing rate of oxidation.

OKO2

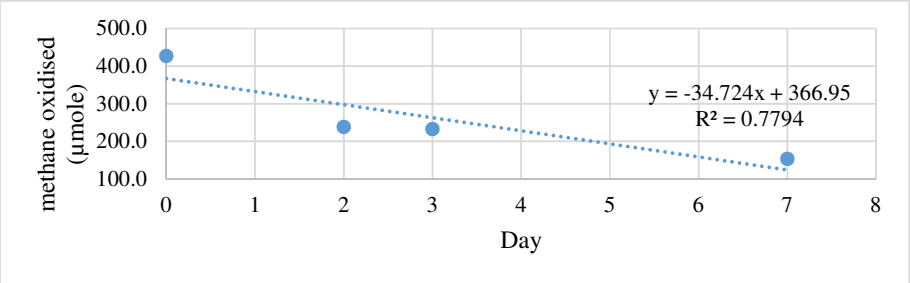

TKT67

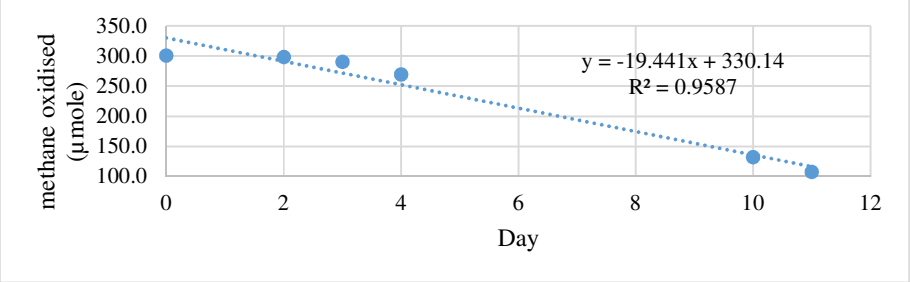

TKT68

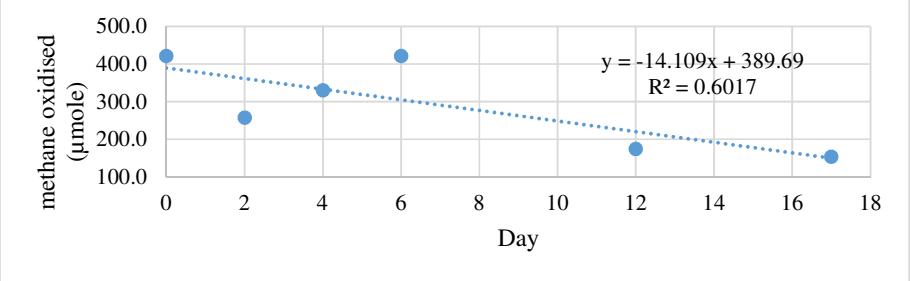

TOK17

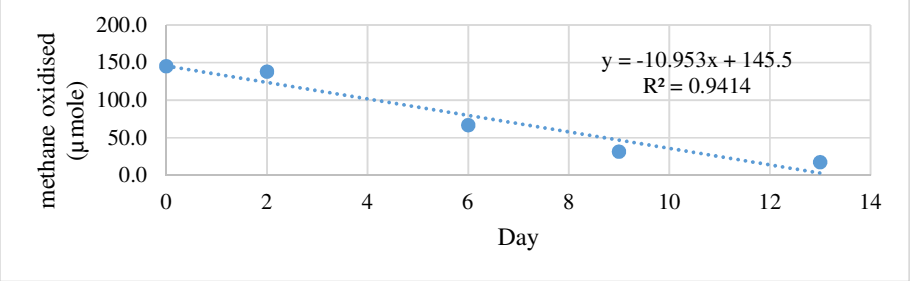

WTV1

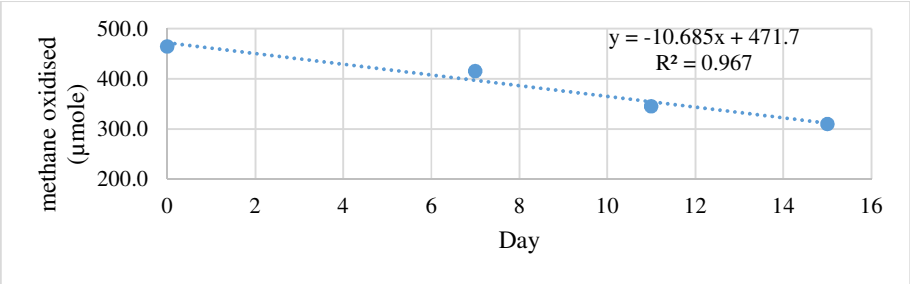

TOK7

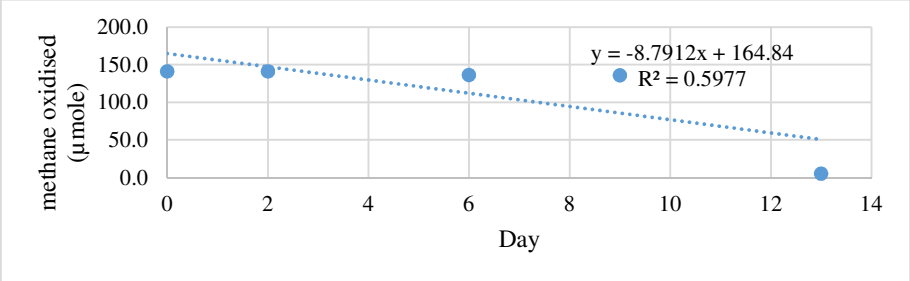

LPR14

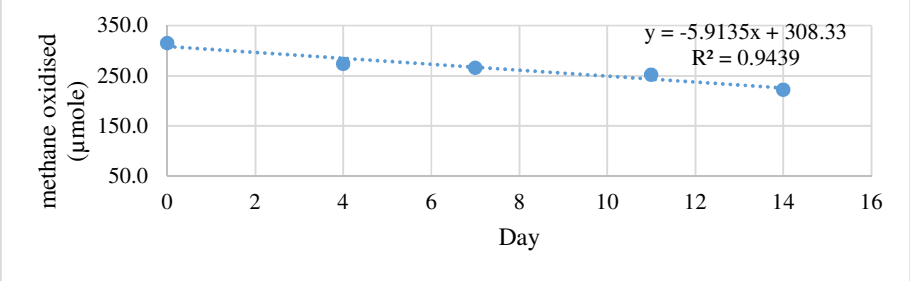

TOK10

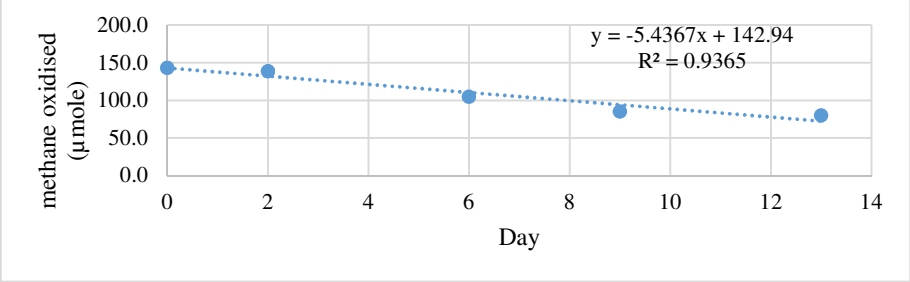

TKA9

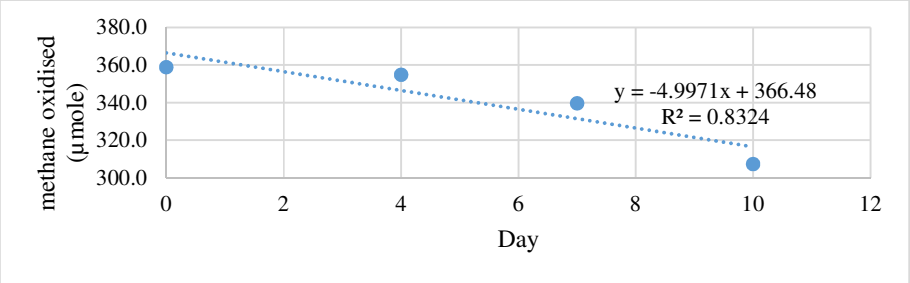

GDS2

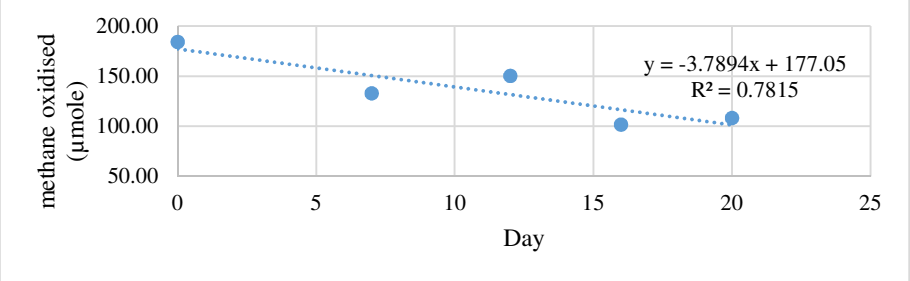

WHV12

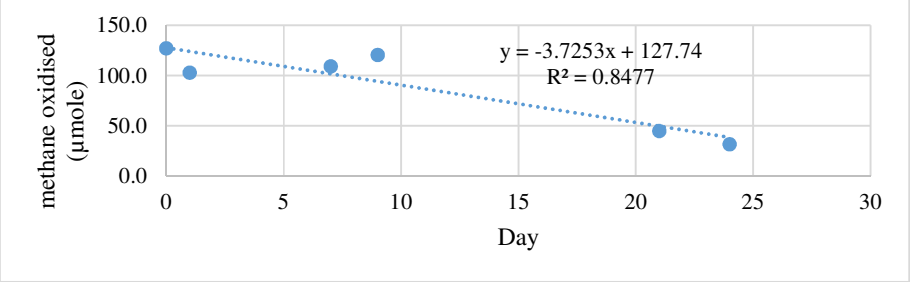

WHV18

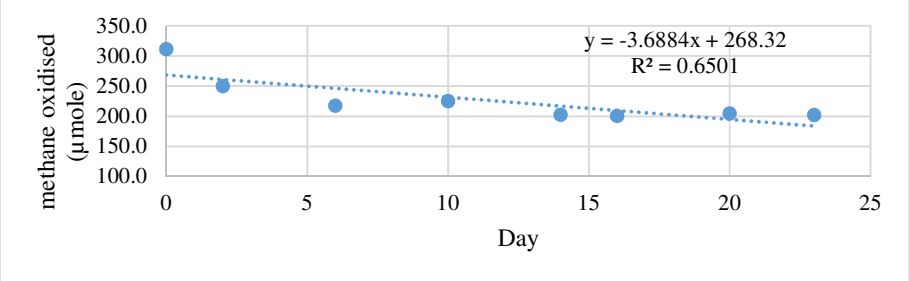

WTV4

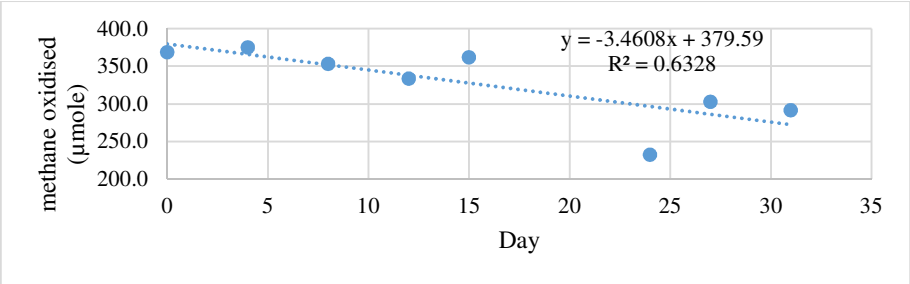

WAM36

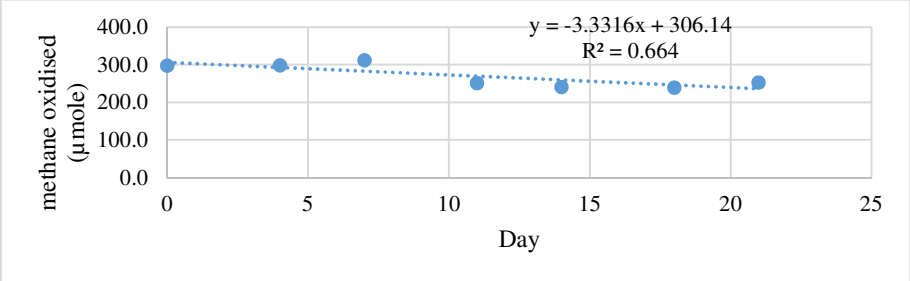

TOK12

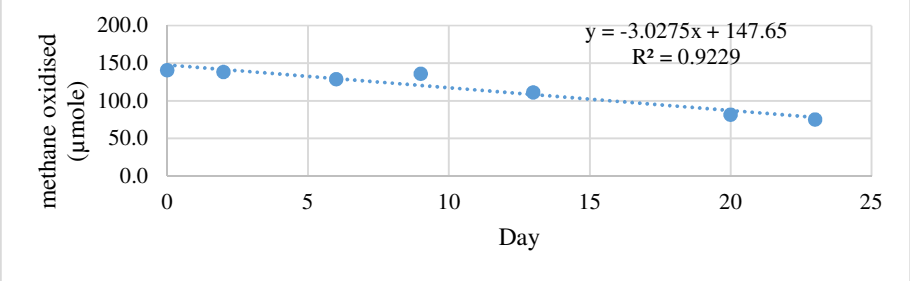

TKA16

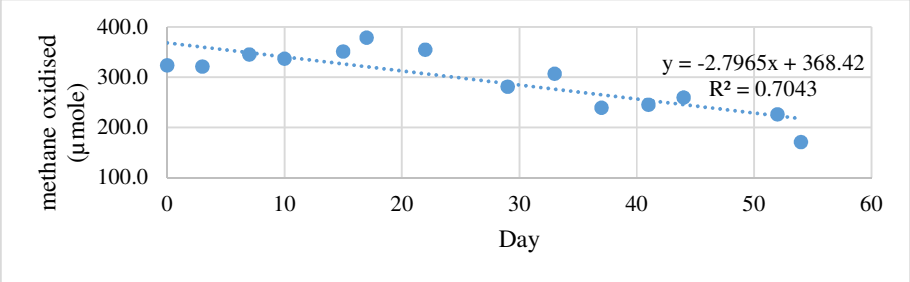

WTV2

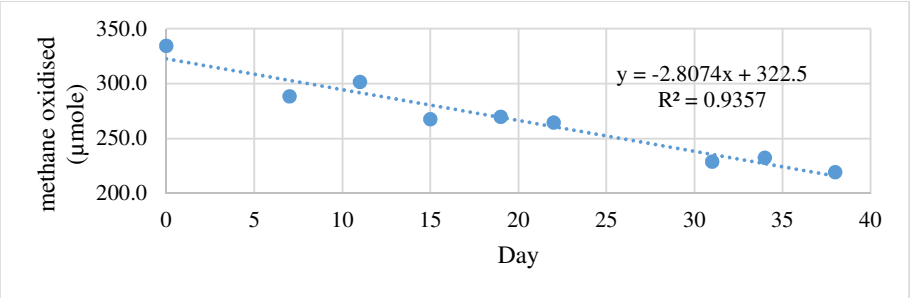

GDS1

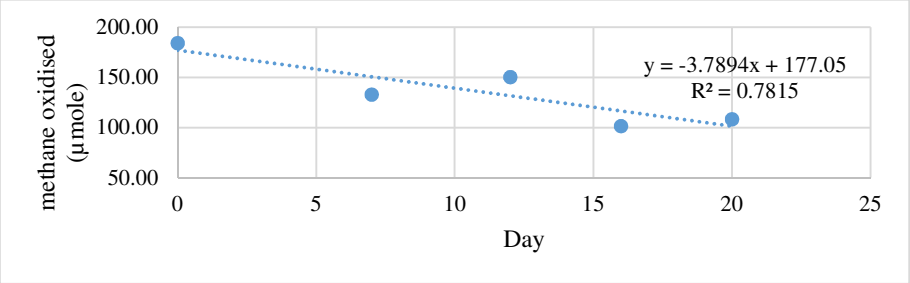

LPR17

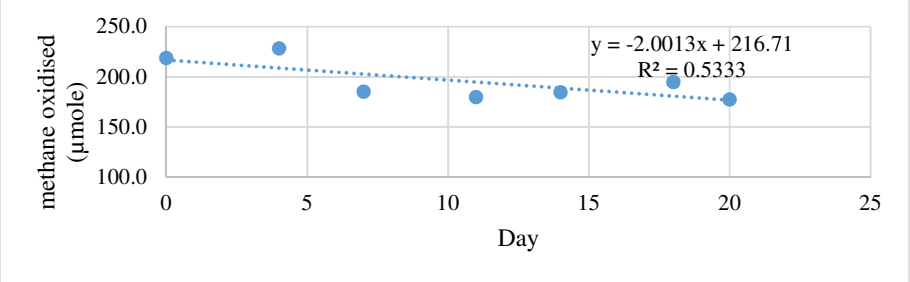

WKT45

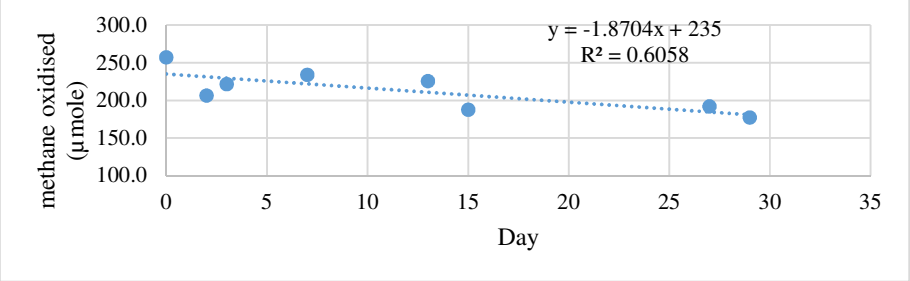

TKA13

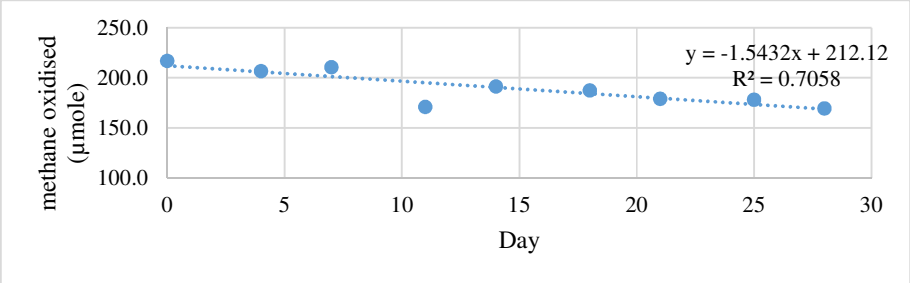

WHV15

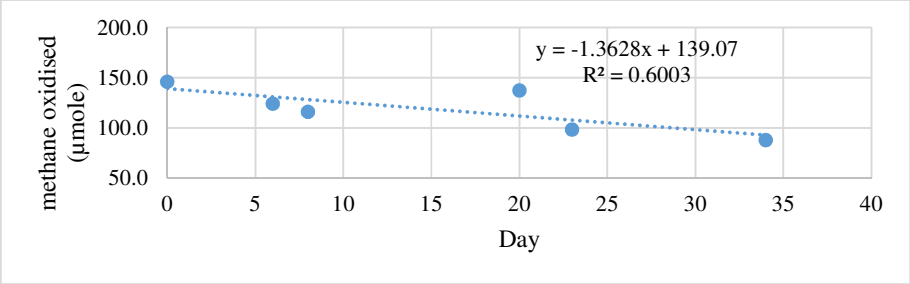

TKA15

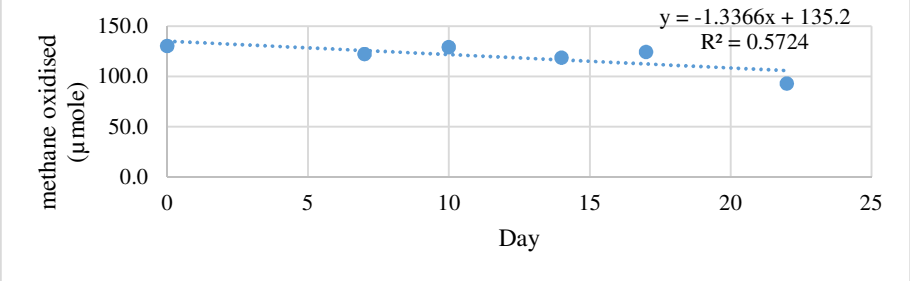

TKA8

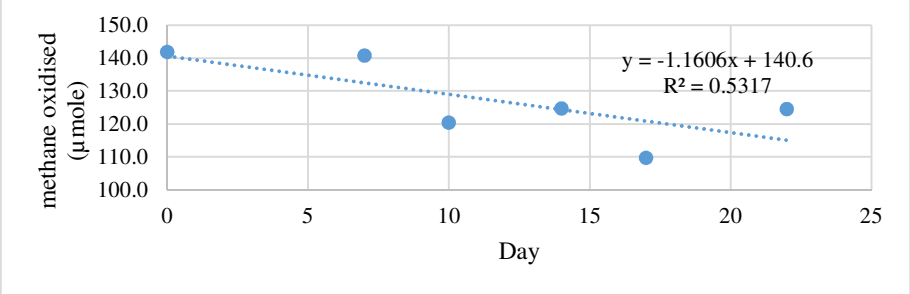

TOK15

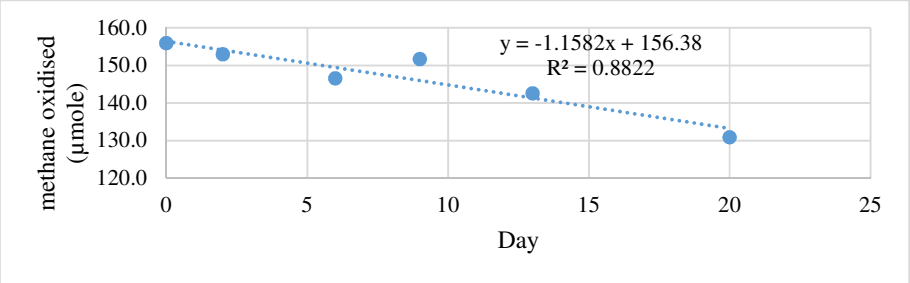

LPR16

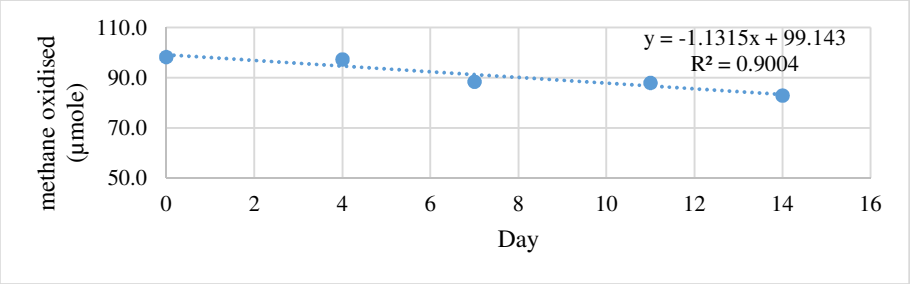

WHV13

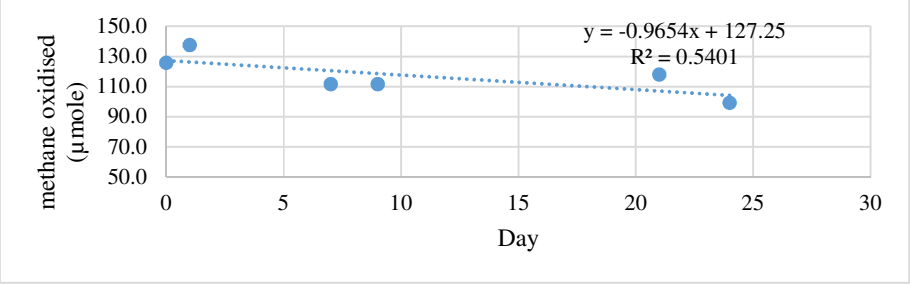

7.2 Sequencing pipeline scripts

Trimming and Quality Control

```
$mkdir raw_reads; mkdir trimmed; mv *.fastq raw_reads/

$for read1 in raw_reads/*_1.fastq; do
read2=$(echo $read1|sed 's/_1.fastq/_2.fastq/');
trim_galore -q 20 --paired $read1 $read2 -o trimmed --
fastqc;
done

$mv trimmed/*val_*.fq ./

$rename -v 's/(.*)_(.*)_val_(.*).fq/$1_$2.fastq/' *.fq
```

Merge demultiplexed reads

```
$for file in *_1.fastq
do
 if [ -f "$file" ]; then
 sampleID=$(echo "$file" | cut -d "_" -f1) # "_" as
delimiter
 usearch70 -fastq_mergepairs $file -reverse
${file%_1.fastq}
_2.fastq -fastqout "${sampleID}_merged.fastq"
fi
done &> merged_log.txt
```

Convert FASTQ to FASTA, filter low quality reads

```
$for file in *merged.fastq; do
 sampleID=$(echo "$file" | cut -d "_" -f1)
 usearch70 -fastq_filter "${sampleID}_merged.fastq" -
fastaout "${sampleID}_filtered.fasta" -fastq_maxee 1.0
done &> filtered_log.txt
```

Rename files and concatenate

```
$for filename in $(ls *_filtered.fasta); do
samplename=$(echo $filename | cut -d '_' -f1)
sed "-es/^>\(.*\)/>;barcodelabel=$samplename;/" <
"$filename" > ${samplename}_renamed.fasta
done

$for filename in *renamed.fasta; do
cat $filename >> "all_samples_filtered.fasta"
done
```

Remove homopolymers and short and long sequences

```
$mothur
trim.seqs(fasta=all_samples_filtered.fasta,
minlength=200, maxlength=500, maxhomop=6, processors=8)
summary.seqs(fasta=all_samples_filtered.trim.fasta)
quit
```

Process unfiltered reads

```
$for file in *merged.fastq; do
 sampleID=$(echo "$file" | cut -d "_" -f1)
 usearch70 -fastq_filter "${sampleID}_merged.fastq" -
fastaout "${sampleID}_unfiltered.fasta"
done &> unfiltered_log.txt

$for filename in $(ls *_unfiltered.fasta); do
samplename=$(echo $filename | cut -d '_' -f1)
sed "-es/^>\(.*\)/>;barcodelabel=$samplename;/" <
"$filename" > ${samplename}_unfiltered_renamed.fasta
done

$for filename in $(ls *unfiltered_renamed.fasta); do
cat $filename >> "all_samples_unfiltered.fasta"
done
```

Remove short and long sequences

```
$mothur
trim.seqs(fasta=all_samples_unfiltered.fasta,
minlength=200, maxlength=400, processors=8)
summary.seqs(fasta=all_samples_unfiltered.trim.fasta)
quit

$mkdir merged | mv *_merged.fastq merged/
mkdir filtered | mv *_filtered.fasta filtered/
mkdir renamed | mv *_renamed.fasta renamed/
mkdir unfiltered | mv *_unfiltered.fasta unfiltered/
mkdir mothur_output | mv all_samples* mothur_output/ |
mv mothur.* mothur_output/
mv *.fastq trimmed/

$mv mothur_output/all_samples_filtered.trim.fasta
mothur_output/all_samples_unfiltered.trim.fasta ./
```

Create de novo database

```
$usearch70 -derep_fulllength
all_samples_filtered.trim.fasta -output derep.fa -
sizeout

$usearch70 -sortbysize derep.fa -output derep_2.fa -
minsize 2

$usearch70 -cluster_otus derep_2.fa -otus rep_set.fa

$fasta_number.py rep_set.fa "OTU_" >
rep_set_numbered.fa
```

Align unfiltered reads to de novo database

```
$usearch70 -usearch_global
all_samples_unfiltered.trim.fasta -db
rep_set_numbered.fa -id 0.97 -strand plus -uc
readmap.uc

$sed 's/\t\t\t/\t/' readmap.uc > readmap_2.uc

$create_otu_table_from_uc_file.py -i readmap_2.uc -o
otu_table.txt

$source activate qiime1

$biom convert -i otu_table.txt -o otu_table.biom --
table-type="OTU table" --to-json
```

Assign taxonomy to OTUs

```
$assign_taxonomy.py -m rdp -i rep_set_numbered.fa -o
rdp_assigned_taxonomy -c 0.5 -t
~/software/db_files/SILVA/SILVA_123/taxonomy/16S_only/9
7/consensus_taxonomy_7_levels.txt -r
~/software/db_files/SILVA/SILVA_123/rep_set/rep_set_16S
_only/97/97_otus_16S.fasta --rdp_max_memory 24000

$biom add-metadata -i otu_table.biom --observation-
metadata-
fp rdp_assigned_taxonomy/rep_set_numbered_tax_assignmen
ts.txt --sc-separated taxonomy --observation-header
OTUID,taxonomy -o otu_table_wTax.biom
```

Remove unwanted taxa

```
$filter_taxa_from_otu_table.py -i otu_table_wTax.biom -
o otu_table_wTax_noChloroMito.biom -n
D_2__Chloroplast,D_4__Mitochondria
```

```
$biom summarize-table -i
otu_table_wTax_noChloroMito.biom -o
otu_table_wTax_noChloroMito_smry.txt
```

Rarefy data

```
$single_rarefaction.py -i
otu_table_wTax_noChloroMito.biom -o
otu_table_wTax_noChloroMito_149400.biom -d 149400

$biom convert -i
otu_table_wTax_noChloroMito_149400.biom -o
rare_otu_table.txt --to-tsv --header-key taxonomy
```

Make a phylogenetic tree

```
$parallel_align_seqs_pynast.py -i rep_set_numbered.fa -
o pynast_aligned -O 30

$filter_alignment.py -i
pynast_aligned/rep_set_numbered_aligned.fasta -o
pynast_aligned/

$make_phylogeny.py -i
pynast_aligned/rep_set_numbered_aligned_pfiltered.fasta
```

Run Core Diversity workflow

```
$core_diversity_analyses.py -i rare_otu_table.biom -o
core_output/ -m mapping_file.txt -e 149400 -c Oxidation
-t tree.tre -a -O 30 -p parameter_file.txt
```

Create distance matrices for variables and compare

```
$distance_matrix_from_mapping.py -i mapping_file.txt -c
Temperature -o temp_dm.txt

$distance_matrix_from_mapping.py -i mapping_file.txt -c
pH -o pH_dm.txt

$distance_matrix_from_mapping.py -i mapping_file.txt -c
Soil_type -o soil_type_dm.txt

$distance_matrix_from_mapping.py -i mapping_file.txt -c
methane_oxidation_umole_g_day -o methane_umole_dm.txt

$distance_matrix_from_mapping.py -i
new_mapping_file.txt -c in_situ -o in_situ_dm.txt

$distance_matrix_from_mapping.py -i
new_mapping_file.txt -c Latitude,Longitude -o
lat_long_dm.txt

$compare_distance_matrices.py --method=mantel -i
weighted_unifrac_dm.txt,pH_dm.txt,temp_dm.txt,soil_type
_dm.txt,methane_umole_dm_matrix.txt,in_situ_dm.txt,lat_
long_dm.txt -o weighted_mantel_out -n 999
```

Compare OTU frequencies

```
$group_significance.py -i rare_otu_table.biom -m
new_mapping_file.txt -c Oxidation -s kruskal_wallis -o
kw_sig.txt
```

7.3 Putative aerobic methanotroph OTUs and their most closely related species

#OTU ID	Length of sequence (bp)	Closest related genus	Closest related species	Accession number	% coverage	% identity
OTU_762	292	*Crenothrix*	*polyspora*	DQ295898	96	94
OTU_8761	292	*Crenothrix*	*polyspora*	DQ295898	97	96
OTU_4745	292	*Methylacidimicrobium*	*cyclopophantes*	NR126315	96	98
OTU_1233	291	*Methylacidiphilum*	*infernorum*	CP000975	95	100
OTU_2239	292	*Methylacidiphilum*	*infernorum*	CP000975	95	100
OTU_2289	291	*Methylacidiphilum*	*infernorum*	CP000975	97	97
OTU_2357	292	*Methylacidiphilum*	*infernorum*	CP000975	96	96
OTU_2679	292	*Methylacidiphilum*	*infernorum*	CP000975	100	97
OTU_2728	290	*Methylacidiphilum*	*infernorum*	CP000975	96	97
OTU_2794	292	*Methylacidiphilum*	*infernorum*	CP000975	100	97
OTU_2869	292	*Methylacidiphilum*	*infernorum*	CP000975	96	98
OTU_2978	293	*Methylacidiphilum*	*infernorum*	CP000975	96	97
OTU_3268	292	*Methylacidiphilum*	*infernorum*	CP000975	100	96
OTU_3459	292	*Methylacidiphilum*	*infernorum*	CP000975	100	96
OTU_3635	290	*Methylacidiphilum*	*infernorum*	CP000975	100	97
OTU_3962	292	*Methylacidiphilum*	*infernorum*	CP000975	100	96
OTU_4025	292	*Methylacidiphilum*	*infernorum*	CP000975	100	97
OTU_4153	291	*Methylacidiphilum*	*infernorum*	CP000975	97	97
OTU_4154	292	*Methylacidiphilum*	*infernorum*	CP000975	96	96
OTU_4172	292	*Methylacidiphilum*	*infernorum*	CP000975	96	97
OTU_4263	291	*Methylacidiphilum*	*infernorum*	CP000975	100	96
OTU_4489	291	*Methylacidiphilum*	*infernorum*	CP000975	98	95
OTU_4493	292	*Methylacidiphilum*	*infernorum*	CP000975	96	97
OTU_4519	291	*Methylacidiphilum*	*infernorum*	CP000975	100	96
OTU_4551	292	*Methylacidiphilum*	*infernorum*	CP000975	96	97
OTU_4597	292	*Methylacidiphilum*	*infernorum*	CP000975	100	96
OTU_4907	294	*Methylacidiphilum*	*infernorum*	CP000975	93	97
OTU_5004	292	*Methylacidiphilum*	*infernorum*	CP000975	96	98
OTU_5005	292	*Methylacidiphilum*	*infernorum*	CP000975	100	95
OTU_5069	292	*Methylacidiphilum*	*infernorum*	CP000975	96	98
OTU_5090	292	*Methylacidiphilum*	*infernorum*	CP000975	100	96
OTU_5120	292	*Methylacidiphilum*	*infernorum*	CP000975	100	96
OTU_5157	291	*Methylacidiphilum*	*infernorum*	CP000975	100	91
OTU_5266	292	*Methylacidiphilum*	*infernorum*	CP000975	100	98

OTU_549	292	*Methylacidiphilum*	*infernorum*	CP000975	96	98
OTU_5532	292	*Methylacidiphilum*	*infernorum*	CP000975	100	95
OTU_5608	291	*Methylacidiphilum*	*infernorum*	CP000975	100	96
OTU_6031	292	*Methylacidiphilum*	*infernorum*	CP000975	100	97
OTU_6056	292	*Methylacidiphilum*	*infernorum*	CP000975	100	97
OTU_6492	291	*Methylacidiphilum*	*infernorum*	CP000975	100	95
OTU_6585	291	*Methylacidiphilum*	*infernorum*	CP000975	96	96
OTU_6713	292	*Methylacidiphilum*	*infernorum*	CP000975	96	96
OTU_6797	292	*Methylacidiphilum*	*infernorum*	CP000975	98	97
OTU_6847	292	*Methylacidiphilum*	*infernorum*	CP000975	96	96
OTU_6870	292	*Methylacidiphilum*	*infernorum*	CP000975	100	97
OTU_6975	290	*Methylacidiphilum*	*infernorum*	CP000975	100	98
OTU_7009	291	*Methylacidiphilum*	*infernorum*	CP000975	98	96
OTU_7031	292	*Methylacidiphilum*	*infernorum*	CP000975	98	98
OTU_7200	293	*Methylacidiphilum*	*infernorum*	CP000975	100	96
OTU_7212	292	*Methylacidiphilum*	*infernorum*	CP000975	100	96
OTU_7517	467	*Methylacidiphilum*	*infernorum*	CP000975	100	99
OTU_7551	292	*Methylacidiphilum*	*infernorum*	CP000975	96	97
OTU_7691	291	*Methylacidiphilum*	*infernorum*	CP000975	95	97
OTU_7707	291	*Methylacidiphilum*	*infernorum*	CP000975	96	96
OTU_7924	292	*Methylacidiphilum*	*infernorum*	CP000975	100	97
OTU_7990	292	*Methylacidiphilum*	*infernorum*	CP000975	96	96
OTU_8	292	*Methylacidiphilum*	*infernorum*	CP000975	100	98
OTU_8005	291	*Methylacidiphilum*	*infernorum*	CP000975	97	97
OTU_8091	257	*Methylacidiphilum*	*infernorum*	CP000975	90	97
OTU_8163	293	*Methylacidiphilum*	*infernorum*	CP000975	96	97
OTU_8193	292	*Methylacidiphilum*	*infernorum*	CP000975	91	99
OTU_8255	292	*Methylacidiphilum*	*infernorum*	CP000975	96	96
OTU_8342	292	*Methylacidiphilum*	*infernorum*	CP000975	100	96
OTU_8363	291	*Methylacidiphilum*	*infernorum*	CP000975	96	98
OTU_8467	292	*Methylacidiphilum*	*infernorum*	CP000975	96	96
OTU_8508	291	*Methylacidiphilum*	*infernorum*	CP000975	97	98
OTU_8539	292	*Methylacidiphilum*	*infernorum*	CP000975	96	94
OTU_8545	289	*Methylacidiphilum*	*infernorum*	CP000975	98	97
OTU_8592	292	*Methylacidiphilum*	*infernorum*	CP000975	100	96
OTU_8687	292	*Methylacidiphilum*	*infernorum*	CP000975	96	97
OTU_8745	292	*Methylacidiphilum*	*infernorum*	CP000975	96	97
OTU_8791	292	*Methylacidiphilum*	*infernorum*	CP000975	100	96
OTU_8831	293	*Methylacidiphilum*	*infernorum*	CP000975	94	96
OTU_8906	300	*Methylacidiphilum*	*infernorum*	CP000975	94	92
OTU_9070	292	*Methylacidiphilum*	*infernorum*	CP000975	100	97
OTU_9081	214	*Methylacidiphilum*	*infernorum*	CP000975	100	98
OTU_9140	292	*Methylacidiphilum*	*infernorum*	CP000975	100	97
OTU_9161	292	*Methylacidiphilum*	*infernorum*	CP000975	96	96
OTU_7154	292	*Methylobacter*	*marinus*	LT220841	96	95

OTU_4562	292	*Methylobacter*	*tundripaladum*	NR042107	96	98
OTU_1127	292	*Methylocaldum*	*marinum*	NR126189	96	94
OTU_2113	292	*Methylocaldum*	*tepidum*	NR026062	100	96
OTU_5729	292	*Methylocapsa*	*palsarum*	NR137418	96	93
OTU_1481	292	*Methylococcus*	*capsulatus*	AE017282	96	96
OTU_2594	292	*Methylococcus*	*capsulatus*	AE017282	100	94
OTU_474	292	*Methylococcus*	*capsulatus*	AE017282	96	98
OTU_1207	292	*Methylocystis*	*echinoides*	KY114785	100	98
OTU_7334	292	*Methylocystis*	*parvus*	AF150805	96	99
OTU_5233	288	*Methylomarinum*	*vadi*	KU740210.1	95	95
OTU_6536	292	*Methylomicrobium*	*alcaliphilum*	NR074649	96	93
OTU_7537	292	*Methylomicrobium*	*alcaliphilum*	NR074649	96	96
OTU_5994	292	*Methylomonas*	*aurantiaca*	NR029243	96	95
OTU_8093	292	*Methylomonas*	*aurantiaca*	NR029243	100	95
OTU_97	292	*Methylomonas*	*aurantiaca*	NR029243	96	97
OTU_5609	292	*Methylomonas*	*denitrificans*	CP014476	100	97
OTU_6282	292	*Methylomonas*	*lenta*	NR133783	96	98
OTU_7159	293	*Methylomonas*	*lenta*	NR133783	98	96
OTU_1890	292	*Methylomonas*	*methanica*	CP002738	96	95
OTU_6715	291	*Methylomonas*	*methanica*	CP002738	95	96
OTU_8861	292	*Methylomonas*	*methanica*	CP002738	96	96
OTU_3590	292	*Methylomonas*	*rubra*	AF150807	100	95
OTU_4951	292	*Methylosinus*	*trichosporium*	AB648997.1	96	99
OTU_5700	292	*Methylosinus*	*trichosporium*	AB648997.1	96	91
OTU_1502	292	*Methylothermus*	*subterraneus*	NR113020	100	94
OTU_2388	292	*Methylothermus*	*subterraneus*	NR113020	100	92
OTU_3240	292	*Methylothermus*	*subterraneus*	NR113020	96	95
OTU_3433	292	*Methylothermus*	*subterraneus*	NR113020	100	90
OTU_3946	292	*Methylothermus*	*subterraneus*	NR113020	96	92
OTU_3987	291	*Methylothermus*	*subterraneus*	NR113020	96	93
OTU_4048	292	*Methylothermus*	*subterraneus*	NR113020	96	94
OTU_4544	291	*Methylothermus*	*subterraneus*	NR113020	97	95
OTU_5125	288	*Methylothermus*	*subterraneus*	NR113020	100	93
OTU_69	292	*Methylothermus*	*subterraneus*	NR113020	96	94
OTU_6968	292	*Methylothermus*	*subterraneus*	NR113020	100	92
OTU_7028	292	*Methylothermus*	*subterraneus*	NR113020	96	94
OTU_7340	292	*Methylothermus*	*subterraneus*	NR113020	97	93
OTU_7727	291	*Methylothermus*	*subterraneus*	NR113020	96	93
OTU_8026	292	*Methylothermus*	*subterraneus*	NR113020	100	93
OTU_8617	292	*Methylothermus*	*subterraneus*	NR113020	96	93
OTU_8768	292	*Methylothermus*	*subterraneus*	NR113020	96	94
OTU_9052	292	*Methylothermus*	*subterraneus*	NR113020	97	94

7.4 Media recipes

Trace metal solutions and other media additives are in Appendix 7.5

7.4.1 Modified NMS

$NaNO_3$	0.084 g	
$MgSO_4.7H_2O$	0.135 g	
$CaCl_2.6H_2O$	0.026 g	
KCl	0.035 g	
K_2HPO_4 *OR* KH_2PO_4	0.029 g	
Copper rich trace metal solution	1 ml	
ddH_2O to 1 l		pH adjusted to that of sample

7.4.2 NMS

$MgSO_4.7H_2O$	1.000 g	
KNO_3	1.000 g	
$CaCl_2.6H_2O$	0.200 g	
Yeast extract	0.01 g	
$NiCl_2.6H_2O$	trace	
Trace element solution	1 ml	
FeEDTA solution	10 ml	
Phosphate buffer solution	2 ml	
ddH_2O to 1 l		pH 6.8

7.4.3 dNMS

$Na_2HPO_4.12H_2O$	0.40 g	
$MgSO_4.7H_2O$	0.20 g	
KNO_3	0.20 g	
$CaCl_2.6H_2O$	0.04 g	
Methanotrophs trace metal solution	0.20 ml	
FeEDTA solution	0.20 ml	
ddH_2O to 1 l		pH 6.8

7.4.4 ANMS

KNO_3	0.250 g	
NH_4Cl	0.250 g	
KH_2PO_4	0.130 g	
$Na_2HPO_4.12H_2O$	0.358 g	
$MgSO_4.7H_2O$	0.400 g	
$CaCl_2.2H_2O$	0.100 g	
$Na_2MoO_4.6H_2O$	trace	
$NiCl_2.6H_2O$	trace	
B-Forte vitamin capsule	0.010 g	
Methanotrophs trace metal solution	0.5 ml	
FeEDTA solution	0.2 ml	
ddH_2O to 1 l		pH 6.8

7.4.5 mmj

NaCl	3.00 g	
$NaHCO_3$	0.50 g	
$MgCl_2.6H_2O$	0.42 g	
$MgSO_4.7H_2O$	0.34 g	
NH_4Cl	0.25 g	
$NaNO_3$	0.25 g	
$CaCl_2$	80.0 mg	
KCl	33.0 mg	
K_2HPO_4	14.0 mg	
$CuSO_4$	3.7 mg	
$Fe(NH_4)_2(SO_4)_2.6H_2O$	2.0 mg	
B-Forte vitamin capsule	0.01 g	
Wolin trace mineral solution	1 ml	
ddH_2O to 1 l		pH 6.2

7.4.6 V4

NH_4Cl	0.40 g	
KH_2PO_4	0.05 g	
$MgSO_4.7H_2O$	0.02 g	
$CaCl_2.6H_2O$	0.01 g	
FeEDTA solution	3.0 ml	
Methanotrophs trace metal solution	3.0 ml	
Wolin trace mineral solution	1.0 ml	
1 mM $Ce(SO_4)_2$	0.2 ml	
1 mM $La_2(SO_4)_3$	0.2 ml	
ddH_2O to 1 l		pH 2.5

7.5 Media additives

Copper rich trace metal solution

$CuSO_4.5H_2O$	4.100 g
$ZnSO_4.7H_2O$	0.327 g
$FeSO_4.7H_2O$	0.268 g
$MnCl_2.4H_2O$	0.116 g
$CoCl_2.6H_2O$	0.043 g
$Na_2MoO4.2H_2O$	0.027 g
$NiCl_2.6H_2O$	0.012 g
H_3BO_3	0.008 g
Na_2-EDTA	2.032 g
ddH_2O to 100 ml	

NMS trace element solution

$CuSO_4.5H_2O$	200 mg	
$ZnSO_4.7H_2O$	10 mg	
$MnCl_2.4H_2O$	3 mg	
H_3BO_3	30 mg	
$CoCl_2.6H_2O$	10 mg	
$Na_2MoO_4.7H_2O$	10 mg	
ddH_2O to 1 l		pH 4.0

NMS phosphate buffer solution

$Na_2HPO_4.12H_2O$	35.8 g
KH_2PO_4	13.6 g
ddH_2O to 100 ml	

FeEDTA solution

$FeSO_4.7H_2O$	1.54 g
Na_2-EDTA	2.06 g
dd H_2O to 1 l	

Methanotrophs trace metal solution

$ZnSO_4.7H_2O$	0.44 g
$Na_2MoO_4.2H_2O$	0.06 g
$MnCl_4H_2O$	0.19 g
$CuSO_4.5H_2O$	0.20 g
H_3BO_3	0.10 g
$CoCl_2.6H_2O$	0.08 g
ddH_2O to 1 l	

Clinicians B-Forte vitamin capsules (Douglas Pharmaceuticals, Auckland, New Zealand)

Choline bitartrate	182 mg
Ascorbic acid	100 mg
Thiamin hydrochloride	84 mg
Riboflavin	75 mg
Inositol	75 mg
Nicotinamide	75 mg
Pyridoxine hyrdrochloride	61 mg
Calcium pantothenate	55 mg
Folic Acid	0.3 mg
Biotin	0.1 mg
Cyanocobalamin	0.05 mg

Wolin trace metal solution [466]

Nitrilotriacetic acid	1.5 g
$Fe(NH_4)_2(SO_4)_2 \cdot 6H_2O$	0.2 g
$Na_2SeO4.10H2O$	0.44 g
$CoCl_2 \cdot 6H_2O$	0.1 g
$MnSO_4 \cdot 4H_2O$	0.12 g
$Na_2MoO_4 \cdot 2H_2O$	0.1g
$NaWO_4 \cdot 2H_2O$	0.1 g
$ZnSO_4 \cdot 7H_2O$	0.1 g
$AlCl_3 \cdot 6H_2O$	0.04 g
$NiCl_2 \cdot 6H_2O$	0.025 g
H_3BO_3	0.01 g
$CuSO_4 \cdot 5H_2O$	0.01 g
ddH_2O to 1 l	

7.6 Rates of methane oxidation for geothermal enrichment microcosm cultures.

Samples are arranged by decreasing rate of oxidation.

GDS1

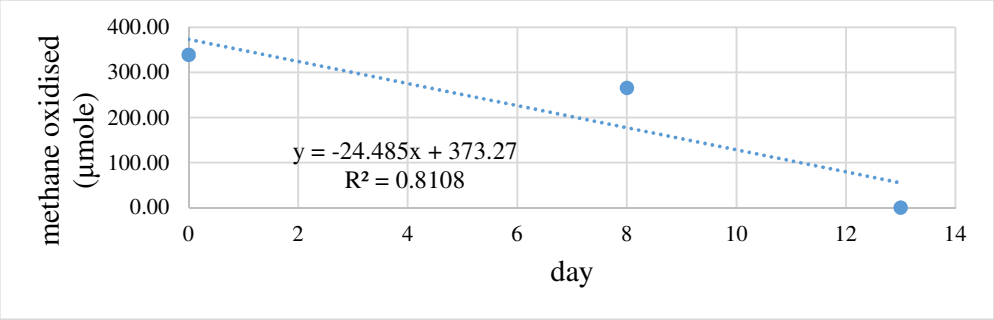

GDS2

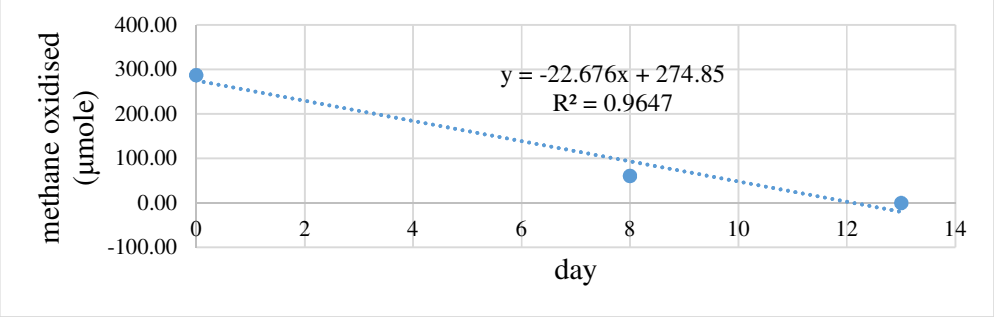

NGM91

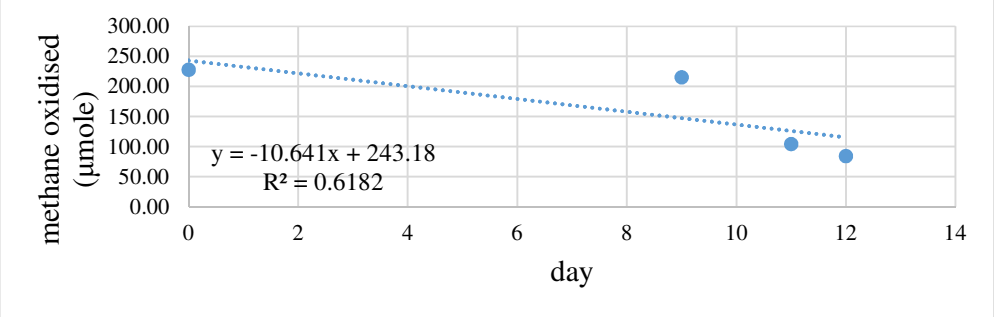

TOK12

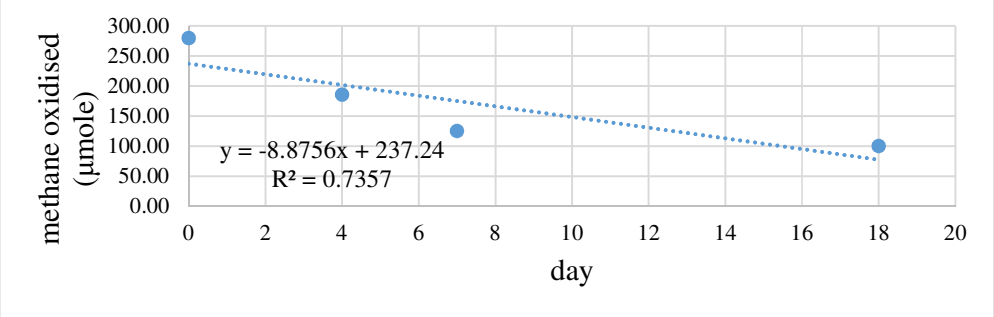

TOK10

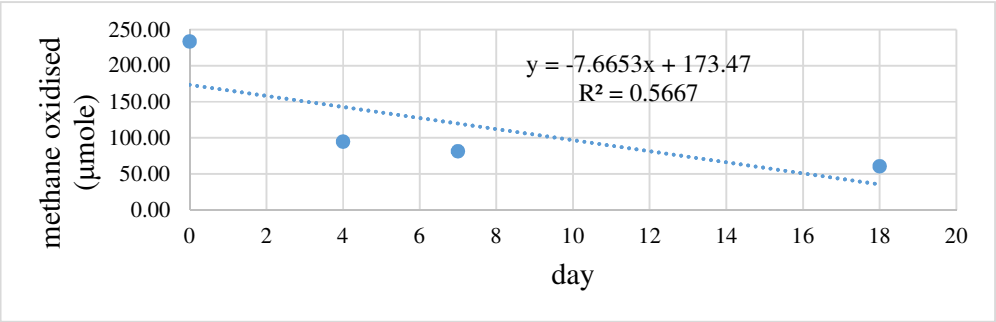

WHV12

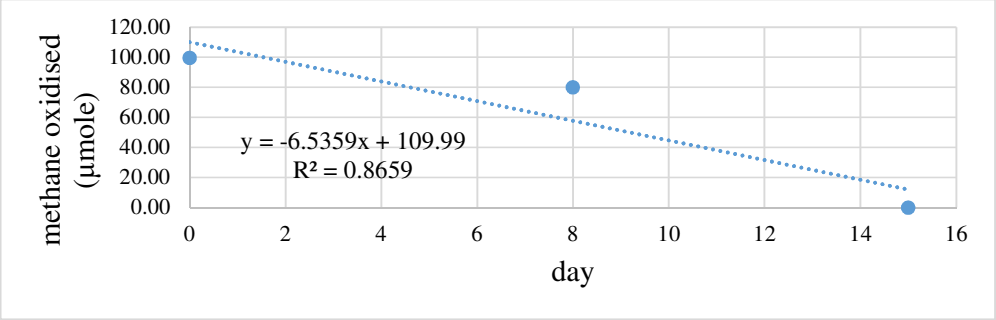

TOK17

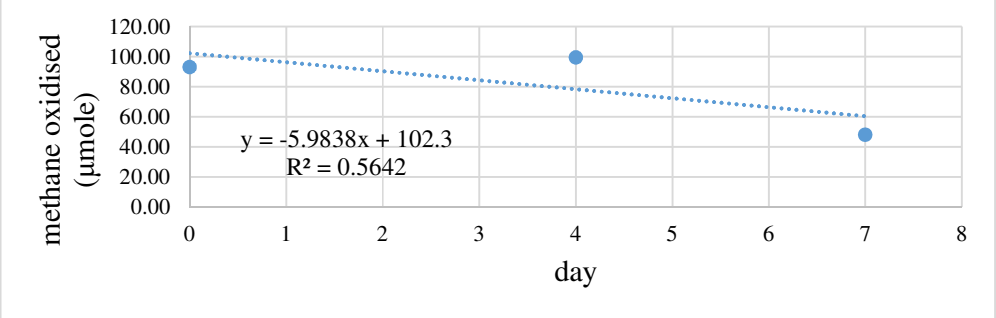

NGM89

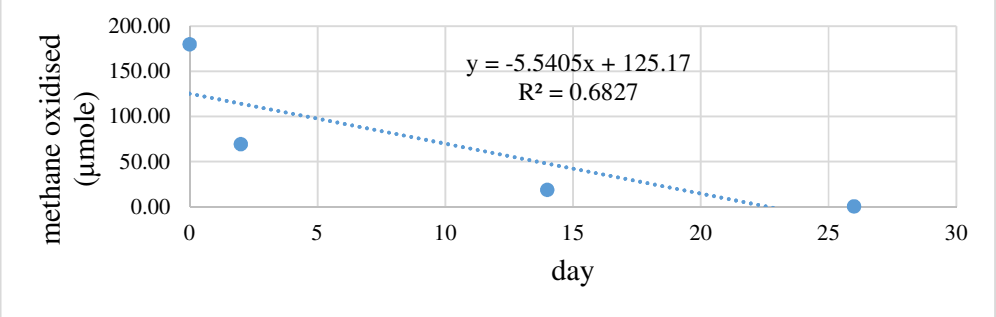

TKA13

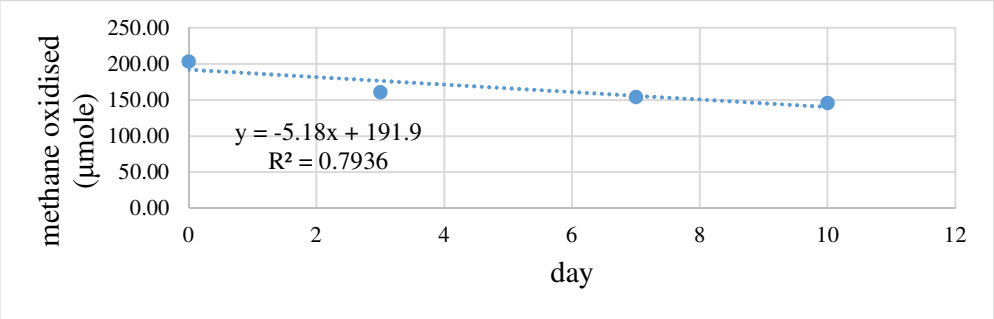

LPR16

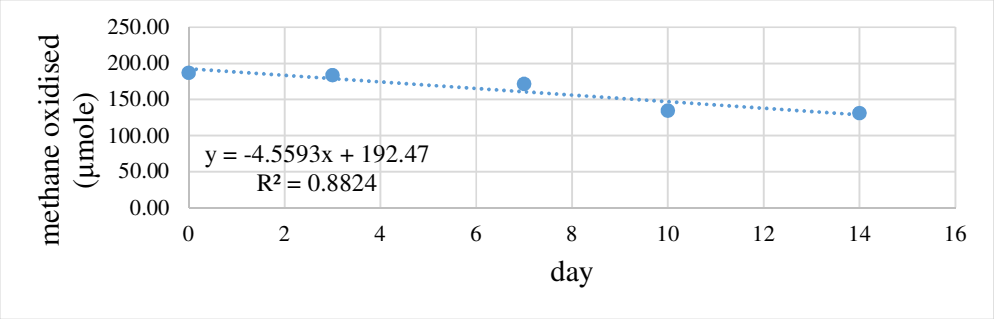

WAP11

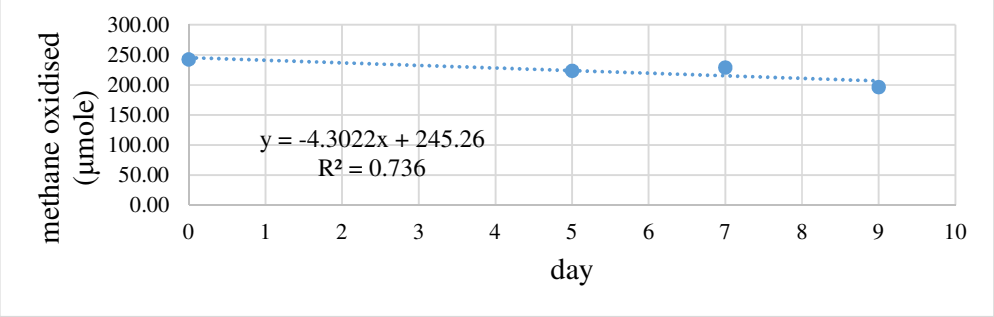

TOK7

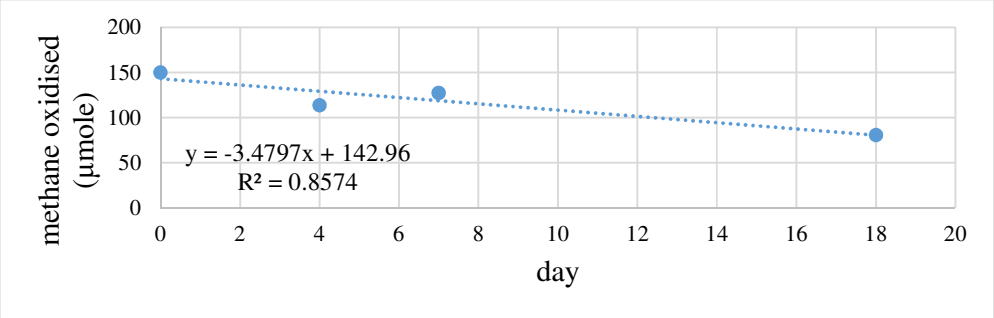

TKA9

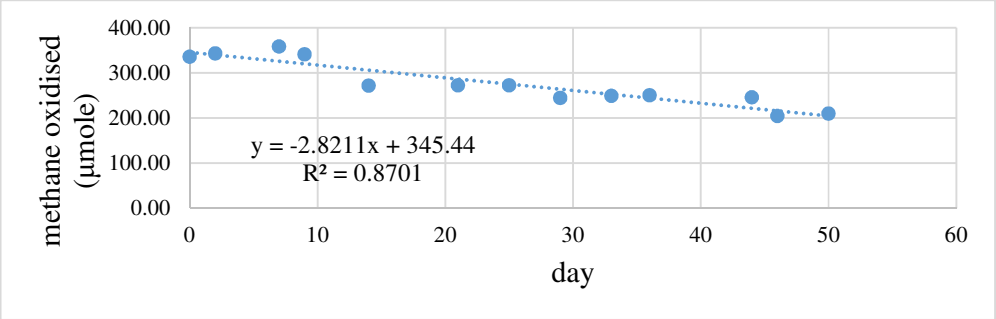

WTV2

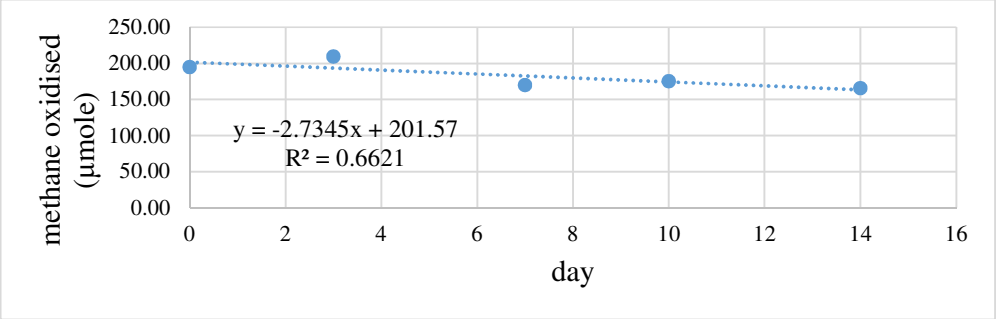

NGM91R

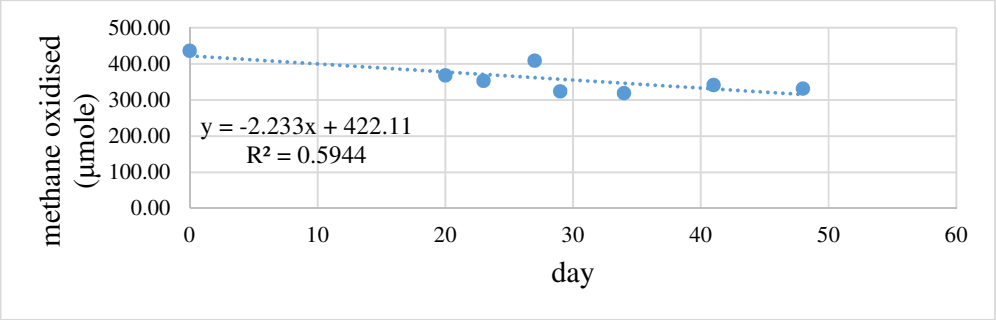

WTV1

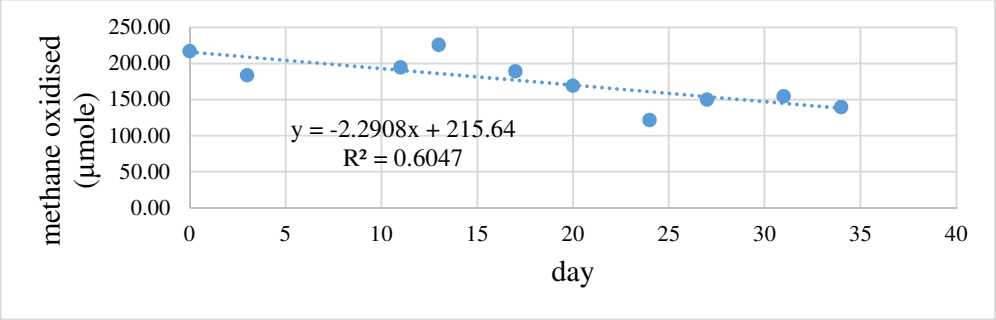

WHV18

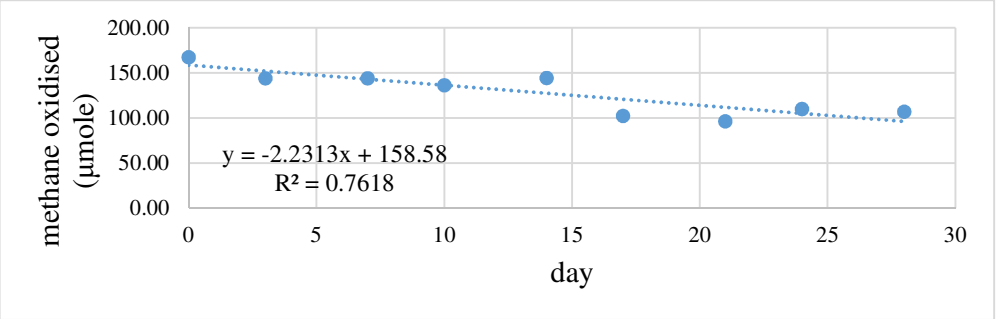

TKA16

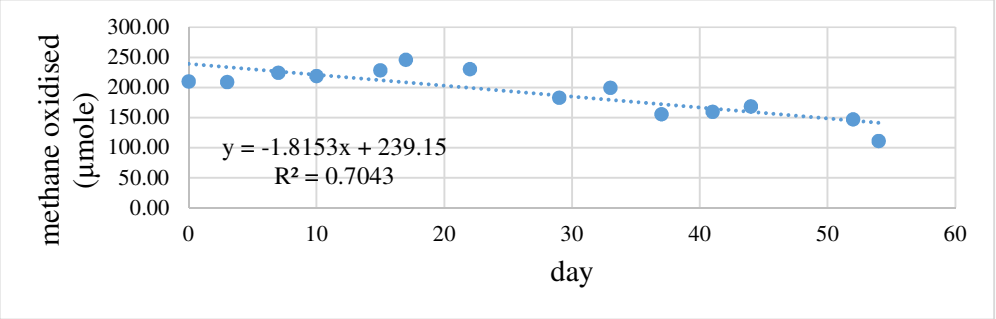

TKA8

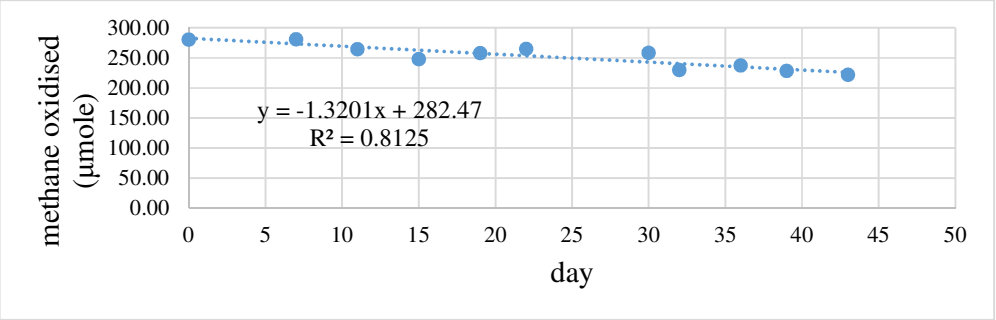

LPR17

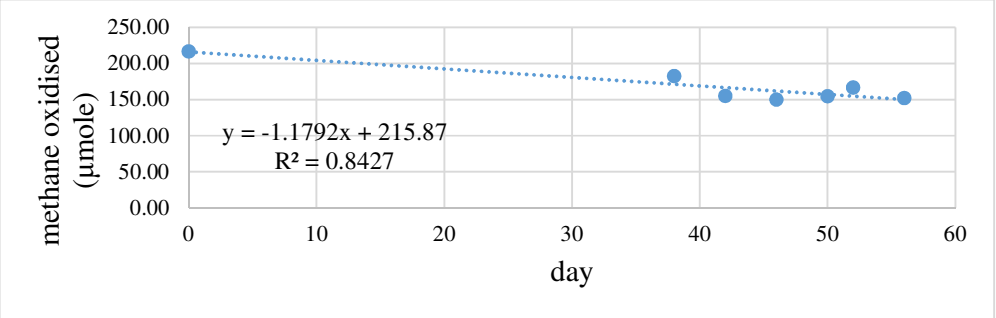

TKA15

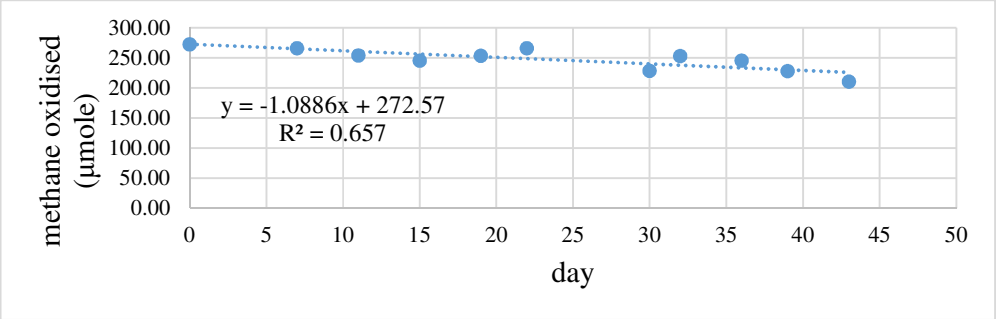

WHV16

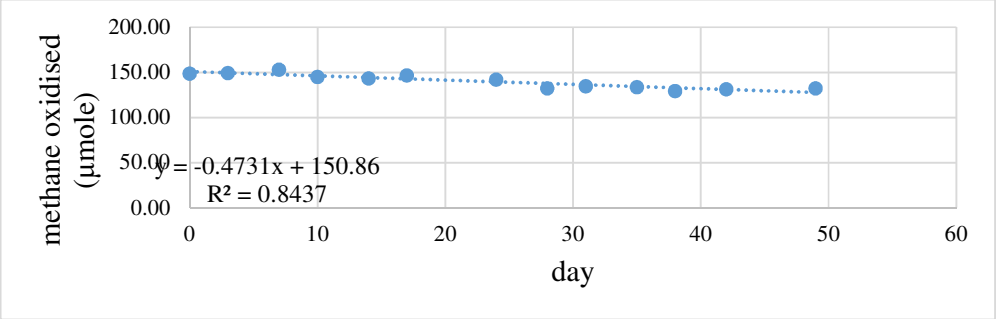

OKO2

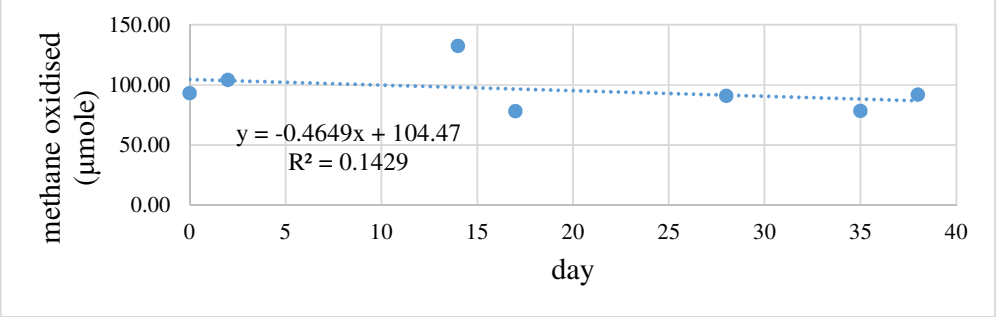

TKT67

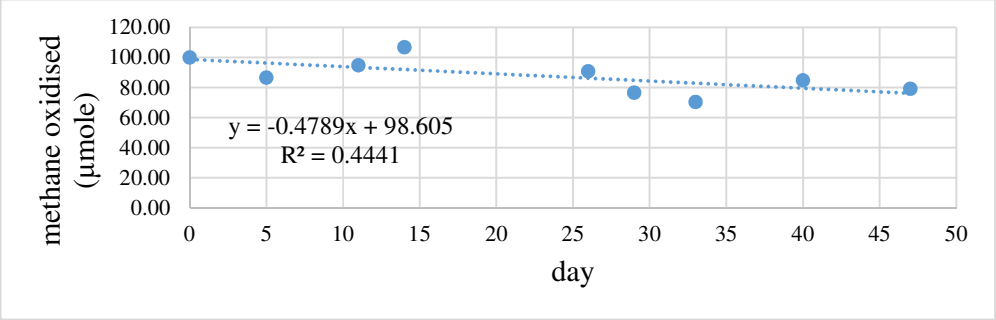

TKT68

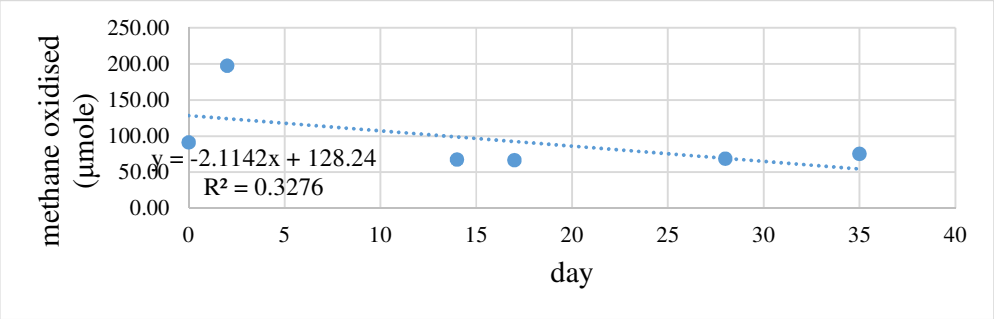

LPR14

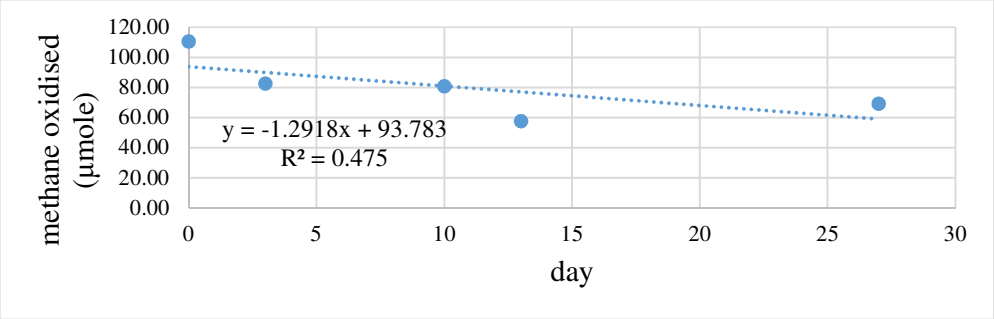

WTV4

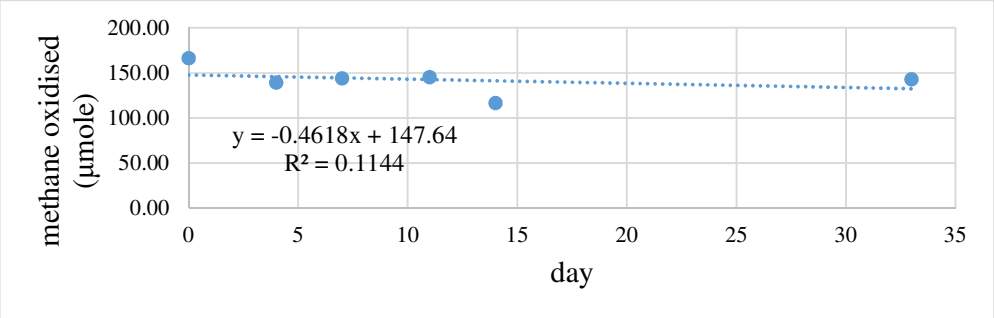

WAM36

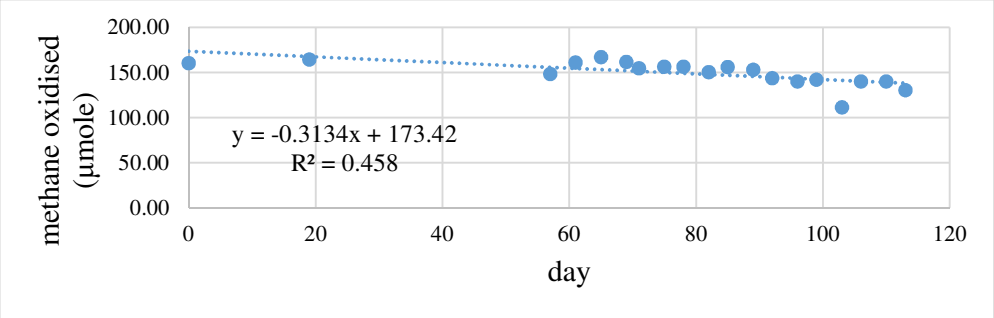

WKT45

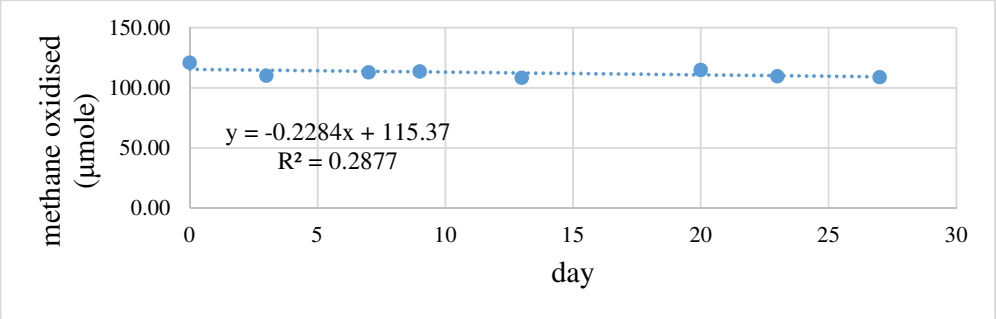

WHV15

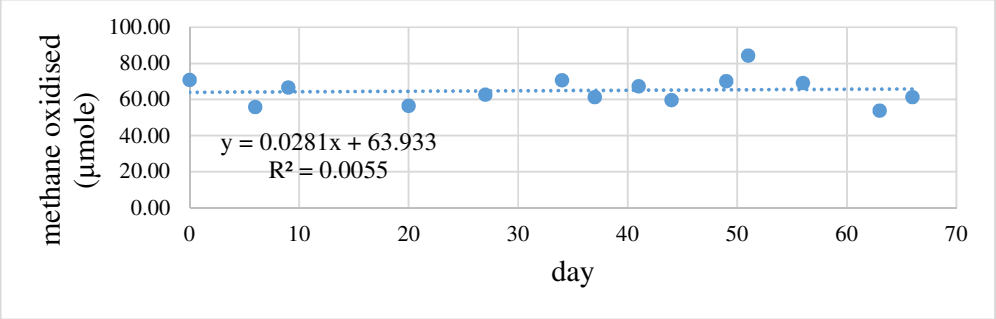

TOK15

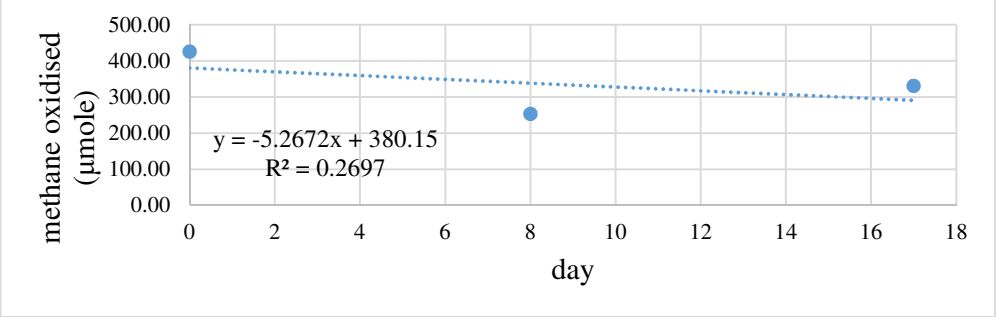

WHV13

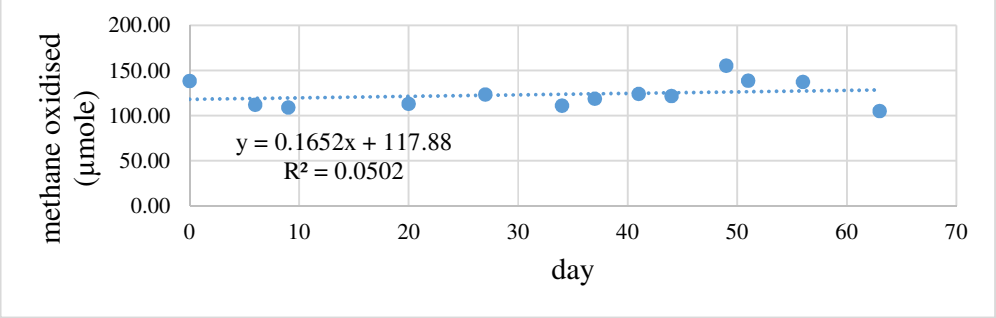

7.7 Methane oxidation of samples selected for transcriptome analysis, before stabilisation and storage of RNA. In all graphs, the three colours indicate each of the three biological replicates of the sample.

GDS1 (37 °C)

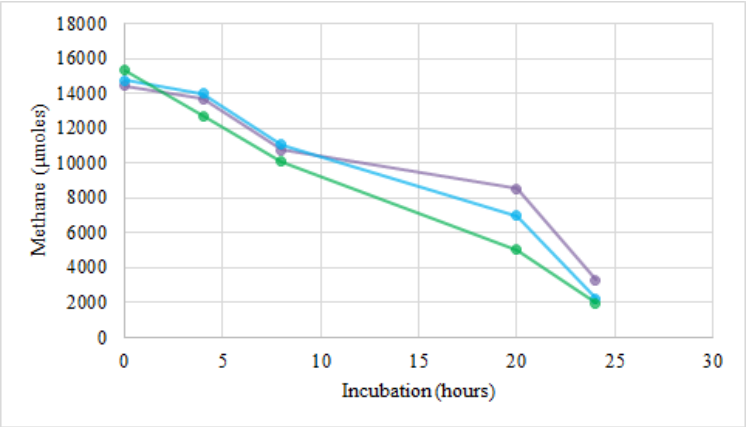

TOK7 (46 °C)

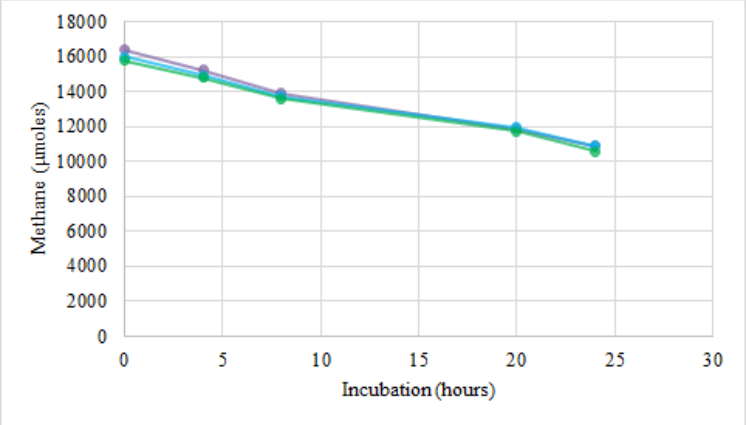

NGM89 (60 °C)

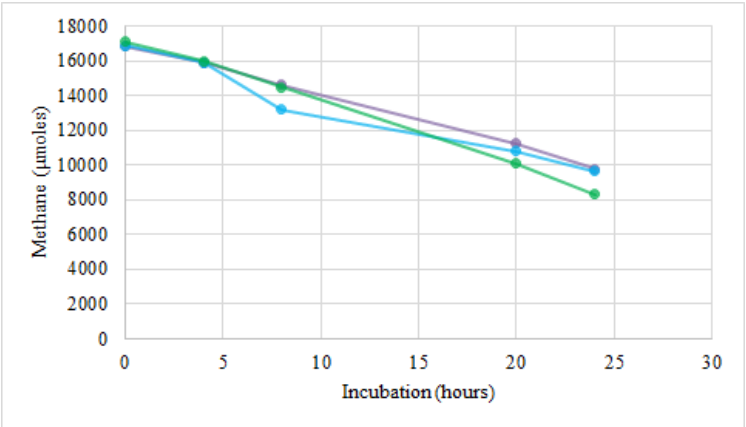

7.8 Inferred amino acid sequence alignment of 3d hydrogenases from Methylococcus GDS2.4, M. capsulatus and M. fibrata. L1 and L2 motifs of hydrogenase are highlighted in bold.

GDS2_4_3d	----------DPVTRVEGHGKITLLLDDDN
M. capsulatus 3d	MYDHLETAENPENLKRVVIDPVTRVEGHGKVTLLLDDDD
M. fibrata 3d	MYDHLETAENVHNLKRVVIDPVSRVEGHGKITLLLDEAG
GDS2_4_3d	HVRQARLHIVEFRGFERFIQGRPYWELPVL**VQRLCGCIP**
M. capsulatus 3d	HVRQARLHIVEFRGFERFIQGRPYWELPVL**VQRLCGCIP**
M. fibrata 3d	RVRQARLHIVEFRGFERFIQGRPYWELPIL**VQRLCGCIP**
GDS2_4_3d	**VSH**HLAAAKAIDQVVGVD?-?LTPAAEKLRRLMHFGQFL
M. capsulatus 3d	**VSH**HLAAAKAIDQIVGVD?-?LTPAAEKLRRLMHFGQFL
M. fibrata 3d	**VSH**HLAAGKAIDQLVGVDPDELTPSATKLRQLLHFGQVL
GDS2_4_3d	QSHALHFFHLATPDLLFGFDSPAGRRNIFEVLKEYPDVG
M. capsulatus 3d	QSHALHFFHLATPDLLLGFDSPAGRRNIFEVLKEYPDVG
M. fibrata 3d	QSHALHFFYLASPDLLFGFESDIHKRNIFSVLEDYPDIG
GDS2_4_3d	LEGVRMRKYGQEVIRLISGKRIHGSAAIPGGMNKALTAE
M. capsulatus 3d	LEGVRMRKYGQEVIRVISGKRIHGSASIPGGMNKALTCE
M. fibrata 3d	LQAVKVRKYGQEVIRAVAGKRIHGSGAIAGGMNKSLSSA
GDS2_4_3d	ERDFLLQDIDTVLGWCRNALALIRRIYLANREHHERFGL
M. capsulatus 3d	ERDFLRQDIDEVLGWCRNALALIRRIYLANREHHERFGL
M. fibrata 3d	ECEALLADIDQIIAWSSAAVLLIQKILYSDRAFYDDFAT
GDS2_4_3d	IRSNFMGLIRDDGAFEIYHGGLRAKDASGRTIFDKLDYR
M. capsulatus 3d	IRSNFMGLIRDDGAFEIYHGGLRAKDASGRTIFDKLDYR
M. fibrata 3d	LRSLYLGLTRPDGALELYHGGLRVKDAEGGTILDHVDYC
GDS2_4_3d	GYTGILREEVRSWSYMKFPYLEALGKDNGWYRVGPLAR
M. capsulatus 3d	GYTGILREEVRSWSYMKFPYIEALGKENGWYRVGPLAR
M. fibrata 3d	DYNSYIHEEVRSWTYMKFPYLLSLGKENGWYRVGPLAR
GDS2_4_3d	INNCDFMPTPLAEAARQDFLAQGAGGPVHGSLAFHWAR
M. capsulatus 3d	INNCDFIPTPLAEEARQDFLAHGAGGPVHGSLAFHWAR
M. fibrata 3d	VNNCDFIDTPLAEAARLEFKAHGTEAMVHNTLATHWAR
GDS2_4_3d	MIETLHCAESIRDLLHD?----------
M. capsulatus 3d	MIETLHCAESIRELLDDPELLGTDLVVHGERRPEGIGVI
M. fibrata 3d	MIETLHCAERIKELLRDPDIRGHDLVTQGEKRYEGIGVI
GDS2_4_3d	----------
M. capsulatus 3d	EAPRGTLFHHYQVDENDLVTRANLIVSTTQNNQAMNESI
M. fibrata 3d	EAPRGTLFHHYRIDENDIVVKANLIVSTTHNNRAMNESV
GDS2_4_3d	----------
M. capsulatus 3d	RQVAAEYLDGQTITEGLLNHIEVAIR**AYDPCLSCATH**ALG
M. fibrata 3d	RQVAARYLSGRELTEPLLNNLEVAVR**AYDPCLSCATH**AVG